The American Mineralogist

Journal of the Mineralogical Society of America

VOL. 43 JULY–AUGUST, 1958 Nos. 7 and 8

Contents

(Continued on Cover 2)

Published bi-monthly by the Society

The enlarged issues of this journal for 1958 are made possible by a grant from the Penrose Fund of the Geological Society of America.

The American Mineralogist—Journal of the Mineralogical Society of America

The journal, containing articles on mineralogy, crystallography, and allied sciences, is issued every two months. Contributions are invited.

Authors are requested to submit two copies of each manuscript, typewritten on standard size paper, 8½×11 inches. Photographs submitted for cuts should be glossy prints.

Beginning with Vol. 43, 1958, authors are entitled to 50 free reprints, without covers, of each article published.

Sent to all members and fellows of the Mineralogical Society of America. Membership dues $4.00 annually, fellowship dues $5.00 annually, which includes receipt of the American Mineralogist and GeoTimes, which is published by the American Geological Institute. Subscriptions for libraries, colleges, institutions, companies and similar organizations $6.00 annually.

Entered as second class matter at the post office at Menasha, Wis., under Act of March 3, 1879. Acceptance for mailing at the special rate of postage provided for in section 1103, Act of Oct. 3, 1917, paragraph 4 section 429 P. L. & R. authorized March 13, 1922.

Notice of change of address, orders, and remittances should be sent to Mineralogical Society of America, Dr. Earl Ingerson, Treasurer, U. S. Geological Survey, Washington 25, D.C.

Printed by the George Banta Company, Inc., Menasha, Wisconsin
Printed in the United States of America

Leitz®

SATISFIES THE MOST EXACTING REQUIREMENTS

RESEARCH POLARIZING MICROSCOPE

DIALUX-POL

The new *LEITZ* DIALUX-pol is the most advanced, universal polarizing research microscope ever manufactured. It was designed for the geologist, minerologist, petrographer, paleontologist, and the industrial research microscopist.

The DIALUX-pol maintains the principle of interchangeability, famous with all *LEITZ* precision instruments, so that it is readily used for transmitted light as well as for reflected-polarized light. With the simple addition of a connecting bar, it provides synchronous rotation of polarizer and analyzer.

In addition to a built-in light source and condenser system, the DIALUX-pol features many other operational advantages: unique single-knob control of both coarse and fine adjustment by alteration of the stage height (and not the tube), thus focusing with maximum operational ease.

Within seconds, the DIALUX-pol, through *LEITZ* accessories, converts for photography (through combined monocular-binocular tube and Leica camera), for ore microscopy (through vertical illuminator), or will accommodate the *LEITZ* Universal Stage, Sodium Vapor Lamp, and other facilities.

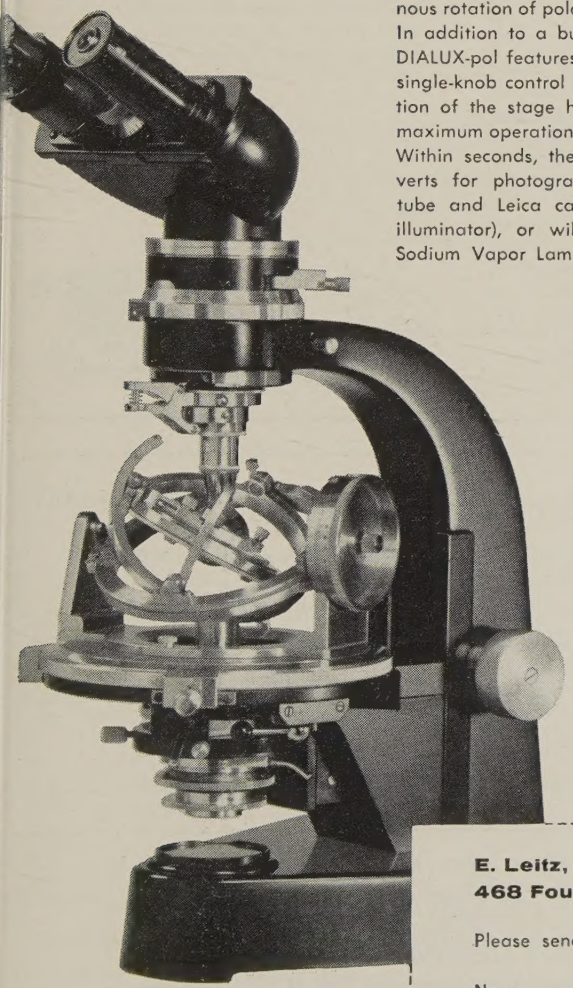

- monocular or binocular vision
- combination tube FS for photography
- synchronous polarizer-analyzer rotation upon request
- dual coarse and fine focusing
- built-in light source; 6-volt, 2.5-amp, variable intensity
- vertical illumination for ore microscopy
- polarizing filters or calcite prisms
- adaptable to all universal stage methods

Send for the DIALUX-pol information bulletin—then see and examine this fine instrument for yourself.

E. Leitz, Inc., Department AM-8
468 Fourth Ave., New York 16, N. Y.

Please send me the *LEITZ* DIALUX-pol brochure.

Name_____

Street_____

City_____ Zone_____ State_____

25150

E. LEITZ, INC., 468 FOURTH AVENUE, NEW YORK 16, N. Y.
Distributors of the world-famous products of
Ernst Leitz G. m. b. H., Wetzlar, Germany—Ernst Leitz Canada Ltd.
LEICA CAMERAS · LENSES · MICROSCOPES · BINOCULARS

THE AMERICAN MINERALOGIST

JOURNAL OF THE MINERALOGICAL SOCIETY OF AMERICA

Vol. 43 JULY–AUGUST 1958 Nos. 7 and 8

ADSORPTION AND RETENTION OF AN ORGANIC MATERIAL BY MONTMORILLONITE IN THE PRESENCE OF WATER*

G. W. BRINDLEY AND MAHMOUD RUSTOM, *Department of Ceramic Technology, The Pennsylvania State University.*

ABSTRACT

The adsorption of a polyethylene glycol ester of oleic acid on montmorillonite is studied in relation to the water content of the system. At low concentrations of organic material to clay mineral, 70% of the organic material is adsorbed on the clay and 30% remains in solution. The lattice spacings of the clay-organic complexes, when dried at 110° C., are studied for clays saturated with Na, Ca and Mg ions. Ordered complexes are found containing one layer or two layers of organic material between silicate layers, and in the appropriate composition ranges mixtures of 1-layer and 2-layer types are observed rather than mixed sequences. Repeated washings reduce 2-layer to 1-layer type sequences, but a single organic layer between silicate sheets is firmly held.

INTRODUCTION

The adsorption of organic molecules by montmorillonite and the resultant expansion of the crystalline lattice have been intensively studied and general surveys have been given by MacEwan (1951) and by Grim (1953). These studies have been made mainly with liquids, either organic liquids or solutions in water, but in a few instances with organic vapors. Glaeser and Mering (1952, 1954), and Barrer and MacLeod (1955) have studied the adsorption and desorption isotherms of montmorillonite for a number of gases and vapors in relation to the relative vapor pressure; comparable studies for organic materials dissolved in water appear not to have been made.

In the present investigation an attempt has been made to study equilibrium in a system comprising montmorillonite, an organic material, and water. In particular, attention has been given to (i) the partition of the organic material between the clay and the liquid phase, (ii) the change in character of the clay-organic complex as the organic com-

* Contribution No. 57–20 from the College of Mineral Industries, The Pennsylvania State University, University Park, Pennsylvania.

ponent is increased from small amounts up to saturation, and (iii) the retention or fixation of the organic material by the clay.

In recent years much attention has been given to the adsorption of cationic organic complexes on clays (see Gieseking (1939), Hendricks (1941), Jordan (1949, 1954), Franzen (1955), Talib-Udeen (1955), Barrer and MacLeod (1955), Haxaire and Bloch (1956)). The results indicate that in addition to a cation exchange reaction, physical adsorption processes also occur. It seemed desirable, therefore, to study the adsorption of a non-ionic complex before considering situations in which exchange reaction take place.

Materials

Organic material

The experiments have been carried out with a commercial wetting agent, "Nonisol 250", supplied by the Geigy Chemical Corporation, the choice of which was partly fortuitous. This is an ester of polyethylene glycol and oleic acid, with the following chemical formula:

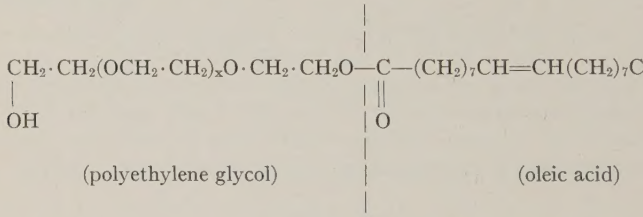

The material is normally a paste, readily soluble in water and in most organic solvents. It is recoverable from solution in water by drying at 105° C. with less than a 1% weight loss, and with no significant change in the *x*-ray powder diagram. The material is therefore chemically stable to solution in water and re-drying.

Clay material

Montmorillonite has advantages over non-swelling clays since the expansion of the crystal lattice can be measured by *x*-rays and this provides an accurate method of studying adsorbed surface layers which is not applicable to the non-swelling clays.

A purified Wyoming bentonite was supplied by Dr. J. L. McAtee, of the Baroid Sales Division, National Lead Company, Houston, Texas. This is a relatively well-crystallized form of montmorillonite. The precise purification process is not known but is believed to be one of sedimentation and/or centrifugation. The sample supplied had Na and Ca ions as exchangeable cations and contained a trace of cristobalite impurity.

Experimental Procedures

Clay mineral preparation

By repeated treatment with 1-N solutions of the respective chlorides, clay samples were prepared saturated with Ca, Na and Mg ions. Following sedimentation and repeated washings of the clays with distilled water, the remaining traces of excess chloride were removed by dialysis through cellophane tubing, using the silver nitrate test. The clay samples were then dried in air at 110° C. and stored in a dessicator over activated alumina.

Clay-organic adsorption procedure

The experiments were designed mainly on a volumetric basis. A suspension of montmorillonite containing 1 gm. clay/liter water, and an organic solution containing 1 gm./liter water were prepared. Requisite volumes of clay suspension, organic solution, and water were mixed and agitated intermittently for 4 hours. After centrifugation, an aliquot of the clear solution was analysed for organic material, and the clay was removed for *x*-ray examination.

Organic analysis

To determine the organic matter left in solution, a direct weighing method was tried using very thin Pyrex bulbs as evaporating dishes. The method was found to be capable of giving reasonable accuracy but was very inconvenient.

A titration method was developed making use of the C=C bond in the oleic acid part of the molecule. Adsorption of bromine by the double bond was determined by measuring excess bromine with a thiosulphate titration. A calibration curve was obtained using organic solutions of known concentration. The conditions for the bromine absorption and the subsequent titration were standardized precisely. The method was found to be accurate and measurements could be repeated.

X-ray analysis

The clay samples were prepared as thin, oriented layers on glass slides and were examined with a Philips Norelco diffractometer with CuKα radiation. The atmosphere surrounding the specimen was controlled by air circulation, either dry air or air of humidity approaching 100%. The latter was used with wet clay films prior to any drying treatment and ensured that the clay film remained wet during the *x*-ray examination, usually about 30 min.-1 hr.

Results

(*a*) *Partition of organic material between clay and water for constant initial concentration of organic material*

The three components, clay, organic material and water, were mixed to provide an initial concentration of 300 mg. organic material/liter water, and to cover a range of values for the ratio of organic material to clay.

In Fig. 1, the organic material adsorbed per gm. clay is plotted against total organic material in the system per gm. clay. The adsorption curve tends smoothly to an asymptotic limit of about 0.6 gm. adsorbed organic

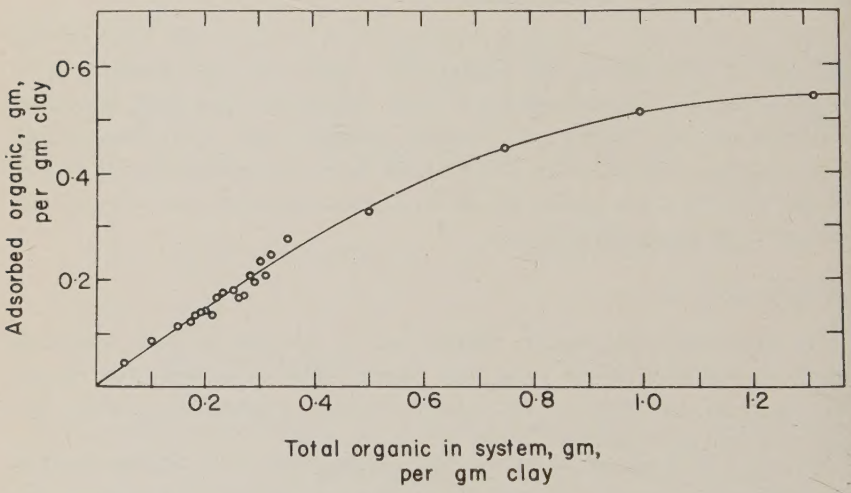

Fig. 1. Adsorption of polyethylene glycol ester of oleic acid on montmorillonite in an aqueous system.

material per gm. clay. In the region of about half maximum adsorption a large number of observations were made to check for a possible departure from the smooth curve, but within the accuracy of the determinations, no deviations were found.

Up to about 50% of maximum adsorption, the curve is linear with a gradient corresponding to about 70% of the total organic material being adsorbed on the clay. At about 90% of maximum adsorption, the clay adsorbs about 50% of the total organic material.

(*b*) *X-ray examination of the wet clay-organic films prior to drying*

After centrifugation, the clear liquid was drained from the clay, a few ml. of water were added, and several drops of the clay suspension placed on a glass slide. Evaporation in air was allowed to proceed until

a coherent but still moist clay film was obtained. This was placed in the diffractometer enclosure and kept moist by passing air of almost 100% R.H.

The lattice spacing $d(001)$ was 18.5–19 Å largely irrespective of the exchangeable cations and the amount of adsorbed organic material. The results are set out in Table 1. For Na-montmorillonite, the spacing ranged up to 22 Å for small quantities of adsorbed organic material, but otherwise conformed to the values found for Ca- and Mg-montmorillonites. These results suggest that prior to drying the lattice spacing is determined principally by water remaining between the silicate sheets.

Table 1. Lattice Spacings of Wet Montmorillonite Films Containing Adsorbed Polyethylene Glycol Ester of Oleic Acid (Nonisol 250); Values of $d(001)$ in Å

Exchangeable cations	Na	Ca	Mg
Clay films prior to any drying treatment	18.0–22.0	18.6	18.8–19.2
Clay films re-wetted after drying at 110° C.	18.4–19.6	18.4–18.8	18.4–19.0

(*c*) *X-ray examination of the dried clay-organic films*

The clay-organic films were now dried at 110° C. and maintained in a dry atmosphere during storage and during *x*-ray examination with the diffractometer.

The results vary according to the exchangeable cation and the total organic/clay ratio. Typical diffractometer recordings for selected organic/clay ratios are shown in Figs. 2, 3, and 4, and the lattice spacings, $d(001)$, are shown in Figs. 5, 6, and 7.

Figs. 5, 6, and 7 show that the lattice spacing expands to nearly stationary values of about 14 Å and 17.5 Å as the total organic content is increased. The detailed results, see Table 2, show that the mean lattice expansions with respect to clays dried at 250° C. and without organic material are 4.20 Å and 7.70 Å. These expansions are regarded as corresponding to one and two layers of organic material respectively between the montmorillonite sheets.

It is of particular interest to consider whether, with increasing organic content, the clay-organic complexes form regular structures at certain compositions, and irregular or interstratified structures at intermediate compositions. The evidence in Figs. 2–7 points to the formation of regular structures as the main feature of these organic complexes. Although there is some evidence for irregular stratifications of the clay-organic layers, this does not appear to be a major characteristic of the present system.

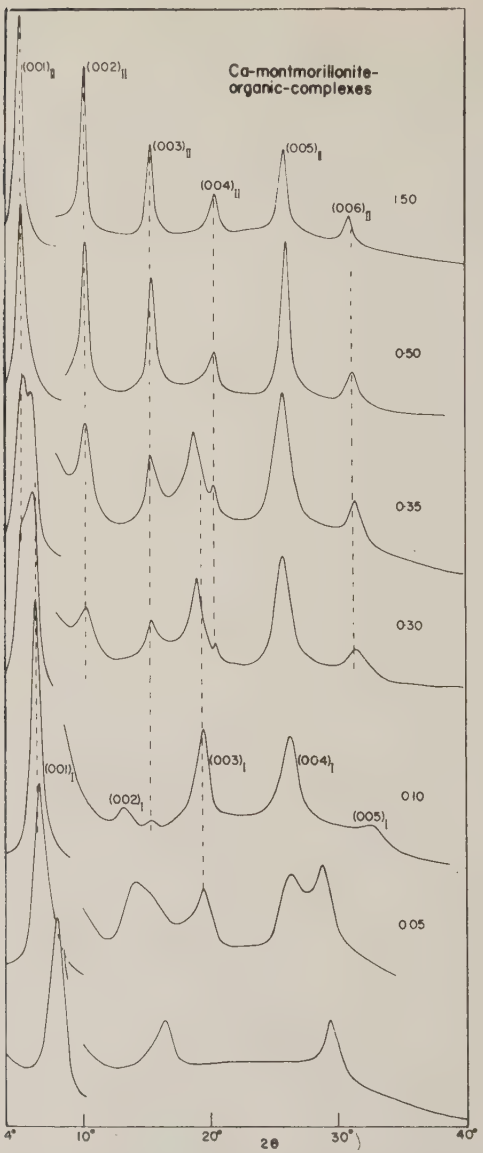

FIG. 2. Diffractometer recordings of Ca-montmorillonite-organic complexes. The ratio of total organic material in the system to the amount of clay is shown by the value at the right hand side of each diagram.

The breaks in the curves at about $2\theta = 10°$ arise from a change of the intensity scale for the higher order reflections.

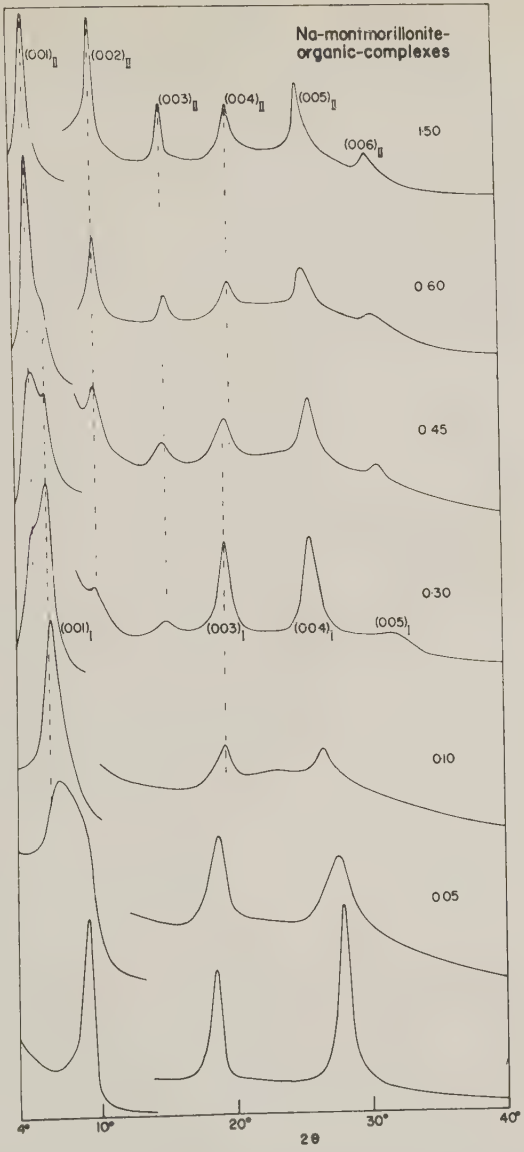

FIG. 3. Diffractometer recordings of Na-montmorillonite-organic complexes. The ratio of total organic material in the system to the amount of clay is shown by the value at the right hand side of each diagram.

The breaks in the curves at about $2\theta = 10°$ arise from a change of the intensity scale for the higher order reflections.

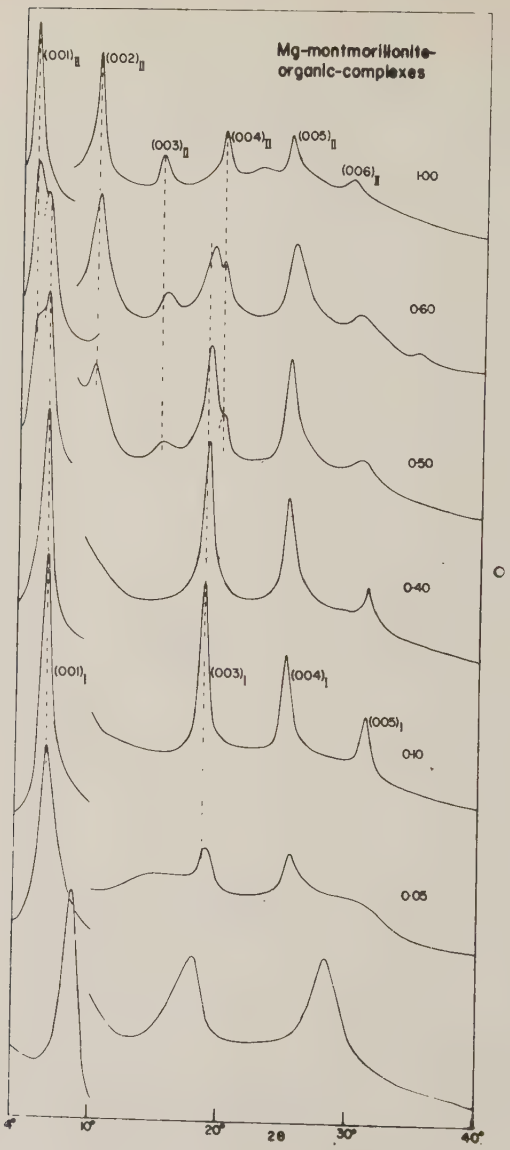

FIG. 4. Diffractometer recordings of Mg-montmorillonite-organic complexes. The ratio of total organic material in the system to the amount of clay is shown by the value at the right hand side of each diagram.

The breaks in the curves at about $2\theta = 10°$ arise from a change of the intensity scale for the higher order reflections.

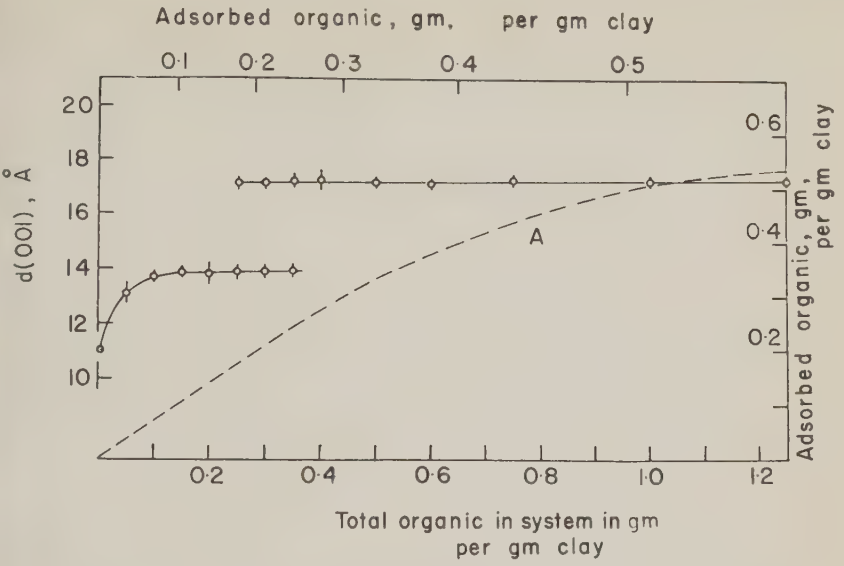

FIG. 5. Lattice spacings in Å of dried Ca-montmorillonite-organic complexes with increasing organic material in the reacting system.

Curve A is the adsorption curve of Fig. 1.

Regularity of a layer structure is indicated by the formation of an integral series of Bragg reflections; the lattice spacing calculated from each reflection with its assumed integral order should then have a constant

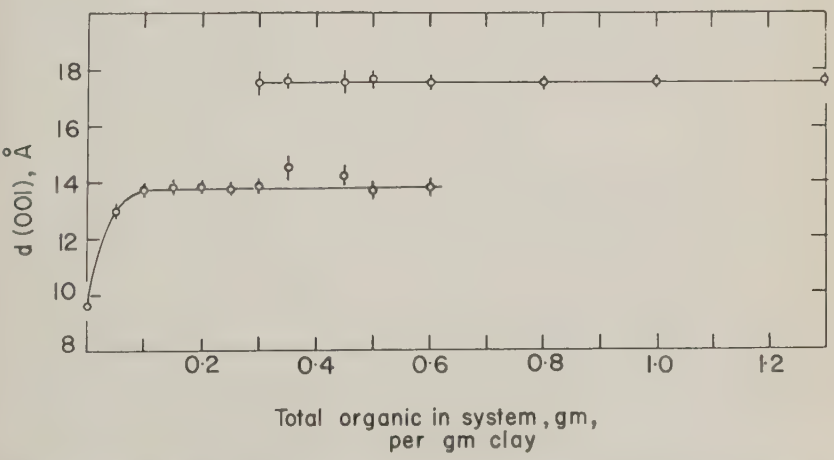

FIG. 6. Lattice spacings in Å of dried Na-montmorillonite-organic complexes with increasing organic material in the reacting system.

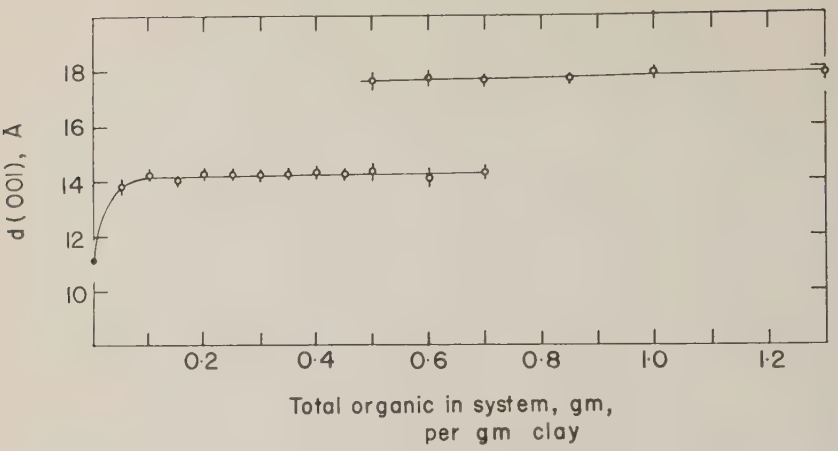

Fig. 7. Lattice spacings in Å of dried Mg-montmorillonite-organic complexes with increasing organic material in the reacting system.

value. Mixed-layer sequences do not give truly integral orders of reflection and if integral orders are assumed, then the lattice spacings derived on this basis do not have a constant value. In Figs. 5, 6, and 7, mean values of $d(001)$, obtained from the observed reflections with the assumption of integral orders, are recorded and the short vertical lines indicate the mean deviations of individual values from the average values. The fact that the mean deviations are generally small means that, for the most part, the integral Bragg law is obeyed, i.e., the structures are regular.

Between the composition ranges in which only one basal spacing

Table 2. Lattice Spacings, in Å, of Dried Films of Montmorillonite Containing Adsorbed Polyethylene Glycol Ester of Oleic Acid (Nonisol 250)

Exchange ion	Fully dried clay	Expanded clays			
		First stage of expansion		Second stage of expansion	
		d	Δd	d	Δd
Na	9.6_5	13.8	4.1_5	17.5	7.8_5
Ca	9.7_5	13.9	4.1_5	17.3	7.5_5
Mg	10.0	14.2_5	4.2_5	17.7	7.7
		Mean	4.2_0	Mean	7.7_0

$d(001)$ is recorded, there is a region in which two basal spacings are found simultaneously. This means that in a composition range where irregular interstratified sequences might well have been anticipated, two different ordered phases are found. This is illustrated in Figs. 2, 3, and 4 where reflections arising from structures with one organic layer, and with two organic layers are marked $(00l)_{I}$ and $(00l)_{II}$ respectively. It is noticeable in Figs. 5, 6, and 7 that where two basal spacings are found together, the lattice spacings are somewhat less regular than when a single basal spacing occurs.

Between the pure clay end-member and the complex with one organic layer, superpositions of corresponding reflections are not observed, but a progressive shift is found indicating that interstratification of dissimilar layers occurs when the first small amounts of organic material are added to the system. However, the clay lattice expands very quickly to an ordered arrangement with one layer of organic material between the silicate sheets.

(*d*) *X-ray examination of re-wetted clay-organic films*

After examination of the dried films, a few drops of water were placed on each clay-organic film which was then left over-night in a humid atmosphere. Results for the re-wetted films, summarized in Table 1, agree with those for the initial wet films with the one exception that the Na-clay with little organic material did not expand beyond about 19.6 Å.

(*e*) *Stability of the clay-organic films to washing*

The effect of repeated washing of the clay-organic complexes was studied both before and after a drying treatment. After each washing the clay was centrifuged, the liquid removed, fresh water added and a further washing carried out.

The results set out in Table 3 show the dry spacings of Na-, Ca-, and Mg-clays after repeated washings. Two layers of adsorbed organic material can be reduced to one layer, but beyond this stage the organic material could not be removed. A Sohxlett extraction also failed to remove the single adsorbed layer.

Discussion

The similarity of the results for the Na-, Ca- and Mg-clays shows that essentially the same processes are involved in all three clays. However, the adsorption curve, Fig. 1, has been determined only for the Ca-clay. The discussion will therefore be limited to Ca-clay in the first instance. The adsorption curve is superposed on the lattice spacing curves in Figure 4 so that it can be seen at a glance how the swelling of the clay is re-

Table 3. Lattice Spacings, in Å, of Dried Montmorillonite-Nonisol Complexes After Repeated Washings in Water

Na-Montmorillonite		Mg-Montmorillonite		Ca-Montmorillonite	
No. of washings	d(001)	No. of washings	d(001)	No. of washings	d(001)
—	17.2 (2-layers)	—	17.8 (2-layers)	—	17.3 (2-layers)
5	13.9 (1-layer)	5	15.5	4	17.2 (2-layers)
		10	13.7 (1-layer)	12	17.2 (2-layers)
		20	13.8 (1-layer)	20	14.0 (1-layer)
—	13.7 (1-layer)	—	14.2 (1-layer)	—	13.8 (1-layer)
5	13.8 (1-layer)	8	14.2 (1-layer)	4	13.9 (1-layer)
10	13.7 (1-layer)	12	13.8 (1-layer)	12	13.9 (1-layer)
15	13.8 (1-layer)	16	13.9 (1-layer)	20	13.8 (1-layer)
				25	13.8 (1-layer)

lated to the adsorbed organic material and to the total organic material in the system.

It has already been noted that there is a marked tendency towards the formation of ordered complexes containing either one layer or two layers of organic material between successive silicate sheets. If P(n) denotes a regular phase containing n organic layers between successive silicate sheets, and P(n,m) an irregular sequence in which n or m organic layers occur randomly between successive silicate sheets, then the sequence of phases observed as the amount of organic material increases in the clay lattice, is as follows:

$$\text{P(0)},\quad \text{P(0, 1)},\quad \text{P(1)},\quad \text{P(1)} + \text{P(2)},\quad \text{P(2)}.$$

P(0) symbolizes the pure montmorillonite. P(0, 1) appears as an irregular sequence extending from zero to about 0.07 gm. adsorbed organic material per gm. clay which corresponds to about 12% of the saturation value.

The ordered phase P(1) extends from about 0.07–0.17 gm. adsorbed organic per gm. clay, i.e., 12%–30% of the saturated value. The lattice spacing of the P(1) phase is almost constant at 13.9 Å and increases only slightly as the organic content increases. It might be expected that the limit of the P(1) phase would correspond to 50% saturation of the clay. However, when 30% of saturation is reached, some two-layer complex makes its appearance and the mixed phases P(1)+P(2) co-exist in the range 0.17–0.25 gm. adsorbed organic per gm. clay, i.e., 30%–42% of the saturation value.

This symbol, P(1)+P(2), implies that the co-existing phases are regu-

lar structures, which is essentially the case, but the regularity is somewhat less perfect than in the single phase ranges. One may therefore picture the P(1) phase as containing a small proportion of two-layer complex and the P(2) phase a small proportion of one-layer complex, but the proportions are too small to make any appreciable change in mean lattice spacing except perhaps in the case of the Na-clay, see Fig. 6.

When the adsorbed organic exceeds 0.25 gm. per gm. clay (42% of saturation), then P(2) alone is formed. This means that even though the organic material is not quite sufficient to fill one layer to maximum capacity, a regular two-layer structure is formed. From 42%–100% saturation, the two-layer complex becomes increasingly filled with organic molecules. Adsorption beyond a two-layer complex does not occur.

In order to visualize how the adsorption complexes are formed, it must be remembered that the adsorption takes place initially when the silicate layers are separated in water. The spacing of the dried films is the result of bringing two adsorbing surfaces together. If each surface had 50% of its maximum adsorption, then it might be expected that the molecules adsorbed on one surface could be accommodated in vacant positions on the adjacent surface, thereby producing one completely filled layer. The results show that for Ca-clay when each surface adsorbs 42% of its maximum capacity, a regular two-layer structure is formed. It must be concluded that the organic molecules are held rather tightly and are not sufficiently mobile to give a close-packed single layer.

The maximum adsorption on each surface to give a single layer P(1) complex occurs at 30% of its maximum adsorptive capacity. When the adsorbed organic content exceeds 30% of saturation, the P(2) complex makes its appearance along with the P(1) complex. It is difficult to explain why some clay particles contain wholly or almost wholly the P(1) complex and others contain wholly or almost wholly the P(2) complex. One is almost forced to conclude that there are minor differences between individual clay particles such that certain particles tend to build up a P(2) complex at a lower organic content than do other clay particles. In consequence, as the organic content in the liquid phase is increased, more and more particles pass over from the P(1) to the P(2) type of complex.

Presumably these differences between particles are not sufficient to influence the initial organic adsorption, for here a mixed-layer phase P(0,1) is produced rather than a mixture of pure montmorillonite P(0), plus a one-layer complex, P(1).

One might hazard a guess that the hypothetical minor differences arise from differences in chemical composition giving rise to different exchange capacities and different layer charges. On this basis it is con-

ceivable that when the organic content in the liquid phase approaches a certain range of values, some particles will be extended to P(2) complexes while others still remain as P(1) complexes.

Acknowledgments

This work forms part of a program made possible by a Grant-in-Aid from the Gulf Research and Development Company, Harmarville, Pa. The purified montmorillonite was kindly made available by Dr. J. L. McAtee, and the Baroid Sales Division, National Lead Company, Houston, Texas, and the organic agent by the Geigy Chemical Corporation.

References

Barrer, R. M., and MacLeod, D. M. (1955), Activation of montmorillonite by ion-exchange and sorption complexes of tetra-alkyl ammonium montmorillonites, *Trans. Faraday Soc.*, **51,** 1290–1300.

Franzen, P. (1955), *X*-ray analysis of an adsorption complex of montmorillonite with cetyltrimethyl ammonium bromide (lissolamine), *Clay Min. Bull.*, **2,** 223–225.

Gieseking, J. E. (1939), Mechanism of cation exchange in the montmorillonite-beidellite-nontronite type of clay minerals, *Soil Sci.*, **47,** 1–14.

Glaeser, R., and Méring, J. (1952), Les propriétés des associations organo-argileuses, *Congrès Geol. Inter., Alger.*, **18,** 117–121.

Glaeser, R., and Méring, J. (1954), Isothermes d'hydratation des montmorillonites bi-ioniques (Na, Ca), *Clay Min. Bull.*, **2,** 188–193.

Glaeser, R. (1954), Complexes organo-argileux et rôle des cations échangeables, 1–68, Thèse (Paris)

Greene-Kelly, R. (1955), An unusual montmorillonite complex, *Clay Min. Bull.*, **2,** 226–232.

Grim, R. E. (1953), "Clay Mineralogy", Ch. X, pp. 250–277, McGraw-Hill, New York.

Haxaire, A., and Bloch, J. M. (1956), Sorption de molécules organiques azotées par la montmorillonite. Étude du méchanisme, *Bull. Soc. Franç. Min. Crist.*, **79,** 464–475.

Hendricks, S. B. (1941), Base-exchange of the clay mineral montmorillonite for organic cations and its dependence upon adsorption due to Van der Waals forces. *J. Phys. Chem.*, **45,** 65–81.

Jordan, J. W. (1949), Organophilic bentonites, I. Swelling in organic liquids, *J. Phys. and Coll. Chem.*, **53,** 294–306.

Jordan, J. W. (1949), Alteration of the properties of bentonite by reaction with amines, *Min. Mag.*, **28,** 598–605.

Jordan, J. W., and Williams, F. J. (1954), Organophilic bentonites. III. Inherent properties, *Koll-Zeit.*, **137,** 40–48.

MacEwan, D. M. C. (1951), The montmorillonite minerals; Ch. IV, pp. 86–137, in "*X*-ray Identification and Crystal Structures of Clay Minerals" Mineralogical Society, London.

Méring, J., and Glaeser, R. (1954), Sur le rôle de la valence des cations échangeables dans la montmorillonite, *Bull. Soc. Franç. Min. Crist.*, **77,** 519–530.

Talib-Udeen, O. (1955), Complex formation between montmorillonite clays and amino-acids and proteins, *Trans. Faraday Soc.*, **51,** 582–590.

Manuscript received Oct. 5, 1957

THE AMERICAN MINERALOGIST, VOL. 43, JULY-AUGUST, 1958

FACTORS EFFECTING MAXIMUM HYDROTHERMAL STABILITY IN MONTMORILLONITES

L. L. Ames* and L. B. Sand,** *Dept. of Mineralogy*
University of Utah, Salt Lake City, Utah.

Abstract

The relative importance of the factors effecting maximum thermal stability in montmorillonites in hydrothermal systems was investigated. The influencing factors considered were 1) interlayer cations, 2) composition, and 3) types of lattice substitutions.

Initial studies were concerned with the aluminum and magnesium montmorillonites because they are most commonly found in hydrothermal alteration zones associated with ore deposition.

The absence of an interlayer alkali cation (Na) causes low decomposition temperatures of about 300° C. for magnesium montmorillonites and 400° C. for aluminum montmorillonites as compared to 750° C. and 480° C., respectively, when the alkali is present. With optimum substitution, saponites have considerably higher maximum stabilities then the aluminum montmorillonites. Lattice substitutions (in all cases to give excess charge corresponding to maximum base exchange capacity) in montmorillonites effecting maximum hydrothermal stability are as follows:

A. for aluminum montmorillonites
   1. substitution of Al for Si in tetrahedral coordination

$$Al_2(Si_{3.67}{}^{Na_{.33}}Al_{.33})O_{10}(OH)_2 \xrightarrow{480^\circ\ C.} \text{paragonite, pyrophyllite, mullite}$$

   2. substitution of Mg for Al in octahedral coordination

$$(Al_{1.67}{}^{Na_{.33}}Mg_{.33})Si_4O_{10}(OH)_2 \xrightarrow{480^\circ\ C.} \text{saponite, albite, cristobalite}$$

B. for magnesium montmorillonites
   1. substitution of Al for Si in tetrahedral coordination

$$Mg_3(Si_{3.67}{}^{Na_{.33}}Al_{.33})O_{10}(OH)_2 \xrightarrow{750^\circ\ C.} \text{talc} \xrightarrow{780^\circ\ C.} \text{enstatite, quartz}$$

   2. substitution of Li for Mg in octahedral coordination

$$(Mg_{2.67}{}^{Na_{.33}}Li_{.33})Si_4O_{10}(OH)_2 \xrightarrow{750^\circ\ C.} \text{talc} \xrightarrow{780^\circ\ C.} \text{anthophyllite}$$

Equivalent stabilities within experimental error result if optimum substitution is in the octahedral or the tetrahedral layer. A marked decrease in stability results when substitution in the lattice deviates from the optimum amounts, although still retaining electrostatic balance by changing the amounts of other cations; for example, in the saponites: $Al_{.33}$ (750° C.), $Al_{.22}$ (680° C.), $Al_{.11}$ (275° C.), and $Al_{.00}$ (255° C.).

Introduction

The hydrothermal stabilities of several critical aluminum and magnesium montmorillonite compositions were determined in an attempt

* Present address: General Electric Research Laboratories, Richland, Washington.
** Present address: Tem-Pres, Inc., State College, Pennsylvania.

to establish the relationships between composition and thermal stability for this largest family of montmorillonites. Much of the stability data reported, especially on the magnesium montmorillonites, have been on compositions without the most common exchange ion, sodium. The stability data herein reported are on compositions including sodium as the exchange cation, in addition to a few compositions without sodium to demonstrate the effect on stability when exchangeable sodium is absent.

Early syntheses of montmorillonites are summarized by Ross and Hendricks (1945). These contributions were not concerned with stabilities. Aluminum montmorillonites were synthesized by Roy and Osborn (1954) who reported a maximum hydrothermal stability of 420° C. for a pure aluminum montmorillonite with H^+ as the base exchange cation. Roy and Roy (1955) synthesized magnesium-aluminum-silica montmorillonites of widely variable compositions which were stable to a maximum of 480° C. These authors considered Mg, or a hydrated complex, as the exchangeable base in the above compositions. A pure magnesium saponite was found by them to have a stability of $275 \pm 20°$ C.

Sand (1955) reported the hydrothermal decomposition temperature of hectorite as about 800° C. at 1000 atmospheres water pressure. Mumpton and Roy (1956) studied the influence of ionic substitution on the hydrothermal stabilities of montmorillonoids. Decomposition temperatures of 430° C. and 565° C. respectively were reported for hectorite and an aluminous saponite. Two areas of montmorillonoid formation were indicated. The natural dioctahedral montmorillonites were reported by them to be stable generally to about 465° C. and the trioctahedral saponites to about 550° C. at 20,000 psi water vapor pressure.

Recent work on the hydrothermal stability of synthetic and natural hectorite by Sand and Ames (1957) has indicated that trioctahedral hectorite is stable to 750° C. at 1000 atmospheres.

Methods of Investigation

Hydrothermal equipment used was essentially of the kind described by Roy, Roy, and Osborn (1950). "Test tube" type reactor vessels were employed in conjunction with a water pressure system with a limit of 2000 atmospheres.

Synthetic mixtures of calcined silicic acid and nitrates, oxides plus a sodium salt, and calcined nitrates plus ethyl orthosilicate were used as starting materials. These mixtures were contained in gold envelopes.

X-ray diffraction and infrared absorption techniques were employed for identification of the resulting phases. All samples were either vapor

or "wet" solvated with ethylene glycol to identify the montmorillonites by the characteristic 17 Å basal spacing, using the technique of Brunton (1955).

Results

Approximately 150 stability and synthesis runs were made on the compositions shown in Table 1.

Table 1. Critical Runs

Composition	T	P(atm.)	Time	Phases
Trioctahedral Montmorillonites				
Tetrahedral substitution				
$Na_{.33}Mg_{3.00}Si_{4.00}$	230	1000	5 days	mont.
$Na_{.33}Mg_{3.00}Si_{4.00}$	260	1000	5 days	talc
$Na_{.33}Mg_{3.00}(Al_{.11}Si_{3.89})$	260	1000	2 days	mont.
$Na_{.33}Mg_{3.00}(Al_{.11}Si_{3.89})$	285	1000	3 days	talc and mont.
$Na_{.33}Mg_{3.00}(Al_{.16}Si_{3.84})$	540	1000	3 days	mont.
$Na_{.33}Mg_{3.00}(Al_{.16}Si_{3.84})$	560	1000	3 days	talc and mont.
$Na_{.33}Mg_{3.00}(Al_{.22}Si_{3.78})$	665	1000	3 days	mont.
$Na_{.33}Mg_{3.00}(Al_{.22}Si_{3.78})$	690	1000	3 days	talc and mont.
$Na_{.33}Mg_{3.00}(Al_{.33}Si_{3.67})$	740	1000	2 days	mont.
$Na_{.33}Mg_{3.00}(Al_{.33}Si_{3.67})$	780	1000	2 days	talc and enstatite
Octahedral substitution				
$Na_{.33}(Mg_{2.67}Li_{.33})Si_{4.00}$	450	1000	3 days	mont. (>mica spacing on drying)
$Na_{.33}(Mg_{2.67}Li_{.33})Si_{4.00}$	740	1000	1 day	mont. (talc spacing on drying)
$Na_{.33}(Mg_{2.67}Li_{.33})Si_{4.00}$	750	1000	5 days	mont. and talc
$Na_{.33}(Mg_{2.67}Li_{.33})Si_{4.00}$	760	1000	8 days	talc
$Na_{.33}(Mg_{2.67}Li_{.33})Si_{4.00}$	780	1000	5 days	talc and anthoph.
$Na_{.33}(Mg_{2.67}Li_{.33})Si_{4.00}$	800	1000	7 days	anthoph.
Nat. hectorite	425	1000	7 days	mont. (>mica spacing on drying)
Nat. hectorite	560	1000	8 days	mont. (talc spacing on drying)
Nat. hectorite	750	1000	5 days	mont. and talc
Nat. hectorite	765	1000	4 days	talc
Nat. hectorite	820	1000	8 days	anthoph.
Both octahedral and tetrahedral substitution				
Nat. saponite (Milford, Utah)	530	1000	2 days	mont.
$(Ca/2)_{.21}(Mg_{2.85}Al_{.04})$ $(Al_{.30}Si_{3.70})$	550	1000	2 days	talc

Table 1. (continued)

Composition	T	P(atm.)	Time	Phases
$Na_{.33}(Mg_{2.83}Li_{.17})(Al_{.16}Li_{3.84})$	740	1000	5 days	mont.
$Na_{.33}(Mg_{2.83}Li_{.17})(Al_{.16}Li_{3.84})$	760	1000	5 days	talc and anthoph.
		No alkali exchangeable ion		
$Mg_{3.00}(Al_{.16}Si_{3.84})$	300	1000	7 days	mont.
$Mg_{3.00}(Al_{.16}Si_{3.84})$	325	1000	7 days	talc
$(Mg_{2.67}Li_{.33})Si_{4.00}$	250	1000	3 days	mont.
$(Mg_{2.67}Li_{.33})Si_{4.00}$	300	1000	3 days	talc
		Dioctahedral Montmorillonites		
		Tetrahedral substitution		
$Na_{.33}(Al_2(Al_{.33}Si_{3.67})$	470	1000	5 days	mont.
$Na_{.33}Al_2(Al_{.33}Si_{3.67})$	490	1000	5 days	paragonite+pyrophyllite+mullite
		Octahedral substitution		
$Na_{.33}(Al_{1.67}Mg_{.33})Si_{4.00}$	470	1000	5 days	mont.
$Na_{.23}(Al_{1.67}Mg_{.33})Si_{4.00}$	490	1000	5 days	ab+saponite+cristobalite

Table 1 gives the critical runs and resulting decomposition temperatures, within $\pm 10°$ C., and products.

Table 2 is a summary of the maximum hydrothermal stabilities of the various compositions.

Table 3 lists the relative intensities and "*d*" spacings for the synthetic saponite, $Na_{.33}Mg_{3.00}(Al_{.33}Si_{3.67})O_{10}(OH)_2$, dried at 110° C. and also vapor solvated with ethylene glycol. Note the second order basal spacing on the dried sample.

Discussion

The assumption is made here that the ions actually went into the structural positions indicated in these montmorillonite compositions given in Table 1. Runs made on compositions that gave defects or "holes" in the structure, or when sodium was omitted as a base exchange ion (leaving H^+), yielded montmorillonites of much lower maximum stability. As the cation exchange capacity cannot be explained reasonably unless the ions in the resulting montmorillonites are in the structural positions indicated, and the high hydrothermal stabilities resulted when the compositions had optimum substitution for maximum base exchange capacity, this assumption is believed to be valid.

There appears to be little or no overlapping of the trioctahedral and dioctahedral montmorillonite fields except at low temperatures. These low temperature hybrids usually form defect structures that are less

TABLE 2. A SUMMARY OF STABILITY DATA FOR THE VARIOUS MAGNESIUM MONTMORILLONITE COMPOSITIONS AT 1000 ATMOSPHERES OF WATER PRESSURE

Starting Composition	Maximum Stability
Tetrahedral substitutions	
$Na_{.33}Mg_{3.00}Si_{4.00}$	255° C.
$Na_{.33}Mg_{3.00}(Al_{.11}Si_{3.89})$	275° C.
$Na_{.33}Mg_{3.00}(Al_{.16}Si_{3.84})$	550° C.
$Na_{.33}Mg_{3.00}(Al_{.22}Si_{3.78})$	680° C.
$Na_{.33}Mg_{3.00}(Al_{.33}Si_{3.67})$	750° C.
Octahedral substitutions	
$Na_{.33}Mg_{2.00}Si_{4.00}$	255° C.
$Na_{.33}(Mg_{2.67}Li_{.33})Si_{4.00}$	750° C.
$Na_{.33}(Mg_{2.67}Li_{.33})Si_{4.00}$ [natural hectorite]	750° C.
Na vs. H as base exchange cation	
$Na_{.33}Mg_{3.00}(Al_{.16}Si_{3.84})$	550° C.
$Mg_{3.00}(Al_{.16}Si_{3.84})$	310° C.
$Na_{.33}(Mg_{2.67}Li_{.33})Si_{4.00}$	750° C.
$(Mg_{2.67}Li_{.33})Si_{4.00}$	275° C.
Both octahedral and tetrahedral substitution	
$Ca/2_{.21}(Mg_{2.85}Al_{.04})(Al_{.30}Si_{3.70})$ natural saponite	540° C.
$Na_{.33}(Mg_{2.83}Li_{.17})(Al_{.16}Si_{3.84})$	750° C.

stable than the 480° C. maximum of the dioctahedral montmorillonite of optimum composition.

Sand, Roy, and Osborn (1957) reported the maximum stability of dioctahedral montmorillonites in the system $Na_2O \cdot Al_2O_3 \cdot SiO_2 \cdot H_2O$ to be 480° C. at 1000 atmospheres of water vapor pressure. The maximum hydrothermal stability occurs on the composition $Na_{.33}Al_{2.00}(Al_{.33}Si_{3.67})$ according to Sand and Crowley (1956). An equivalent stability within experimental error results when optimum substitution is in the octahedral layer: $Na_{.33}(Mg_{.33}Al_{1.67})Si_{4.00}$. These compositions represent optimum substitutions for maximum base exchange capacity in dioctahedral montmorillonites. As the composition of the starting material deviates from this composition, the hydrothermal stability becomes lower than 480° C. The dioctahedral (aluminum) montmorillonites are, in effect, defect structures with two-thirds of their octahedral positions filled. This condition weakens the structure so that a maximum hydrothermal stability of 480° C. is reached with optimum substitution of aluminum for silicon in the tetrahedral position or magnesium for aluminum in the octahedral layer.

With the same optimum substitutions in the trioctahedral (magne-

TABLE 3. X-RAY DIFFRACTION POWDER DATA FOR THE SYNTHETIC SAPONITE $Na_{.33}Mg_{3.00}(Al_{.33}Si_{3.67})O_{10}(OH)_2$. INTENSITIES WERE VISUALLY ESTIMATED

Dried at 110° C.		Vapor solvated with ethylene glycol	
I/I_0	d, Å	I/I_0	d, Å
10	12.3	10	17.0
2	6.15	5	8.5
4	4.58	4	5.69
5	3.10	5	4.58
4	2.63	8	3.37
3	2.53	3	2.81
1	2.34	4	2.58
1	2.295	1	2.36
1	2.067	1	2.30
2	1.734	1	2.106
7	1.529	1	2.085
3	1.323	1	1.868
1	1.274	3	1.738
1	1.054	7	1.535
1	.999	3	1.326
2	.886	1	1.277
		1	1.233
		1	1.055
		2	1.002
		3	.887

sium) montmorillonites, a maximum hydrothermal stability of 750° C. is attained. The magnesium trioctahedral montmorillonites, with optimum substitution, exceed the hydrothermal stability of aluminum dioctahedral montmorillonites by 270° C. The optimum exchange capacity of the trioctahedral montmorillonites also can be achieved in three ways: 1) by substitution of lithium in the octahedral position for magnesium, 2) substitution of aluminum in the tetrahedral position for silicon or 3) a combination of octahedral and tetrahedral substitution. (Ross and Hendricks, 1945). Either manner of attaining maximum cation exchange capacity results in a maximum hydrothermal stability of 750° C. at 1000 atmospheres pressure. These montmorillonites cannot have identical decomposition temperatures, but appear equivalent within the experimental error of $\pm 10°$ C.

The results also clearly indicate that magnesium, acting as the base exchange cation with or without H^+, forms either a hydrogen-based montmorillonite or a defect structure. Either of the above conditions results in a much lower hydrothermal stability than if the proper amount of base exchange cation is added to the starting composition. The low hydrothermal stabilities reported by Roy and Roy (1955) for montmoril-

lonites synthesized in the system magnesia-alumina-silica-water were due to either the formation of defect structures or H^+ based montmorillonites. The maximum stability of 430° C. for natural hectorite reported by Mumpton and Roy (1956) might have been due to misidentification of the "talc" decomposition phase (Sand and Ames, 1957).

These results emphasize the existence of the two distinct structural series, the dioctahedral (aluminum) montmorillonite and the trioctahedral (magnesium) montmorillonites, with some overlapping of these two series at lower temperatures by formation of defect structures. These latter montmorillonites have lower hydrothermal stabilities than the optimum compositions and separate into the di- and trioctohedral montmorillonite at higher temperatures before the dioctahedral montmorillonite decomposes, with the trioctahedral montmorillonite persisting to higher temperatures. This was demonstrated on an aluminum montmorillonite containing some magnesium from Hector, California (Sand and Ames, 1957) and on a defect saponite from an occurrence near Milford, Utah. Determination of the stabilities of these defect montmorillonites formed by hydrothermal alteration can fix the upper temperature limit of the altering solutions.

Summary and Conclusions

The controlling factors which result in a montmorillonite composition having the highest hydrothermal stability are as follows:

1. All possible cation positions in the lattice occupied; e.g., a trioctahedral montmorillonite such as hectorite.
2. Optimum substitution in either tetrahedral or octahedral coordination to provide excess negative charge for maximum base-exchange capacity.
3. The presence of exchangeable ions, other than H^+, to satisfy the interlayer charge.

All three conditions must obtain; when they do, a maximum hydrothermal stability of 750° C. results for saponite as compared to 480° C. for aluminum montmorillonite. Deviations from these optimum conditions have a more pronounced affect on the stability of the saponites than on the aluminum montmorillonites.

As the montmorillonite lattice can accommodate many variations in both kinds and amounts of ion substitution, including in a negative sense the defect structures, as well as variations in layer stacking, hydrothermal treatment effects a reorganization of some of the montmorillonites into a montmorillonite composition of higher stability plus other decomposition products such as mica and a silica polymorph. Even in hectorite, which satisfies all three conditions for high hydrothermal

stability but which was formed in a hot spring environment, a structural change is caused by the high P-T treatment. Although still remaining an expanding montmorillonite, it approaches talc closely in structure when dried. Electron micrographs of the hydrothermally treated hectorite show it to be recrystallized into thicker stacks of very well defined pseudo-hexagonal crystals as compared to the very thin laths of the as-formed hectorite.

Studies of this type on a wide range of compositions of natural montmorillonites, formed in a variety of environmental conditions, would be informative, as most of these are formed during the operation of kinetic processes which cannot be duplicated in the laboratory under the equilibrium conditions currently employed and necessitated by present equipment limitations.

Acknowledgments

The authors wish to acknowledge the financial assistance of National Science Foundation Project G-2934, and the University of Utah Research Fund. Prof. J. J. Comer, The Pennsylvania State University, kindly provided us with electron micrographs.

References

Ames, L. L., Sand, L. B., and Goldich, S. S., A contribution on the Hector, California bentonite deposit: *Econ. Geol.* (in press).

Brunton, G. (1955) Vapor pressure glycolation of oriented clay minerals: *Am. Mineral.*, **40,** 124–126.

Cahoon, H. P. (1954) Saponite near Milford, Utah: *Am. Mineral.*, **37,** 222–230.

Mumpton, F. A., and Roy, R. (1956) The influence of ionic substitution on the hydrothermal stability of montmorillonoids: *Nat. Research Council Publication* **456,** 337–339.

Ross, C. S., and Hendricks, S. B. (1945) Minerals of the montmorillonite group: *U. S. Geol. Survey Prof. Paper* **205-B.**

Roy, D. M., and Roy, R. (1955) Synthesis and stability of minerals in the system MgO-Al_2O_3-SiO_2-H_2O: *Am. Mineral.*, **40,** 147–178.

Roy, R., and Osborn, E. F. (1954), The system Al_2O_3-SiO_2-H_2O: *Am. Mineral.*, **39,** 853–885.

Roy, R., Roy, D. M., and Osborn, E. F. (1950) Compositional and stability relationships among the lithium alumino-silicates; eucryptite, spodumene and petalite: *Jour. Am. Ceram. Soc.*, **33,** 152–159.

Roy, R., and Sand, L. B. (1956) A note on some properties of synthetic montmorillonites: *Am. Mineral.*, **41,** 505–509.

Sand, L. B. (1955) Montmorillonites stable at high temperatures: *Geol. Soc. Am. Bull.*, **66,** Part II, 1610–1611 (abstract).

Sand, L. B., and Ames, L. L. (1957) Stability and decomposition products of hectorite: Proc. of Sixth National Clay Conference (in press).

Sand, L. B., and Crowley, M. S. (1956), Comparison of a natural bentonite with its synthetic analogue: *Nat. Research Council Publication* **456,** 96–100.

Sand, L. B., Roy, R., and Osborn, E. F. (1957) Stability relations of some minerals in the Na_2O-Al_2O_3-SiO_2-H_2O system: *Econ. Geol.*, **52,** 169–179.

Manuscript received October 12, 1957.

THE AMERICAN MINERALOGIST, VOL. 43, JULY-AUGUST, 1958

CLAY-CARBONATE-SOLUBLE SALT INTERACTION DURING DIFFERENTIAL THERMAL ANALYSIS

R. Torrence Martin

Massachusetts Institute of Technology, Cambridge, Massachusetts.

Abstract

In the majority of fine grained soils the qualitative and even quantitative determination of carbonate minerals, calcite and dolomite, by DTA, is a relatively simple matter. However, in some soils it has been found that as much as 40 per cent carbonate may completely escape detection by DTA. Thermograms are presented to show that this anomalous behavior arises from a combination of factors. The data reveal that in the most severe cases soluble salts react with some of the more active silicate from the clay; then the product of this reaction reacts with the carbonate mineral to produce the observed anomalous thermal effects. The thermograms indicate that the anomalous behavior is as pronounced for calcite as for dolomite. Even in the absence of soluble salts, some hydrous micas seriously distort the characteristic calcite thermogram.

Introduction

Differential thermal analysis (DTA) is a very common method of determining the kind and amount of carbonate minerals present in fine grained soils. The most common carbonate minerals, calcite and dolomite, have thermal reactions at somewhat higher temperatures than the most important clay reactions. Because of the large amount of heat adsorbed in the carbonate thermal reaction, detection of a few per cent carbonate mineral is expected by differential thermal analysis. In the majority of soils, clay and carbonate thermal reactions occur independently; therefore, detection of a few per cent of carbonate by DTA is realized. Unfortunately, DTA records only the net heat effect which may result in seriously distorted thermograms when several reactions proceed simultaneously. In fact, as much as 40 per cent calcite and/or dolomite may go undetected by DTA because of the complex reactions occurring between clay, soluble salts and the carbonates.

Berg (1943) and Graf (1952) observed that readily soluble salts have a pronounced influence upon the first endotherm of dolomite. Berg (1943) remarked that the salt had no effect upon the dissociation of calcite; therefore, the effects reported here are different from any previously reported anomalies because the soluble salt appears to have a strong influence upon the calcite decomposition.

Natural Soils

The types of anomalous differential thermal behavior encountered in natural soils are shown by illustrative examples in Fig. 1. Other perti-

nent data for these soils are given in Table 1. Prior to DTA[1] the samples were treated as follows:

a. Natural soil—the minus 74 micron fraction, air dried and crushed.
b. Water washed—a 10 gram subsample from "*a*," extracted five times with 200 ml. portions of water, air dried and crushed.
c. Water washed plus NaCl—NaCl added to a suspension of a subsample from "*b*" to bring the conductivity of the suspension to that of the natural soil, air dried and crushed.
d. Minus carbonates—natural soil digested with 2N acetic acid to completely destroy all carbonate minerals, washed free of salts, air dried and crushed.

Table 1. Salt Content, Carbonate Mineral, and Phyllosilicate Clay for Typical Soils with Anomalous Thermograms

Soil Number	Soluble Salts (g. NaCl/100 g. Soil)*	Carbonate Mineral		Phyllosilicate† Clay
		Species	g./100 g. Soil	
633	1.16	Dolomite	25	K, I, M
366	0.48	Calcite	40	I, M

* Computed from conductivity of a 2:1 water clay suspension assuming all soluble salts are NaCl.

† K = kaolinite, I = illite, M = montmorillonoid.

From the thermograms on the natural soils Curves A and E, Fig. 1, the presence of carbonate minerals to the extent of 25 to 40 per cent would hardly be anticipated. Thermograms obtained after the samples were water washed, treatment *b*, clearly show carbonate mineral thermal reactions, Curves C and G, Fig. 1. Treatment *c*, where NaCl was added to the soil that had been washed free of salt, restored the thermogram to nearly that of the natural soil, Curves B and F, Fig. 1.

[1] DTA Experimental Conditions:

Heating rate:	12.5° C./min with maximum variation of less than 1° C./min.
Thermocouples:	Pt-Pt (10% Rh)
Temperature Couple:	In Ni steel block, peak temperature uncorrrected
Sample Pre-treatments:	As indicated; no relative humidity control so the thermogram below 400° C. is not reproduced in the figure. Approximately 1 gram samples.
Calibration:	50% quartz and 50% $BaCO_3$ Quartz $\alpha \rightleftharpoons \beta$ at 573 ± 3° C. $BaCO_3$ to α at 819 ± 3° C. $BaCO_3$ to β at 988 ± 3° C.

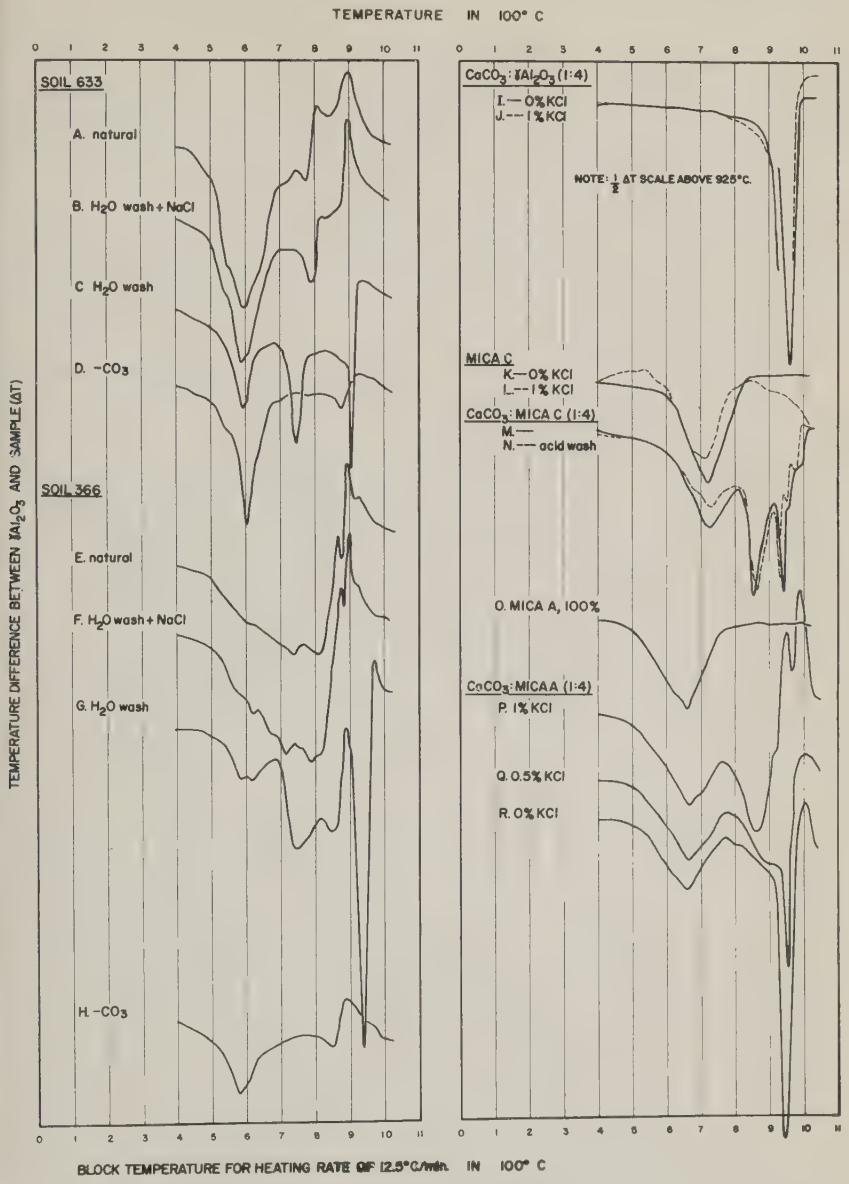

FIG. 1. Thermograms on natural soils and prepared mixtures showing anomalous carbonate peaks.

These results demonstrate that even a trace amount of NaCl (<1 per cent) may be sufficient to mask completely normal carbonate mineral thermal reactions even when the carbonate mineral is calcite. Graf (1952)

found that chloride salts of the alkali and alkaline earth elements were about equally effective in changing the low temperature endotherm of dolomite. That the same group of salts are responsible for the thermal effects observed here is indicated by the fact that LiCl, which has a much lower melting point than NaCl, produced the same thermal effect as NaCl.

The shape of the anomalous thermogram bears no relation to the kind of carbonate mineral nor to the particle size of the carbonate so long as the particles are less than 74 microns. Where the natural soil displays an anomalous thermal reaction, the removal of soluble salt yields a repressed thermal peak for both calcite and dolomite.

The dolomite thermal peaks for soil No. 633 (Curve C, Fig. 1) are both about 1/3 as large as they should be for the 25 per cent dolomite present in this soil. The thermogram for soil No. 366 (Curve G, Fig. 1) after removal of soluble salt shows a typical calcite reaction of approximately 1/2 the amplitude expected from the calcite percentage present. There is, in addition to the calcite peak, an anomalous endothermic reaction between 700 and 900° C. The endotherm between 700 and 900° C. is truly anomalous because careful *x*-ray examination of the sample showed clay minerals and calcite as the only components that could contribute to the thermal curve. Further, after complete removal of carbonates from soil No. 366, the addition of 40 per cent c.p. $CaCO_3$ gave a thermogram very similar in both shape and size to that obtained for the natural soil washed free of soluble salts.

Additional evidence as to the influence of soluble salt on the carbonate mineral decomposition was obtained from samples heated in the differential thermal analyzer to various temperatures, air quenched, and the products examined by *x*-ray diffraction. The soil used, No. 634, gave an anomalous thermogram similar to soil No. 633; however, the *x*-ray patterns showed that the soil No. 634 contained calcite and dolomite. Nevertheless, the changes in the *x*-ray patterns enumerated in Table 2 verify, qualitatively, that soluble salts lower the carbonate decomposition temperature.

Artificial Mixtures

In an attempt to evaluate the effect of soluble salt and clay on the decomposition of carbonate minerals, a few exploratory DTA investigations have been made: (*a*) calcite plus soluble salt, (*b*) mica plus soluble salt, (*c*) mica plus calcite, and (*d*) mica plus calcite plus soluble salt. Ground mica was chosen as the clay because by varying the method of preparation, differences in availability of the various clay constituents should be obtained. Total potash content of mica prepared by different methods is given in Table 3.

TABLE 2. EFFECT OF A SOLUBLE SALT ON THE DECOMPOSITION TEMPERATURE OF CARBONATE MINERAL IN A NATURAL SOIL

	Relative Intensity of *X*-ray Reflections after Heating to Temperature Indicated					
	Soil No. 634—Natural			Soil No. 634—Water Washed		
Temperature °C / *d* value	25	700	800	700	800	900
3.03 Å (Calcite Reflection)	10	10	—	10	10	—
2.88 Å (Dolomite Reflection)	10	—	—	10	—	—

During DTA the alkali metal ions of hydrous micas may be released. If the clay structure permits rapid release of alkali ions, these ions may interact with the carbonate minerals in a manner similar to alkali ions obtained from soluble salt. Generally, this release of alkali ions is inadequate to affect the carbonate thermal reactions. Graf (1953) found no effect on the thermograms of dolomite from the addition of illite.

As evidenced by the similarity of Curves I, and J, Fig. 1, addition of 1 per cent KCl to a mixture of 25 per cent $CaCO_3$ and 75 per cent γ-Al_2O_3 had no significant effect upon the calcite decomposition, confirming

TABLE 3. PREPARATION METHOD AND TOTAL POTASH CONTENT FOR MICA*

Sample	Preparation	Total Potash Content (%)
A	Mica batch No. 1 ground wet in a muller grinder. Sieved wet to minus 74 microns	7.8
B	Mica batch No. 2 prepared same as Sample A. Fine size fraction.	8.15
C	Mica batch No. 2; prepared same as Sample A; intermediate size fraction	8.75
D	Sample C(5g) extracted 6 times with 200 ml portions of 6N HCl; washed free of chlorides	8.70
E	Mica batch No. 2; ground dry in mechanical mortar and pestle; sieved wet to minus 74 microns	6.40

* Muscovite mica, batch No. 1 and No. 2 gave identical *x*-ray diffraction patterns.

Berg's observation that soluble salts have no direct effect upon the calcite decomposition. Therefore, soluble salts must act through the clay to produce the observed anomalous calcite thermogram. Evidence that soluble salt acts first on the clay is shown by the effect of 1 per cent KCl on ground mica, compare Curves K and L, Fig. 1.

In the absence of soluble salt, clay-carbonate interactions may be quite marked as indicated by natural soils, Curves C and G, Fig. 1, and representative thermograms for mica mixed with 25 per cent $CaCO_3$, Curves M, N, and R, Fig. 1. Although all of the thermograms for ground mica and $CaCO_3$ are not shown, in every instance there was a reaction between the mica and calcite. When mica rather than alundum was used to dilute the calcite, the carbonate reaction was either greatly reduced or occurred as a double endothermic peak. Since mica Sample C showed the greatest interaction between mica and calcite, a subsample of mica C was extracted with strong acid (Sample D), in the hope that all readily extractable potassium ions would be removed and thereby alter the thermal effects. The acid extraction changed neither the thermal effects, compare Curves M and N, Fig. 1, nor the potash content. Mica Sample E which gave an endothermic reaction 130° C. lower than did mica C and which had 24 per cent less K_2O than did mica C, showed anomalous calcite decomposition identical to that revealed by mica C plus calcite. Acid extraction of mica E, as with mica C, changed neither the thermal effects nor the total potash content.

From these few experiments it would appear that some component other than alkali ions is a major cause for the anomalous thermal behavior of calcite mixed with mica clay. The 850° C. endothermic peak on Curves M and N in Fig. 1 must arise from interaction between mica and calcite since this peak is not present in the thermogram for either component. A possible reaction could be silicate from the mica and Ca ions from the calcite combining to form a calcium silicate. To check this hypothesis, a thermogram was obtained on a mixture containing 25 per cent Na silicate, 25 per cent $CaCO_3$ and 50 per cent Al_2O_3. The resultant thermogram gave endothermic peaks at 840 and 960° C. that were just slightly larger than the 860 and 930° C. peaks on Curve M in Fig. 1. A thermogram on Na silicate diluted with Al_2O_3 gave no thermal reaction above 400° C. Therefore, anomalous thermal behavior of calcite and clay mica has been traced to a reaction between the silicate and calcium. The reason that many soils containing calcite reveal no anomalous thermal behavior is probably due to differences in the reactivity of the silicate in the temperature range 800 to 950° C.

The addition of KCl to a mica-carbonate mixture produces thermal effects similar to those observed for natural soils containing carbonates and

soluble salts (see Curves P, Q, and R, Fig. 1) and these thermal effects are much more pronounced than those observed for mica-carbonate mixtures in the absence of KCl. These data confirm the hypothesis that the soluble salts act on the clay and then some product of this first reaction tion produces the anomalous carbonate decomposition.

Conclusions

It is concluded from this investigation that as much as 40 per cent carbonate mineral may escape detection by DTA. The cause of this anomalous thermal behavior is demonstrated to result from the interaction of hydrous mica clay and soluble salts with the carbonate minerals. Hydrous mica clay has a direct influence on the calcite decomposition because hydrous mica can distort the calcite thermal reaction. Soluble salts have an indirect influence on the carbonate decomposition because while trace quantities of soluble salt in addition to certain hydrous micas completely obscure the calcite decomposition, soluble salts have no effect on the calcite thermal peak in the absence of the hydrous mica.

References

Berg, L. G., 1943, Influence of Salt Admixtures upon Dissociation of Dolomite. *C. R. Acad. Sci., U.R.S.S.*, **38,** 24–27.

Graf, D. L., 1952, Variation in Differential Thermal Curves of Dolomite, *Am. Mineral.*, **37,** 1–27.

Manuscript received September 27, 1957

THE AMERICAN MINERALOGIST, VOL. 43, JULY–AUGUST, 1958

BISMUTOFERRITE, CHAPMANITE, AND "HYPOCHLORITE"*

CHARLES MILTON, JOSEPH M. AXELROD, AND BLANCHE INGRAM,
U. S. Geological Survey, Washington 25, D. C.

ABSTRACT

Bismutoferrite, $Bi(OH)Fe_2(SiO_4)_2$ or $Bi_2O_3 \cdot 2Fe_2O_3 \cdot 4SiO_2 \cdot H_2O$ in substantial agreement with Frenzel's (1871) $Bi_2Fe_4Si_4O_{17}$, occurring as a yellow powder associated with bismuth ores at Schneeberg, Saxony, and nearby localities, gives a unique x-ray diffraction pattern and consistent chemical analyses. It is therefore to be considered a valid mineral species. The term "hypochlorite" has been used for a green mixture of bismutoferrite with quartz and chalcedony. The original analysis in 1832 was of such material; the first analysis of reasonably pure bismutoferrite was by Frenzel in 1871. A substance also termed "hypochlorite" was found at Bräunsdorf, Saxony, but it contains antimony instead of bismuth. Recognition of the composite character of "hypochlorite" and uncertainty as to whether it contained bismuth or antimony or both, with failure to accept Frenzel's work as valid, have until now left the status of bismutoferrite and "hypochlorite" dubious. Data presented here establish chapmanite (Walker, 1924) as the antimony analogue of bismutoferrite. Recognition of the proper valence states of antimony and iron (both three) in chapmanite leads to a correct interpretation of the formula from the original analysis. Bismutoferrite and chapmanite therefore form a homologous and presumably isostructural group of two valid species; the name "hypochlorite," which has been used to designate a characteristic mixture of either of these minerals dispersed in quartz or chalcedony, may well be discarded.

HISTORICAL

"Hypochlorite" was the name given by Schüler (1832) to a highly siliceous bismuth-bearing yellow-green material from Schneeberg, Saxony. Dana (1870) summarized the original account as follows: "minute crystalline, also earthy: H=6, G-2.9-3.04. Color green, streak light green, brittle, fracture even to flat conchoidal," and he cites an analysis (Table 3, A). Schüler is quoted by Frenzel (1871) as saying that "hypochlorite" occurs rarely; associated with quartz, chalcedony, bismuth, cobaltite, and arsenopyrite in veins in shale at Schneeberg; with quartz, bismuth, galena, and silver ores in mica schist at Johanngeorgenstadt; and with quartz and pyrite in mica schist at Bräunsdorf near Freiberg.

Frenzel states that Schüler's analysis was forthwith considered to be of a mixture, the question being raised by the editor of the journal that published Schüler's paper; and this view was concurred in by Dana (1868), Breithaupt (1871), and H. Fischer (1870), who pronounced it to be microscopically a mixture of three substances, namely, quartz, an opaque green substance as the most abundant constituent, and radial

* Publication authorized by the Director, U. S. Geological Survey.

spheroidal aggregates of brown needles. (The "opaque green substance" presumably was the "hypochlorite" proper, and the brown needles possibly goethite.)

A few years after Schüler's report on (bismuth) "hypochlorite," a paper by Kersten (1844) appeared, giving an analysis of the "hypochlorite" from Bräunsdorf ("Neu Hoffnung Gottes") in which he found antimony, but no bismuth. This apparent conflict with the earlier work may well have contributed to the misgivings which became associated with these substances.

In 1871, Frenzel carefully reviewed the status of "hypochlorite" and proposed the name bismutoferrite for what he considered a valid species (correctly, in our opinion); and he clarified the ambiguous relationships of "hypochlorite" and "antimony-hypochlorite." He suggested the existence of an antimony compound "isomorphous" with bismutoferrite. The following year, in 1872, Frenzel further discussed "hypochlorite," in particular the early work of Kersten on the Bräunsdorf antimony-"hypochlorite." He cites Kersten's analysis (Table 5, H) and notes its essential agreement with his own (Table 5, I, J, K). Concerning bismutoferrite, he says that beyond doubt it must be considered as a valid mineral species. He refers again to his observations (1871) that the bismutoferrite which he analyzed (Table 3, D) contained crystals too small for precise observations, but which were apparently monoclinic.

We may observe here that our own work, almost a century later and with modern tools available, fully confirms that of Frenzel, and we agree that bismutoferrite is entitled to species rank and that the antimony-"hypochlorite" is indeed the antimony analogue of bismutoferrite dispersed in quartz or chalcedony. Further, as will be shown, the substantially pure antimony compound has been known since 1924 as chapmanite (Walker, 1924) from Ontario. Antimony-"hypochlorite" has also been found in Alaska by W. T. Schaller, U. S. Geological Survey (personal communication). Chapmanite with quartz (antimony-"hypochlorite") also occurs with sulfide ore from Velardeña, Durango, Mexico.

Nevertheless, Frenzel's contemporaries and successors were not convinced of the validity of his work, and bismutoferrite and "hypochlorite" have been consigned to the limbo of discredited species or mixtures. Thus Dana (1892) refers to Schüler's "hypochlorite" as "beyond doubt a mixture," and to Frenzel's bismutoferrite as a "supposed bismuth iron silicate." Doelter (1917) notes that bismutoferrite is a mixture, like "hypochlorite." Ramdohr (1936) lists bismutoferrite as an obsolete term for a mixture of bismuth and iron minerals, and "hypochlorite" similarly. Hey (1950) refers to "hypochlorite" as "very doubtful; probably a mixture," and lists bismutoferrite in small type, that is, not of species rank.

In 1924, Walker described an "olive-green" powdery mineral from South Lorraine, Ontario, whose composition was given as $5FeO \cdot Sb_2O_5 \cdot 5SiO_2 \cdot 2H_2O$ and which he named chapmanite. Except for ferrous instead of ferric iron and other minor variations, this formula is not greatly different from that of bismutoferrite, $2Fe_2O_3 \cdot Bi_2O_3 \cdot 4SiO_2 \cdot H_2O$. From the extremely close similarity of the x-ray diffraction patterns (Table 6), the calculations of average index of refraction by Gladstone and Dale's law as given below, and critical review of the original Walker-Todd analysis of chapmanite, it will be shown that bismutoferrite is homologous (isostructural?) with chapmanite. Although chapmanite has been accepted as a recognized species, its relationships have not been known, nor has it been reported until now from any locality except the original Ontario source. Walker's formula, as will be shown, is erroneous, and because of this the relationship between bismutoferrite and chapmanite has gone unrecognized.

Material Studied and Acknowledgments

At the suggestion of Clifford Frondel, of Harvard University, we have restudied all available material labeled bismutoferrite, chapmanite, and "hypochlorite," (as well as stibiaferrite,[1] (Goldsmith, 1873) and jujuyite,[2] (Ahlfeld, 1948) both of which have been found to be unrelated to this present study). To him and to George Switzer, of the United States National Museum, and Brian Mason, of the American Museum of Natural History, New York City, all of whom supplied the specimens studied, we express thanks. Michael J. Milton studied the specimens by the x-ray fluorescence method (Adler and Axelrod, 1956) in the U. S. Geological Survey. Robert G. Coleman and Alfred H. Truesdell, also of the Geological Survey helped greatly in the purification of the analyzed sample of bismutoferrite, in particular by removal of microscopic particles of sulfides through the use of the Mayeda flotation cell (Kerr, 1950).

The 30 specimens labeled "hypochlorite" or bismutoferrite from the three Museum collections that were examined fall into four groups, as follows:

Group I contains more or less pure bismutoferrite, all from Saxony.
Group II contains bismutoferrite dispersed in quartz or chalcedony, that is, "bismuth hypochlorite"—all from Saxony.
Group III contains chapmanite dispersed in quartz or chalcedony:

[1] Stibiaferrite has been studied by Vitaliano and Mason (1952) and found to consist of wulfenite, bindheimite, and jarosite in quartz.

[2] Jujuyite also studied by Brian Mason (personal communication 1957) is tripuhyite and quartz.

that is, antimony "hypochlorite" –all from Saxony except one from Mexico and one from Hungary.

Group IV is a miscellaneous lot of mislabeled specimens mostly nontronite, only one of which is reported as from Saxony.

Others specimens from the National Museum labeled chapmanite included three more or less pure chapmanites from Ontario; and one from Alaska, termed "hydrous ferrous antimonate" (W. T. Schaller) which has been identified as essentially antimony "hypochlorite" or chapmanite dispersed in silica. Two others labeled chapmanite from Ontario from the American Museum of Natural History collections are also chapmanite from the type Ontario locality.

Group I. *Bismutoferrite*

Table 1 lists specimens identified as bismutoferrite. All of these are either soft, bright yellow and powdery, or hard and green; all tested (by *x*-ray fluorescence) are essentially compounds of bismuth and iron (and silica, not detectable by the *x*-ray spectrographic methods used), and have at most traces of antimony; eight are from Schneeberg, and one from Ullersreuth; none is from Bräunsdorf. A consistent *x*-ray diffraction pattern (Table 6) was obtained from the six of these so examined. Chemical analysis (Table 3, C) gave a reasonable formula, $Bi(OH)Fe_2(SiO_4)_2$, in striking agreement with the older analyses (Table 3, D and E) on which Frenzel based the species bismutoferrite.

Group II. *Bismuth-"hypochlorite" (Quartz and bismutoferrite)*

In Table 1, Bismutoferrite, it will be noted that Harvard 47001 is represented by three *x*-ray diffraction patterns, two of "hard green" material, one of "soft yellow," the former identified as quartz and more or less bismutoferrite. By *x*-ray fluorescence all three spindles show major bismuth and iron, and no antimony. In this specimen both types of material are present in sharply defined areas. Material of the same nature, but more easily recognized as essentially drusy quartz, is present in the five specimens listed in Table 2.

Chemical analyses substantiating the *x*-ray fluorescence are given in Table 3: Schüler's original analysis of "hypochlorite" (A and B) and Frenzel's (F).

Group III. *Antimony-"hypochlorite" (Quartz and chapmanite)*

So far, all the substances described have been bismuth minerals, essentially pure or admixed, with no antimony. We now come to a group of eight specimens listed in Table 4, Group III, very much alike, all char-

TABLE 1. GROUP I—BISMUTOFERRITE

Specimen	Labeled	Locality	X-ray Film	Identification	Composition (X-ray fluorescence)			Remarks
					Major	Minor	None	
U.S.N.M. R3998	Bismutoferrite-hypochlorite	Schneeberg	11432	Bismutoferrite	Bi, Fe	As	Sb	
U.S.N.M. C3306	Bismutoferrite	Schneeberg			Bi, Fe	As, Sb trace		
U.S.N.M. 93338	Bismutoferrite	Schneeberg			Bi, Fe	As, Sb trace		
U.S.N.M. 16698	Hypochlorite	Ullersreuth	11441, 11198	Bismutoferrite and bismutite	Bi, Fe	As trace	Sb	
U.S.N.M. R9803	Hypochlorite with bismuth	Schneeberg						Similar to others; not further studied
Harvard 46981	Hypochlorite	Schneeberg	8957	Bismutoferrite and trace of unidentified	Bi, Fe			
Harvard 46981	Hypochlorite	Schneeberg	8912	Bismutoferrite	Bi, Fe	As	Sb	Chemical analysis; soft yellow
Harvard 10880	Hypochlorite with bismuth, etc.	Schneeberg	8921	Bismutoferrite				This and the following are two fragments of (originally) a single specimen
Harvard 47011	Hypochlorite	Schneeberg	8919	Bismutoferrite				
Harvard 47001	Hypochlorite	Schneeberg	8923	Quartz and bismutoferrite	Bi, Fe	As	Sb	Hard Green
Harvard 47001	Hypochlorite	Schneeberg	11431	Quartz and less bismutoferrite				Hard Green
Harvard 47001	Hypochlorite	Schneeberg	11430	Bismutoferrite				Soft Yellow

TABLE 2. GROUP II BISMUTOFERRITE DISPERSED IN SILICA (BISMUTH-"HYPOCHLORITE")

Specimen	Labeled	Locality	*X*-ray Film	Identification	Composition (*X*-ray fluorescence)			Remarks
					Major	Minor	None	
Harvard 47031	Hypochlorite	Gersdorf	8915, 11439	Quartz, with a little bismutoferrite	Bi, Fe	—	Sb, As	Thin section studied
U.S.N.M. C3307	Hypochlorite	Schneeberg			Bi, Fe	As	Sb	Locality questioned, Thin section studied
U.S.N.M. 12815	Hypochlorite	Ullersreuth						Thin section studied
Am. Mus. Nat. Hist. 12573	Hypochlorite	Schneeberg	11931	Quartz and bismutoferrite				With bismuth sulfides
Harvard 274	Hypochlorite	Schneeberg						Thin section studied

The last (Harvard 274) showed in thin section extremely minute prismatic (?) crystals in dense aggregates (Fig 1). Thin sections of Harvard 47031 and U.S.N.M. C3307 were similar.

TABLE 3. CHEMICAL ANALYSES "HYPOCHLORITE" (BISMUTH) AND BISMUTOFERRITE

	A	B	C	D	E	F	G
Bi_2O_3	13.02	13.08	42.5	43.26	42.83	4.76	44.65
Al_2O_3	14.65	14.65	.3	—	—	—	—
SiO_2	50.24	50.34	23.9	23.08	24.05	88.45	23.02
FeO	—	—	1.8	—	—	—	—
Fe_2O_3	10.54	10.54	29.3	33.33	33.12	6.00	30.60
Sb_2O_3	—	—	—	—	—	—	—
P_2O_5	9.62	9.62	—	—	—	—	—
As_2O_3	—	—	.08	—	—	—	—
H_2O^+	—	—	1.8	—	—	—	1.73
SO_3 MgO MnO	trace	—	—	—	—	—	—
	98.07	98.23	99.7	99.67	100.00	99.21	100.00
Sp. gr.			>3.3	4.47			

A. "Hypochlorite," Schneeberg, G. Schüler, analyst (Schüler, 1832), as cited in Dana, 3rd Ed. (Dana, 1870).

B. "Hypochlorite," Schneeberg, G. Schüler, analyst (Schüler, 1832), as cited by Frenzel (Frenzel, 1871).

C. Bismutoferrite, Schneeberg, Blanche Ingram, U. S. Geol. Survey, analyst, 1956, Harvard 46981.

D. Bismutoferrite, Schneeberg, A. Frenzel, analyst (Frenzel, 1871).

E. Bismutoferrite, Schneeberg, A. Frenzel, analyst (Frenzel, 1872).

F. Bismuth-"hypochlorite" (quartz and bismutoferrite), A. Frenzel, analyst (Frenzel, 1871).

G. Bismutoferrite, theoretical, $Bi(OH)Fe_2(SiO_4)_2$.

acterized by antimony and containing no bismuth. They contain a mineral dispersed in quartz or chalcedony, with an x-ray diffraction pattern almost identical with that of bismutoferrite. This mineral is chapmanite, discussed below.

It will be observed that Harvard 46972 is labeled as from Schneeberg; three other Harvard specimens, apparently very similar to it, are ascribed to Bräunsdorf. Schneeberg is the probable source of all the bismuth minerals in question, and Bräunsdorf, of the antimony minerals. The original label of this particular specimen has been lost (C. Frondel, personal communication, 1956) and the present label may well be erroneous. Our questioning of the Schneeberg locality for Harvard 46972 and suggestion that it too should be Bräunsdorf, is borne out by Frenzel's statement (1871, page 361) that no bismuth minerals occur at Bräunsdorf.

The first four specimens are similar in appearance; hard, dull olive-green, massive, with small holes; they form part of quartz veins, with pyrite and associated minerals, between the green mineral and the vein

TABLE 4—GROUP III—ANTIMONY-"HYPOCHLORITE" (QUARTZ AND CHAPMANITE)

Specimen	Labeled	Locality	*X*-ray Film	Identification	Composition (*X*-ray Fluorescence)			Remarks
					Major	Minor	None	
U.S.N.M. R4024	Hypochlorite	Bräunsdorf			Sb, Fe	As	Bi	This is very similar to H46972
Harvard 46972	Hypochlorite	Schneeberg (error)	8913	Quartz and a little chapmanite	Sb, Fe		Bi, As	Locality should be Bräunsdorf?
Harvard 10881	Hypochlorite	Bräunsdorf	8914	Quartz and a little chapmanite	Sb, Fe	As trace	Bi	
Harvard 105310	Antimony-Hypochlorite	Bräunsdorf	8917, 11440	Quartz and a little chapmanite	Sb	As	Bi	
Harvard 47021	Hypochlorite	Hungary	8916, 11438	Quartz and a little chapmanite, nontronite	Fe		As, Sb, Bi	
U.S.N.M. 105722	Hydrous ferrous antimonate	Venesela Mt., Alaska	11747	Quartz and chapmanite				Collected by J. B. Mertie, Jr., examined by W. T. Schaller
Am. Mus. Nat. Hist., N.Y.C. No number	Unlabeled	Velardeña, Durango, Mexico	11914	Quartz and chapmanite	Fe, Sb		Bi	
Am. Mus. Nat. Hist., N.Y.C. 12574	Hypochlorite	Freiberg, Saxony	11915	Quartz and chapmanite				Soft yellow and hard green

TABLE 5. ANALYSES OF "ANTIMONY-HYPOCHLORITE" (QUARTZ AND CHAPMANITE) AND CHAPMANITE

	H	I	J	K	L	M
Sb_2O_3	3.01	5.0	5.56	7.3	—	33.6
Sb_2O_5	—	—	—	—	31.65	—
SiO_2	88.50	86.0	86.40	78.0	28.28	27.6
FeO	—	—	—	—	33.91	—
Fe_2O_3	5.01	7.8	8.04	11.4	—	36.8
P_2O_5	2.03	trace	trace	—	—	—
H_2O	1.00	—	—	1.0	3.46	2.1
NiO	—	—	—	—	.36	—
CoO	—	—	—	—	.03	—
Cu	—	—	—	—	.17	—
Bi	—	—	—	—	.20	—
As	—	—	—	—	1.28	—
Al_2O_3	—	—	—	—	.28	—
	99.55	98.8	100.00	97.7	99.62	100.1

H. "Antimony-hypochlorite," Bräunsdorf, Kersten, analyst (1844) (SO_3, MgO, MnO, trace).
I. "Antimony-hypochlorite," Bräunsdorf, A. Frenzel, analyst (1871).
J. "Antimony-hypochlorite," Bräunsdorf, A. Frenzel, analyst (1871).
K. "Antimony-hypochlorite," Bräunsdorf, A. Frenzel, analyst (1871).
L. Chapmanite, Ontario, E. W. Todd, analyst (Walker 1924).
M. Chapmanite, theoretical, $Sb(OH)Fe_2(SiO_4)_2$.

quartz. Microscopically, the color is seen best with the condenser in, under high magnification. The needles are too small for optical study; their abundance agrees with what would be expected if Kersten's analysis (Table 5, H) is of a mixture with quartz. The fifth specimen in Table 4 is mostly nontronite, containing a little antimony "hypochlorite."

A somewhat nondescript material (U.S.N.M. 105722) collected by J. B. Mertie, of the U. S. Geological Survey, in 1938, from Venesela Mountain, Alaska (Lat. 60°41′ N Long. 155°43′ W) containing iron, antimony, and water, was found by *x*-ray to be essentially the same as the Bräunsdorf "antimony hypochlorite," that is, chapmanite, dispersed in quartz.

Analyses of the material—"antimony hypochlorite," actually, chapmanite dispersed in quartz or chalcedony —are given in Table 5. Also, in this table, are given the original analysis of the Ontario chapmanite (Walker, 1924); and the true composition inferred from its relationship to bismutoferrite. It will be observed that the two analyses are not greatly different. *X*-ray data are given in Table 6 for bismutoferrite and chapmanite.

Gladstone and Dale's Law Applied to Bismutoferrite and Chapmanite

Howard Jaffe (1956) has recently called attention to the usefulness of Gladstone and Dale's law (Larsen and Berman, 1934) in checking the validity of proposed compositions of minerals where the refractive indices and density are known with reasonable certainty. Although, because of minute grain size, precise optical determinations on bismutoferrite are difficult, it is possible to use what data are available, and to obtain, on one hand, corroboration of the formula proposed by us for bismutoferrite and chapmanite, and, on the other hand, strong indication of the untenability of Walker's formula for chapmanite.

Available data are:

For bismutoferrite

(a) indices of refraction $\alpha=1.93$, $\beta=1.97$, $\gamma=2.01$ (determined by us)
(b) density 4.47 (Frenzel, 1871)
(c) proposed formula $Bi_2O_3 \cdot 2Fe_2O_3 \cdot 4SiO_2 \cdot H_2O$
(d) specific refractive energies of above oxides, as given by Larsen and Berman (1934) except for Fe_2O_3, as given by Jaffe (1956).

For chapmanite

(a) indices of refraction $\alpha=1.85$, $\gamma=1.96$ (Walker, 1924)
(b) density 3.58 (Walker, 1924)
(c) proposed formula $Sb_2O_3 \cdot 2Fe_2O_3 \cdot 4SiO_2 \cdot H_2O$
Walker's formula $Sb_2O_5 \cdot 5FeO \cdot 5SiO_2 \cdot 2H_2O$
(d) Specific refractive energies of above oxides with alternate values for Sb_2O_3 0.209 and 0.232 and for Sb_2O_5 0.152 and 0.222 (Larsen and Berman, 1934).

Calculation using this data gives

	Density	Indices of Refraction Observed	Average Observed	Average Calculated
Bismutoferrite	4.47	$\alpha=1.93$ $\beta=1.97$ $\gamma=2.01$	1.97	1.96
Chapmanite (Correct formula)	3.58	$\alpha=1.85$ $\gamma=1.96$	1.905	1.86, 1.89
Chapmanite (Walker's formula)	3.58	$\alpha=1.85$ $\gamma=1.96$	1.905	1.673, 1.752

Evidently, the agreement of observed average index of refraction with the calculated index for bismutoferrite is excellent; for chapmanite (our formula) good; but for chapmanite, using Walker's formula, very poor. In summary, application of Gladstone and Dale's law supports the

formula $Bi_2O_3 \cdot 2Fe_2O_3 \cdot 4SiO_2 \cdot H_2O$ for bismutoferrite, and $Sb_2O_3 \cdot 2Fe_2O_3 \cdot 4SiO_2 \cdot H_2O$ for chapmanite.

The Composition of Chapmanite

Still other reasons exist for rejecting E. W. Todd's (Walker, 1924) analysis of chapmanite and Walker's formula based upon it. Michael Fleischer has pointed out (oral communication) that the formula derived from Todd's analysis is open to serious question. Walker says that "the state of oxidation of the iron was determined by dissolving the mineral in hydrofluoric acid and titrating with potassic permanganate." Todd and Walker assumed that ferrous iron was thereby oxidized to ferric. In our opinion, what actually happened was that antimonous oxide was oxidized to antimonic. Indeed, titration of antimonous salts with permanganate is a standard analytical method for the determination of antimony (Scott, 1939). Considering the two oxidation reactions,

$$2Sb_2O_3 + 4O = 2Sb_2O_5$$
$$2FeO + O = Fe_2O_3$$

it is evident that the amount of oxygen (or the equivalent permanganate) necessary to oxidize four moles of FeO is equal to that necessary to oxidize one mole of Sb_2O_3. Todd, therefore, mistook the oxidization of a mole of Sb_2O_3 for the oxidation of a substantially equivalent amount (actually, five moles) of FeO. He was, of course, familiar with this standard analytical procedure for the quantitative analysis of antimony, and it is therefore clear that he wrongly assumed that the antimony in the mineral was unaffected by permanganate, that is, it was in the pentavalent state, Sb_2O_5. Hence, his formula is erroneous with respect to valence states of both iron and antimony.

Walker further notes that "at 270° the mineral lost its green color and became pale brownish, due, apparently, to a change in the state of oxidation which would result in an increase of weight." We do not regard this color change as necessarily indicating oxidation of ferrous iron; it could reflect decomposition of the silicate mineral, with release of ferric oxide as such. Many ferric silicates are green, not yellow or brown.

Unlike Sb_2O_3, Bi_2O_3 is not oxidized by permanganate. Titration of FeO in bismutoferrite by permanganate as in Mrs. Ingram's analysis is therefore a valid procedure; and it may be noted that she found the iron present to be almost wholly ferric iron.

Finally, the remarkable similarity of the x-ray diffraction patterns of bismutoferrite and chapmanite is further weighty evidence for their formulas being homologous. We therefore reject Walker's formula for chapmanite and accept chapmanite as $Sb(OH)Fe_2(SiO_4)_2$ or $Sb_2O_3 \cdot 2Fe_2O_3 \cdot 4SiO_2 \cdot H_2O$, homologous or isostructural with bismutoferrite $Bi(OH)Fe_2(SiO_4)_2$ or $Bi_2O_3 \cdot 2Fe_2O_3 \cdot 4SiO_2 \cdot H_2O$.

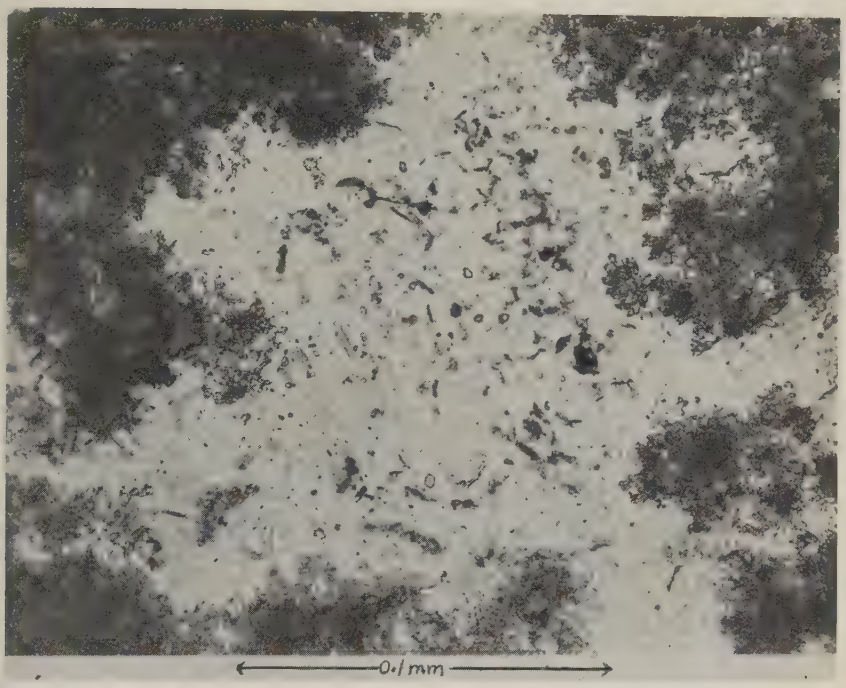

FIG. 1. Thin section of "hypochlorite (bismutoferrite in quartz), Schneeberg, Saxony. Harvard 274. Shows typical aspect of "hypochlorite" (the same for both bismuth and antimony types). At the edges of the dense aggregates of bismutoferrite, extremely small, poorly developed single crystals are discernible. Ordinary light.

X-RAY DATA

Except for the several specimens which were identified as nontronite and other extraneous species, *x*-ray powder patterns of the specimens labeled "bismutoferrite" and "hypochlorite", and chapmanite included one distinctive pattern. The pattern varied slightly from sample to sample, as is not unusual for a mineral species. However, when *x*-ray spectroscopy showed a mutual exclusion of bismuth and antimony, the most obvious variation, that in the relative *d*-spacings of a medium intensity triplet around 2.59Å, was re-examined; the triplet 2.66-2.59-2.53Å is characteristic for the bismuth mineral and the triplet 2.67-2.59-2.54Å is characteristic for the antimony mineral. Other variations in spacing conform so there are actually two slightly different patterns, those of bismutoferrite and chapmanite. Intensity relationship differences between the two patterns in Table 6 result at least in large part from preferred orientation in bismutoferrite. Lines obviously strengthened in some patterns by preferred orientation are marked by a plus sign and those weakened are marked by a minus sign.

TABLE 6. *X*-RAY POWDER DIFFRACTION PATTERNS OF BISMUTOFERRITE AND CHAPMANITE

$\lambda = 1.548$ Å (Cu/Ni)
$r = 114.6$ mm.

Bismutoferrite HMM 46981 Film No. 8912 Max. *d*-spacing cutoff 14.73		Chapmanite U.S.N.M. 94866 Film No. 11748 Max. *d*-spacing cutoff 13.59		Bismutoferrite HMM 46981 Film No. 8912 Max. *d*-spacing cutoff 14.73		Chapmanite U.S.N.M. 94866 Film No. 11748 Max. *d*-spacing cutoff 13.59	
d	*I*	*d*	*I*	*d*	*I*	*d*	*I*
7.63	100−	7.63	100−	1.471	3	1.471	5
4.52	6−			1.456	2		
4.47	6	4.44	3	1.451	1		
4.18	18+	4.17	25	1.435	4	1.443	5
3.87	100−	3.88	90−	1.394	1b	1.397	5
3.79	2	3.80	5	1.370	4	1.373	12
3.58	35+	3.58	100	1.360	1		
3.18	50+	3.19	90	1.329	1		
2.90	70−	2.90	70	1.299}	1	1.296	9
2.66	12+	2.67	25	1.291}	1		
2.59	35+	2.59	70	1.282	<1	1.281	3
2.53	25−	2.54	35	1.257–1.252	1	1.256	5
2.383	10	2.380	18			1.241	2
		2.344	9	1.224	1	1.228	3
		2.287	3	1.215	1	1.221	5
2.251	9	2.243	18	1.203	2	1.204	5
2.225	3			1.184	1		
2.201	9−	2.217	18	1.176	<1		
2.162	15−	2.156	18	1.169	1	1.167	3
2.086	5	2.085	18	1.161	<1		
2.040	9	2.044	18	1.143	1	1.142	2
2.011	1			1.124	1	1.124	6
1.976	<1			1.106	<1	1.109	3
1.935	12−	1.941	15	1.093	1		
1.907	9	1.910	18	1.080	1b		
1.891	6−			1.067	<1		
1.863	3	1.873	5	1.049	1		
1.835	3	1.838	6	1.037	<1	1.016	2
1.785	1	1.785	9	.9830	2	.9826	5
1.744	3			.9736	<1		
1.719	12	1.725	22	.9418	<1b		
1.694	4	1.698	9	.9286	<1b	.9259	2
1.683	6−	1.683	12	.9188	<1		
1.659	2	1.659	3	.9096	<1		
1.637}	9	1.634	12	.9045	1		
1.628}	3	1.613	12	.8967	<1b	.8978	1
1.608	9	1.605	12	.8872	<1		
1.592	4	1.590	12	.8770	1		
1.570	1	1.570	5			.8755	1
1.542	1b	1.544	6			.8659	2
1.516	4	1.523	5			.8285	1
1.504	12	1.501	25			.7964	1

b = broad line.
} = band with peaks.
+ = strengthened by preferred orientation.
− = weakened by preferred orientation.

TABLE 7. GROUP IV—MISCELLANEOUS SPECIMENS LABELED (ERRONEOUSLY) "HYPOCHLORITE" OR "BISMUTOFERRITE"

Specimen	Labeled	Locality	*X*-ray Film	Identification	Composition (*X*-ray Fluorescence)			Remarks
					Major	Minor	None	
Harvard 46971	"Hypochlorite"	Goritz, Reuss.	8918	Nontronite				
Harvard 46991	"Hypochlorite"	Haar, near Passau, Bavaria	8920	Nontronite and tremolite (?)				
Harvard (No number)	"Hypochlorite"	(No locality)	8922	Nontronite	Fe	Sb	Bi(?)	
U.S.N.M. R4025	"Hypochlorite"	Schneeberg	11433	Mostly talc, also white pyroxene, graphite, etc.				
Am. Mus. Nat. Hist. 12576	"Hypochlorite"	Schneeberg	11933	Copper sulfate in opaline silica on magnetite				Clear glassy green
Am. Mus. Nat. Hist. 26395	"Bismutoferrite"	Schneeberg	11916	Bindheimite				Pb and Bi by chemical test. Waxy yellow.
Am. Mus. Nat. Hist. 12575	"Hypochlorite"	Schneeberg	11932	Nontronite				No Bi or Sb, much Fe.

The patterns of the two minerals are remarkably similar and the pair may be classed with such pairs as scheelite-powellite and magnesite-siderite in which one element completely substitutes for another with very little change in the x-ray patterns.

Group IV. *Miscellaneous substances termed "Hypochlorite" or "Bismutoferrite"*

In all three Museum collections were found specimens labeled "hypochlorite" which proved to be something different. These are listed in Table 7. Apparently nontronite is easily mistaken for "hypochlorite" which it superficially resembles.

Bibliography

Adler, I., and Axelrod, J. M., 1956, Application of X-ray fluorescence spectroscopy to analytical problems: *Norelco Reporter*, v. **3,** 65–68.

Ahlfeld, F., 1948, An unusual antimony deposit in Argentina, *Econ. Geol.*, **43,** 598–602.

Breithaupt, A., 1871, "Oral communication", cited by Frenzel.

Dana, E. S., 1892, System of Mineralogy, 6th ed., p. 562, J. Wiley & Sons Inc., New York.

Dana, J. D., 1870, System of Mineralogy, 3rd ed., p. 392, J. Wiley & Sons Inc., New York.

Doelter, C., 1917, Handbuch der Mineralchemie, Band 2, Abt. 2, p. 164, Steinkopff, Dresden.

Fischer, H., 1870, Critische, mikroscopisch-mineralogische Studien: *Berichte der Naturf. Gesellsch., Freiburg,* Band **5,** Hft. 2, pp. 1–64.

Frenzel, A., 1871, Hypochlorit: *Journal Prakt. Chemie,* (N.F. **4**) 353–362.

Frenzel, A., 1872, Letter to Prof. H. G. Beinitz: *Neues Jahrb für Mineral.*, 514–517.

Goldsmith, E., 1873, *Proc. Acad. Philadelphia*, 366.

Hey, M. H., 1950, Chemical Index of Minerals, pp. 102, 199. British Museum, London.

Jaffe, H. W., 1956, Application of the rule of Gladstone and Dale to minerals, *Am. Mineral.*, **41,** 757–777.

Kerr, P. F., Mineralogical studies of uraninite and uraninite-bearing deposits: AEC Interim Technical Report, July 1, 1948, to June 30, 1950, p. 12.

Kersten, C. M., 1844, Ueber die chemische Zusammensetzung einiger sächsischer Mineralien und Gebirgsarten: *Berg. und Hütten. Zeitung,* **3,** 59.

Larsen, Esper S., and Berman, Harry, 1934, Microscopic determination of the nonopaque minerals. *U. S. Geological Survey Bulletin* **848.**

Ramdohr, P., 1936, Klockmann's Lehrbuch der Mineralogie, Enke Verlag, Stuttgart, pp. 601, 603.

Schüler, 1832, Sogenannter Grüneisenerde von Schneeberg, Hypochlorit: *Jour. für Chemie und Physik,* **66,** p. 41.

Scott, W. W., 1939, Standard methods of chemical analysis, p. 76, D. Van Nostrand & Co., New York.

Vitaliano, C. J., and Mason, Brian, 1952, Stibiconite and cervantite: *Am. Mineral.*, **37,** 982–999.

Walker, T. L., 1924, Chapmanite, a new mineral from South Lorraine, Ontario, *Univ. of Toronto Studies, Geol. Ser.* **17,** p. 5.

Manuscript received October 10, 1957

THE AMERICAN MINERALOGIST, VOL. 43, JULY-AUGUST, 1958

A WHITE CHLORITE FROM COBARGO, N.S.W.

F. C. Loughnan and G. T. See, *New South Wales University of Technology, Kensington, N.S.W., Australia.*

Abstract

A white chlorite from Cobargo, N.S.W., previously described as pyrophyllite, is shown to be of approximate composition $Mg_5Al(Si_3Al)O_{10}(OH)_8$. The chlorite is associated with small amounts of montmorillonite, talc, vermiculite, mica, rutile and pulverized felspar. The mineral assemblage has resulted from magnesium solutions of hydrothermal origin, acting on a fine to medium grained albitite, a differentiate of the Bega granodiorite.

The Cobargo deposits have been worked sporadically for many years as a source of a white filler clay for the manufacture of rubber and paint. Whitworth (1949), and later Fisher and Canavan, described the deposit, referring to the material as pyrophyllite, though Whitworth suggested that gibbsite may be present in quantity. The suggestion was based on one chemical analysis which showed a high alumina value (53.4%) while the magnesia content was insignificant (1.1%). Material corresponding to this analysis was not encountered in the present survey.

Occurrence

The deposits, which are located a few miles to the south of Cobargo, occur as relatively small lenticular masses in granodiorite (Brown 1933) and pits have been opened out on three of these lenses, two on Portions 73–80 Ph Narira Co. Dampier, and the third, a disused pit, on Portion 13 of the same Parish. Several small shears parallel the strike of the lenses and thin cross-fibered veins, up to an inch or two in width, follow the fissures. Quartz veins, showing obvious signs of a later shearing movement, are located within the fissures while large masses of unaltered fine to medium grained albitite occur throughout the deposit.

The more westerly pit on Portions 73/80, the only lens being worked at present, has been opened out for a distance of 40 ft. along the strike and to a depth of 20 to 25 ft. while the maximum width reached is 18 ft. The walls appear to be still in clay.

The following samples were obtained from the three pits for analyses.

1. "Run-of-mine" clay from the more westerly pit on Portions 73/80. The clay is white, dense, soapy and unstressed. Comparative reflectance value was 87% of MgO.

1A. Same pit as above. Soft powdery clay hand picked from within the shear planes.

1B. Same pit as above. Pale greenish material occurring in cross-fibred veins paralleling the fissures.

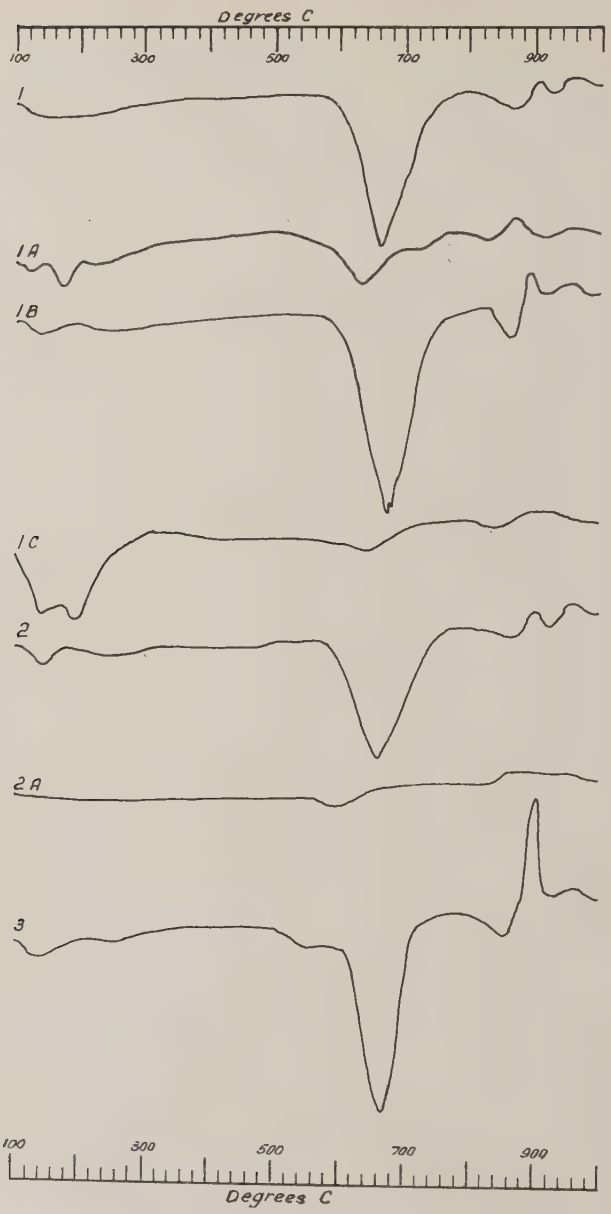

FIG. 1. Differential thermal curves of chlorite and associated minerals from Cobargo, N.S.W.

1C. Same pit as above. Small blebs of dark brown and light yellow material obtained from in and about the shear planes.
2. "Run-of-mine" clay from a disused pit located 100 yds. east of pit 1. Shearing is less pronounced. Comparative reflectance value was 85% of MgO.
2A. Soft powdery material obtained from small cross fissures in pit 2.
3. "Run-of-mine" clay taken from a disused pit on Portion 13, half a mile north of pits 1 and 2. Comparative reflectance value was 82% of MgO.

Mineralogy

The samples were examined by differential thermal, *x*-ray and chemical techniques.

Differential Thermal Analysis: The differential thermal curves (see Fig. 1) for samples 1, 1B, 2 and 3 show the characteristic reactions for chlorite. However the presence of small but definite endothermic reactions in the region of 120° to 180° C. suggests the presence of other minerals, possibly montmorillonite and/or vermiculite. Sample 1A has weak chlorite and montmorillonite and/or vermiculite reactions while sample 1C is that typical of a montmorillonite. The indeterminate graph given by sample 2A indicates the presence of a considerable amount of a non-reactive mineral shown by *x*-ray data to be felspar.

X-ray Data: *X*-ray analyses were made on untreated clay, glycerol treated clay and on clay preheated to 700° C. for 2 hours. Data are given in Table 1. Samples 1, 1B, 2, 2A and 3 remained unaffected by glycerol treatment, indicating the absence of montmorillonite.

From the *x*-ray data the following conclusions regarding the mineralogy may be made.

1. Chlorite with a little vermiculite.
1A. Talc, montmorillonite and chlorite in approximately equal amounts with some felspar.
1B. Chlorite with a little talc and vermiculite.
1C. Montmorillonite with a little chlorite.
2. Chlorite with a small amount of vermiculite.
2A. Predominantly felspar but talc is abundant and chlorite present in a small amount.
3. Chlorite with a small amount of mica and vermiculite.

Chemical Analyses: Chemical data are given in Table 2. Applying the rational analysis technique described by Brindley and Gillery to sample 1, the chlorite has the composition $Mg_5Al(Si_3Al)O_{10}(OH)_8$. The presence of a small amount of vermiculite, approximately 5% in this sample, though not seriously affecting the results, nevertheless renders the composition, as determined, an approximation only.

Fine needles and somewhat coarser stumpy crystals of rutile were present to a small extent in all samples, while zircons, though rare, were noted similarly.

TABLE 1. *X*-RAY DATA

Sample 1				Sample 1A						Sample 1B				Sample 1C				Sample 2				Sample 2A		Sample 3			
a		c		a		b		c		a		c		a		b		a		c		a		a		c	
d	*I*	*d*	*I*	*d*	*I*	*d*	*I*	*d*	*I*	*d*	*I*	*d*	*I*	*d*	*I*	*d*	*I*	*d*	*I*	*d*	*I*	*d*	*I*	*d*	*I*	*d*	*I*
						17.7	8									17.7	10										
14.0	9	14.4	10	14.6	10	14.6	4	14.6	10	14.0	10	14.4	10	14.6	10	14.3	1	14.0	10	14.4	10	14.1	1	14.0	10	14.4	10
																								10.2	1	10.1	1
		9.4	2	9.3	9	9.5	10	9.5	7	9.3	1	9.6	2			9.0	4			9.6	2	9.3	7			9.5	4
7.10	10	7.25	4	7.15	2	7.20	3			7.10	10	7.15	1	7.10	1	7.4	1	7.05	10	7.20	2			7.10	10		
				6.40	1	6.44	1					6.44	1									6.40	3				
4.74	10	4.78	4	4.80	4	4.80	2	4.82	1	4.78	8	4.77	4	4.78	1	4.78	3	4.72	10	4.70	2	4.72	1	4.72	9	4.67	2
4.59	1	4.61	4	4.51	4	4.51	6	4.55	4	4.59	1			4.51	6	4.59	8	4.59	1	4.53	2	4.49	1			4.53	2
4.26	1													4.24	1			4.24	1								
				4.04	1	4.04	2			4.04	3	4.05	1	4.05	1							4.04	6				
3.90	1																	3.92	1			3.77	4				
				3.69	1			3.75	2	3.69	1	3.70	2									3.67	5				
3.55	10	3.56	6	3.56	3	3.58	4			3.55	10	3.55	2	3.55	1	3.58	3	3.53	10	3.56	4	3.52	2	3.54	10	3.53	4
3.35	1	3.36	2	3.36	2	3.36	1			3.35	1	3.36	2	3.36	1	3.35	1	3.35	2	3.36	1	3.36	2			3.39	1
		3.21	1	3.20	5	3.20	5	3.23	3	3.19	2	3.21	5	3.19	1	3.20	1					3.20	10				
				3.10	7	3.12	6	3.14	4													3.10	2			3.06	1
				2.94	1					2.95	1			2.96	1							2.96	3			3.01	1
2.85	4	2.85	8	2.85	1	2.86	1			2.85	4	2.84	4	2.88	1			2.84	4	2.84	4	2.86	1	2.84	3	2.86	8
2.59	1	2.61	1	2.62	1			2.68	1	2.65	1	2.65	6			2.62	4	2.65	1	2.67	3	2.65	1			2.67	7
2.55	5	2.55	2	2.55	1	2.55	2			2.59	2	2.61	1	2.59	2			2.59	3	2.61	2			2.58	1	2.61	2
				2.49	1	2.48	2	2.49	6	2.53	3	2.56	1			2.55	2	2.53	6	2.55	1	2.55	2	2.53	6	2.56	2
2.44	3	2.46	6	2.44	1					2.44	2	2.46	6	2.45	1	2.45	2	2.44	4	2.46	6	2.45	2	2.44	4	2.46	6
2.38	1			2.39	1					2.37	1							2.38	2					2.37	1		
2.25	1	2.27	2	2.21	2					2.26	1	2.27	3			2.27	2	2.26	2	2.26	3	2.29	2	2.25	2	2.27	4
2.03	1			2.11	2			2.13	1			2.14	1									2.13	3			2.20	1
2.00	4	2.01	2	2.01	3					1.99	3	1.99	1	2.01	1	2.01	2	1.98	4	2.01	2	2.07	1	2.00	6	2.01	2
1.88	1	1.89	2	1.88	1	1.90	2	1.88	2	1.88	1	1.89	1					1.88	2	1.89	2	1.91	1	1.88	2	1.88	1
1.83	1	1.83	1	1.82	1					1.82	1			1.82	1			1.82	2			1.82	2	1.82	2		
				1.79	1									1.78	1							1.79	1				
				1.73	1											1.73	1	1.74	1			1.73	1	1.66	1		
1.57	2	1.67	1	1.67	1	1.60	1			1.57	3			1.56	1	1.57	1	1.57	4			1.69	1	1.56	6		
1.53	4	1.55	5	1.54	3	1.54	3	1.53	1	1.54	4	1.55	6	1.54	1	1.53	3	1.53	6	1.55	6	1.54	3	1.53	6	1.55	4
1.50	1	1.51	2	1.50	1	1.51	2			1.50	1			1.52	3	1.51	1	1.50	1					1.50	1	1.51	1

a—Untreated.
b—Glycerol treated.
c—Preheated 700° C. 2 hours.

Table 2. Chemical Analyses

	Albitite*	1	1A	1B	2	3
SiO_2	62.8	33.0	52.0	33.7	34.1	35.7
Al_2O_3	20.5	22.8	18.1	21.0	24.5	28.9
Fe_2O_3	0.5	0.2	0.2	0.5	0.3	0.4
TiO_2	0.6	0.4	0.3	0.4	0.4	0.9
CaO	Tr	0.1	0.4	0.3	0.1	0.1
MgO	4.5	29.7	16.9	28.2	25.9	20.4
Na_2O	8.2	—	—	—	—	—
H_2O	2.8	11.9	7.2	12.0	12.7	12.4
H_2O^-		0.5	2.8	0.7	1.3	1.2
Total	99.6	98.6	97.9	96.8	99.3	100.0

* After Whitworth (1949).

Origin

As Whitworth (1949) suggested, the parent material for the formation of the mineral assemblage is a fine to medium grained albitite, a differentiate of the Bega granodiorite. A gradation may be seen in thin section from the unaltered rock, which contains sphene and apatite to the extent of one or two per cent in addition to albite, through sections with chlorite filled vugs, to relatively pure chlorite. The partly altered rock shows obvious signs of shearing with granulated albite, coarse and chalcedonic quartz together with wisps of chlorite infilling the fissures. The quartz, unlike the albite, does not display undulous extinction. Skeletal grains of sphene altering to rutile may be seen in thin section also.

As shown by the following reaction,

$$2NaAlSi_3O_8 + 5MgO + 4H_2O \rightarrow Mg_5Al(AlSi_3)O_{10}(OH)_8 + 3SiO_2 + Na_2O$$

198 cc. 205 cc.

for the chloritization of the albite, a considerable amount of magnesia and water must enter the system with a corresponding loss of all the soda and half the silica. Magnesium metasomatism at the expense of soda and silica has been recorded frequently elsewhere, the only surprising feature in this instance is the paucity of iron.

The unstressed nature of the quartz infilling the fractures in the partly altered rock suggests that the alteration postdated the fissuring, for the intimate association of quartz and chlorite can leave little doubt that the former is the product of silica released during the chloritization process.

An unusual feature is the occurrence of fine pulverized felspar along

the shear zones, for it would be expected that if fissuring preceded the alteration, then the fine state of subdivision of the felspar would have rendered it more reactive and hence more readily convertible to chlorite than the massive rock. There appears to be no simple explanation for this unless it be accepted that the chloritization proceeded in different parts of the mass at different times interspersed with a period or periods of shearing. This would account for the sheared nature of the quartz veins (as distinct from the unstressed quartz in the partly altered rock) for these veins must have intruded early in the alteration process. A further possibility is that these veins also represent silica released by the chloritization process.

References

Brindley, G. W., and Gillery, F. H. (1956) *X*-Ray Identification of Chlorite. *Am. Mineral.*, **41,** 169–186.

Brindley, G. W., and Robinson, K. (1951) *X*-Ray Identification and Crystal Structures of Clay Minerals. Mineralogical Society, London (Clay Minerals group), 173–198.

Brown, I. A. (1933) The Geology of the South Coast of N.S.W. with Special Reference to the Origin and Relationships of the Igneous Rocks. *Proc. Linn. Soc. N.S.W.*, **58,** 339–362.

Fisher, N. H., and Canavan, F. (1950) Talc, Steatite and Pyrophyllite. *Bur. Min. Res. Aust.*, Sum. Rept. **15.**

MacEwan, D. M. C. (1944) Glycerol-montmorillonite. *Nature*, **154,** 577.

Walker, G. F. (1951) *X*-Ray Identification and Crystal Structures of Clay Minerals. Mineralogical Society, London (Clay Minerals group), 199–223.

Whitworth, H. F. (1949) The Pyrophyllite Deposits of the Cobargo and Pambula Districts. N.S.W. *Dept. Mines. Ann. Rept.*, 101–102.

Manuscript received October 9, 1957

THE AMERICAN MINERALOGIST, VOL. 43, JULY–AUGUST, 1958

SANTAFEITE, A NEW HYDRATED VANADATE FROM NEW MEXICO*

MING-SHAN SUN AND ROBERT H. WEBER, *New Mexico Bureau of Mines and Mineral Resources, Socorro, New Mexico.*

ABSTRACT

Santafeite is a new hydrated vanadate found in the Grants uranium district, McKinley County, New Mexico, in the spring of 1951. It has the formula $Na_2O \cdot 3MnO_2 \cdot 6(Mn,Ca,Sr)O \cdot 3(V,As)_2O_5 \cdot 8H_2O$. The mineral occurs as an encrustation of small rosettes of acicular crystals on an outcrop joint surface of Todilto limestone. Physical and optical properties are: perfect (010) and distinct (110) cleavages, very brittle, measured density 3.379, black color, brown streak, subadamantine luster, readily fusible in an alcohol flame to a dull black bead; translucent only in very small fragments, pleochroic from dark reddish brown to yellowish brown, with absorption $X > Y > Z$; $X = c$, $\alpha = 2.01$, and distinct dispersion. *X*-ray studies by rotation, Laue, Weissenberg, and powder diffraction methods indicate orthorhombic symmetry, space group $B22_12$, D_2^5, with cell dimensions: $a_0 = 9.25 \pm .02$ Å; $b_0 = 30.00 \pm .02$ Å; $c_0 = 6.33 \pm .02$ Å.

The mineral is named santafeite, after the Atchison, Topeka and Santa Fe Railroad Company, in recognition of its pioneer exploration and development of the uranium deposits in New Mexico.

INTRODUCTION

In the course of a reconnaissance of uranium mineral deposits in the Grants district in the spring of 1951, a small sample of santafeite was collected by Weber from a cliff-face outcrop of the Jurassic Todilto limestone in section 25, T. 13 N., R. 10 W. The locality is about 12 miles north of Grants; approximately one mile northward in McKinley County from the McKinley-Valencia County line, New Mexico.

Preliminary optical, *x*-ray, and semiquantitative spectrographic analysis (which reported significant amounts of silica, alumina, manganese, and vanadium) led to the tentative identification of the mineral as ardennite (abstract, *Am. Mineral.*, **40**, 338, 1955). Through the courtesies of Drs. Hugo Strunz and Clifford Frondel the writers received a sample of ardennite from Salm Chateau, Belgium. Comparison of the *x*-ray powder pattern of the Grants material with the Salm Chateau ardennite showed conclusively that the Grants material was not ardennite. A second, more precise, semiquantitative spectrographic analysis revealed that the unknown mineral was not a silicate, but a hydrated manganese vanadate.

Insufficient material was present in the original sample to permit a

* Published by permission of the Director, New Mexico Bureau of Mines and Mineral Resources.

complete chemical analysis, so the locality was revisited by the writers in the summer of 1954. It was found that the outcrop from which the original sample was taken had been destroyed by subsequent mining operations, and none of the santafeite left exposed in 1951 remained. A second search of most of the cliff edge and surface mine workings in the Todilto limestone between San Mateo road and Haystack Mountain in 1955 was also fruitless. Fortunately, however, an additional 100 milligram sample of santafeite was collected in the summer of 1956 by Mr. Robert Thaden and Dr. Alice D. Weeks of the U. S. Geological Survey, from a shallow open pit along the rim outcrop of the Todilto limestone in Section 26, which adjoins the location of the original sample.

The name santafeite (san-ta-fay-ite) was adopted in recognition of the work of the Atchison, Topeka and Santa Fe Railroad Company, which pioneered in the exploration and development of the uranium deposits of what soon became the most important producing district in New Mexico, and on whose property the mineral was first discovered.

Occurrence

Santafeite was originally found at one point on the cliff-face outcrop of the Todilto limestone, which in this area is a thin-bedded sequence aggregating 8 to 16 feet in thickness (Towle and Rapaport, 1952). A subsequent discovery by Mr. Robert Thaden, and identification by Dr. Alice D. Weeks is noted above. The Todilto limestone is underlain by Entrada sandstone, and capped by what is probably the equivalent of the Summerville formation, succeeded upward by the Morrison formation. The mineral occurred as an encrustation on, and intergrowth with, crystalline calcite coating a nearly vertical joint surface in the limestone. Deposition of both santafeite and calcite was clearly controlled by jointing. Sparse flecks of cuprosklodowskite are present on some of the santafeite crystals, and more conspicuously developed along an irregular surface that roughly parallels the plane of the bedding of the limestone. The occurrence is adjacent to exploratory pits that expose yellow uranium-vanadium minerals. Other minerals that have been identified in Todilto limestone deposits of the area, but not known to be directly associated with the santafeite, include carnotite, tyuyamunite and metatyuyamunite, uranophane, beta-uranotil, uraninite, fluorite, barite, marcasite, pyrite, galena, psilomelane, hematite, and montmorillonite (Gruner, Towle, and Gardiner, 1951; Towle and Rapaport, 1952; Gruner, Gardiner, and Smith, 1954; Weeks and Thompson, 1954).

Physical and Optical Properties

Santafeite occurs as well-defined rosettes of radially oriented acicular crystals (Fig. 1). Individual rosettes range from about 1.5 mm. to 4 mm.

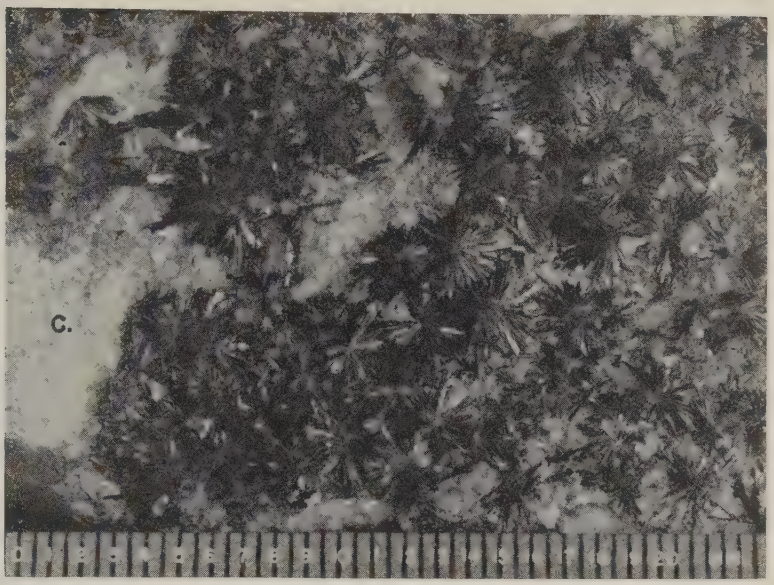

FIG. 1. Santafeite rosettes with associated calcite (c) on joint surface of Todilto limestone.

in diameter. Some of them are triangular in profile along the diameter, suggesting an original spherulitic form from which the upper two-thirds has been broken away. A typical rosette 2.8 mm. in diameter consists of crystals measuring approximately 0.3 mm. along the *a*-axis, 0.07 mm. along the *b*-axis, and 1.4 mm. along the *c*-axis. The small size and fragile character of individual crystals prohibited optical goniometric measurements. Of the forms present, however, the *b*-face is especially prominent.

Cleavages are (010) easy and perfect, and (110) distinct; very brittle; color black; streak brown; luster subadamantine; readily fusible in an alcohol flame to a dull black bead. The density, determined by suspension in Clerici's solution, is 3.379. The mineral is transluscent only in very small fragments, which show pronounced pleochroism ranging from dark reddish brown to yellowish brown, with absorption $X > Y > Z$. Extinction is parallel, with $X = c$, $\alpha = 2.01$ by the immersion method. Dispersion is distinct.

CHEMICAL COMPOSITION

Acting upon the courteous suggestion of Dr. Michael Fleischer, a sample of santafeite was submitted to the Geochemistry and Petrology Branch of the U. S. Geological Survey for spectrographic and microchemical analysis. According to Dr. Alice D. Weeks (letter of April 1, 1957), "The mineral sample looks quite pure and consists of clean, micro-

scopic, prismatic crystals, but the spectrographic analysis shows many trace constituents. Although the mineral appears to be essentially a hydrated calcium manganese vanadate, many of the minor elements must substitute for the major constituents. Several of the minor elements have to be determined in order to make a satisfactory total for the analysis." The results of the semi-quantitative spectrographic analysis are listed in Table 1.

The small amount of the original sample, and the additional 100 mg. of santafeite subsequently collected by Mr. Robert Thaden and Dr. Alice D. Weeks were processed for partial quantitative micro-chemical analysis in the U. S. Geological Survey Laboratory. The results of this analysis are listed in Table 2. At the suggestion of Mr. Robert Meyrowitz, the analyst, a footnote describing the procedures and methods used is at the end of Table 2, so that "one can better evaluate the reliability of an analytical result when the method used for the determination is known. This is especially true in the analysis of small amounts of material," (Robert Meyrowitz, letter of June 10, 1957). The writers believe that the procedures and methods used by Mr. Meyrowitz provide a valuable reference for those who have similar problems in the chemical analysis of small samples of a complex mineral.

The chemical formula of santafeite, calculated from the partial quantitative micro-chemical analysis, is $Na_2O \cdot 2MnO_2 \cdot 6(Mn,Ca,Sr)O \cdot 3(V,As)_2O_5 \cdot 8H_2O$. The Fe_2O_3, CoO, NiO, CO_2, CuO, UO_3, and SiO_2 shown by the chemical analysis to be present in santafeite are considered to be impurities contributed by associated hematite, limestone, and cuprosklodowskite.

Because of the complex nature of the chemical composition, and the small quantity of the analyzed sample, the calculated chemical formula of santafeite may be subject to revision. The analysis shows a total of 96.2 per cent, of which several per cent probably represent impurities. Based on the measured density and the unit cell dimensions of the mineral, the calculated molecular weight of santafeite is 1787.41, assuming that there are two molecules in the unit cell. However, the molecular weight based on the calculated chemical formula of santafeite is only 1449.12. The measured density is 3.379, but some crystals deviate slightly from this value, leading one to suspect that a portion of the discrepancy in the molecular weights may be due to the difference in density of the individual crystals.

X-Ray Analysis

Cell dimensions are $a_0 = 9.25 \pm .02$ Å, $b_0 = 30.00 \pm .02$ Å, and $c_0 = 6.33 \pm .02$ Å, calculated from the $h00$, $0k0$, and $00l$ reflections on the Weis-

TABLE 1. SEMI-QUANTITATIVE SPECTROGRAPHIC ANALYSIS OF SANTAFEITE FROM MCKINLEY COUNTY, NEW MEXICO

Analyst: Katherine E. Valentine, Naval Gun Factory Laboratory, Geochemistry and Petrology Branch, U. S. Geological Survey

Si	.3	Eu	0	Ru	0
Al	.1	F	—	Sb	0
Fe	.3	Ga	0	Sc	.001
Mg	.1	Gd	0	Sn	.003
Ca	.3	Ge	0	Sr	1.0
Na	1.0	Hf	0	Sm	0
K	0	Hg	0	Ta	0
Ti	.01	Ho	0	Tb	0
P	0	In	0	Te	0
Mn	M	Ir	0	Th	0
Ag	0	La	.01	Tl	0
As	.3	Li	0	Tm	0
Au	0	Lu	0	U	.1
B	0	Mo	.001	V	M
Ba	.1	Nb	0	W	0
Be	0	Nd	.03	Y	.003
Bi	0	Ni	.1	Yb	.0003
Cd	0	Os	0	Zn	0
Ce	.1	Pb	.03	Zr	.003
Co	.1	Pd	0		
Cr	.0003	Pr	.01		
Cs	0	Pt	0		
Cu	.1	Rb	0		
Dy	.03	Re	0		
Er	.03	Rh	0		

Figures are reported to the nearest number in the series 10, 3, 1, .3 etc., in per cent. Eighty per cent of the reported results may be expected to agree with the results of quantitative methods.

Symbols used are: — not looked for; 0 looked for, but not detected; M major constituent greater than 10%.

NOTE: The standard sensitivities for the elements determined by the semi-quantitative spectrographic method are those established by the Naval Gun Factory Laboratory, Geochemistry and Petrology Branch, U. S. Geological Survey.

senberg photographs. *X*-ray powder diffraction data obtained through use of a Norelco 114.59 mm. diameter powder camera, and a Nore'co Geiger counter *x*-ray diffractometer, and the calculated indices of reflections are listed in Table 3. The measured *d* values are in fairly good agreement with the calculated values. The space group, designated as

Table 2. Partial Chemical Analysis of Santafeite

(Analyst: Robert Meyrowitz, Naval Gun Factory Laboratory, Geochemistry and Petrology Branch, U. S. Geological Survey, Washington, D. C.

Constituent	%	Footnote	Constituent	%	Footnote
V_2O_5	35.6	h	CoO	0.1	d, g
MnO_2	16.6	i	NiO	0.1	e, g
MnO	13.7	i	CuO	0.5	f, g
CaO	6.2	j, o	UO_3	0.3	n, o
SrO	6.0	k, o	Insol+SiO_2	0.8	b, g
Na_2O	4.1	l, o	H_2O	8.8	q
K_2O	<0.1	m, o	CO_2	0.3	q
As_2O_5	2.2	p	Total	96.2	
Fe_2O_3	0.9	c, g	$H_2O(-)$	0.2	a, g

$B22_12$, D_2^5, was determined according to the condition of non-extinction of reflections shown by Weissenberg photographs. The criteria of non-extinction are: $(h+l)$ is even for hkl, l is even for $0kl$, h is even for $hk0$, $(h+l)$ is even for $h0l$, h, k, and l are even for $h00$, $0k0$, and $00l$ respectively.

Santafeite is highly brittle, tending to break even under very slight pressure. Small grains about 0.2 mm. long and 0.1 mm. thick were selected for single crystal study by Laue, rotation, and Weissenberg methods. Laue photographs were taken with the x-ray beam parallel to each of the three crystallographic axes. The Laue photograph with x-ray beam parallel to the a-axis (Fig. 2A) shows most reflections sharply defined. A photograph with beam parallel to the c-axis is similar to Fig. 2A. A photograph with beam parallel to the b-axis is shown in Fig. 2B, in which both sharp reflections and diffuse streaks are evident. Indices of some of the reflections were obtained from a gnomonic projection of this photograph. An orthorhombic symmetry is indicated for santafeite by the Laue patterns.

Rotation photographs about the a-axis and c-axis (Fig. 2D) show only layer lines of the first kind, with sharp reflections. The rotation photograph about the b-axis (Fig. 2C), however, shows so-called layer lines of the second kind that are characterized in part by sharp spots, and in part by diffuse streaks. Indices of the reflections along the zero layer line, derived by the graphic method, are listed in Table 4. Indices of the diffuse streaks on the zero layer line are 101, 301, 103, and 303. It appears that the diffuse streaks result from layer displacements of santafeite in the ac plane.

TABLE 3. X-RAY POWDER DIFFRACTION DATA: Fe RADIATION, Mn FILTER
FeKα=1.93728 Å

	d, Å, (Meas.)	*d*, Å (Calc.)	*hkl*	I
1	14.88	15.00	020	10
2	7.47	7.50	040	5
3	5.01	5.00	060	1
4	4.56	4.57	210	1
5	4.19	4.20	230	1
6	3.66	3.66	250	3
7	3.39	3.39	260	3
8	3.13	3.14	270	2
9	2.908	2.913	280	3
10	2.788	2.799	052	4
11	2.702	2.704	290	5
12	2.607	2.612	202	3
13	2.600	2.600	341	2
14	2.461	2.467	242	1
15	2.395	2.408	082	1
16	2.311	2.313	400	1
17	2.197	2.199	2 12 0	2
18	2.139	2.135	0 14 0	1
19	2.106	2.111	1 13 1	1
20	2.033	2.036	3 10 1	1
21	1.862	1.867	402	2
22	1.826	1.835	432	2
23	1.817	1.812	442	2
24	1.746	1.748	531	1
25	1.710	1.712	472	1
26	1.667	1.667	0 18 0	4
27	1.656	1.657	2 14 2	2
28	1.579	1.583	004	2
29	1.539	1.542	600	1
30	1.514	1.513	4 15 0	2
31	1.493	1.494	2 19 0	1
32	1.458	1.462	2 17 2	1
33	1.401	1.405	2 18 2	2
34	1.385	1.389	513	2
35	1.366	1.367	5 14 1	1
36	1.205	1.206	791	2

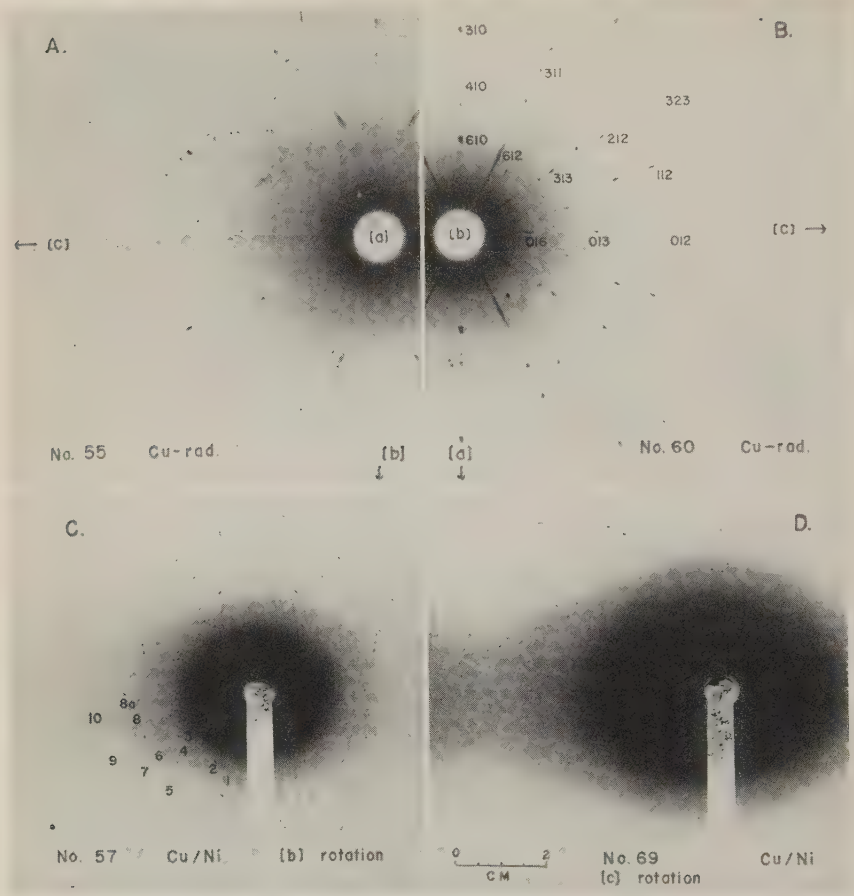

FIG. 2. A. Laue photograph of santafeite, x-ray beam parallel to a-axis. B. Laue photograph with x-ray beam parallel to b-axis; distance between crystal and film 6.64 cm. Note sharp spots and diffuse streaks reflections. C. b-axis rotation photograph. Note sharp spots and diffuse streaks of layer lines of the second kind. D. c-axis rotation photograph; camera diameter 57.3 mm. Scale of all four photographs indicated on Fig. 2D.

ACKNOWLEDGMENTS

The writers gratefully acknowledge the essential contributions to this report of several persons, all of whom are staff members of the U. S. Geological Survey. Dr. Michael Fleischer, at whose suggestion, and through whose courtesies the analyses were provided. Dr. Alice D. Weeks, who facilitated the analytical work in the Naval Gun Factory Laboratory of the Geochemistry and Petrology Branch, generously sup-

Table 4. Indices of Sharp Spot and Diffuse Streak Reflections of the *b*-Axis Rotation Photograph

Nos of layer lines of the 2nd kind	ξ	*hkl* (along zero layer line)		I
		Diffuse reflections	Sharp reflections	
1	.30	101		vs
2	.33		200	s
3	.56	301		m
4	.60		202	m
5	.67		400	w
6	.75	103		w
7	.83		402	s
8	.89	303		w
8a	.98		004	vs
9	1.02		600	vw
10	1.11		602	w

plied additional material for analysis that she and Mr. Robert Thaden collected, and offered many helpful suggestions. Mr. Robert Meyrowitz made the very difficult quantitative microchemical analysis, and provided the footnote outline of the procedure used. Miss Katherine E. Valentine contributed the spectrographic analysis. To these and others who assisted them, the writers extend their sincere thanks.

Dr. Abraham Rosenzweig of the University of New Mexico kindly helped in the space group interpretation.

The selection of the procedures used for the chemical analysis was based on the semi-quantitative spectrographic analysis of the mineral by Katherine E. Valentine, TWS-2841, August 31, 1956.

Footnotes:

(a) Dried to constant weight at 110±5° C.

(b) The "Insoluble+SiO_2" was determined gravimetrically by dehydration in a hydrochloric acid solution of the mineral using a quartz crucible.

(c) Fe_2O_3 was determined spectrophotometrically by the *o*-phenanthroline procedure using an aliquot of the filtrate from the "Insoluble+SiO_2" determination.

(d) CoO was determined spectrophotometrically by the nitroso-R salt procedure (Acetate Medium) as described by E. B. Sandell, "Colorimetric Determination of Traces of Metals, 2nd edition, 1950, page 277, using an aliquot of the filtrate from the "Insoluble+SiO_2" determination.

(e) NiO was determined spectrophotometrically using dimethylglyoxime according to the procedure of W. Oelschläger, *Z. Anal. Chem.*, **146**, 346–50 (1955). An aliquot of the filtrate from the "Insoluble+SiO_2" determination was used.

(f) CuO was determined spectrophotometrically using sodium diethyldithiocarbamate according to the procedure of K. L. Cheng and R. H. Bray, *Anal. Chem.*, **25,** 655–59 (1953). An aliquot of the filtrate from the "Insoluble+SiO_2" determination was used.

(g) The sample size for the $H_2O(-)$, "Insoluble+SiO_2," Fe_2O_3, CoO, NiO and CuO determinations was approximately 18 mg.

(h) The total vanadium calculated as V_2O_5 was determined spectrophotometrically using the hydrogen peroxide procedure. The sample was dissolved using hydrochloric acid. After oxidation by ammonium peroxydisulfate, the precipitate of manganese dioxide formed was dissolved by the addition of hydrogen peroxide. Orthophosphoric acid was used to mask the iron present. The sample size was approximately 4 mg. It was found that the mineral was not completely decomposed by boiling (1+3) H_2SO_4. The mineral was completely decomposed by evaporation to SO_3 fumes.

(i) The total manganese was determined spectrophotometrically using the peroxydisulfate procedure described by E. B. Sandell, Colorimetric Determination of Traces of Metals, 2nd Edition, 1950, pages 433–34. The sample size was approximately 2 mg. The total "available oxygen" was determined as follows: The sample and a weighed amount of $FeSO_4 \cdot (NH_4)_2SO_4 \cdot 6H_2O$ were boiled in a (1+9) H_2SO_4 solution under an atmosphere of N_2. The sample was completely decomposed. After the addition of ortho-phosphoric acid, the solution was titrated with standard 0.03N $K_2Cr_2O_7$ using sodium diphenylamine sulfonate as an indicator, to determine the excess $Fe(SO_4) \cdot (NH_4)_2SO_4 \cdot 6H_2O$. The sample size was approximately 7 mg. The "available oxygen" was arbitrarily calculated as MnO_2 after correcting for that due to V_2O_5. The remaining manganese is reported as MnO.

(j) CaO was determined by flame photometry (wave length = 554 mμ). The sample solution was compared to standard calcium solutions containing approximately the same concentration of sodium, strontium, vanadium, manganese, and iron present in the solution of the sample.

(k) SrO was determined by flame photometry (wave length = 461 mμ). The sample solution was compared to standard strontium solutions containing approximately the same concentration of calcium, sodium, vanadium, manganese, and iron present in the solution of the sample.

(l) Na_2O was determined by flame photometry (wave length = 589 mμ). The sample solution was compared to standard sodium solutions containing approximately the same concentrations of calcium, strontium, vanadium, manganese, and iron present in the solution of the sample.

(m) K_2O was determined by flame photometry (wave length = 765 mμ). The sample solution was compared to standard potassium solutions containing approximately the same concentrations of sodium, calcium, strontium, vanadium, manganese, and iron present in the solution of the sample.

(n) UO_3 was determined fluorimetrically by Grafton J. Daniels.

(o) A hydrochloric acid solution of the sample was used for the CaO, SrO, Na_2O, K_2O and UO_3 determinations. The sample size was approximately 16 mg. A Beckman Flame Spectrophotometer (DU) was used for the flame photometry. The flame was hydrogen-oxygen.

(p) As_2O_5 was determined spectrophotometrically after separation as the bromide according to a modified procedure of J. C. Bartlet, Margaret Wood, and R. A.

Chapman, *Anal. Chem.*, **24**, 1821–24 (1952). The sample size was approximately 1.3 mg.

(q) H_2O and CO_2 were determined by use of modified microcombustion train of the type used for the determination of carbon and hydrogen in organic compounds. The sample was decomposed by ignition at 900° C. in a stream of oxygen. The sample size was approximately 20 mg.

References

Buerger, M. J. (1942) *X-ray Crystallography*, John Wiley and Sons, Inc.

Gossner, B., and Strunz, H. (1932) Über strukturelle Beziehungen zwischen Phosphaten (Triphylin) und Silikaten (Olivin) und über die chemische Zusammensetzung von Ardennit: *Zeit. Krist.*, **83,** 419.

Gruner, J. W., Towle, C. C., and Gardiner, Lynn (1951), Uranium mineralization in Todilto limestone near Grants, McKinley County, New Mexico (abstract): *Bull. Geol. Soc. Am.*, **62,** 1445.

Gruner, J. W., Gardiner, Lynn, and Smith, D. K., Jr. (1954) Mineral associations in the uranium deposits of the Colorado Plateau and adjacent regions: *U. S. Atomic Energy Comm.*, **RME-3092,** 37–38.

Towle, C. C., and Rapaport, Irving (1952) Uranium deposits of the Grants district, New Mexico: *Min. Eng.*, **4,** 1039.

Weeks, A. D., and Thompson, M. E. (1954) Identification and occurrence of uranium and vanadium minerals from the Colorado Pleateaus: *U. S. Geol. Survey, Bull.* **1009-B,** 37–40.

Manuscript received August 6, 1957

GORCEIXITE FROM DALE COUNTY, ALABAMA*

CHARLES MILTON, J. M. AXELROD, M. K. CARRON, AND F. STEARNS MACNEIL, *U. S. Geological Survey, Washington 25, D. C.*

ABSTRACT

Two specimens of hydrous alkali-earth rare-earth aluminum phosphate from Eocene marl in southeastern Alabama have compositions approximating $RAl_3(PO_4)_2(F,OH)_5(H_2O)_3$ and $R_{0.8}Al_{4.6}(PO_4)_2(F,OH)_{10}(H_2O)_{0.3}$ respectively; the *x*-ray diffraction pattern of each is that of the alunite-plumbogummite-beudantite group. The mineral is isotropic, with n about 1.61, d about 3.09. No explanation of the difference in composition is offered; it is noted that the other recorded analyses of similar minerals show similar differences.

OCCURRENCE IN ALABAMA

Gorceixite, essentially $(Ba,Ca,Sr,Ce)Al_3(PO_4)_2(OH)_5 \cdot H_2O(?)$, occurs in four localities a few miles apart in southeastern Alabama, and is also found in Arkansas (Young, 1958). These occurrences are the first reported discoveries in North America of what may be a fairly widespread mineral, for it can be easily confused with bauxite, chert nodules, and similar appearing material. The Alabama occurrences are of special interest because of a substantial content (6–8 per cent) of rare earths.

The Alabama gorceixite is found as irregular nodules up to several inches across, in the weathered outcrops of the Bashi marl, the basal member of the Hatchetigbee formation, which is the youngest formation of the lower Eocene Wilcox group of Alabama. MacNeil first noted these nodules in 1943 in the vicinity of Ariton and Ozark, Dale County, Alabama. The Bashi is a highly fossiliferous glauconitic sand; it maintains a thickness of between 3 and 15 feet in the eastern Gulf region and is one of the most continuous single beds in the Tertiary of the Gulf Coast.

Gorceixite has been found at these four Dale County localities (the analyzed specimens are from A and B).

A. Road cut NW¼NE¼ sec. 18, T. 7 N., R. 24 E., about 2 miles southeast of Ariton, Dale County, Alabama.
B. Near the railroad on highway 53, 1 mile north of Dill, Dale County, Alabama.
C. Four hundred feet west of railroad cut on highway 53, near western boundary of Ariton, Dale County, Alabama.
D. On old road parallel to highway 53, about 0.9 mile west of intersection of these roads, at Ariton, Dale County, Alabama.

Nodular material superficially resembling gorceixite is present in many localities in Dale County. However, study by *x*-ray fluorescence of several of these nodules, in some instances further confirmed by *x*-ray diffraction, showed that none of this material is gorceixite.

* Publication authorized by the Director, U. S. Geological Survey.

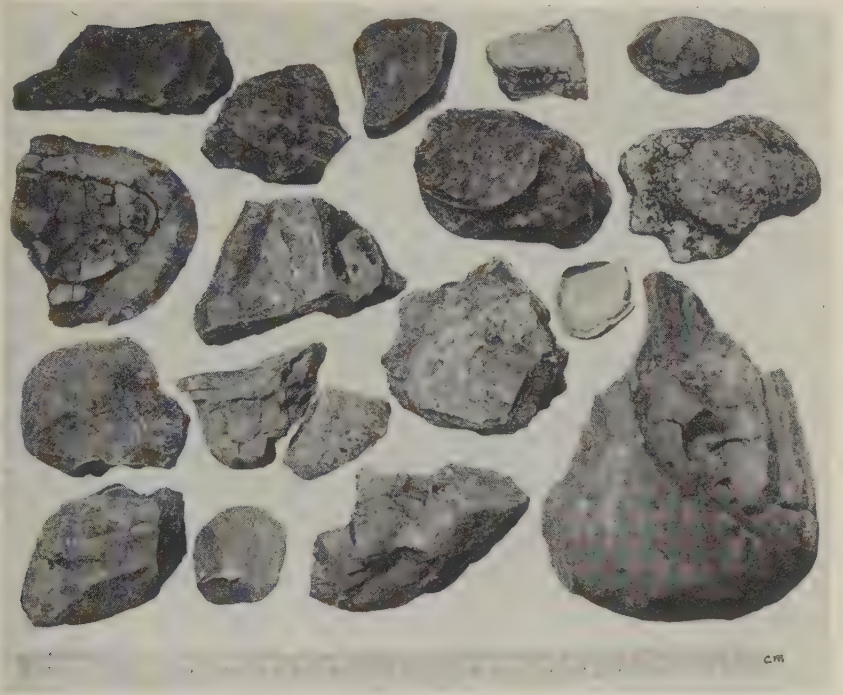

FIG. 1. Gorceixite nodules from Bashi marl member of the Hatchetigbee formation, Dale County, Alabama, one mile north of Dill. Shows typical aspect of nodules. These are free from glauconite, and are the material analyzed as sample B.

PHYSICAL PROPERTIES

The *x*-ray diffraction pattern of the gorceixite is very similar to those of svanbergite from Sweden, U. S. National Museum no. C 4444, harttite (calcian svanbergite) from Brazil, U. S. National Museum no. 94797, and gorceixite from Brazil, U. S. National Museum no. C 4296. These are all members of the alunite-plumbogummite-beudantite group.

The density of the Alabama gorceixite (analysis A, including quartz and calcite) is 2.93, with correction for quartz and calcite (analysis A_1) the density is computed as 3.09. The index of refraction of the isotropic substance is 1.61. The color of the nodules is generally dirty white; there are dark specks of glauconite in some nodules. The nodules are firmly coherent. Thin sections (Figs. 2 and 3) indicated as much as 70 per cent of apparently isotropic gorceixite, with lesser quartz and glauconite (the latter removed before analysis by the electromagnet and hand-picking). Sample $B\text{-}B_1$ is nodular gorceixite (free from glauconite); typical such nodules are shown in Fig. 1.

FIG. 2. Thin section of nodule, such as shown in Fig. 1. The white areas are quartz, the dark spots are light brown organic (phosphatic) material. The gray matrix is gorceixite.

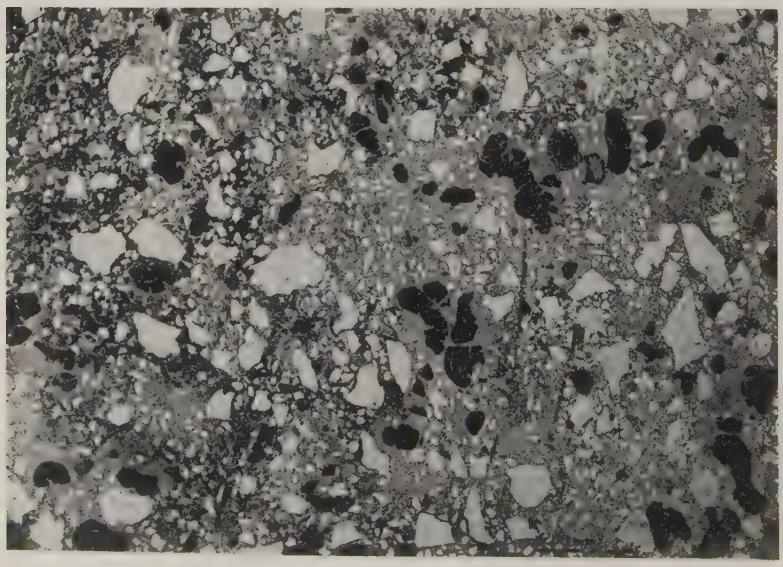

FIG. 3. From 2 miles southeast of Ariton, Alabama. Thin section of glauconitic marl, showing abundant quartz (white) and glauconite (dark). The gray matrix is gorceixite. Material such as this was analyzed after removal of glauconite (Sample A).

Analyses

Gorceixite is one of the plumbogummite group of hexagonal minerals of general formula,

$AB_3(XO_4)_2(OH)_5H_2O_{(1-0)}$ where A may be Pb, Ba, Sr, Ca, or Ce; B may be Al, or Fe, and X may be P or As.

Chemical analyses of two specimens were made by M. K. Carron; supplementary spectrographic investigations of the rare-earth content of specimen A were made by H. J. Rose, and of minor elements, including rare earths, of specimen B by Harry Bastron. The analyses are given in Tables 1, 2, and 3.

Discussion of Analyses

Analysis A_1, corrected for quartz and calcite, agrees reasonably well with the theoretical $BaAl_3(PO_4)_2(OH)_5 \cdot H_2O$ (although H_2O is 3 instead of 1). This formula is by no means fixed, in fact, it is expressly stated to be "uncertain," "perhaps $BaAl_3(PO_4)_2(OH)_5 \cdot H_2O$." (2). The same uncertainty is noted about other members of the plumbogummite group, in particular plumbogummite itself and crandallite. One source of uncertainty may be analytical, involving the troublesome estimation of the respective alkaline earths, another may be the valence state of cerium, CeO_2 or Ce_2O_3. At any rate, scrutiny of the three analyses of gorceixite cited by Palache, Berman, and Frondel (1944), shows a much closer approximation to $BaAl_5(PO_4)_2(OH)_{11}$. This, again, is close to our analysis B_1 which computes near to (Ba,Sr,Ca,RE, etc.)$Al_5(PO_4)_2 \cdot (F,OH)_{11}$.

The excess of Al_2O_3 and H_2O, in sample B as compared to sample A, cannot be referred to any impurity, observable either optically or by *x*-ray pattern; in particular, diaspore, gibbsite, or boehmite. Because the quartz present is practically equivalent to the total silica, there can be little if any mica or clay.

In summary, analyses of gorceixite, one of the two from Alabama included, tend to show an excess of $Al(OH)_3$ over the simple formula generally given; however, this excess cannot be referred to any specific mineral as admixture.

The mineral from Alabama which we have called gorceixite contains more or less equivalent amounts of Ba, Sr, Ca, and rare earths, corresponding to the recognized end member minerals gorceixite, goyazite, crandallite, and florencite. Thus, the name given is not entirely satisfactory, but a new name does not seem warranted.

The origin of these gorceixite nodules is an unsolved problem. They

TABLE 1. CHEMICAL ANALYSES OF GORCEIXITE, DALE COUNTY, ALABAMA
M. K. Carron, analyst

	A	A_1	B	B_1
SiO_2	31.90	—	17.82	—
Al_2O_3	17.17	25.70	33.72	41.14
Fe_2O_3	2.58	3.86	1.03	1.26
P_2O_5	18.30	27.40	20.10	24.52
BaO	4.56	6.83	2.90	3.54
SrO	3.56	5.33	3.94	4.81
CaO	2.14	2.29	1.02	1.24
MgO	.08	.12	.22	.27
Ce_2O_3	1.29	1.93	3.88*	4.73*
La_2O_3, etc.	3.91	5.85		
TiO_2	.54	.81	.03	.04
Na_2O	.05	.07	.17	.21
K_2O	.24	.36	.48	.58
PbO	—	—	.08	.10
H_2O-	1.32	1.98	1.15	1.40
H_2O+	10.16	15.21	11.93	14.56
CO_2	.48	—	—	—
SO_3	.29	.43	.73	.89
F	2.11	3.16	1.01	1.23
	100.68	101.33	100.21	100.52
$O=F_2$	−.89	−1.33	−.43	−.52
	99.79	100.00	99.78	100.00

Density: 2.93 (measured). 3.09 (corrected).

* Total rare earth oxides.

A—Gorceixite associated with glauconite, etc., in nodules about 2 miles southeast of Ariton, Dale County, Alabama.

A_1—Analysis A, recalculated after deducting 31.90 per cent SiO_2 (quartz) and 1.09 per cent $CaCO_3$ (based on 0.48 per cent CO_2).

B—Gorceixite from glauconite-free nodules 1 mile north of Dill, Dale County, Alabama.

B_1—Analysis B, recalculated after deducting 17.82 per cent SiO_2 (quartz).

Analysis A_1 is computed to:

$(Ba_{0.23}Sr_{0.26}Ca_{0.21}Mg_{0.02}RE_{0.24}Na_{0.01}K_{0.04})$ $\Sigma=1.01$

$(Al_{2.58}Fe^{3+}_{0.25}Ti^{4+}_{0.05})$ $\Sigma=2.88$

$(PO_4)_{1.97}(SO_4)_{0.03}$ $\Sigma=2.00$

$(F_{0.85}(OH)_{4.07})$ $\Sigma=4.92$

$(H_2O_{2.85})$ $\Sigma=2.85$

giving (Ba, Sr, Ca, RE, etc.)(Al, Fe, Ti)$_3$$(PO_4)_2(F, OH)_5$$(H_2O)_3$

Analysis B_1 is computed to:

$(Ba_{0.13}Sr_{0.26}Ca_{0.12}Mg_{0.04}RE_{0.16}Pb_{0.003}Na_{0.04}K_{0.07})$ $\Sigma=0.82$

$(Al_{4.53}Fe^{3+}_{0.09}Ti^{4+}_{0.003})$ $\Sigma=4.62$

$(PO_4)_{1.94}(SO_4)_{0.06}$ $\Sigma=2.00$

$(F_{0.36}(OH)_{9.29})$ $\Sigma=9.65$

$(H_2O_{0.34})$ $\Sigma=0.34$

giving (Ba, Sr, Ca, RE, etc.)$_{0.82}$(Al, etc.)$_{4.6}$$(PO_4)_{2.0}(F, OH)_{10.0}$$(H_2O)_{0.3}$

Essentially this formula is equivalent to that of A_1 with excess of $(Al)_{1.6}(OH)_{5.0}$, or $[Al(OH)_{3.0}]_{1.6}$, and deficiency of $(H_2O)_{2.7}$.

TABLE 2. RARE EARTH DISTRIBUTION (SPECTROGRAPHIC) OF GORCEIXITE, DALE COUNTY, ALABAMA (COMPOSITION OF THE 5.20 PER CENT TOTAL RARE EARTHS OF ANALYSIS A, TABLE 1)

Harry Ross, U. S. Geological Survey, analyst

CeO_2	36.8
La_2O_3	16.5
Nd_2O_3	25.0
Pr_6O_{11}	5.9
Y_2O_3	4.1
Yb_2O_3	—
Sc_2O_3	—
ThO_2	.0
Sm_2O_3	6.1
Gd_2O_3	3.9
	98.3

TABLE 3. MINOR ELEMENT CONTENT (SPECTROGRAPHIC) OF GORCEIXITE, DALE COUNTY, ALABAMA, ANALYSIS B, TABLE 1

Harry Bastron, U. S. Geological Survey, analyst

Cu	0.002			
Pb	.06			
Cr	.003			
V	.005			
Ti	.1			
Zr	.01			
Be	.01			
Sr	1.2			
Ba	4.5			
B	.01			
Ce	1.5	=	Ce_2O_3	1.75
La	1.0	=	La_2O_3	1.17
Nd	1.0	=	Nd_2O_3	1.16
Pr	.2	=	Pr_2O_3	.23
Y	.07	=	Y_2O_3	.09
Yb	.005			
Sc	.02			4.40

NOTE: The total of rare earths spectrographically 4.40 per cent is reasonably close to the chemically determined (weighed) total rare earths 3.88 per cent. The spectrographic and chemical Ba and Sr differ: Spectrographic (BaO) 5.0, (SrO) 1.4, chemical (BaO) 2.90, (SrO) 3.94. This discrepancy may reflect the difficulty of separating Ba and Sr chemically. The sum of the two oxides spectrographically is 6.4, chemically 6.8.

may have been deposited as such on the sea floor, or accumulated in the sediment during its diagenesis. Or, they may have formed subaerially during the weathering of the Bashi marl member, either directly, or perhaps as partial replacement of more common calcareous phosphate concretions.

Acknowledgment

We are indebted to Mr. Hugh D. Pallister, Geologist of the Alabama State Geological Survey, for his friendly interest in this investigation, and guidance in a field study of these occurrences.

References

Young, Edward J., (1958) An occurrence of gorceixite in Arkansas: *Am. Mineral.* **43,** 762.

Palache, C., Berman, H., and Frondel, C. (1944) Dana's System of Mineralogy, 7th ed., vol. 2, p. 833.

Manuscript received October 10, 1957

THE AMERICAN MINERALOGIST, VOL. 43, JULY-AUGUST, 1958

AN APPARATUS FOR THE STUDY OF THERMOLUMINESCENCE FROM MINERALS*

G. E. Ashby[1] and R. C. Kellagher,[2] *U. S. Geological Survey, Washington 25, D. C.*

Abstract

An apparatus has been constructed to record the thermoluminescence of a mineral in the form of a powder or a single crystal at temperatures from −100° C. to +400° C. Glow curves are obtained by heating the sample at a constant rate and recording the intensity of thermoluminescence as a function of temperature. The apparatus has provision for the irradiation of the sample with *X*-rays or ultraviolet light and for measurement of the induced luminescence during any part of the experiment. Upon termination of the irradiation the measurement of the luminescence can be continued at any desired temperature and rapidly decaying phosphorescence can be detected. In all these experiments the sample remains undisturbed, and the problems associated with the heterogeneity of the sample are thus reduced.

Introduction

Recent studies (Daniels and Saunders, 1951; Daniels, Boyd, and Saunders, 1953; Saunders, 1953, Pitrat, 1956, and Zeller, Wray, and Daniels, 1957) have shown that a study of the thermoluminescence of minerals and rocks can provide information applicable to problems in stratigraphy, geologic age determination, and geothermometry. It has been established that some minerals have electron traps that are the result of imperfections in the crystal structure such as vacant lattice sites, interstitial atoms, foreign atoms in either interstitial or substitutional positions, and dislocations (Seitz, 1952), and that these imperfections are a function of the environmental conditions during crystallization and the subsequent history of the mineral. Excited electrons produced by ionizing radiations interacting with the mineral are trapped by the lattice imperfections. The time that the trapped electrons exist in a metastable energy state depends on the binding energy of the trap and the temperature of the solid. Some electrons exist in a metastable state throughout geologic history and can be released at a future time by the application of heat. A solid is termed thermoluminescent if the electrons detrapped by heat make energy transitions that yield wavelengths in the visible region.

Several designs of apparatus for studying thermoluminescence have been described. Randall and Wilkins (1945) obtained glow curves from

* Publication authorized by the U. S. Geological Survey and the Atomic Energy Commission.

[1] Present address: W. R. Grace Company, Washington Research Center, Clarksville, Maryland.

[2] Present address: Melpar Company, Falls Church, Virginia.

sample material brushed on the prepared surface of an electrically heated copper box. A thin layer of sample is spread on the surface of the box, using a slight smear of glycerol as a binder. A thermocouple is soldered to the same surface and a helical coil of resistance wire is arranged within the box to function as a heater. The entire apparatus is cooled by liquid air. When the sample reaches the desired temperature, it is activated by irradiation with the light from a mercury arc until the electron traps are filled. After activation of the sample the box is removed from the coolant and placed in the dark before an electron multiplier tube. The heater is then energized and and the sample is heated at a constant rate to produce luminescence. A glow curve is obtained by recording the intensity of the luminescence as a function of temperature.

Daniels and Saunders (1951) described a similar apparatus in which glow curves are obtained from room to incandescence temperatures from a sample spread on the surface of an electrically heated silver block. Sample materials are reactivated by *x*-ray, gamma-ray, or ultraviolet light irradiation before being placed in the apparatus. In a later design by Daniels, a tungsten strip is substituted for the silver block in order to obtain a higher heating rate and increased sensitivity. Heckelsberg (1951) has described an apparatus that permits a sample to be reactivated at liquid air temperatures with *x*-rays, and that will yield glow curves from liquid air to room temperatures.

In the present paper an apparatus is described that will record the thermoluminescent properties of a sample in the form of a powder or single crystal, at temperatures from −100° C. to +400° C., at either fast or slow controlled heating rates. It has provision for the irradiation of the sample with *x*-rays or ultraviolet light and for the measurement of the induced luminescence during any part of the experiment. Upon termination of the irradiation the measurement of the luminescence can be continued and rapidly decaying phosphorescence can be detected. In all of these experiments the sample remains undisturbed and the problems associated with the heterogeneity of the sample are thus reduced.

We wish to acknowledge our discussions of the problems in measuring thermoluminescence with C. L. Christ, U. S. Geological Survey, and Farrington Daniels, University of Wisconsin. The apparatus was constructed by E. L. Curtis and J. F. Abell of the U. S. Geological Survey. This report concerns work conducted by the Geological Survey on behalf of the Division of Research of the U. S. Atomic Energy Commission.

Description

The thermoluminescence apparatus consists of an electrically-heated sample stage positioned under a photomultiplier tube in a light- and gas-

tight cylinder (Fig. 1). This cylinder is an assembly of three individual units, a barrel to house the photomultiplier tube, a cap containing the tube-socket assembly, and a base containing the heater. Mounting studs

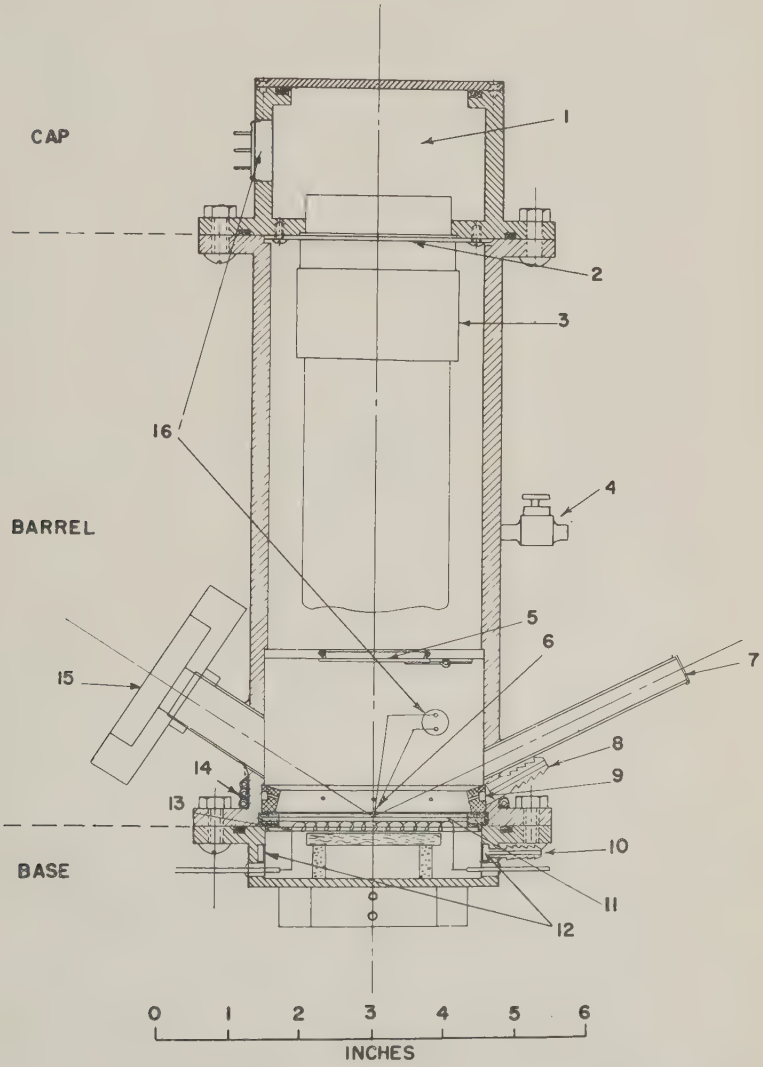

FIG. 1. Thermoluminescence apparatus: (1) space for electrical circuits, (2) tube socket, (3) photomultiplier tube, (4) gas exhaust valve, (5) shutter, (6) thermocouple, (7) X-ray collimator, (8) gas inlet, (9) gas manifold, (10) water connections, (11) sample stage, (12) water conduit, (13) heating element, (14) water cooling coils, (15) filter adapter, and (16) ceramic plugs for electrical connections.

on the flange of the heater unit and on the upper flange of the barrel are used to position the units for assembly. Ring seals between the flanges form light- and gas-tight barriers when the unit is assembled. This construction permits easy access to the internal parts of the apparatus and enables the operator to change samples with a minimum of effort.

The largest unit, the barrel, is a machined brass cylinder $8\frac{1}{2}$ in. long with a diameter of $3\frac{1}{4}$ in. and has a $\frac{3}{4}$ by $\frac{1}{4}$ in. flange on each end. Inside the barrel is a brass diaphragm $2\frac{1}{4}$ in. from the bottom face. The diaphragm has a 1-in. diameter aperture with a circular shutter that can be opened or closed from outside the barrel by means of a knob.

A gas manifold containing eight ports is at the base of the barrel. Its purpose is to direct a flow of inert gas onto the sample stage. Gas is introduced into the manifold through a fitting soldered into the barrel wall and controlled by adjusting an exhaust valve in the wall of the upper chamber.

A brass tube of $\frac{3}{8}$-in. inside diameter is soldered into the side of the lower chamber at an angle of 26° with the axis of the barrel at a point 1 inch above the base. This tube acts as an x-ray collimator and permits irradiation of the center of the stage with x-rays. The tube is closed at the outer end with a beryllium foil 0.007-in. thick to make it light- and gas-tight. This foil is transparent to x-rays.

Opposite the x-ray collimator and similarly mounted is a tube of $\frac{3}{4}$-in. inside diameter that is used principally to allow light transmission to and from the sample through the barrel wall. This tube is also useful for final positioning of samples and adjusting thermocouples before an experimental run. An adapter, fitted to the tube, will accommodate one or more 2-by-2-in. light filters. These filters are useful for restricting the wavelengths of the light that strike the sample and for spectral analysis of the thermoluminescent light. The tube is normally closed with a black rubber stopper when light from the room cannot be tolerated.

Temperature measurements are made with two chromel-alumel thermocouples in the sample chamber. The leads of the thermocouples are connected to a terminal strip on the outside surface of the barrel and enter the sample chamber through a light- and gas-tight ceramic plug mounted in the barrel wall. The ceramic plug and terminal strip have provision for additional leads for electrical conductivity measuring apparatus. In addition, the barrel is water-cooled to protect the photomultiplier tube and ring seals from damage. The water flows through a three-turn coil soldered around the base of the barrel.

The cap or photomultiplier tube socket assembly holds the tube socket in position and contains part of the electrical circuits for the tube. The cap has a brass collar, $3\frac{1}{4}$ in. in diameter by $2\frac{1}{4}$ in. long, with a $\frac{3}{4}$-by-$\frac{1}{4}$-in.

flange on one end. The socket is centrally mounted with the tube side of the socket flush with the flange surface and held in position by two screws. A distance of approximately $1\frac{1}{2}$ in. extends above the socket to accommodate electrical circuits. This space is closed by a cover plate and sealed with a ring seal. A ring seal is also placed in the flange to seal the connection between this assembly and the barrel. A light- and gas-tight ceramic plug soldered in the collar allows electrical connections to be made from the tube socket to an external terminal strip.

The base (Fig. 2) consists of the heating element, sample stage, and a housing. A nichrome-V wire spiral of 50 ohms resistance wound over a

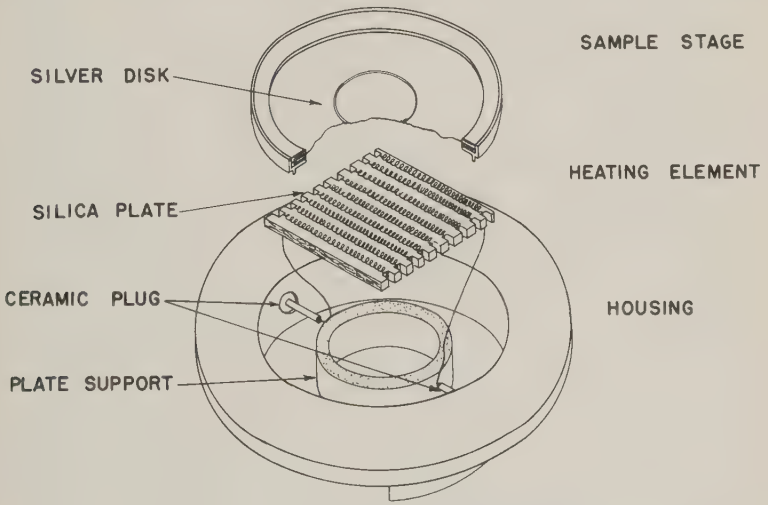

Fig. 2. An exploded view of the base of the thermoluminescence apparatus.

silica plate 2-by-2-by-$\frac{1}{8}$-in. serves as the heating element. The plate is notched to position the winding and is designed to space ten spirals across the surface. Ceramic beads are placed on the windings to prevent shorting between adjacent spirals and between the windings and the silver stage.

A sample stage, composed of a silver disk 0.02 in. thick and $2\frac{3}{4}$ in. in diameter, is mounted in a brass ring between asbestos gaskets. The ring positions the stage over the heating element and forms a light-tight seal between the heating element and photomultiplier tube. A silver ring with a diameter of $\frac{7}{8}$ in., a wall height of $\frac{1}{8}$ in., and a thickness of 1/32 in., is silver-soldered to the center of the stage to retain the sample in position under the photomultiplier tube.

The heating element is contained in a flanged brass cup $\frac{7}{8}$ in. deep and 3 in. in diameter and is positioned with the upper surface of the element flush with the cup rim. A silver sample stage is placed above this surface and in contact with the ceramic beads on the element. A water conduit in the wall of the housing surrounds the element and keeps the wall of the cup at approximately room temperature while the heater is in operation. Electrical connections for the element are made through gas-tight

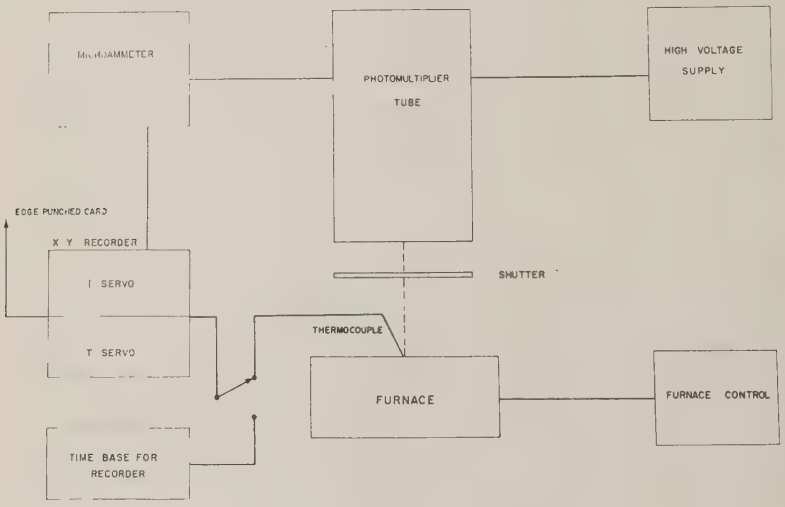

FIG. 3. Block diagram of the electrical circuits.

ceramic plugs. The base of the heater has been machined to fit a standard camera track of an x-ray diffraction unit.

Controlled low temperatures of $-100°$ C. to room temperature are obtained in the sample chamber by a nitrogen cooling system. The lower part of the apparatus is immersed in liquid nitrogen to obtain a $-100°$ C. temperature. When a higher temperature is desired the heating element is energized and controlled with a 0 to 115 volt autotransformer.

Electrical circuits for the apparatus are shown in a block diagram, (Fig. 3) and in a wiring diagram (Fig. 4). High voltage for the operation of the photomultiplier tube is supplied by a battery pack containing twenty-four 45-volt batteries connected in series. Selected voltages from 855 volts to 1080 volts, in increments of 45 volts, are supplied to the tube through a six-position selector switch on the power supply chassis. A conventional voltage divider connected to this high-voltage supply provides the voltages necessary for each dynode of a 5819 photomultiplier tube.

The photomultiplier tube develops an anode current that is directly proportional to the amount of light striking the photosensitive cathode. Current from the anode is measured by a modified ultrasensitive direct-current microammeter. An anode current of 0.01 microamperes is sufficient to give full scale deflection on the meter of this instrument with an overall accuracy of ± 5 per cent. Full scale currents of 0.1, 1.0, 10, 100, and 1000 microamperes can also be selected with a range switch.

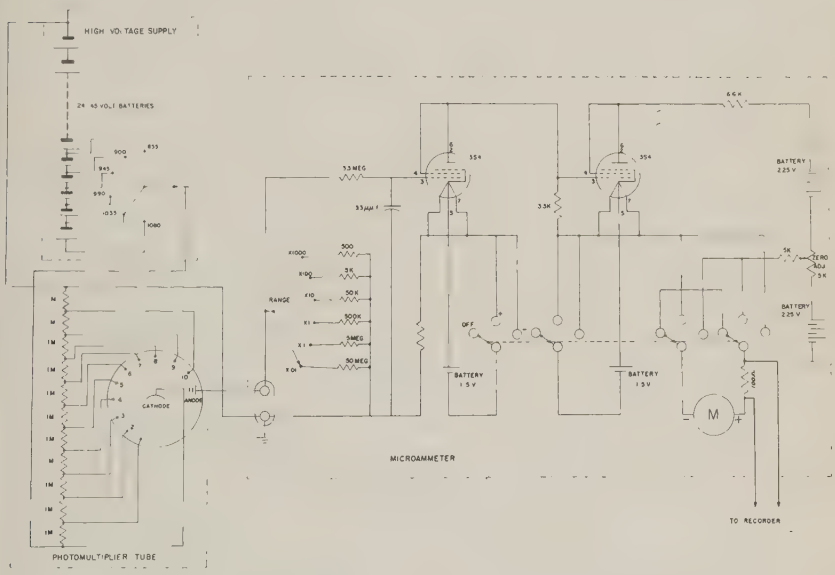

FIG. 4. Wiring diagram of the high voltage supply, photomultiplier tube, and microammeter.

An output signal suitable for a strip-chart recorder is obtained from the microammeter by a slight modification of the circuit. A 100-ohm resistor in series with the meter develops approximately a 10-millivolt voltage drop at full scale on all ranges. This voltage drop is used as an output signal to the recorder.

The recorder consists of two servo units: a pen-drive unit operating from the output signal of the microammeter, and a chart-drive unit operating from either a thermocouple or time-base generator. Both of these servos operate on the principle of a self-balancing potentiometer. In each, a servo motor rotates a potentiometer to produce a direct-current voltage that exactly cancels the applied direct-current signal, and thus determines the position of the writing pen or chart. These servo units

have a full-scale sensitivity of 10 millivolts with a 2.5-second full-scale response time.

The chart servo unit can be connected to either a thermocouple signal or time signal by a selector switch. At the thermocouple setting of the switch a chromel-alumel thermocouple is connected in series with a voltage-dividing resistor. A voltage change produced by the thermocouple will move the chart with respect to the pen an amount proportional to the change. With the switch in this position and with the thermocouple in contact with the sample, current from the photomultiplier is displayed on the chart as a function of the temperature of the sample. The scale factor of the chart may be adjusted to any value from 5° C. to 20° C. per division by the voltage-dividing resistor.

A voltage varying as a linear function of time is introduced into the chart-servo from the time-base generator when the selector switch is on the "time" setting. This generator consists of a 10-turn potentiometer with a wiper driven by a $\frac{1}{2}$-rpm synchronous motor. By adjusting the voltage supplied to the potentiometer, the rate of change of the voltage output of the generator can be varied from $\frac{1}{2}$ millivolt to 5 millivolts per minute. Variable chart speeds can be obtained in this manner. With the switch on the "time" setting, the current from the anode of the photomultiplier is displayed as a function of time.

The photomultiplier, microammeter, and time-base generator are all powered by batteries in order to reduce the pickup of stray currents and thus to increase the stability of the servo system.

The charts for the recorder are printed on cards 12 inches long. With the chart in this form, the drive sprocket holes along its edge may be punched and the chart indexed and sorted as an edge-punched card.

Operation

The apparatus is designed to perform three basic thermoluminescence experiments: (1) to heat a sample at a constant rate and measure the light emission as a function of temperature—that is, to produce the glow curve; (2) to irradiate the sample at a known temperature and measure the light emission as a function of time—that is, to produce the saturation curve; and (3) to measure the phosphorescence from a sample as a function of time—that is, to produce the decay curve. The procedure for operating the apparatus varies with each type of experiment. In all experiments, the method of mounting the sample, the positioning of the thermocouple, and adjustment of the light recording equipment is identical. The sample, a specimen of mineral or rock in the form of a powder or thin slab is mounted in an area of $\frac{7}{8}$-in. diameter at the center of the stage. When the barrel is assembled to the heater unit the thermocouple is

positioned on the surface of the sample. Observation and manipulation of the thermocouple can be made through the larger tube in the barrel wall to insure contact with the sample.

The adjustment of the light recording equipment consists of: (1) selecting a voltage for the photomultiplier tube, (2) selecting the range setting for the microammeter, (3) zeroing the microammeter and pen servo system. The photomultiplier tube is usually operated at 855 volts but occasionally higher voltages are used when increased sensitivity is de-

FIG. 5. A typical glow curve for calcite obtained after activation with x-rays.

sired. In selecting a range setting a value should be used that will make the maximum response during the experiment approach the full-scale value of the microammeter. This selection is, of course, impossible in most experiments without prior knowledge of the result. The operator can, however, from experience with the behavior of different types of samples predict approximately the range setting for the experiment. In general, the setting is usually 0.1, 1, or 10 microamperes. The microammeter and pen servo are adjusted to zero with the apparatus assembled and the shutter in the closed position. A zero-adjusting resistor is used to balance the bridge circuit of the microammeter. The pen servo system is adjusted to give a zero pen position on the chart when the microammeter is at zero.

After mounting the sample and adjusting the circuits the equipment is ready for determination of either a glow curve, saturation curve, or decay curve. To obtain a glow curve, the sample is heated at a constant rate by controlling the voltage supplied to the heater with a 0-to-115-

volt autotransformer. Before the sample is heated, the chart is adjusted to show the initial temperature of the sample. This temperature is obtained by comparing the voltage developed by the thermocouple on the sample to that developed by a thermocouple at 0° C. The glow curve is recorded with the thermoluminescence intensity expressed as the ordinate and the sample temperature as the abscissa (Fig. 5).

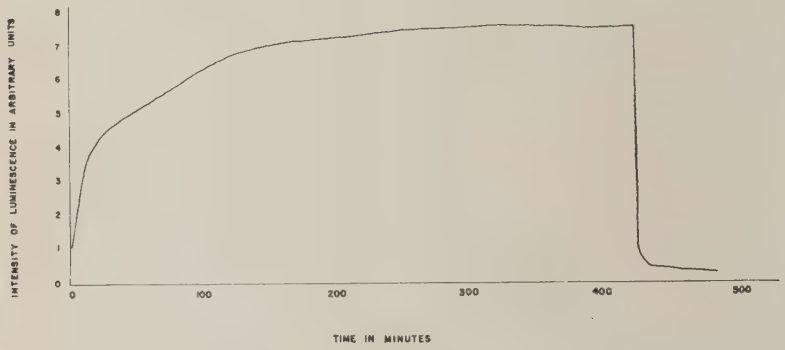

FIG. 6. Typical saturation and decay curves for calcite. *X*-ray irradiation was terminated after 428 minutes.

The saturation curve is obtained by recording the fluorescence intensity as a function of the time of irradiation by *x*-rays or light (Fig. 6). When *x*-ray irradiation is desired the apparatus is mounted on a standard camera track of an *x*-ray diffraction unit (Fig. 7) so that the *x*-ray beam passes through the *x*-ray collimator in the barrel wall and strikes the sample. As the photomultiplier is only sensitive to wavelengths between 3000 and 6600 Å, it will not record *x*-ray photons. When ultraviolet light is used for excitation, the apparatus is positioned so that the light source is adjacent to the filter adapter. Filters are selected and mounted in the adapter that will transmit only the desired wavelengths to the sample. In addition, a filter can be placed on the diaphragm between the photomultiplier and the stage to absorb reflected light from the sample stage.

PERFORMANCE

The following data illustrate the performance of the apparatus:

(1) Maximum constant heating rate: 2.7° C. per second
(2) Optimum maximum temperature of stage: 400° C.
(3) Average cooling time from 400° C. to room temperature: $2\frac{1}{2}$ minutes
(4) Optimum minimum temperature of stage: −100° C.
(5) Maximum light sensitivity (at 4900 Å): 4.2×10^{-12} lumens per chart division.

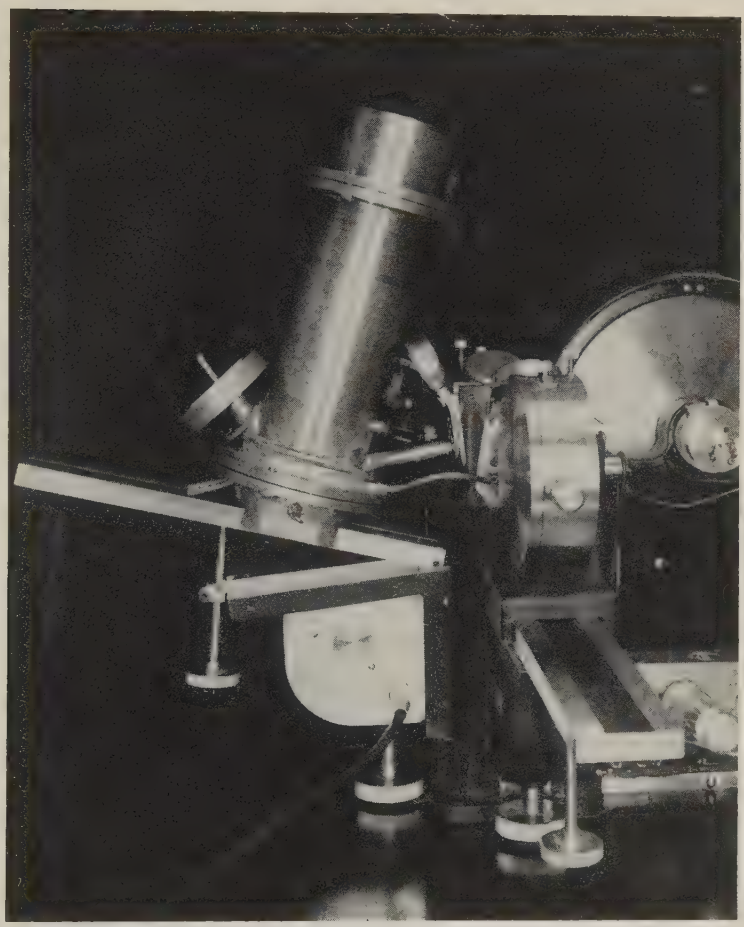

FIG. 7. The thermoluminescence apparatus mounted on an x-ray diffraction camera track.

(6) Noise at maximum sensitivity: 5.0 chart division or 2.0×10^{-11} lumens
(7) Response time of recorder: 3.0 seconds for full scale on either servo
(8) Accuracy of microammeter: ±5 per cent of full scale
(9) Accuracy of recorder: ±1 per cent of full scale

The most probable sources of error in the measurement of the temperature of the sample are in the heat loss through the thermocouple leads and variation in contact between the thermocouple and sample. If these errors are negligible and the voltage at the ends of the thermocouple leads is a true measure of the sample temperature, then the chart will indicate the temperature to within $\pm2°$ C.

References

Daniels, Farrington, Boyd, C. A., and Saunders, D. F., 1953, Thermoluminescence as a research tool: *Science*, **117**, 343–349.

Daniels, Farrington, and Saunders, D. F., and others, 1951, The thermoluminescence of crystals—Final Report: U. S. Atomic Energy Comm. AECU-1583, 26 chap. Microcard copy on file in U. S. Atomic Energy Comm. depository libraries.

Heckelsberg, L. F., 1951, Thermoluminescence and related properties of the alkalies, chap. 5, p. 1–29, *in* Daniels, Farrington, and Saunders, D. F., and others, The thermoluminescence of crystals—Final Report: U. S. Atomic Energy Comm. AECU-1583, 26 chap. Microcard on file in U. S. Atomic Energy Comm. depository libraries.

Pitrat, C. W., 1956, Thermoluminescence of limestones of Mississippian Madison group in Montana and Utah: *Am. Assoc. Petroleum Geologists Bull.*, **40**, 943–952.

Randall, J. T., and Wilkins, M. H. F., 1945, Phosphorescence and electron traps I. The study of trap distributions: *Royal Soc. London Proc. A*, **184**, 366–389.

Saunders, D. F., 1953, Thermoluminescence and surface correlation of limestones: *Am. Assoc. Petroleum Geologists Bull.*, **37**, 114–124.

Seitz, Frederick, 1952, Imperfections in nearly perfect crystals: A synthesis, *in* Shockley, W., and others, eds., Imperfections in nearly perfect crystals, Symposium held at Pocono Manor, October 12–14, 1950: New York, John Wiley and Sons, Inc., 490 p.

Zeller, E. J., Wray, J. L., and Daniels, Farrington, 1957, Factors in age determination of carbonate sediments by thermoluminescence: *Am. Assoc. Petroleum Geologists Bull.*, **41**, 121–129.

Manuscript received October 11, 1957

THE AMERICAN MINERALOGIST, VOL. 43, JULY-AUGUST, 1958

SYNTHESIS OF THE CHLORITES AND THEIR STRUCTURAL AND CHEMICAL CONSTITUTION*

BRUCE W. NELSON,[1] AND RUSTUM ROY, *College of Mineral Industries, Pennsylvania State University, University Park, Pennsylvania, U.S.A.*

ABSTRACT

Experimental hydrothermal studies on both synthetic and natural phases in a portion of the system MgO-Al_2O_3-SiO_2-H_2O reveal the polymorphic relationship between 7 Å sheet trioctahedral phases and true 14 Å-chlorites. Each polymorphic type allows continuous extensive isomorphous replacement of 2 Al^{3+} for $Si^{4+}+Mg^{2+}$ terminating at the amesite composition. The equilibrium maximum stability temperature for the chlorites appears to reach a maximum at the composition of clinochlore (710° C. at 20,000 psi) and to decrease slightly (~20° C.) towards both penninite and amesite. The nomenclature and relations among the various chlorites is discussed in the light of this information.

INTRODUCTION

An entirely satisfactory systematization of the chlorite group is difficult primarily because of the discrepancies between chemical and structural data now available for the chlorites. A recent review of the chlorite problem has been given in Hey's excellent paper (1954). The continuous nature of chemical variation between different end member molecules has been shown by chemical analysis of natural chlorites, and Tschermak (1890, 1891) and Winchell (1926) explained the compositional differences between chlorites through isomorphism. Structural investigations reveal that most chlorites contain alternating mica-type and brucite-type layers in their crystal structures (Pauling, 1930). But other chlorites, notably amesite, cronstedtite, many chamosites, and the serpentine or antigorite minerals, and, in fact, all of the end member compositions in Winchell's classification are represented by layer structures consisting of trioctahedral 7 Å units. This lack of isostructural regularity in the chlorite group seems to preclude the existence of isomorphism between the end members. In the course of hydrothermal mineral synthesis studies we have found two isostructural series within the chlorite group which bear a polymorphic relationship to each other. The existence of these two polymorphic isostructural series supplies a significant advance in our understanding of the chlorites.

This paper discusses the magnesian chlorites. A series of trioctahedral

* Contribution No. 56-58 from the College of Mineral Industries, University Park, Pennsylvania.

[1] Now in the Department of Geology, Virginia Polytechnic Institute, Blacksburg, Virginia.

7 Å phases, herein called septechlorite* structures, extends between the serpentine composition, $6MgO \cdot 4SiO_2 \cdot 4H_2O$, and the amesite composition, $4MgO \cdot 2Al_2O_3 \cdot 2SiO_2 \cdot 4H_2O$.† A series of normal chlorite structures extends continuously between the penninite composition, $21MgO \cdot 3Al_2O_3 \cdot 13SiO_2 \cdot 16H_2O$, and the amesite composition. Both synthetic and natural septechlorite structures ranging from penninite to amesite in composition can be converted into normal chlorite structures under proper temperature and pressure conditions. The change from one structural type to the other is a polymorphic transition.

The experimental work described herein was carried out in 1952–53. Since that time much more detailed x-ray work has been done in this laboratory, and the reader is referred to forthcoming papers for details.

Experimental Methods and Previous Work

The magnesian chlorites occur as synthetic phases in the quaternary system MgO-Al_2O_3-SiO_2-H_2O (see Fig. 1). The general phase equilibrium relations in the system were studied by Yoder (1952) and Roy and Roy (1952, 1955). In both investigations two different phases were synthesized at the clinochlore composition, $5MgO \cdot Al_2O_3 \cdot 3SiO_2 \cdot 4H_2O$. A normal chlorite structure formed under relatively high water vapor pressures and high temperatures. At 1000 atmospheres this structure was said to be stable up to 680° C. Under relatively low water vapor pressures and at lower temperatures a septechlorite structure formed, which above 450° C. and in sufficiently long runs at high water vapor pressures was transformed into the normal chlorite phase. The Roys observed variable unit cell dimensions for septechlorite phases obtained in three phase assemblages from other more aluminous compositions in the system. They reasoned that solid solution must extend beyond clinochlore along the clinochlore-amesite join. Yoder, however, was unable to synthesize a single phase assemblage at the amesite composition, largely because he was unable to prepare a sufficiently reactive mixture. Chrysotile at the serpentine composition had been synthesized previously by Bowen and Tuttle (1949) and was stable up to 500° C. under 1000 atmospheres water vapor pressure.

* See later for etymology. This trioctahedral unit repeats with a 7 Å periodicity along the c-axis. Minerals containing the unit are chlorites in both the mineralogical and chemical sense and are related, as discussed in this paper, to normal chlorites by a polymorphic rearrangement. We have suggested previously (Nelson and Roy, 1954), therefore, that such minerals should be called septechlorites, or 7 Å chlorites. The mineralogical distinctions between these septechlorites and the dioctahedral kaolin minerals is so fundamental that it seems desirable to avoid referring to them as "kaolin-type" minerals.

† This series may, in fact, not be continuous due to the question of tubular magnesium chrysotile and "platy" aluminous members. This is discussed later.

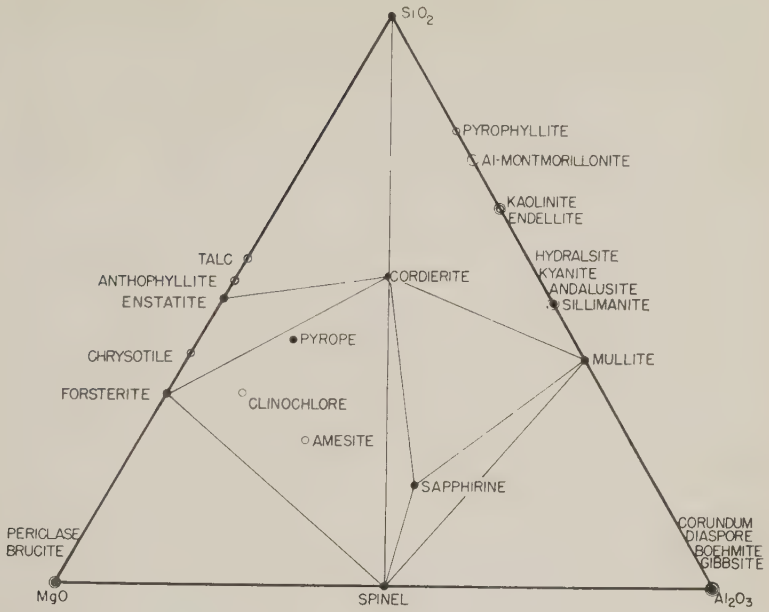

FIG. 1. Mol. per cent composition diagram showing phases in the quaternary system MgO-Al_2O_3-SiO_2-H_2O with compositions projected on to the anhydrous base. Solid dots represent anhydrous phases. Open circles represent hydrated phases actually lying above the plane of the paper. Double open circles indicate more than one phase present at the projected composition point, with the phases differing in water content. Seven compositions studied lie in the join chrysotile-amesite extended. (See Table I for compositions.)

In this investigation a study of compositions lying along the serpentine-amesite join was made in order to determine:

1) whether solid solution extends continuously between the serpentine and amesite compositions,
2) what limits of alumina substitution exist in the magnesian chlorites,
3) whether polymorphic normal chlorite and septechlorite structures extend over the entire range of chlorite composition.

This study was conducted by means of apparatus and techniques that have been described fully in other papers from this laboratory (e.g., Roy and Osborn, 1952, 1954; Roy and Roy, 1952, 1955; Roy, Roy and Osborn, 1953, etc.). The starting compositions, corresponding to those shown in Fig. 1 and Table I, were prepared in the form of amorphous "gels" of alumina, magnesia, and silica (Roy and Roy, 1955; Roy, 1956). The phases were identified in every case by comparing *x*-ray diffractometer traces of the synthetic products with traces obtained from "standard"

TABLE 1. RESULTS OF REPRESENTATIVE HYDROTHERMAL RUNS

Temperature (° C.)	Pressure (psi)	Duration (days)	Phases Present[1]
	a. Composition S-I: $23MgO \cdot Al_2O_3 \cdot 15SiO_2$		
420	10,000	3	SC
440	10,000	17	SC
477	20,000	15	SC
485	30,000	19	SC+tr. For
515	10,000	$2\frac{1}{2}$	SC+For+?
700	18,000	$3\frac{3}{4}$	For+Sp+?
700	10,000	17	For+?
	b. Composition S-II: $11MgO \cdot Al_2O_3 \cdot 7SiO_2$		
440	10,000	17	SC
477	20,000	15	SC
515	10,000	$2\frac{1}{2}$	SC+For+?
660	20,000	36	Cl+SC (used for next run)
680	20,000	7	Cl+SC+For
700	18,000	$3\frac{3}{4}$	For+Sp+Talc
700	10,000	17	For+Talc+Sp
	c. Composition S-III: $21MgO \cdot 3Al_2O_3 \cdot 13SiO_2$		
440	10,000	17	SC
477	20,000	15	SC
515	10,000	$2\frac{1}{2}$	SC
700	10,000	17	For+Talc+Sp
	d. Clinochlore, Composition: $5MgO \cdot Al_2O_3 \cdot 3SiO_2$		
120	5,000	30	SC
160	5,000	55	SC
234	5,000	$9\frac{1}{2}$	SC
266	5,000	11	SC
285	5,000	22	SC
360	15,000	30	SC
410	10,000	19	SC
440	10,000	23	SC
515	10,000	$2\frac{1}{2}$	SC
590	6,000	14	SC
610	15,000	30	Cl
650	10,000	9	SC+tr (For+Talc)
660	20,000	36	Cl (used in next run)
680	20,000	7	Cl
700	18,000	$3\frac{1}{2}$	SC+For+Talc+Sp
720	15,000	$1\frac{1}{2}$	For+Talc+Sp
700	10,000	17	For+Talc+Sp+SC (?)
	e. Composition AS-I: $9MgO \cdot 3Al_2O_3 \cdot 5SiO_2$		
120	5,000	30	SC
160	5,000	55	SC
234	5,000	$9\frac{1}{2}$	SC
285	5,000	23	SC
310	5,000	18	SC
350	10,000	30	SC
405	18,000	14	SC

TABLE 1 (*continued*)

Temperature (° C.)	Pressure (psi)	Duration (days)	Phases Present[1]
495	16,000	14	SC+Cl
585	6,000	14	SC
610	18,000	30	Cl
660	20,000	36	Cl (used in next run)
680	20,000	7	Cl+For+?
700	18,000	3½	SC+Cl+Sp
700	10,000	17	SC ? For+Talc+Sp
720	15,000	1½	SC+For+Sp+Talc
	f. Amesite Composition A: $4MgO \cdot 2Al_2O \cdot 2SiO_2$		
160	5,000	55	SC
180	5,000	31	SC+Boehm
280	5,000	14	SC+Boehm
265	5,000	10½	SC+Boehm
310	5,000	18	SC
350	10,000	30	SC
400	10,000	26	SC+Sp
415	10,000	7	SC
495	16,000	14	SC
580	5,000	7	SC
610	18,000	30	Cl
650	10,000	9	SC
660	20,000	36	Cl (used in next run)+SC (?)
680	20,000	7	Cl+For+Sp (?)
700	18,000	3½	For+Talc+Sp
700	10,000	17	For+Talc+Sp
	g. Composition A-I: $15MgO \cdot 9Al_2O_3 \cdot 7SiO_2$		
360	10,000	30	SC (spacing 7.06)+Boehm
520	18,000	30	Cl+Sp+?
610	18,000	30	Cl+Sp+?
	h. Composition A-II: $7MgO \cdot 5Al_2O_3 \cdot 3SiO_2$		
266	5,000	11	SC+Boehm+?
400	10,000	26	SC (spacing 7.06)+Sp+Cor (?)

Mineral	Temperature (° C.)	Pressure (psi)	Duration (days)	Phases Present
	i Natural Minerals			
(Antigorite, Antigorio-Frondel)	605	20,000	26	Cl+For+Talc
(Antigorite, Antigorio-Foshag)	605	20,000	26	Cl+For+Talc
(Amesite, Urals)	605	20,000	26	SC+Cl
(Serpentine,* Manchuria-Faust)	605	20,000	26	For+Talc
(Serpentine,* Faust)	605	20,000	26	For+Talc

[1] Abbreviations used: SC=septechlorite; For.=forsterite; tr.=trace; Sp.=spinel; Cl.=14 Å chlorite; Boehm.=boehmite.

* Analysis shows very low Al_2O_3 content ($\leq 1.0\%$).

TABLE 2. X-RAY POWDER DATA FOR SEPTECHLORITE OF AMESITE COMPOSITION—SYNTHESIZED HYDROTHERMALLY AT 500° C., 10,000 PSI, 3 DAYS CuKα, 5 HRS., CAMERA RADIUS: 7 CM.

d-spacing	Intensity	*d*-spacing	Intensity
7.08	vs	1.704	w
4.62	s	1.664	m, d
3.97	w	1.617	mw
3.55	vs	1.564	w, d
2.65	s	1.540	vs
2.59	m	1.504	mw
2.505	m	1.414	mw, d
2.396	s, d	1.326	w, d
2.270	w	1.294	w
2.110	w	1.130	vw, d
2.013	m, d	1.005	w, d
1.942	w	0.995	w, d
1.886	w		
1.745	w, d		

natural and synthetic materials, supplemented by the usual microscope techniques. In addition to the synthetic compositions, several natural septechlorite minerals were used as starting materials.

EXPERIMENTAL DATA

Approximately two hundred hydrothermal runs were made with synthetic compositions and natural minerals as starting materials. Table I summarizes the phases formed at particular temperatures and pressures.

These data show that a septechlorite phase can be synthesized for each composition along the serpentine-amesite join. Solid solution extends to but not beyond amesite, since compositions more aluminous than amesite give three-phase assemblages at all temperatures and pressures. The septechlorite phase in the three-phase assemblages has the same unit cell dimensions as the amesite phase; amesite, therefore, is the maximum limit for alumina substitution in the septechlorite isostructural series.* Table II gives powder diffraction data for a typical member of this series, a septechlorite of amesite composition.

Above about 500° C. and under relatively high water vapor pressures normal chlorite structures form slowly from the septechlorite phases from all compositions more aluminous than that designated

* In our more recent detailed *x*-ray studies different polytypes within the septechlorite group have been recognized, but this does not affect the conclusions reported.

S-III. S-III corresponds approximately to the composition of a magnesian penninite. Compositions more aluminous than amesite yield a three phase assemblage, including a normal chlorite structure with the same unit cell dimensions as that forming at the amesite composition. Solid solution in the normal chlorite isostructural series extends continuously from penninite to amesite. Compositions *less* aluminous than penninite form three-phase assemblages above about 500° C., and one phase is always a normal chlorite (or a septechlorite phase in short and low pressure runs) whose unit cell dimensions correspond to phases formed at the penninite composition.

The lowest temperature at which a normal chlorite structure has thus far been synthesized is 450° C., the minimum attained at the clinochlore composition by Roy and Roy (1955). There is a question as to which of the polymorphs is the stable phase below 450° C., and particularly whether or not the septechlorite phases have any true stability range even at low temperatures. The transition from the septechlorite to the normal chlorite structure is extremely sluggish at all temperatures and is favored by higher pressures. Thus, normal 14 Å chlorites are formed in three to four weeks at 1000 atmospheres, but require only a week at 3000 atmospheres and 550° C. It is possible that the 14 Å chlorite structure is the stable one even at low temperatures, an alternative that we tend to favor even though the experimental data allow no unequivocal choice.

There is an experimental limitation on the attempts to resolve this point. When 7 Å phases are converted to 14 Å ones, the powder pattern shows the appearance of new reflections which form the odd orders of the 14 Å series. When, however, we attempt to reverse the process, partial conversion to a 7 Å phase is very difficult to detect since one can only expect minor changes in the relative intensities of the basal reflections. No evidence was found, which would show that the 14 Å phases were less stable than the 7 Å ones under particular conditions. Should the normal chlorite structure be stable at all temperatures one must consider the possibility that the normal chlorite solid solution series could extend from amesite all the way to the serpentine composition. However, we favor the view that a minimum alumina content is necessary to stabilize the normal chlorite structure for reasons discussed later, based both on our experiments and natural occurrences.

In the presence of high water vapor pressures the maximum stability temperature for the normal chlorite structure is about 710° C. at 1000 atmospheres. Normal chlorites of the penninite and amesite compositions appear to have lower maximum stability temperatures than those near the clinochlore composition. However, for a given water vapor pressure

there is probably no more than twenty or thirty degrees difference in the maximum equilibrium decomposition temperatures. The usual products of decomposition are forsterite, spinel and cordierite, but naturally these depend on the composition.

The data in Table I obtained from natural minerals that have been used as starting materials are consistent with the data from synthetic compositions. For example, after hydrothermal treatment a normal chlorite structure is formed from the Urals septeamesite. The transition appears to be similar to the polymorphism observed for the synthetic compositions rich in alumina. The Antigorio antigorite contains a relatively small percentage of alumina. After hydrothermal treatment a three-phase assemblage of normal chlorite, forsterite, and talc are formed and this harmonizes with the experimentally derived phase equilibrium relations. The purely magnesian serpentines (chrysotiles) give only the two-phase assemblage forsterite and talc after hydrothermal treatment at high temperatures.

The results of hydrothermal heating should not be confused with the results of "dry" heating experiments with chlorites. Our dry heating experiments have been reported earlier (Nelson and Roy, 1954) and they showed for the first time that the strengthening of a "14 Å" line on heating supposed "chlorites" could not be used as evidence for the presence of the 14 Å chlorite. In each case, both dry and hydrothermal, heating a septechlorite results in the appearance of a "14 Å" line in the powder pattern. In the hydrothermal case this is the first order reflection of the chlorite structure and is sharp and accompanied by all the other reflections of the chlorite structure. The "dry" heating gives only a very diffuse peak nearer 13.5 Å and is accompanied by the partial destruction of the other reflections.

Unit Cell Dimensions and Structural Data

Further evidence for the existence of solid solution along the serpentine-amesite join is obtained by observing the regular change in unit cell dimensions that accompanies an increase in alumina content in both the normal chlorite and the septechlorite structures. Figs. 2 and 3 show this change. Values for the basal spacings were determined by slow speed scanning on high angle diffractometers using the (10.1) Lake Toxaway quartz line as a standard. Values for the b_0 parameter were calculated from measurements on the (060) spacing determined in similar fashion using the (21.1) quartz line as a standard. The numerical values represent relative, not absolute, spacings—although they are probably not less accurate than values hitherto reported. The differences recorded are thought to be quite significant since reproducibility to $\pm 0.01°$ 2θ can

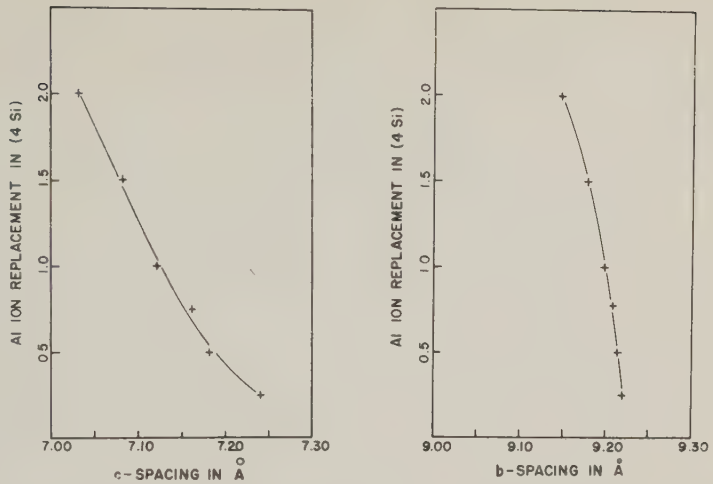

FIG. 2. *a*. Variation in the *c*-spacing of the (7 Å) septechlorite solid solutions up to amesite (Al replacement = 2).

b. Variation in the b_0 parameter of the (7 Å) septechlorite solid solution.

be obtained. The basal spacing of both septechlorite and normal chlorite structures becomes smaller with increasing alumina content, by about 2% in the case of normal chlorites between the clinochlore and amesite compositions. The magnitude of the change is greater in the normal chlorites than in the septechlorites. The septechlorites have a slightly smaller basal spacing than the corresponding normal chlorites. The

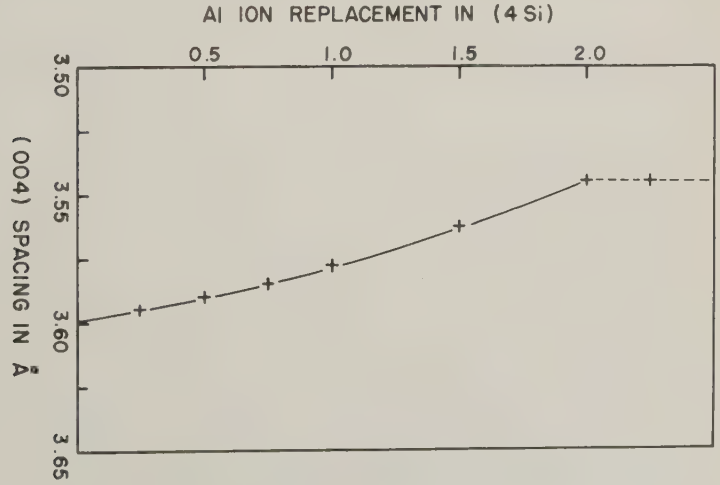

FIG. 3. Variation of the 004 spacing of the (14 Å) normal chlorites.

difference is about 0.16 Å in terms of a first order spacing of approximately 14 Å. The *b* parameter varies in a similar manner decreasing somewhat more slowly than the basal spacing.

Phase Equilibrium Relations

From the data obtained (Table I) new conclusions regarding the phase relations in the system MgO-Al_2O_3-SiO_2-H_2O may be drawn. The compatibility triangles in Fig. 4 show the effect of solid solution along the join on phase equilibrium relations in other regions of the quaternary system. The compositions are plotted as projections on the MgO-Al_2O_3-SiO_2 base of a tetrahedron following the usual procedure. The new triangles are revisions of those given by Yoder (1952) and Roy and Roy (1955), and only the critical relations are shown. The triangles show relations ac-

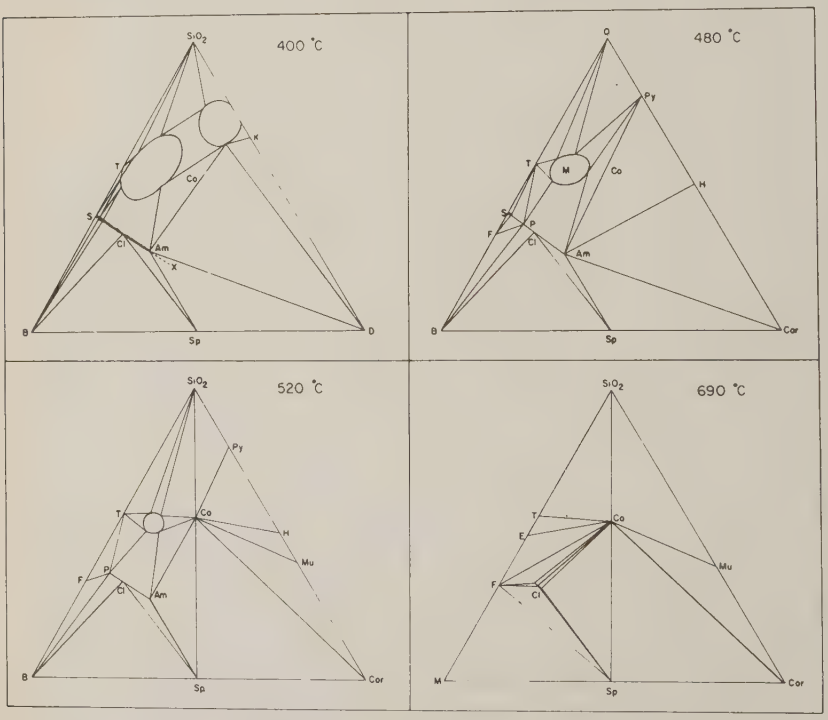

Fig. 4. Four selected isobaric (1000 atm) isothermal (temperature indicated) compatibility triangles for the quaternary system MgO-Al_2O_3-SiO_2-H_2O. Abbreviations can be compared to Fig. 1 where full names are given. The round quaternary solid solution areas are the various montmorillonoids. These revised data are taken from the work of Mumpton and Roy (1955). The precision in such triangles is of a much lower order than for example in isothermal sections of ordinary "dry" equilibrium diagrams.

tually encountered under experimental conditions up to 1500 atmospheres water vapor pressure. Alternative possibilities that could exist at other water vapor pressures (Yoder, 1952) are indicated by dashed lines. Another type of presentation of the results is shown in Fig. 5 which is the partly binary t-x section of greatest interest here. The system becomes quaternary as soon as any solid phase dissociates, e.g., it is binary only at the lower temperatures and the diagram must, therefore, be used with care. Two alternative diagrams are presented, one regarded as more likely than the other. The choice hinges around two incompletely resolved points.

First, chrysotile and synthetic phases of pure serpentine composition have a tubular habit, while the septechlorite phases of more aluminous composition crystallize in very small, well defined, hexagonal plates (see Fig. 6). Solid solution between the tubular and platy habits implies a gradual transition from tube (rolled sheet) to plate. Electron microscope studies of several septechlorites lying between serpentine and penninite in composition failed to reveal any evidence for a gradual change in habit. In general a mixture of tubes and plates was noted, and this suggests the discontinuity shown in Fig. 5*a*. If, on the other hand, high confining pressure or shearing stress produces a flat sheet habit for phases of chrysotile composition, the continuous relations shown in Fig. 5*b* are suggested. The occurrence of tubular chrysotiles and platy antigorites in nature supports Fig. 5*a*. However, most natural antigorites contain some R_2O_3, and previous synthesis work (Roy and Roy, 1954) suggests that a minimum R_2O_3 content is necessary to stabilize the platy habit.

Second, the septechlorites may or may not have a range of thermodynamic stability, a question already discussed. The experimental data do not settle this question. The fact that it is not possible to make 14 Å chlorites with a low alumina content and is more difficult to synthesize normal chlorites from the very high alumina compositions also suggests that if there is a stability range for the septechlorites, this range reaches a maximum temperature near the amesite composition (as shown in Fig. 5*b*). That there may be a true stability range for the least aluminous septechlorites is suggested by the numerous low-R_2O_3 "antigorite" phases in nature *for which no 14 Å polymorph exists*, and for the high-R_2O_3 ones, stability is suggested by the natural occurrences at Chester, Massachusetts and Saranovskoye, Northern Urals. The occurrence of diaspore with amesite at Chester implies a stability range even under moderate temperature ($<\sim 400°$ C.) and pressure conditions, and the paragenetic relations of amesite and corundophyllite suggest inversion to the septechlorite with lowering temperature. If the Chester association is metastable the relations in Fig. 5*a* apply. The question may be answered by a

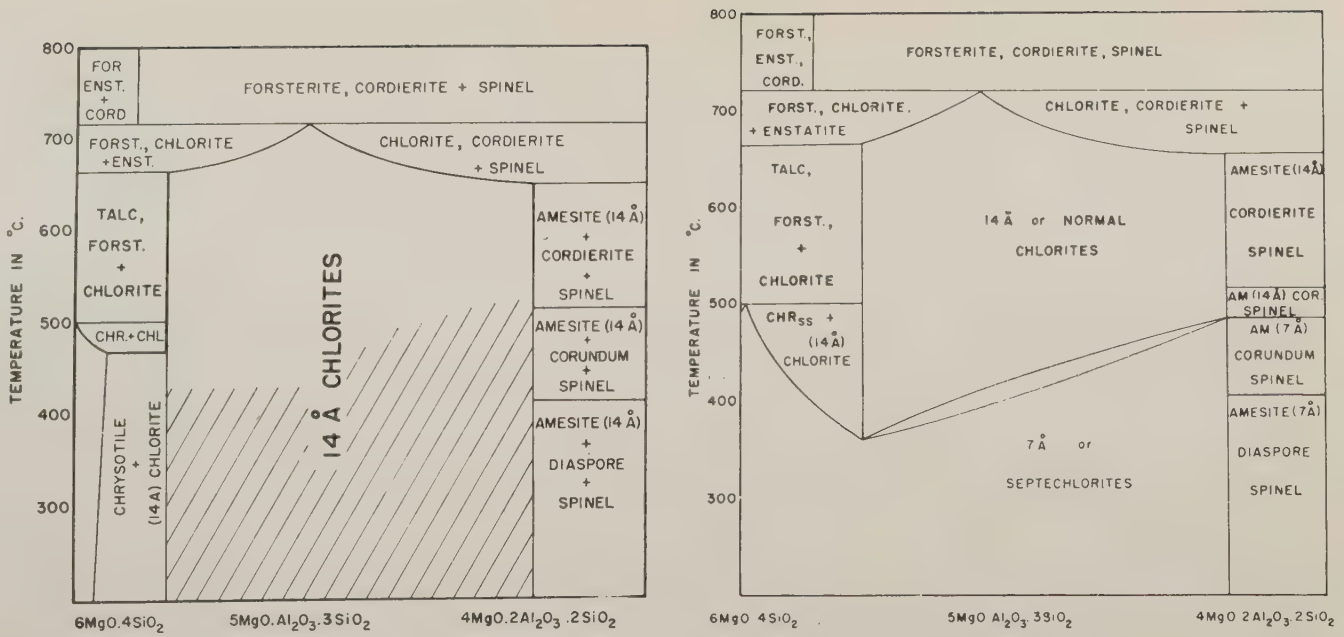

FIG. 5. *a*. Preferred version of a composition-temperature diagram drawn for a pressure of 1000 atmospheres, for the join chrysotile-amesite extended. The lower part of the diagram is a true binary join, above this, however, the equilibrium is quaternary and the diagram shows only the stable solid phases at various compositions as a function of temperature. Precision in such diagrams is poor (±15° C.) especially in the area of solid solutions which decompose to other solid solutions. The preferred version shows as a shaded area the p-t range in which (7 Å) septechlorites form and persist metastably (?) for long periods. Note also the 2-phase region chysotile+chlorite showing a discontinuity in solid solubility along the "chlorite-join."

FIG. 5. *b*. Possible alternative to Fig. 5 *a*. with septechlorites now shown as stable low temperature polymorphic forms of chlorites.

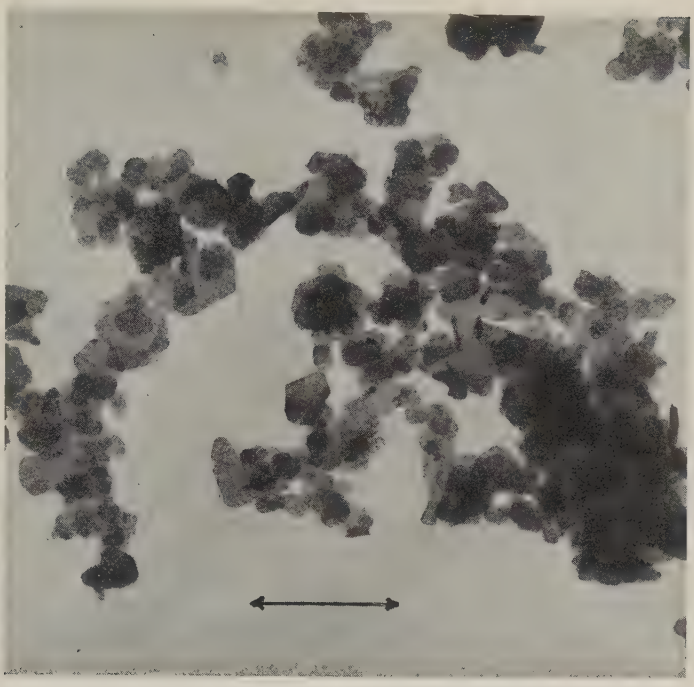

FIG. 6. Electron micrograph showing euhedral well-crystallized septechlorite material (Composition: clinochlore, 450° C., 15,000 psi).

detailed study of the influence of much higher pressures than have been used so far.

In both alternatives of Fig. 5, a minimum alumina content is shown as necessary for formation of the 14 Å normal chlorite structures due to the failure to synthesize normal chlorites containing less alumina than penninite. This is also more easily explained on a structural basis. It should be recalled that changes in composition in the chlorites occur through *simultaneous* substitution of aluminum ions for silicon ions in the tetrahedral layers *and* of aluminum ions for magnesium ions in the octahedral layers. This very important point was first made by Gruner (1944). In Pauling's structural scheme for the layer silicates the chlorites are related to the micas in that a charged brucite-type sheet occupies the interlayer cation position of the micas. A certain minimum charge on this brucite-type sheet may, therefore, be necessary to hold the mica-type layers together. The composition corresponding to a particular brucite layer charge cannot be determined, because different amounts of substitution and charge may occur in the interlayer brucite and the mica-unit octahedral layer. The maximum charge on the interlayer brucite is

achieved if all the octahedral substitution occurs in the interlayer brucite. In this case the octahedral layer within the mica-type unit would be uncharged. Substitutions confined to the interlayer brucite would give an interlayer charge equal to the interlayer charge in muscovite with a minimum alumina content corresponding to the clinochlore composition. The possible substitutions are shown schematically in Fig. 7. The normal chlorite isostructural series extends from amesite only as far as penninite, therefore, probably because of the minimum interlayer charge requirements on the brucite-type layer. A detailed structural study of synthetic gallium and nickel analogues of the normal chlorites is being pursued in an attempt to determine the nature of the actual octahedral substitutions and reveal the minimum interlayer charge requirements for mica-type structures.

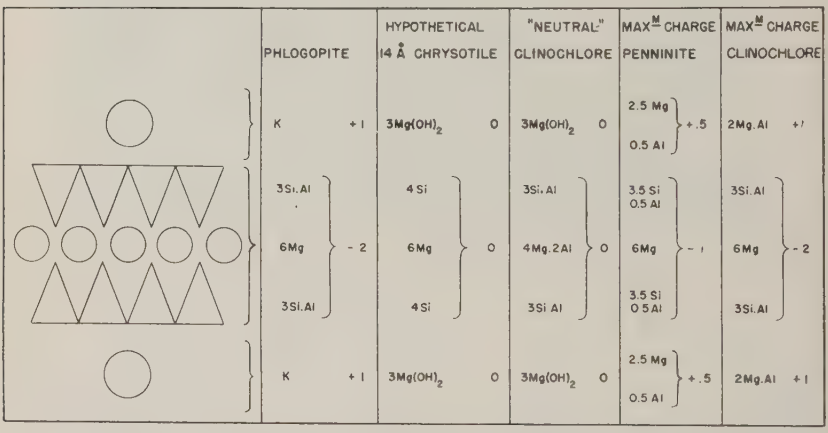

FIG. 7. Schematic illustration of various possibilities in filling the different "layers" of penninite or clinochlore. If the minimum charge required on the layers is the same as in a mica, then the *minimum* Al_2O_3 content with which this can be achieved corresponds to the clinochlore composition.

DISCUSSION OF THE RESULTS

The preceding experimental data allow us to reconsider the problems of chlorite constitution and classification. The following significant points should be borne in mind. A complete sequence of normal chlorite structures with a 14 Å series of basal x-ray reflections can be synthesized for compositions ranging from amesite to penninite. From the same compositions, but generally at lower temperature and water vapor pressure conditions, a second sequence of trioctahedral kaolin-type or "septechlorite" structures with a 7 Å series of basal reflections can be synthesized. For a given composition within this range there exist two poly-

morphic forms of the chlorite phase. (Each polymorph may, in addition, exist in more than one polytype.) These results were obtained not only for the synthetic compositions but also with the natural minerals studied.

This study did not involve experimental work with chlorites containing large amounts of either ferrous or ferric iron. However, ferrous iron analogues of both the septechlorites and normal chlorites have been

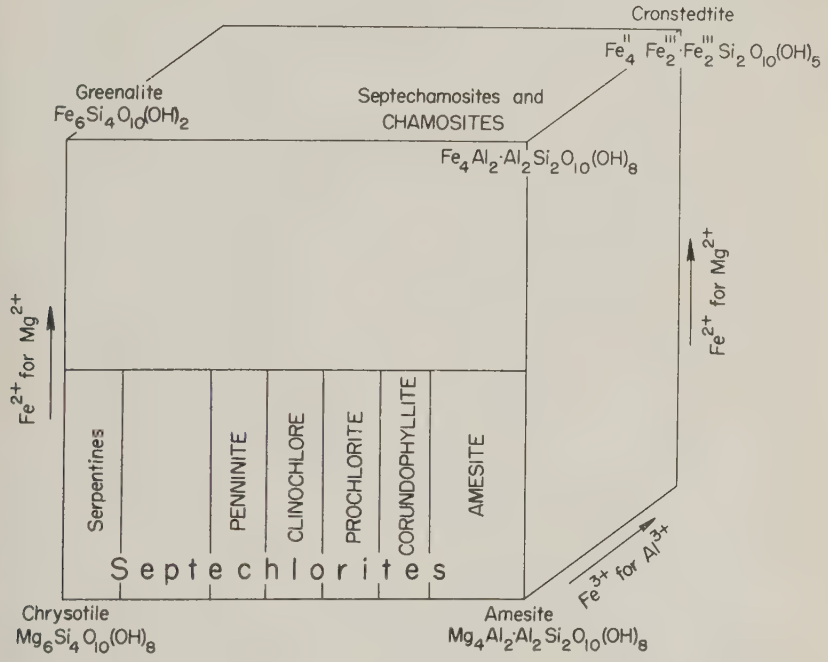

FIG. 8. A revised "Winchell-type" scheme showing compositional relationships among the members of the chlorite group. The septechlorites (roughly equivalent to Winchell's term antigorite) can occur as the low temperature polymorph at any composition which forms a chlorite. In nature Ni^{2+} and Mn^{2+} analogues of the magnesian members are known, and fit directly into the scheme.

described (Brindley, 1951) among the chamosites. Polymorphic relations similar to those described here are almost sure to exist in the iron chlorites.

The compositions of magnesian and ferroan chlorites can be represented diagrammatically in terms of four end members as has been done in Fig. 8. Chamosite has been used as one end member because both septechlorite and normal chlorite structures are already known from materials described by this name. Most chamosites are rich in alumina and lie close to the end member composition of this diagram. The amesite

end member is represented also by both septechlorite and normal chlorite structures. Tschermak's divisions of the orthochlorite series have been used, since they are in common use. Figure 8 is an extension of Winchell's ideas except that we have used molecular proportions as the basis of our subdivisions following Tschermak, instead of weighting the corners. This method of plotting has the double advantage of showing the relative proportions of each end-member in the particular composition under consideration and of indicating the number of substituted aluminum ions in each layer of the structure, a characteristic of particular significance in chlorites. The structural formulae for such chlorite compositions as clinochlore and amesite should, of course, be written: $(Mg_5Al)(AlSi_3)O_{10}(OH)_8$ for clinochlore and $(Mg_4Al_2)(Al_2Si_2)O_{10}(OH)_8$ for amesite. Designations familiar in other mineral groups might also be used. Thus where Sp represents the molecular proportion of the septechlorite end-member and At the molecular proportion of the amesite end-member, penninite might cover the range $Sp_{60}At_{40}$–$Sp_{50}At_{50}$ and clinochlore the range $Sp_{50}At_{50}$–$Sp_{40}At_{60}$, etc. (after Tschermak). If it is remembered that each composition can exist in two polymorphs it is obvious that the one diagram suffices for both the septechlorite and the normal chlorite forms of the same composition, although for plotting optical and other properties two diagrams perhaps will be required.

The introduction of Fe^{3+} for Al^{3+} is another common possibility in nature. This also has been sketched in on Fig. 8 with the Fe^{3+} for Al^{3+} replacement plotted as a third dimension coming out of the plane of the paper. The only important end-member mineral which needs to be considered here is cronstedtite, which is then the amesite analogue with both Fe^{2+} substitution for Mg^{2+} and Fe^{3+} for Al^{3+}.

The ability of synthetic septechlorite structures to accept isomorphous replacements by Mg, Fe^{2+}, Fe^{3+}, Ni, Mn, Cr, Ge and Ga has been studied by Roy and Roy (1954).

Other natural chlorites also show examples of this dimorphism. Thus, in the nickel family one finds both 7 Å and 14 Å material. In the case of the natural samples of schuchardite one cannot be sure whether the 7 Å phase contains much aluminum, or is really an end-member garnierite. In the laboratory both 7 Å and 14 Å members can be prepared, though it has been found to be impossible to convert a sample at the $Ni_5Al \cdot AlSi_3O_{10}(OH)_8$ composition entirely into the 14 Å polymorph.

No synthetic work has as yet been done with the manganese phases but here again it is quite reasonable to presume the existence of the two polymorphs in the "grovesite" sample studied by Hey (1954). Similarly, delessite (=melanolite) and gonyerite correspond then to two isomorphous 14 Å members (with different amounts of substitution of R^{3+})

whereas the 7 Å polymorph is represented by bementite (see Frondel, 1955) and related species.

Summary

In summary, our present concept of the constitution of the chlorites is based on the chemical, structural, and phase equilibrium relations that characterize them. Chlorites as they occur in nature are layer lattice silicates of one of two polymorphic types. The one, typically more perfectly and more coarsely crystalline, is analogous to the mica scheme of crystallization. It is a four-layer structure consisting of mica sheets and substituted brucite sheets. The substituted sheets occupy a position and fill a role analogous to the interlayer cations of the micas. The other, characteristically more fine grained and less perfectly crystallized, (although occasionally giving large well-formed crystals) is a two-layer structure of trioctahedral type. Chemical variations of wide, but not unlimited latitude may occur in both types of structures by a specific type of isomorphous replacement within the lattice. Such substitutions are almost certainly continuous from their maximum to their minimum determined extents, and the characterization of individual chlorite species by narrow and discontinuous ranges of composition is therefore unnatural. The ionic substitutions in the chlorite and septechlorite structures are of the type characterized by simultaneous replacements in tetrahedral and octahedral positions by trivalent ions, particularly aluminum ions. The phase equilibrium studies have shown that there is no *simple* replacement of aluminum by magnesium, or the reverse. The mineral kaolinite and its polymorphs are unique entities characterized by the absence of isomorphous replacements. Such replacements in the septechlorites are exceedingly common. The septechlorite and normal chlorite polymorphs, that may occur singly or together in nature, are not unrelated entities, but under proper conditions the one may undergo transformation to the other. It is unnecessary, therefore, to disassociate from the chlorite family such minerals as antigorite, amesite, and chamosite. The main problem of nomenclature involved is to find a name for the trioctahedral two-layer minerals related to chlorites. We have suggested that it is convenient to call them septechlorites, septechamosites, septeamesites, etc. if and when after *x*-ray examination their structural scheme is found to be based on a 7 Å sequence.

Note on the Etymology of "Septechlorite"

As more and more natural assemblages containing chloritic phases with 7 Å series of basal *x*-ray reflections are encountered the problem of naming such minerals and distinguishing them from other chlorites becomes more acute. The problem was recognized by Brindley (1951, p. 65) and by Hey (1954, p. 279) but neither proposed a solution. In our

first paper on the data given detailed treatment here (Nelson and Roy, 1954) we suggested that the 7 Å chlorites be designated *septechlorites* in allusion to their most obvious identifying x-ray diffraction characteristics, while the 14 Å chlorites should be designated *normal chlorites*. Such designations are useful only after x-ray examinations have been made. The field worker and the petrographer naturally will refer to all undifferentiated chloritic minerals as *chlorites* in the presently accepted sense. Most such minerals will be normal chlorites.

Some have used the term "kaolin-layer" to refer to all two-layer assemblages. This usage seems to us undesirable because the kaolin minerals are a unique crystallization. They are dioctahedral and triclinic, or perhaps monoclinic. Their crystal chemistry admits no isomorphous substitutions in the ideal formula (Roy and Roy, 1954). No simple substitution of magnesium, nor any other ion, for octahedral aluminum occurs, and there are no germanium, or germanium and gallium substituted analogues of kaolinite. Solid solution between serpentine and kaolinite or "parakaolinite" (Serdyuchenko, 1948, p. 156) almost certainly does not exist. Finally, the kaolin minerals undergo no polymorphic transitions of the type described for septechlorites. The unique crystallization of kaolin minerals is in contrast to septechlorites. Septechlorites are trioctahedral and the resulting higher symmetry gives rise to rhombohedral (cronstedtite) or orthohexagonal (some chamosites) crystallizations. The septechlorite layer admits a great variety of ions through isomorphous substitutions (Roy and Roy, 1954), including germanium and gallium. Al^{3+} entry always involves simultaneous octahedral and tetrahedral substitutions.

Apart from a "synthetic" name such as "femalsite" (ferromagnesian aluminum silicates) the other most likely names are *antigorite* and *serpentine*. We strongly favoured the former for many years, but crystallographic workers more and more tend to restrict this term to the structure type with long ($\sim$42 Å) a-spacing. Serpentine has been associated with a morphological habit and also restricted to the magnesium-rich compositions: no one would, for instance, call euhedral amesite crystals, "serpentine."

The most fundamental and distinguishing characteristic of septechlorites is that under appropriate natural or simulated conditions septechlorites are converted to their normal chlorite polymorphs. This structural and genetic relationship associates normal and septechlorites in nature and in the laboratory. They should be associated in nomenclature, as well.

We hope mineralogists will agree the term "septechlorite" is a happy solution to the problem of naming 7 Å chloritic minerals. It is, of course, not so important what terms are used so long as the fundamental relations between the two types of chlorites are recognized.

Acknowledgment

We wish to acknowledge the support of this work by the U. S. Army Signal Corps under Contract DA-36-039, sc-5594, Squier Signal Laboratory, Fort Monmouth, New Jersey.

This paper is based on a thesis submitted in partial fulfillment of the requirement for an M.S. degree at the Pennsylvania State University (1953).

Bibliography

Bowen, N. L. and Tuttle, O. F. (1949), "The System MgO-SiO_2-H_2O," *Geol. Soc. Amer. Bull.*, **60**, 439–60.

Brindley, G. W. (1951), "X-ray Identification and Structure of Clay Minerals," Mineralogical Soc., London, p. 345.

FRONDEL, C. (1955), "Two Chlorites: Gonyerite and Melanolite," *Am. Mineral.*, **40,** 1090–94.

GRUNER, J. W. (1944), "The Kaolinite Structure of Amesite," *Am. Mineral.*, **25,** 422–30.

HEY, M. H. (1954), "A New Review of the Chlorites," *Miner. Mag.*, **30** 277–92.

NELSON, B. W. AND ROY, R. (1954), "New Data on the Composition and Identification of Chlorites," Proc. 2nd. Nat. Conf. on Clays and Clay Minerals, *Nat. Res. Council, Pub.* **327,** 335–348.

PAULING, L. (1930), "The Structure of the Chlorites," *Proc. Nat. Acad. Sci.*, **16,** 478–82.

ROY, D. M. AND ROY, R. (1952), "Studies in the System MgO-Al_2O_3-SiO_2-H_2O," *Bull. Geol. Soc. Amer.*, **63,** 1293–94, Abstract.

ROY, D. AND ROY, R. (1955), "Synthesis and Stability of Minerals in the System MgO-Al_2O_3-SiO_2-H_2O," *Am. Mineral.*, **40,** 147–78.

ROY, D., ROY, R., AND OSBORN, E. F. (1953), "The System MgO-Al_2O_3-H_2O and the Influence of Carbonate and Nitrate Ions on the Phase Equilibria," *Am. J. Sci.*, **251,** 337–361.

ROY, D. AND ROY, R. (1954), "An Experimental Study of the Formation and Properties of Synthetic Serpentines and Related Layer Silicate Minerals," *Am. Mineral.*, **39,** 957–75.

ROY, R. (1956), "Some Simple Aids in Hydrothermal Experimentation II: The Preparation of Mixtures," *J. Am. Ceram. Soc.*, **39,** 145–56.

ROY, R. AND OSBORN, E. F. (1952), "Some Simple Aids in Hydrothermal Investigation of Minerals Systems," *Econ. Geol.*, **47,** 717–721.

SERDYUCHENKO, D. P. (1948), "On the Chemical Constitution of Chlorites," *Doklady Akad. Sci. U.S.S.R.*, **60,** 1561–64.

TSCHERMAK, G. (1890), "Die chloritgruppe, II. Theil, Sitzungsber.," *Akad. Wiss. Wien, Math-naturwiss, Kl.*, Abt. I, **99,** 174–278.

——— (1891) "Die chloritgruppe, II. Theil, Sitzungsber.," *Akad. Wiss. Wien, Math-naturwiss, Kl.*, Abt. I, **100,** 29–107.

WINCHELL, A. N. (1926), "Chlorite as a Polycomponent System," *Amer. Jour. Sci.*, ser. 5, Vol. **11,** 283–300.

YODER, H. S. (1952), "The MgO-Al_2O_3-SiO_2-H_2O System and Related Metamorphic Facies," *Amer. Jour. Sci.*, **Bowen Vol.,** 569–627.

Manuscript received October 28, 1957

THE AMERICAN MINERALOGIST, VOL. 43, JULY–AUGUST, 1958

THE CORRECTION FOR ABSORPTION FOR ROD-SHAPED SINGLE CRYSTALS

M. J. Buerger and N. Niizeki, *Crystallographic Laboratory, Massachusetts Institute of Technology, Cambridge, Massachusetts.*

Abstract

There is a simple relation between the forms of the transmission factors for upper levels and the zero levels for rod-shaped specimens. When the equi-inclination technique is used, the several ray paths for a given Υ have lengths x_j for the zero level, while the ray paths for the upper level at the same Υ are $x_j/\cos\nu$. If the form of the transmission factor for the zero level is known, the form for the upper level is therefore the same for the same value of Υ, except that the geometrical scale of the cross-section is increased by the factor $1/\cos\nu$. The resulting correction for absorption for all levels is especially easy to apply if the cross-section of the crystal is circular.

Introduction

If a material has a linear absorption coefficient μ_l, then, after traversing a path of length x, a beam of original intensity I_0 is reduced[1] to

$$I = I_0 e^{-\mu_l x}. \tag{1}$$

If the crystal has a shape such that the various paths have different lengths, x, then (1) must be integrated over the volume of the crystal.

The transmission factor is defined as the ratio of the intensity which is diffracted by the specimen to the intensity which would be diffracted if the specimen had no absorption. Let K be the fraction of the intensity of the direct beam diffracted by a crystal in a particular spectrum. Then the transmission factor for that spectrum is

$$\begin{aligned} T &= \frac{KI}{KI_0} \\ &= \frac{\int^V I dV}{\int^V I_0 dV} \\ &= \frac{\int^V e^{-\mu_l x} dV}{V}. \end{aligned} \tag{2}$$

What is termed the transmission factor here is ordinarily called the

[1] M. J. Buerger. X-ray crystallography. John Wiley and Sons, New York, (1942) 181–182.

"absorption" factor. But, as Joel et al.[2] have pointed out, that usage is confusing. The fraction transmitted is I/I_0, whereas the fraction absorbed is its complement $(I_0-I)/I_0$.

Claasen,[3] and later Bradley,[4] solved (2) for cylindrical samples by graphical integration. As a result, the transmission factor for cylindrical samples is available[4,9] tabulated as a function of the Bragg angle θ and the product $\mu_l R$, where R is the radius of the cylinder. Evidently the transmission factor for a single crystal which has been ground to circular cylindrical form can be treated in the same way[3–8] provided that the correction is required only for reflections from planes parallel to the cylinder axis, and provided that the incident x-ray beam is normal to the cylinder axis. But this corresponds to correcting only the zero level for normal-beam or equi-inclination techniques.

Transmission Factors for the General Case

Fig. 1 shows a cross-section of a crystal ground to circular cross-section. The path of the primary ray to the element of volume dV is x_1, and the path of the diffracted ray from the element of volume is x_2. From this point of view (2) can be written

$$T = \frac{1}{V}\int^{V} e^{-(\mu_l x_1 + \mu_l x_2)} dV. \tag{3}$$

In the general case, Fig. 2, the primary ray makes an angle μ, and the diffracted ray makes an angle ν, with a plane normal to the cylinder axis. The diffracted ray is more completely defined by cylindrical direction coordinates ν (the angular component in the plane of the cylinder axis)

[2] N. Joel, R. Vera, and I. Garaycochea. A method for the estimation of transmission factors in crystals of uniform cross section. *Acta Cryst.*, **6** (1953) 365–468.

[3] A. Claassen. The calculation of absorption in x-ray powder photographs and the scattering power of tungsten. *Phil. Mag.* (**7**) 9 (1930) 57–65.

[4] A. J. Bradley. The absorption factor for the powder and rotating-crystal methods of x-ray crystal analysis. *Proc. Phys. Soc.*, **47** (1935) 879–899.

[5] H. Kersten and W. Lange. Method of preparing crystals for rotation photographs. *Rev. Sci. Instr.* (**12**) 3 (1932) 790–791.

[6] C. A. Beevers and W. Hughes. The crystal structure of Rochelle salt (sodium potassium tartrate tetrahydrate, $NaKC_4H_9O_6 \cdot 4H_2O$. *Proc. Roy. Soc., London* (A) **177** (1941) 251–259.

[7] Ray Pepinsky. Method of cutting and shaping fragile crystals. *Rev. Sci. Instr.*, **24** (1953) 403.

[8] F. Barbieri and J. Durand. Method of cutting cylindrical crystals. *Rev. Sci. Instr.*, **27** (1956) 871–872.

[9] C. Hermann. Internationale Tebellen zur Bestimmung von Kristallstrukturen, Vol. II. Gebrüder Borntraeger, Berlin, (1935) 584.

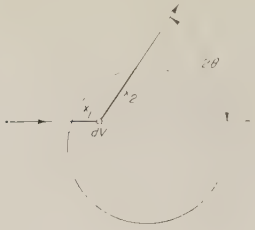

FIG. 1. Crystal ground to a circular cross-section.

and Υ (the angular component in a plane normal to the cylinder axis). Both μ and ν are setting coordinates for any method involving a rotating crystal; Υ is a setting coordinate for a quantum-counter apparatus,[10] also is the coordinate on the Weissenberg film normal to the center line of the film. Now, if one compares the situation for a general level at a value of Υ equal to the 2θ of Fig. 1, it is evident that for the general case, the path x_1 is replaced by $x_1/\cos\mu$ and the path x_2 is replaced by the path $x_2/\cos\nu$. Therefore the transmission factor for the upper level for this reflection has the form similar to equation (3), namely

$$T = \frac{1}{V}\int^{V} e^{-(\mu_i x_1/\cos\mu + \mu_i x_2/\cos\nu)}dV. \tag{4}$$

The integration is equivalent to an integration of x_1 and x_2 over segments of two ellipses, respectively, and then integrating over a change of location of the join of the ellipses.

Absorption Factors for Equi-inclination and Anti-equi-inclination

Relation (4) has a simple solution when $\nu = -\mu$ (equi-inclination, general level) or when $\nu = +\mu$ (anti-equi-inclination, zero level only). In these cases

$$\begin{aligned} T &= \frac{1}{V}\int^{V} e^{-(\mu_i x_1 + \mu_i x_2)/\cos\nu}dV. \\ &= \frac{1}{V}\int^{V} e^{-\mu_i x/\cos\nu}dV. \end{aligned} \tag{5}$$

This is exactly the same as (2) except that every ray path is increased by the factor $1/\cos\nu$.

[10] M. J. Buerger. New single-crystal counter-tube technique. *Acta Cryst.*, **9** (1956) 834.

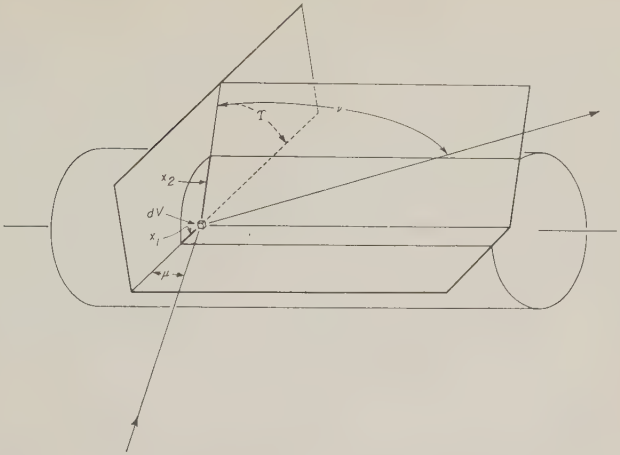

FIG. 2. General case: primary ray makes an angle μ, and the diffracted ray makes an angle ν, with the plane normal to the cylinder axis.

To correct the upper-level equi-inclination reflection for absorption, therefore, one applies the same correction that would be applied at the same value of Υ for the zero level (where $\Upsilon = 2\theta$), except that it should not be looked up under the value of R, but rather $R/\cos \nu$.

This analysis neglects an end effect (for which there is less absorption) for the ends of the cylinder in Fig. 2. This end effect is negligible if the length-to-diameter ratio of the cylinder is large. (If the absolute length of the cylinder is so large that the ends are not in the x-ray beam, then there is no end effect, but there must be a correction for the volume intercepted by the beam. This is proportional to $1/\cos \nu$, so that the "integrated intensity" must be corrected by $\cos \nu$ if the x-ray beam does not bathe the full length of the cylinder.)

EXTENSION TO RODS OF NON-CIRCULAR CROSS-SECTION

If the zero-level transmission factor is found for any rod-shaped specimen of uniform cross-section, it follows from the above discussion that the transmission factor for the upper levels is the same as that of the zero level for the same value of Υ, except that the scale of the cross-section (or else the absorption coefficient) must be regarded as increased by the factor $1/\cos \nu$, provided equi-inclination is used. The simplicity of the absorption correction for equi-inclination provides one more reason for using that technique whenever possible.

Example

To illustrate the importance of making a correction for absorption in data taken from upper levels, an example is given here of the computation of the correction and its application: Three-dimensional data were obtained from a small crystal of wollastonite. The average diameter was 0.0076 cm. The linear absorption coefficient, calculated as outlined elsewhere,[1] is $\mu_l = 215$ cm.$^{-1}$ for CuKα. Thus $\mu_l R = 0.81$. Table 1 shows the computation of the transmission factor. For each level there is derived a

Table 1. Calculation of Correction for Absorption for Rod-Shaped Crystal of Wollastonite

($\mu_l = 215$ cm.$^{-1}$ for CuKα; Radius, $R = .0038$ cm)

		Transmission factor, T								
Υ	level:	0	1	2	3	4	5	6	7	8
	ν:	0°	6°03′	12°10′	18°25′	24°55′	31°47′	39°12′	47°31′	57°26′
	cos ν:	1	.994	.978	.949	.907	.850	.775	.675	.538
	$\mu_l R/\cos \nu$:	.81	.815	.828	.853	.893	.954	1.045	1.20	1.505
0		.264	.262	.257	.248	.233	.213	.185	.146	.088
45°		.274	.272	.267	.258	.243	.224	.198	.160	.103
90°		.302	.300	.295	.287	.273	.255	.230	.195	.141
135°		.334	.332	.328	.320	.307	.291	.268	.235	.181
180°		.353	.351	.347	.339	.326	.308	.285	.251	.199

[11] N. Niizeki and M. J. Buerger. The crystal structure of livingstonite, $HgSb_2S_8$. *Zeit. Krist.*, **109**, 129–157 (1957).

value of $\mu_l R/\cos \nu$. For each of these values, the transmission factor is found by interpolation from the corresponding value of $\mu_l R$ in standard tables.[4,9] To make actual use of these sample values of the transmission, they should be plotted and connected by curves as shown in Fig. 3. Then the transmission factor T for any reflection on any level can be read when the value of Υ for the reflection is known. Since this is a Weissenberg coordinate, and also a setting coordinate for the single-crystal Geiger-counter instrument[10] the value is known for each reflection.

Fig. 3 brings out the importance of making appropriate corrections for absorption in upper-level intensity data. The transmission factors for the higher levels differ so widely from those of the zero level that only a poor residual factor, R, can be expected if the zero-level correction is applied to all levels.[11] The crystal in the example is about as small as can be handled conveniently, yet the transmission factor falls in the range 8% to 35% for CuKα radiation. For MoKα, the value $\mu_l R$ is of the order of only 10% of that for CuKα, and the corresponding transmissions are in the range 90%–100%.

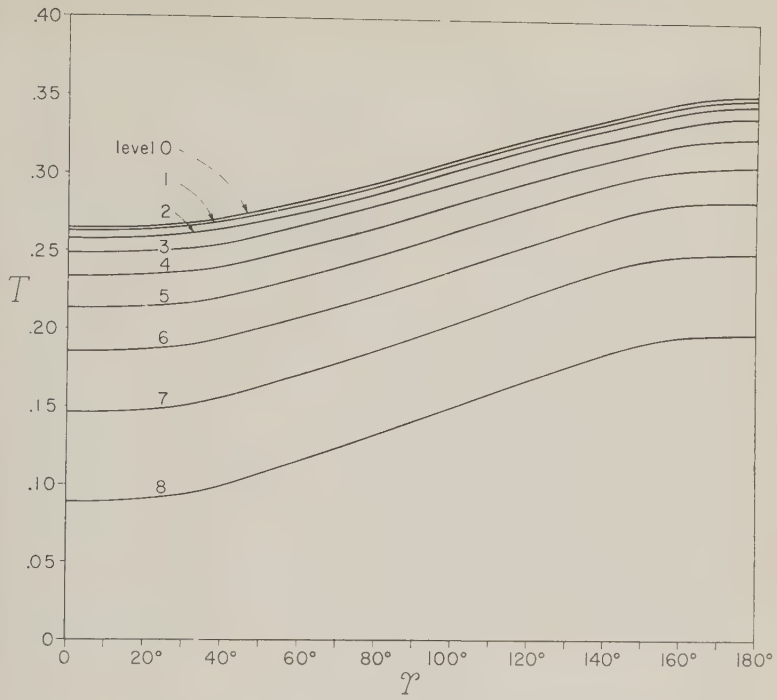

FIG. 3. Transmission factor T plotted against values of Υ for various levels.

This investigation was supported by a grant from the National Science Foundation. We are indebted to Mr. Tibor Zoltai for preparing the illustrations for this paper.

Manuscript received October 31, 1957

DIFFERENTIAL THERMAL ANALYSIS OF SPHALERITE

Otto C. Kopp and Paul F. Kerr, *Columbia University, New York, N. Y.*

Abstract

A relationship between iron content and differential thermal reaction temperature is shown to exist for sphalerite. Samples were heated in air using a modification of a recently developed technique described by Kopp and Kerr (1957). The thermal reaction products consist essentially of sulfur dioxide and zincite, but zinc ferrite or magnetite also appear as the iron content increases.

Several sphalerite samples covering a considerable range in iron content were subjected to differential thermal analysis under controlled conditions using quartz as an internal standard. Peak temperatures decreased from 821° C. for low iron sphalerite (<0.1% Fe) to 767° C. for sphalerite with 13% Fe. Plots of data shown indicate a relationship between D.T.A. peak temperature, iron content and the lattice constant.

Heating rate, grain size and sample weight require close control in determining peak temperature. Peak temperatures are found to decrease at about 3° C. for each ° C. per minute the heating rate is lowered. In the range between 7° C. and 12° C. per minute this correction may apply. Peak temperatures also decrease with a diminution in grain size, especially below 44 microns. The grain size found most suitable for analysis lies in the range 125–149 microns. Peak temperature shows a variation of less than ±3° C. for a sample weight between 40 and 60 milligrams. Samples weighing less than 40 milligrams show a decrease in peak temperature.

Introduction

Recent studies by Hiller and Probsthain (1955) and Kopp and Kerr (1957) have made possible the application of differential thermal analysis to sulfide and arsenide minerals. Sphalerite has been selected for investigation as a part of a series of studies directed toward enlarged application of the D.T.A. method. The wide range in the iron content and common occurrence of sphalerite make it an interesting subject for study.

Kullerud (1953) has offered the significant suggestion that the iron content of sphalerite crystallized in an iron saturated environment is indicative of the temperature of formation. Differential thermal analysis is suggested as a possible supplement to chemical analysis or lattice constant determination in investigating the temperature range of sphalerite.

Procedure

The method of differential thermal analysis used is a slight modification of the technique described by Kopp and Kerr (1957). The heating rate, grain size and sample weight were controlled within essential limits. Since differences of a few degrees are significant, quartz was used as an internal standard to establish a reference peak for temperature control.

The differential thermal peak temperature for quartz with the equipment used was found to be 580±2° C.*

Samples used to obtain a curve showing the relation between iron content and peak temperature were screened.† Only that portion lying in the range 125–149 microns was used. Sample weight was standardized at 50±1 milligrams. Only those thermal curves in which the heating rate showed an average of 11° C. to 12° C. per minute during the oxidation reaction were used, although several tests indicated that it may be sufficiently accurate to apply a correction factor to heating rates as low as 7° C. per minute. All analyses were made at the 200 scale reading on the recorder which corresponds to an amplification of 20× (Kulp and Kerr, 1949).

The samples were mixed with quartz (149–297 microns) in small glass vials and transferred directly to the sample well. The relatively large grains of quartz pack in a uniform manner as they are poured into the sample well. There was no apparent change in packing when the surface of the sample was tamped with a tool fashioned from copper tubing.

As far as possible specimens consisting of single crystals were selected for analysis, but this is difficult for black sphalerite with a high iron content. Megascopic pyrite, pyrrhotite, galena, chalcopyrite and other impurities were removed prior to grinding and the sieved samples were examined with the binocular microscope at 45× magnification. Minor amounts of impurities were removed by hand picking. In general the sphalerite specimens varied in color, except for the high iron sphalerites which were black. Since the peak temperature obtained is thought to reflect the iron present in the sphalerite lattice, the presence of exsolved pyrrhotite will affect the resultant curve. The chemical determination of iron does not in itself distinguish between iron present in sphalerite as FeS from that present as (Zn,Fe)S.

* Keith and Tuttle (1952) determined the inversion temperature for a number of quartz specimens and state that, "Approximately 70 per cent of all natural quartz specimens studied show an inversion break within the range 572.5°–573.5° C." The differential thermal peak temperature for quartz determined without the use of known standards is ordinarily about 7° C. high because it is determined under nonequilibrium conditions.

† For the convenience of the reader standard sieve sizes considered in these experiments are listed as follows:

Sieve No.	*Opening in Microns*
50	297
100	149
120	125
200	74
325	44

Spectrochemical Determination of Iron Content

The authors are indebted to Mr. Arnold Silverman of Columbia University for suggesting the following method of analysis for iron in the sphalerite samples, and providing a standardized curve from which the per cent of iron could be read directly. The method involves dissolving a fixed weight of sample in nitric acid and converting the oxidized material to ferric chloride. The resulting solution is examined by means of the Cary Spectrophotometer. The procedure is as follows:

1. Weigh 0.250 gram of sample.
2. Slowly add 15 milliliters of concentrated nitric acid and after the reaction has subsided, 3 milliliters of 30% hydrogen peroxide.
3. Evaporate to dryness at constant heat.
4. Add 10 milliliters of concentrated hydrochloric acid and boil until all the residue is dissolved.
5. Allow to return to room temperature and bring volume back to 10 milliliters with constant boiling (760 mm. pressure) hydrochloric acid.
6. Decant the solution for an absorption curve on Cary Spectrophotometer.
7. Run the curve in the visible spectrum using slow chart speed; read wavelength in angstroms at optical density 0.5 as pen returns to the base line.

In most cases there was only enough sample for a single iron determination, but the analyses are considered to be accurate to within $\pm 5\%$ of the determined values.

Control of Technique

The range in effects due to heating rate, grain size and sample weight indicates that unless these factors are adequately controlled, peak changes result which exceed the effect of iron content in decreasing the peak temperature of sphalerite. The importance of controlled conditions may be illustrated by noting that the observed temperature range for sphalerite from less than 0.1% to 13% Fe is approximately 54° C., while variations in grain size alone may produce a change in excess of 100° C. Thus prior to any discussion of the range in peak temperature with iron content it becomes necessary to consider the effects of heating rate, grain size, sample weight and proper control.

The Effect of Heating Rate

Ordinarily in D.T.A. determinations, other factors remaining the same, a heating rate between 10° C. and 15° C. per minute yields useful curves. In the current study, however, heating rate variations of as little as 1° C. per minute were observed to cause perceptible changes in peak temperature.

If grain size, sample weight, and heating rate are kept constant, peak temperatures for the same sample analyzed several times agree within

$\pm 3°$ C. However, due to the absence of tight seals in the apparatus, drafts may cause a considerable lowering of the heating rate. In general the heating rate was at least 10° C. per minute, but in a few cases it fell below (as low as 6° C. per minute in one instance). Analyses which showed critical lowering of heating rates were repeated. A group of corresponding peak temperatures obtained for identical samples with different heating rates is shown in Fig. 1. Dashed lines connect points which indicate peak

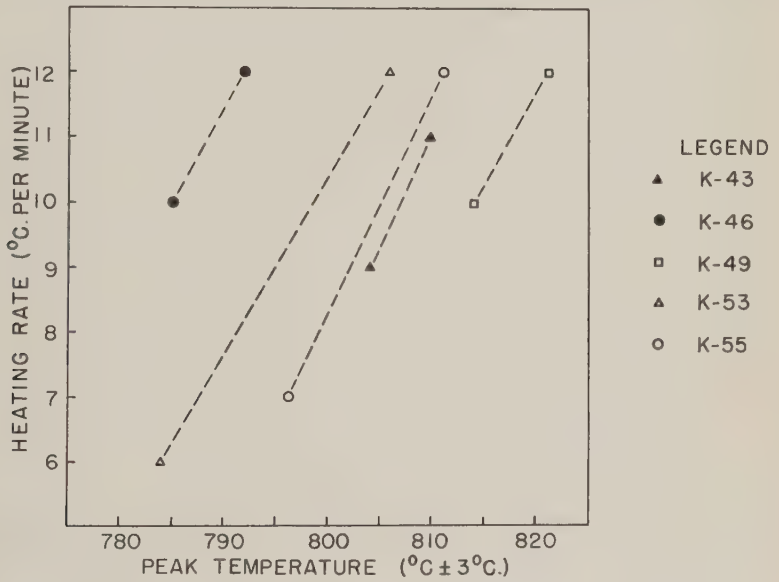

Fig. 1. Heating rate vs. peak temperature. Corresponding slopes of dashed lines connecting data for identical samples at different heating rates indicate an essentially linear relationship between peak temperature and heating rate.

temperatures for the same sample at different heating rates. The lines correspond in slope.

The correction found applicable to low heating rates is illustrated in Fig. 2. The difference in peak temperature noted for the same sample at two different heating rates is plotted against the difference in heating rate for the two runs. A heating rate of 12° C. per minute is considered most satisfactory and serves as a datum for all corrections. Peak temperatures appear to decrease at the rate of about 3° C. for each degree per minute lowering of the heating rate. The slope of the curve appears to change at heating rates below 7° C. per minute.

It appears possible to correct curves in which the heating rate varies between 7° C. per minute and 12° C. per minute. However, in the curve

relating sphalerite peak temperature to Fe content only those differential thermal curves which have a heating rate between 11° C. and 12° C. per minute over the range of the peak were used. A correction of +3° C. was added to peak temperatures obtained at 11° C. per minute and +1° C. to those obtained at 11.5° C. per minute.

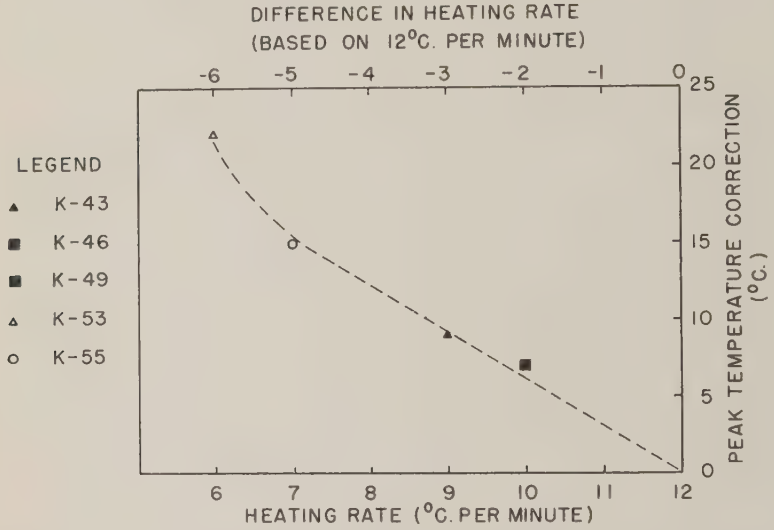

FIG. 2. Peak temperature correction. A correction of about 3° C. for each ° C. the heating rate is lowered appears applicable to heating rates below 12° C. per minute.

Effect of Grain Size

An attempt was made to evaluate the effect of grain size upon the differential thermal peak temperature. Sphalerite from Santander, Spain (Sample No. K-49) was crushed and sieved. The resulting grain size distributions were subjected to differential thermal analysis using a sample weight of 50 ± 1 milligrams (except where noted). The results discussed below indicate that the most suitable grain size for analysis lies in the range 125–149 microns.

The peak temperatures obtained for several size distributions were plotted against the average grain size in microns. The average grain sizes for those samples less than 44 microns and larger than 297 microns are uncertain. The data are listed in Table 1. In order to establish the correct peak temperatures for the various grain sizes, the correction (3° C. per ° C. per minute) was applied.

Figure 3 illustrates a progressive decrease in peak temperature with

TABLE 1. THE EFFECT OF GRAIN SIZE UPON PEAK TEMPERATURE

Sieve No. Range	Diameter Range (Microns)	Peak Temperature (° C. ±3° C.)	Heating Rate (° C. per Min.)	Correction (° C.)	Corrected Peak Temperature (° C. ±3° C.)
< 50	>297	856	7	+15	871
< 50*	>297	851	8	±12	863
50–100	149–297	835	9	+ 9	844
50–100	149–297	833	9	+ 9	842
100–120	125–149	812	9	+ 9	821
100–120	125–149	816	10	+ 6	822
120–200	74–125	802	10	+ 6	808
200–325	44– 74	796	11	+ 3	799
>325	< 44	752	11	+ 3	755

* Sample Weight: 38±1 Milligrams.

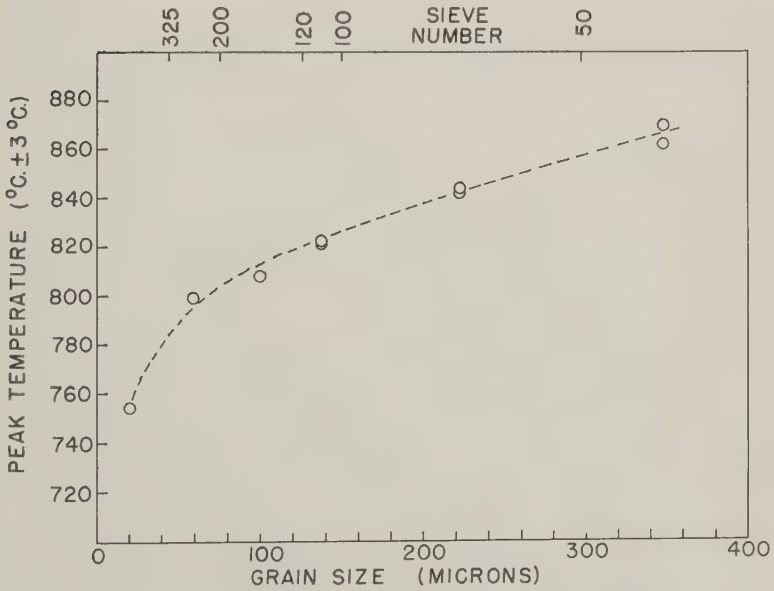

FIG. 3. Grain size vs. peak temperature. Peak temperature decreases with grain size, especially for particles finer than No. 325 sieve.

grain size. This reflects an increase in surface area for the same sample weight as the grain size decreases. Since the reaction is one of oxidation, it is assumed to proceed more rapidly when a greater surface area is available.

The diameter range from 125–149 microns was selected as most suitable for the following reasons:

1. Samples falling within this size range have the smallest possible variation in grain size, i.e. 24 microns, for the sieves available. The next smallest size range lies between 44–74 microns.
2. Samples within this size range lie on a relatively flat portion of the curve. If it were possible to prepare samples consisting essentially of the limiting grain sizes (125 microns and 149 microns) these peak temperatures would not appear to vary by more than ±3° C. from the temperature obtained from the average sample. On the other hand, between 44 and 74 microns the curve is relatively steep and the variation in peak temperatures of the end members might exceed 20° C. Below 44 microns the curve appears to be quite steep. Since the lower size limit cannot be controlled, variations in the average grain size will result in a wide peak temperature range.
3. Samples within this size range are relatively large and inspection under the binocular microscope is not too tedious.
4. During preparation of the specimens for differential thermal analysis, when the grains are mixed in a glass vial with quartz (or alumina) the particles do not adhere to the walls of the vial. This may occur with the finer particles, especially below 44 microns.

Effect of Sample Weight

Samples of sphalerite from Santander, Spain (Sample No. K-49) ranging in weight from 10 milligrams to 60 milligrams (in increments of 10 milligrams) were run to determine the effect of sample weight on peak position and shape.

The peak temperatures, peak heights, peak widths (at one-half the peak height) and estimated peak areas (obtained by multiplying the peak height by the peak width at one-half the peak height) are listed in Table 2. An evaluation of data appears in Fig. 4. Peak temperatures are corrected for heating rate variations.

Table 2. Effect of Sample Weight on Peak Temperature (125–149 Microns)

Weight (Mg.)	Peak Temp. (° C. ±3° C.)	Heating Rate (° C. per min.)	Correction (° C.)	Corrected Peak Temp.	Height (Mm.)	Width (Mm.)	Area (Mm.²)
10	809	12	—	809	22	22	484
20	810	11	+3	812	39	23	897
30	809	10	+6	815	59	24	1316
40	820	11	+3	823	71	24	1704
50	819	12	—	819	94	25	2350
60	820	11	+3	823	103	26	2678

A sample weight of 50 milligrams was found most suitable for comparison. This weight lies on the flat portion of the temperature curve. The variation in peak temperature between 40 and 60 milligrams is within $\pm 3°$ C. The total error in the sample weight analyzed, including possible weighing errors and losses during mixing and transfer of material to the sample well is thought to be within $\pm 5\%$ and in most cases within $\pm 2\%$ of the sample weight.

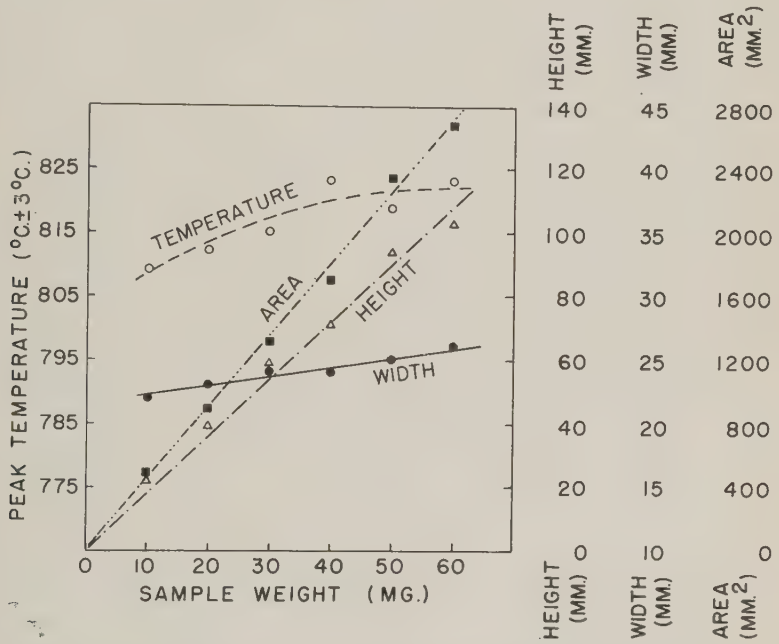

FIG. 4. Sample weight vs. peak dimensions. Peak height, width and area appear to be related linearly to the sample weight. Peak temperature decreases slightly below 40 mg.

A decrease in peak temperature occurs for samples weighing less than 40 milligrams, although the total decrease is only on the order of 10–15° C. The determination of peak temperature for samples weighing less than 40 milligrams becomes increasingly more difficult because the peaks spread and become broader as the sample weight decreases. Peak width decreases slowly compared with peak height. This results in a broader peak for a small sample weight.

The decrease in peak temperature for samples weighing less than 40 milligrams may be of interest. During the oxidation of the sphalerite, sulfur dioxide is produced. This gas must escape from the sample well before oxidation can proceed. The escape of sulfur dioxide and supply of additional oxygen appear to occur simultaneously. As the amount of

sample decreases, the volume of sulfur dioxide produced also decreases. Proportionately more oxygen becomes available and causes more rapid oxidation. Thus, with more rapid oxidation a slightly lower peak temperature may be observed.

Possible application in the determination of the relative constituents of a mineral mixture is suggested by the decreasing size of peaks with respect to height, width and area. For a single specimen, peak height, width and area decrease in a substantially uniform manner. Quantitative determinations may be best related to peak area since peak height and width may vary for the same weight of sample for different specimens.

The Nature of the Reaction

Sphalerite and other zinc sulfide polymorphs are converted to zinc oxide when heated in air. Prewitt-Hopkins and Frondel (1950) state, "Crystals or small cleavage pieces of the five known polymorphs of zinc sulfide when heated in air for 16 hours at 800° C. were found by *x*-ray study to be converted in every instance to the ordinary form of zinc oxide (zincite)."

X-ray examination of sphalerite from Santander, Spain (Sample K-49) indicates that oxidation occurs during the differential thermal analysis of the sample. During the course of the exothermic reaction, the sulfur is oxidized to sulfur dioxide and the zinc to zinc oxide (zincite). The differential thermal curve appears to indicate that the reactions occur simultaneously. The final product is found by *x*-ray study to be zincite (Table 3).

Table 3. Reaction Product of Sphalerite (Sample K-49)

Sample K-49 Residue*		Zincite†	
d(Å)	I	*d*(Å)	I
2.819	70	2.816	71
2.615	40	2.602	56
2.484	100	2.476	100
1.912	20	1.911	29
1.625	30	1.626	40
1.477	30	1.477	35
—	—	1.407	6
1.379	20	1.379	28
1.360	10	1.359	14

* Copper radiation, Debye-Scherrer camera, 11.46 cm. diameter.

† Swanson, H. E. and Fuyat, R. K., 1953, Standard *X*-ray Diffraction Powder Patterns, N.B.S. Circ. 539, v. II, p. 26.

Copper radiation, high angle diffractometer.

The nature of the reaction for sphalerite containing iron is of interest. Sphalerite from Troy, Montana (Sample K-52) which contains 6.9% Fe was examined by means of *x*-ray diffraction after oxidation had been accomplished during differential thermal analysis. Zincite still appears to be the major component, but some additional lines are observed. The spacings of these lines is such that the material formed could be either zinc ferrite or magnetite (Table 4).

TABLE 4. REACTION PRODUCTS OF HIGH IRON SPHALERITE (SAMPLE K-52)

Sample K-52 Residue*		Zincite†		Zinc Ferrite‡		Magnetite§	
d(Å)	I	*d*(Å)	I	*d*(Å)	I	*d*(Å)	I
—	—	—	—	4.84	20	4.86	30
2.97	5	—	—	2.98	50	2.97	60
2.816	70	2.816	71	—	—	—	—
2.601	40	2.602	56	—	—	—	—
2.547	10	—	—	2.53	100	2.53	100
2.473	100	2.476	100	—	—	—	—
—	—	—	—	2.43	10	2.425	10
—	—	—	—	2.10	40	2.097	50
1.912	30	1.911	29	—	—	—	—
—	—	—	—	1.72	40	1.714	40
1.622	50	1.626	40	1.62	70	1.615	60
1.487	5	—	—	1.49	80	1.484	70
1.474	30	1.477	35	—	—	—	—
1.377	20	1.379	28	—	—	—	—
1.357	10	1.359	14	—	—	—	—

* Copper radiation, Debye-Scherrer camera, 11.46 cm. diameter.

† Swanson, H. E. and Fuyat, R. K., 1953, Standard *X*-ray Diffraction Powder Patterns, N.B.S. Circ. 539, **II,** 26.

‡ Posnjak, E., 1930, The crystal structures of magnesium, zinc and cadmium ferrites, *Am. Jour. Sci.*, **19,** 67.

§ Rooksby, H. P., 1951, Oxides and hydroxides of aluminum and iron; *X*-ray Identification and Structures of Clay Minerals, G. W. Brindley, ed., Mineralogical Society, London, 345 pp.

The differential thermal curves for high iron sphalerites indicate that the oxidation reactions occur simultaneously. Sulfur is oxidized to sulfur dioxide, zinc goes to zinc oxide (zincite) and the iron present yields either zinc ferrite, magnetite or both. The pattern obtained is too weak to discern many of the zinc ferrite or magnetite lines. They are closely related in structure and spacings (Table 4), and would be difficult to distinguish even if complete patterns were available. Particles of the

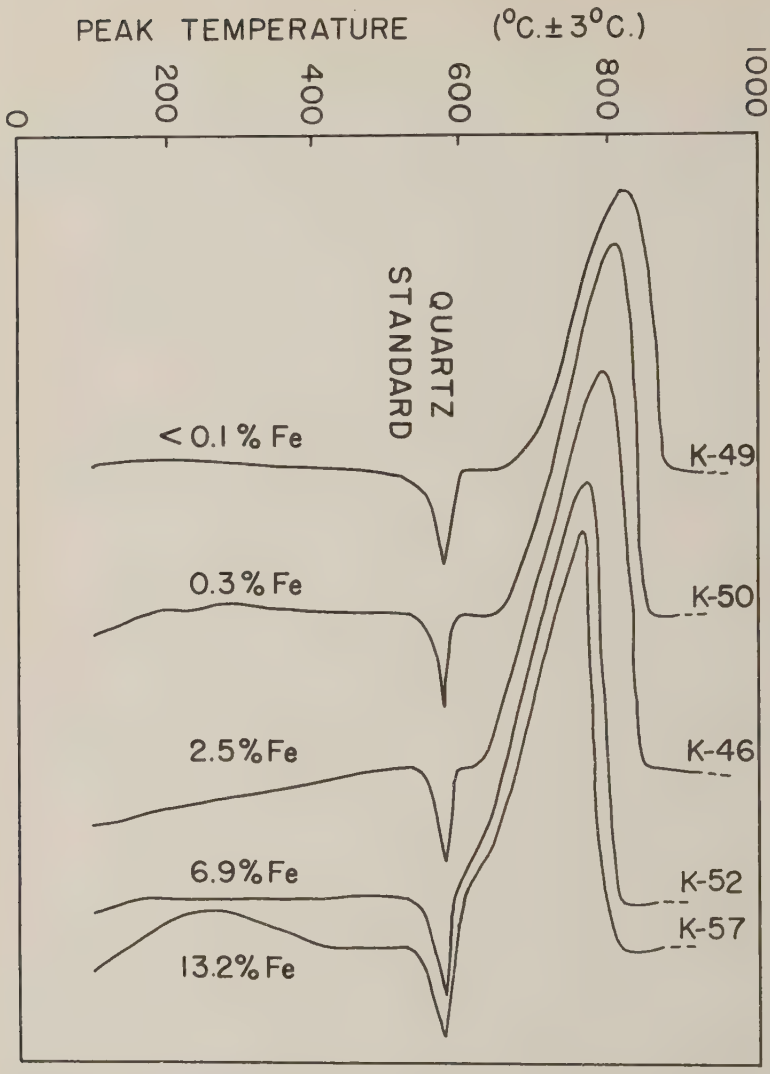

FIG. 5. Selected differential thermal curves of sphalerite. The peak temperature of sphalerite decreases with increasing iron content.

oxidized material tested with an Alnico magnet exhibit no magnetic properties.

IRON CONTENT AND PEAK TEMPERATURE

The peak temperature of sphalerite was observed to decrease with increasing iron content as illustrated in Figs. 5 and 6. Twenty-four

samples were selected for analysis as outlined in the section on procedures. Of these samples twelve were rejected for one or more of the following reasons:

1. Presence of lead, copper or cadmium as indicated by the *x*-ray spectrograph. (Some manganese was present in the high iron samples.)
2. Presence of exsolved pyrrhotite or other impurities in the 125–149 micron fraction visible under 45× magnification.
3. Presence of additional peaks in the thermal record (other than quartz).
4. Peak area of differential thermal curve less than 2000 mm.² for a 50 mg. sample.

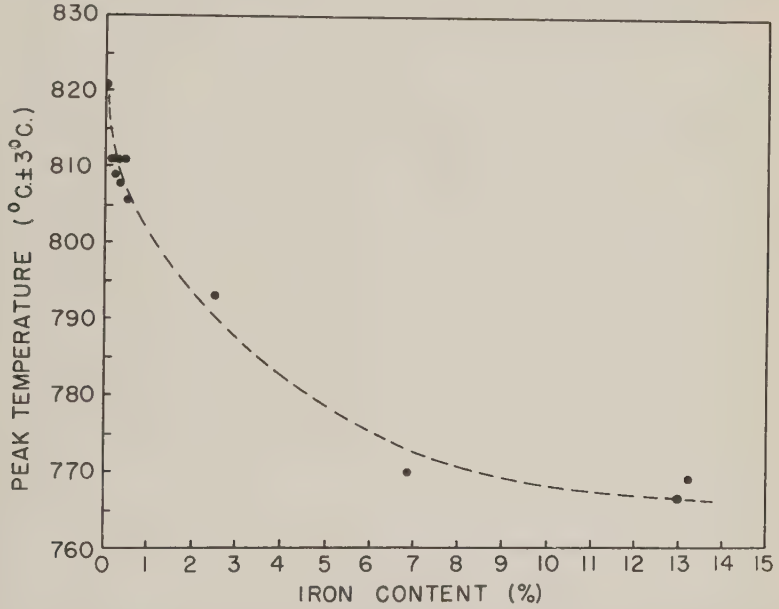

FIG. 6. Iron content vs. peak temperature. The presence of iron in the sphalerite lattice causes a decrease in the peak temperature. Iron contents greater than 7 per cent do not appear to materially affect the peak temperature.

Data for the twelve remaining samples are listed in Table 6 and illustrated in Figs. 5 and 6. Corrected peak temperatures were determined by adding to the observed peak temperatures the correction based on the heating rate and also a correction based on the peak temperature of the quartz standard. This accounts for a temperature difference of $\pm 2°$ C., corresponding to the peak temperature range of $580 \pm 2°$ C. (Table 5).

Thermal records in which the quartz peak did not fall within these limits were rejected. The variation of the quartz peak temperature is apparently due to minor shifts of the thermal head in the furnace.

TABLE 5. QUARTZ PEAK CORRECTION

Quartz Peak (° C.)	Correction (° C.)
578	+2
579	+1
580	0
581	−1
582	−2

TABLE 6. DATA FOR SPHALERITE VS. IRON CONTENT CURVE

Sample Number	Location	Color of Grains	Iron Content (%) (±5% of Value)	Peak Temperature (° C. ±2° C.)	Quartz Peak (° C. ±2° C.)	Heating Rate (° C. per Min.)	Correction (° C.)*	Peak Temperature Corrected (±3° C.)
K-49	Santander, Spain	Colorless —Yellow	less than 0.1	819	578	12	+2	821
K-30	Friedensville, Pennsylvania	Colorless —Yellow	0.1	808	580	11	+3	811
K-44	Cananea, Mexico	Colorless —Orange	0.2	810	580	11.5	+1	811
K-50	Oklahoma	Yellow —Orange	0.3	810	579	12	+1	811
K-43	Minaret, Germany	Yellow —Orange	0.5	810	580	11.5	+1	811
K-33	Kiffin, Ohio	Colorless —Orange	0.2	809	580	12	—	809
K-59	Jasper Co., Missouri	Colorless —Orange	0.3	808	580	12	—	808
K-53	Barren Grounds, N.W. Territory	Colorless —Black	0.5	808	582	12	−2	806
K-46	Cumberland, England	Colorless —Orange	2.5	792	580	11.5	+1	793
K-52	Troy, Montana	Black	6.9	768	579	11.5	+2	770
K-57	Rodna, Transylvania	Black	13.2	771	582	12	−2	769
K-58	Kokomo, Colo.	Black	13.0	768	581	12	−1	767

* The correction applied includes both heating rate changes and also the variation in the peak temperature of quartz.

Figure 6 illustrates the decrease in peak temperature for sphalerite with increasing iron content. The slope of the curve is quite steep at first, but it gradually decreases. Peak temperatures do not decrease appreciably for iron contents greater than 7%, but the validity of the curve in this region is uncertain. Most sphalerite containing iron in excess of 6% is black and it is difficult to determine whether all the iron is present in the sphalerite lattice, or if part of the iron has exsolved as pyrrhotite. In the event that exsolution has occurred, the curve will be displaced, since only that iron which is in the lattice is believed to affect the peak temperature.

Peak Temperatures and Lattice Constants

Kullerud (1953) has shown that the lattice constant of sphalerite increases with replacement of Zn by Fe, Mn and Cd. Replacement by iron causes the lattice constant to increase from 5.3985 ± 0.0001 Å for synthetic sphalerite containing 0% Fe to 5.4134 ± 0.0002 Å for sphalerite containing 36.5% Fe. The rate of increase in lattice constant when Mn substitutes for Zn is greater than for Fe, and the rate of increase when Cd substitutes for Zn is even greater. Kullerud states, "Thus the increase obtained when 1.0 mol. % CdS is dissolved in the ZnS lattice is equal to that caused by 3.6 mol. % MnS or to 11.5 mol. % FeS."

The relationship between the differential thermal peak temperature and the lattice constant appears to be of interest. It was hoped that some correlation could be made between Kullerud's lattice constant determinations based on iron content and the differential thermal peak temperature based on iron content. However, several problems exist. The lattice constant for a synthetic sphalerite (Swanson and Fuyat, 1953) containing 0.01 to 0.1% Cu, 0.001 to 0.01% B, Fe, Mg and Si, and less than 0.001% of Al and Ca was determined to be 5.4060 Å. If this value is placed in Kullerud's curve relating lattice constant with Fe content, the specimen would yield an anomalous 19% Fe. Also, Smith (1955) determined the lattice constants of forty natural specimens of sphalerite. The lattice value ranged from 5.4073 to 5.4246 Å (one specimen from Bolivia had a lattice constant of 5.4806, but this specimen proved to be hexagonal rather than isometric). The relationship of lattice constant to specimen color appears to be rather vague although color is thought to be a good indicator of replacement by foreign ions. Smith also showed that varying amounts of hexagonal packing are to be found in isometric sphalerites.

The lattice constants of seven sphalerite specimens were determined using the Debye-Scherrer method. Iron radiation was used, the period of exposure being from 32 to 48 hours. Films were corrected for shrinkage by the Straumanis technique. All measurements were made on a device

capable of readings to 0.05 mm. The lattice constants were determined from the (511) reflections (Table 7).

Table 7. Lattice Constants of Selected Sphalerite Specimens*

Specimen Number	Lattice Constant†	Per Cent Fe	Peak Temperature (±3° C.)
K-49	5.4082	less than 0.1	821
K-50	5.4087	0.3	811
K-46	5.4103	2.5	793
K-52	5.4160	6.9	770
K-57	5.4196	13.2	769

* Lattice constants for samples K-30 and K-53 are omitted from Table 7 and Figures 7 and 8. Sample K-30 appears to contain a relatively large amount of hexagonal packing which may affect the lattice constant determination. Sample K-53 exhibits a color range from colorless to black which is the widest color range of any of the specimens considered in the entire problem. The lattice constant determined for this specimen is probably questionable, and therefore was not used.

† Fourth place uncertain.

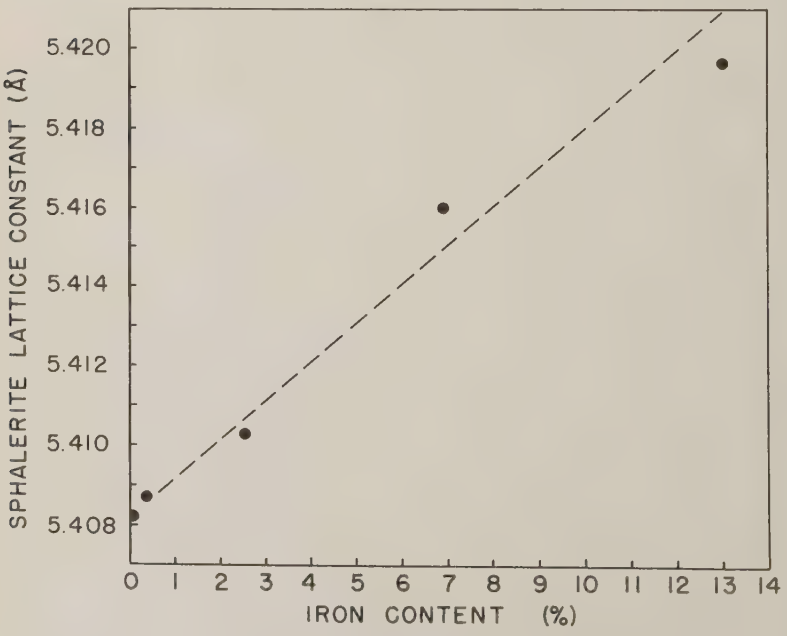

Fig. 7. Iron content vs. lattice constant. The lattice constant appears to increase linearly with increased iron content.

The lattice constant appears to increase with increasing iron content. The relationship of lattice constant to iron content is illustrated in Fig. 7, and that of lattice constant to differential thermal peak temperature is shown in Fig. 8.

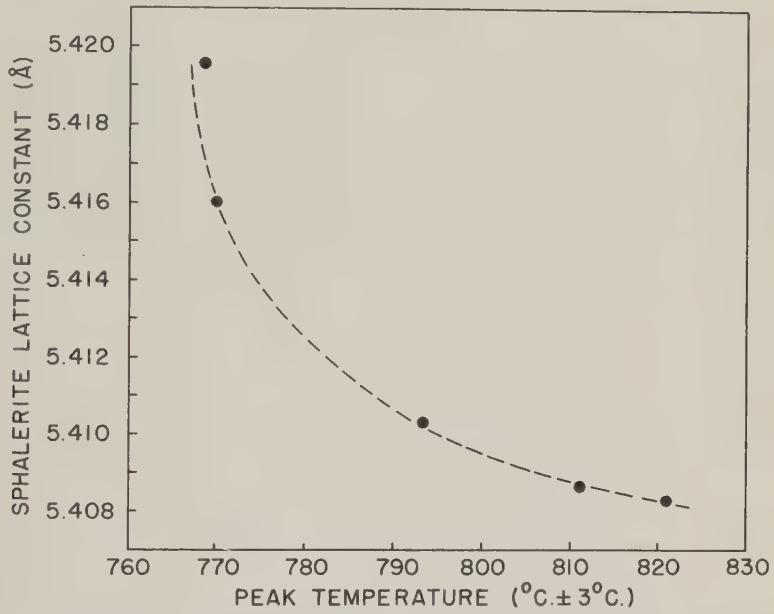

FIG. 8. Peak temperature vs. lattice constant. The peak temperature of sphalerite appears to decrease with increasing lattice constant as a result of increasing iron content.

CONCLUSIONS

Differential thermal analysis has been applied to sphalerite showing a relatively wide range in iron content. The observed progressive change in peak temperature with composition is of interest in investigating composition changes in relation to other factors such as lattice constants and temperatures of formation. Similar studies with other sulfides and arsenides may be possible. Quantitative as well as qualitative mineralogical determinations may be realized if the relation of the peak area to the amount of sample is consistent both in ore mixtures and in purified samples.

REFERENCES CITED

HILLER, J. E. AND PROBSTHAIN, K. (1955), Eine apparatus für die differentialthermoanalyse von sulfiden: Erzmetall, **VIII,** 257–267.

KEITH, M. L. AND TUTTLE, O. F. (1952), Significance of variation in high-low inversion of quartz: *Am. Journ. Sci.*, **Bowen Vol.,** 203–280.

Kopp, O. C. and Kerr, P. F. (1957), Differential thermal analysis of sulfides and arsenides: *Am. Mineral.*, **42,** 445–454.

Kullerud, G. (1953), The FeS-ZnS system, a geological thermometer: *Norsk Geol. Tidssk.*, **32,** 61–147.

Kulp, J. L. and Kerr, P. F. (1949), Improved differential thermal analysis: *Am. Mineral.*, **34,** 839–844.

Posnjak, E. (1930), The crystal structures of magnesium, zinc and cadmium ferrites: *Am. Jour. Sci.*, **19,** 67–70.

Prewitt-Hopkins, J. and Frondel, C. (1950), Thermal decomposition of zinc sulfide polymorphs: *Am. Mineral.*, **35,** 116.

Rooksby, H. P. (1951), Oxides and hydroxides of aluminum and iron: *X*-ray Identification and Structures of Clay Minerals, G. W. Brindley ed., Mineralogical Soc., London, 345 pp.

Smith, F. G. (1955), Structure of zinc sulphide minerals: *Am. Mineral.*, **40,** 658–675.

Swanson, H. E. and Fuyat, R. K. (1953), Standard *X*-ray Diffraction Powder Patterns: *U. S. Bur. Stands. Circ.* **539.**

Manuscript received November 14, 1957

SHERWOODITE, A MIXED VANADIUM(IV)-VANADIUM(V) MINERAL FROM THE COLORADO PLATEAU*

MARY E. THOMPSON, CARL H. ROACH, AND ROBERT MEYROWITZ,
U. S. Geological Survey, Washington 25, D. C.

ABSTRACT

Sherwoodite, a new vanadium mineral that has the probable formula $Ca_3V_8O_{22}\cdot 15H_2O$, has been found in small amounts in many vanadium-uranium mines on the Colorado Plateau. The new mineral occurs as dark blue-black holohedral tetragonal crystals bounded by {110} and {011}. The space group is $I4/amd$, (D_{4h}^{19}), $a_0=27.8\pm0.08$ Å, $c_0=13.8\pm0.08$ Å, $a:c=1:0.4964$, cell contents 16 ($Ca_3V_8O_{22}\cdot 15H_2O$). Sherwoodite is uniaxial negative, $\omega=1.765\pm0.003$, $\epsilon=1.735\pm0.003$, dichroism strong, O green, E blue. The hardness is about 2. The measured specific gravity is 2.8 ± 0.1.

The chemical analysis, in per cent, is as follows: CaO 13.2, MgO 0.5, V_2O_4 5.9, Al_2O_3 2.6, Fe_2O_3 0.8, V_2O_5 50.2, H_2O 23.1, insoluble 3.8, total 100.1.

Sherwoodite is named for Alexander M. Sherwood of the U. S. Geological Survey.

INTRODUCTION AND ACKNOWLEDGMENTS

Sherwoodite was first found in the Matchless mine, Mesa County, Colorado, by Alice D. Weeks and other members of a U. S. Geological Survey field party, in the summer of 1952. Another sample was collected later that summer from the Shadyside mine, on the east side of the Carrizo Mountains, San Juan County, New Mexico, by the same field party, but the two samples contained only enough of the mineral for x-ray powder patterns, preliminary determination of the optical properties, and a qualitative spectrographic analysis.

Early in 1954, as a result of a detailed study of the Peanut mine, Montrose County, Colorado, Carl H. Roach was able to collect enough sherwoodite for a chemical analysis and x-ray study. Because the material used for the mineral description was collected from the Peanut mine, that should be considered the type locality.

More recently, sherwoodite has been found in the vanadium-uranium ores of the J. J. and Mineral Jo mines of the Jo Dandy group in Montrose County, Colorado; the Fall Creek mine of Placerville, San Miguel County, Colorado; and on Wilson Mesa, Grand County, Utah.

We are happy to name this mineral for Alexander M. Sherwood (1888–), an analytical chemist of the U. S. Geological Survey, who has made many excellent and difficult mineral analyses for both the U. S. Bureau of Mines and the U. S. Geological Survey.

Thanks are due to Gabrielle Donnay for the unit-cell data, to C. S. Annell and K. V. Hazel for spectrographic analyses, and to H. T. Evans,

* Publication authorized by the Director, U. S. Geological Survey.

Jr., for advice on the selection of the chemical formula. All are with the U. S. Geological Survey. This work is part of a program being conducted by the U. S. Geological Survey on behalf of the Division of Raw Materials of the U. S. Atomic Energy Commission.

Occurrence

Sherwoodite is evidently widely distributed in the Uravan mineral belt. The Matchless mine, Mesa County, Colorado; the Shadyside mine, San Juan County, New Mexico; the Peanut mine, Montrose County, Colorado, and several other mines in which sherwoodite occurs are in the Salt Wash member of the Morrison formation of Late Jurassic age. Another locality, the Fall Creek mine, San Miguel County, Colorado, is in the Entrada sandstone of Late Jurassic age.

Sherwoodite is an oxidation product of lower valent vanadium minerals. It occurs as coatings on fracture surfaces and along partings in vanadium-bearing sandstones, and along fracture surfaces in mineralized coalified wood. It is commonly associated with hexagonal native selenium, metatyuyamunite, melanovanadite, and an undescribed vanadium mineral resembling hewettite. It alters to an ill-defined, fine-grained green material, probably a poorly crystallized compound of quinquivalent vanadium.

Physical and Optical Properties

Sherwoodite is tetragonal, ditetragonal-dipyramidal ($4/m2/m2/m$). Morphological measurements give a ratio of a:c = 1:0.497, in agreement with the x-ray determination of 1:0.4964 (measurements by Gabrielle Donnay). Crystals display only two forms, $m\{110\}$ and $d\{011\}$ (Fig. 1). The crystals are equant or slightly flattened, and occur singly and as polycrystalline aggregates.

Unaltered sherwoodite is dark blue-black and has a light blue streak,

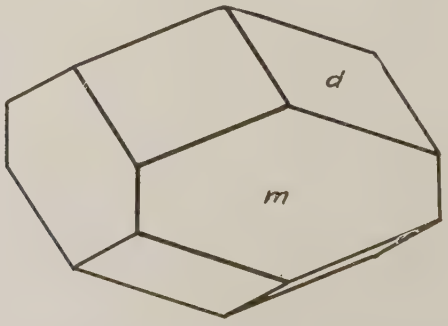

Fig. 1. Crystal drawing of sherwoodite showing the forms m {110} and d {011}.

but slightly altered specimens exhibit an apparently progressive color change to blue-green and yellow-green. This color change is accompanied by only very slight changes in the refractive indices and in the x-ray powder diffraction spacing, and is probably related to the oxidation of quadrivalent vanadium to the quinquivalent state. The luster is vitreous to earthy and the fracture is subconchoidal to uneven. The hardness is about 2. The specific gravity measured by flotation in a mixture of bromoform and acetone is 2.8 ± 0.1.

Sherwoodite is uniaxial negative. The indices of refraction and dichroism of blue-black sherwoodite and yellow-green material are presented below.

Indices	*Dichroism*
Blue-black crystals	
$\omega = 1.765 \pm 0.003$	O green
$\epsilon = 1.735 \pm 0.003$	E blue
Yellow-green material, finer grained	
$\omega = 1.765 \pm 0.003$	O yellow-brown
$\epsilon = 1.738 \pm 0.003$	E deep blue-green

X-Ray Data

X-ray precession photographs by Gabrielle Donnay of the U. S. Geological Survey of crystals of sherwoodite from the Peanut mine yielded the following data: tetragonal, space group $I4/amd$ (D_{4h}^{19}), $a_0 = 27.8 \pm 0.08$ Å, $c_0 = 13.8 \pm 0.08$ Å, $a:c = 1:0.4964$.

X-ray powder diffraction patterns of sherwoodite of various shades of blue and from several localities have been prepared. These patterns all have the three strongest lines in common and these lines on a powder pattern are sufficient for the identification of the mineral, but many of the other lines of the patterns show slight differences in spacing and variations in intensity. It has not been possible to index the powder patterns of sherwoodite with any degree of certainty because the large unit cell results in a very large number of weak and faint diffraction lines.

The unit cell constants and the d-spacings of a powder pattern of sherwoodite, showing the indices of some of the stronger lines, are listed in Table 1. The powder pattern was made by Mary E. Mrose of the U. S. Geological Survey with a Debye-Scherrer camera of 114.59 mm. diameter and CuKα radiation (Ni filter), $\lambda = 1.5418$ Å.

Chemical Analysis

Material for the chemical analysis was taken from samples collected from the Peanut mine, and consisted chiefly of fragments of dark blue

TABLE 1. UNIT-CELL CONSTANTS AND *X*-RAY POWDER DIFFRACTION DATA FOR SHERWOODITE

Tetragonal, $4/m2/m2/m$, space group $I4/amd$ (D_{4h}^{19}), $a_0=27.8\pm0.08$ Å, $c_0=13.8\pm0.08$ Å, $a:c=1:0.4964$, cell contents $16(Ca_3V_8O_{22}\cdot 15H_2O)$?

Cell volume	Density, measured	Molecular weight of cell contents
10,666 A³	2.8±0.1 g/cc	17,985
	Density, calculated for $Ca_3V_8O_{22}\cdot 15H_2O$	Molecular weight of $16(Ca_3V_8O_{22}\cdot 15H_2O)$
$\frac{10,666}{16\times37}=18$ A³ per oxygen	2.86 g/cc.	18,400
	Density, calculated from analysis (table 3)	Molecular weight from analysis (table 3)
	2.82 g/cc.	18,111

I	*d*, measured	*d*, calculated	*hkl*
S	12.3	12.37	011
S	10.0	9.82	220
MS	9.3	9.24	121
W	7.8	7.63	141
W	7.1	6.95	040
W	5.2		
F	5.0		
MW	4.65		
F	4.46		
F	4.19		
F	3.39		
W	3.25		
F	3.21		
W	3.10		
F	3.06		
F	2.96		
W	2.85		
F	2.77		
W	2.71		
M	2.61		
F	2.56		
W	2.28		
M, b	2.10		
W	2.07		
W	1.989		
W, b	1.743		

S strong, M medium, W weak, F faint, b broad.

crystals. The sample was handpicked under the binocular microscope. After a spectrographic analysis indicated that the sample might not be pure, it was rinsed with water, crushed to a slightly smaller grain size, rehandpicked, floated in bromoform of density 2.89 and sunk in bromoform of density 2.7. A second (microqualitative) spectrographic analysis showed no significant change in the proportions of elements present, and it may be that the "impurities" are really contained in the crystals in diadochic substitution for Ca or V. The semiquantitative spectrographic analysis of the handpicked sample gave the following results in per cent:

(C. S. Annell, analyst)

Over 10	V
5–10	—
1 –5	Ca Al Si
0.5 –1	Mg
0.1 –0.5	Fe
0.05 –0.1	Na Sr
0.01 –0.05	Pb Ti Ba
0.005 –0.01	—
0.001 –0.005	Mn Cr Sc
0.0005–0.001	—
0.0001–0.0005	Ag

For the determinations of CaO, Al_2O_3, Fe_2O_3, MgO, $H_2O(-)$, and total vanadium, a sample weighing 16 mg. was dried to constant weight at $110 \pm 5°$ C. The mineral was then dissolved in nitric acid and filtered to separate the insoluble residue.

Calcium oxide was determined as the sulfate after separation from the filtrate as the oxalate. Total vanadium was determined on an aliquot of the filtrate from the CaO determination after the oxalate had been destroyed by boiling with nitric acid. Total vanadium was determined spectrophotometrically using the hydrogen peroxide procedure. Another aliquot of the filtrate from the CaO determination was used to determine Fe_2O_3, which was done spectrophotometrically using the o-phenanthroline procedure.

Another aliquot was used for Al_2O_3, which was determined spectrophotometrically using the ferron procedure after the separation of aluminum, iron, and magnesium from vanadium by the use of 8-hydroxyquinoline. An aliquot of this solution was used for the spectrophotometric determination of MgO, using Clayton Yellow.

The V_2O_4 was determined by dissolving a 15-mg. sample of the mineral in (1+3) sulfuric acid and titrating with approximately 0.03 N standard potassium permanganate. The V_2O_5 was calculated by difference.

The insoluble matter was determined by boiling a 9 mg. sample with

(1+3) sulfuric acid in a weighed Schwarz-Bergkampf micro-filter beaker. The residue was filtered and washed with water and dried to constant weight at 110±5° C. The weighings were made with a microbalance.

Total H_2O was determined by use of a modified micro-combustion train of the type used for the determination of carbon and hydrogen in organic compounds. A 14-mg. sample was decomposed by ignition in a stream of oxygen.

The results of the chemical analysis are shown in Table 2.

TABLE 2. CHEMICAL ANALYSIS OF SHERWOODITE

(Robert Meyrowitz, analyst)

Constituent	Weight Per Cent	Recalculated		$(Ca_3V_8O_{22}\cdot 15H_2O)$
CaO	13.2	13.7	14.2	14.6
MgO	0.5	0.5		
V_2O_4	5.9	6.2	61.8	61.9 (V_8O_{16})
Fe_2O_3	0.8	0.8		
Al_2O_3	2.6	2.7		
V_2O_5	50.2	52.1		
H_2O (total)	23.1	24.0		23.5
Insoluble	3.8	—		
Total	100.1	100.0		100.0
$H_2O(-)$	14.5			

The unit cell contents of sherwoodite have such a large molecular weight that the formula cannot be calculated with absolute certainty from just one analysis. Another source of uncertainty is the problem of whether all the components shown by this analysis belong in the mineral or whether some represent admixed impurities.

The simplest formula having the correct molecular weight, however, was obtained when all of the components shown by the analysis were considered in the calculation (except "insoluble"). The CaO and MgO were summed, as were Al_2O_3, Fe_2O_3, V_2O_4, and V_2O_5. The details of the calculation are shown in Table 3.

The calculation yields the formula

$$(Ca, Mg)_3(V^{+5}_{0.\ell 4}, V^{+4}_{0.84}, Al^{+3}_{0.60}, Fe^{+3}_{0.12})_8O_{22}\cdot 15H_2O. \qquad (Z = 16)$$

This formula is in good agreement with the chemical analysis and the unit cell data, including the molecular weight, and the cell volume per number of oxygen atoms (Table 1).

This formula not only brings into agreement the analytical data, but

TABLE 3. CALCULATION OF THE FORMULA OF SHERWOODITE USING THE MOLECULAR WEIGHT CALCULATED FROM THE UNIT-CELL VOLUME AND THE DENSITY

Component	Analysis, less insoluble, recalculated to 100 per cent	Analysis (×45)[1]	Atomic proportions	Number of molecules per ¼ cell
CaO	13.7	617	11.01	11.57
MgO	0.5	22.5	0.56	
V_2O_4	6.2	279	1.68	15.98
Fe_2O_3	0.8	36	0.23	
Al_2O_3	2.7	121.5	1.19	
V_2O_5	52.1	2345	1288	
H_2O	24.0	1080	60	60
	100.0	4501		

[1] Molecular weight of content of quarter cell approximately 4500, calculated from unit cell volume and measured density.

also offers an explanation for the observed variations in color and *d*-spacings. If V^{+4} and V^{+5} are not distinguished in the sherwoodite structure, the relative amounts shown by this analysis of blue-black material may represent the equilibrium proportions of V^{+4} and V^{+5} under the conditions of formation of sherwoodite. The observed variations then might be related to the oxidation of the V^{+4}, a process that would result in the gradual breakdown of the structure.

Manuscript received November 25, 1957

NOTES AND NEWS

AN IMPROVED SPECIMEN HOLDER FOR THE FOCUSING-TYPE *X*-RAY SPECTROMETER*

MARTIN J. BUERGER AND GEORGE C. KENNEDY, *Massachusetts Institute of Technology, Cambridge, Massachusetts, and Institute of Geophysics, University of California, Los Angeles, California.*

ABSTRACT

A BT-cut quartz oscillator plate may be advantageously used as a specimen mount for a focusing-type *x*-ray spectrometer. The scattered radiation from this kind of mount is much less than that from a glass slide.

A variety of methods for preparing specimens for the focusing-type *x*-ray spectrometer have been described, (Adams and Rowe, 1954). Most of the methods have the objection that a large quantity of sample is required by comparison to that required for *x*-ray powder cameras. Where sample is at a premium, specimens are commonly prepared by mixing very dilute solutions of Duco cement in acetone with the sample and spreading this on the surface of a glass slide.

Scattered radiation from the glass slide, however, seriously interferes with discrimination of minor *x*-ray peaks, or peaks of phases present in small amounts. Specimen mounts of various materials were made up in a search for a specimen mount that would minimize scattered radiation. Among materials tried were various metals, cellophane, lucite and other plastics, and single crystals such as cleavage plates of calcite, cleavage plates of muscovite, and BT-cut quartz oscillator plates. Of these materials, the BT-cut quartz oscillator plate gave by far the best results.

X-ray patterns showing the relative amounts of scattered radiation from a glass slide and from a BT-cut quartz oscillator plate are shown in Fig. 1. These two patterns were made at identical power and gain settings on a North American Phillips *X*-ray Spectrometer.

Calcite cleavage fragments and muscovite cleavage plates also gave low-background scattered radiation, but in both cases major reflections from the single crystals were found within the examined range of 2θ. These strong reflections, of course, mask any reflections which occur in the same angular regions from powders on the holders.

The BT-cut quartz oscillator plate is cut at an angle of 49° from the *c* axis of a quartz crystal, sub-parallel to the $(10\bar{1}1)$ face. A small reflection occurs from a BT-cut oscillator plate at a 2θ value of 68.16° for CuKα

* Publication 88, Institute of Geophysics, University of California, Los Angeles, California.

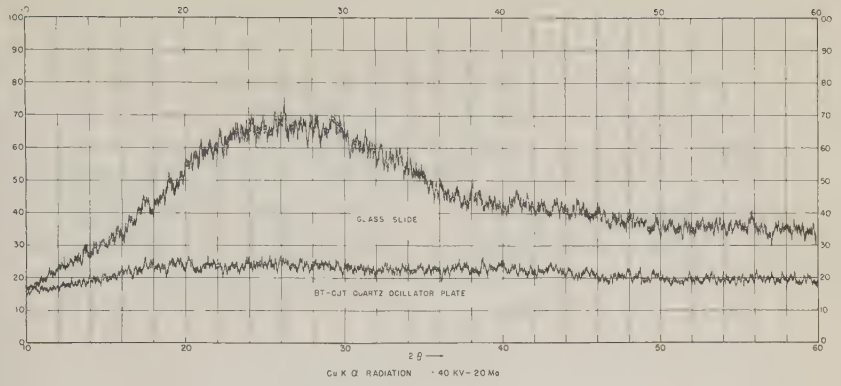

FIG. 1. *X*-ray patterns showing relative amounts of scattered radiation from a glass slide and from a BT-cut quartz oscillator plate.

radiation. This reflection is from the $(20\bar{2}3)$ plane in quartz. At this angle it gives little interference with most powder photography and, indeed, serves usefully on occasions as a built-in internal standard. The BT-cut plate diffracts at a higher angle 2θ than other standard cuts (Parrish and Gordon, 1945, p. 339). Any quartz-crystal plate cut with irrational indices would presumably serve equally well as a mount for powders.

One of the major advantages of quartz plates over glass slides as specimen mounts is that the *x*-ray spectrum can be recorded at very high power and high gain settings without disastrously masking expected reflections by scattered radiation. Thus samples comparable in size to those used in powder camera *x*-ray photography may be used, and several phases in a single small sample may be resolved. This is of particular value to the experimental petrologist where samples are often very small and at a premium.

REFERENCES

ADAMS, L. H. AND ROWE, F. A. (1954), The preparation of specimens for the focusing type *x*-ray spectrometer: *Am. Mineral.*, **39**, 215–221.

PARRISH, WILLIAM, AND GORDON, S. G. (1945), Orientation techniques for the manufacture of quartz-oscillator plates: *Am. Mineral.*, **30**, 296–346.

THE AMERICAN MINERALOGIST, VOL. 43, JULY–AUGUST, 1958

THE LEUCITE NEPHELINE DOLERITE OF MEICHES, VOGELSBERG, HESSEN

C. E. Tilley, *Cambridge University, Cambridge, England.*

The nepheline dolerite of Löbau, Saxony and its leucitic relative, the leucite nepheline dolerite of Meiches in the Vogelsberg, Hessen, are recognized as the type examples of such assemblages in petrographic literature.

The latter rock with its component minerals was early subject to detailed chemical investigation by Knop (1865) and his data have been incorporated in successive editions of Rosenbusch's *Elemente der Gesteinslehre.*

Sommerlad (1883) later provided additional microscopic data on the rock but there appears to be no recent reassessment of its mineralogy and composition.

In view of the phase equilibrium studies in the system $NaAlSiO_4$—$KAlSiO_4$—SiO_2, this Vogelsberg assemblage is of particular interest as it carries the three phases leucite, nepheline and alkali feldspar which are known to co-exist at the ternary point in this system.

In the preliminary account of the experimental system, Schairer and Bowen (1935) delineated the primary phase fields in the quadrilateral $NaAlSi_3O_8$–$KAlSi_3O_8$–$KAlSiO_4$–$NaAlSiO_4$, but tie lines for the principal phases were not then reported.

For some natural assemblages equivalent tie lines joining co-existing nepheline and alkali feldspar solid solutions can be drawn and these data for a number of phonolitic lavas have now been determined (Tilley, 1954, 1956).

Sobolev (1956) has recently used Knop's early analyses of the minerals of the Vogelsberg rock to present graphically the triangle of solid phases (leucite, nepheline, alkali feldspar) for the reaction point of the system, but these analytical data are much too inferior to be of service in this connection; moreover some of Sobolev's deductions on the crystallization phenomena in this system are fallacious.

It is imperative that modern analyses of the Vogelsberg rock and its constituent salic minerals should be available before its crystallization phenomena can be reliably discussed. This chemical analytical work has now been carried out by Mr. J. H. Scoon and is reported below.

The leucite nepheline dolerite of Meiches is built of titaniferous augite in crystals reaching dimensions of one centimeter or more in length, rounded leucites, euhedral nepheline, anhedral sanidine, and as accessories, iron ores and apatite. Biotite and occasional grains of sphene are

also recorded in sections. It is clear that the accessories, the titanaugite and the nepheline crystallized at an early stage and were followed by leucite with sanidine as the last mineral to crystallize. This is evident from the textural relations, for the sanidine envelopes both nepheline and leucite, forming an interstitial cement to the assemblage as a whole.

Table I presents the analyses of the rock and its constituent sanidine

TABLE 1

	1	2	3	Norm of 1		Metal atoms to 32 oxygens in 2	
SiO_2	43.18	42.28	63.62				
Al_2O_3	20.72	33.71	19.12	Lc	22.67	Si 8.18	
Fe_2O_3	2.39	0.80	0.47	Ks	0.47	Al 7.66	15.98
FeO	5.21			Ne	35.07	Fe''' 0.14	
MnO	0.13			An	6.95		
MgO	3.22	0.03	0.05	Cs	0.37	Ca 0.11	
CaO	8.00	0.56	0.05	Di	22.99	Na 6.22	ΣR
Na_2O	7.65	16.61	2.66	Wo	0.46	K 1.43	7.87
K_2O	5.07	5.75	12.09	Il	5.47		
H_2O-	0.42	0.03	nil	Mt	3.48	$Ne_{76.2}Ks_{19.5}An_{2.8}Qz_{1.5}$	
H_2O+	0.67	0.34*	0.11*	Ap	1.01	$(Ne_{78.4}Ks_{20.0}Qz_{1.6})$	
TiO_2	2.90	0.07	0.08	Ct	0.18		
P_2O_5	0.42			Rest	1.09		
BaO	0.12		1.56		100.21		
CO_2	0.08			$(Ne_{60.2}Ks_{29.1}Qz_{10.7})$			
	100.18	100.18	99.81				

* Loss on ignition.

1. Leucite nepheline dolerite, Meiches, Vogelsberg, Hessen.
2. Nepheline } from 1.
3. Sanidine $(Or_{73.0}Ab_{22.9}An_{0.3}Cs_{3.8})$ }

and nepheline. An analysis of the leucite fraction which contained minor amounts of impurity not separable, gave figures for alkalis K_2O 19.42, Na_2O 1.12, these results confirming earlier analytical data on this mineral that replacement of potassium by sodium in rock forming leucites is quite limited. The analyses have been plotted in Figure 1 in the customary manner, the rock analysis by transformation of the salic constituents of the norm, less anorthite, to the co-ordinates of the system $NaAlSiO_4$ · $KAlSiO_4$–SiO_2.

The salic composition of the rock as calculated from the norm falls inside the solid phase triangle Lc-Ne-Sa at N, but with this method of

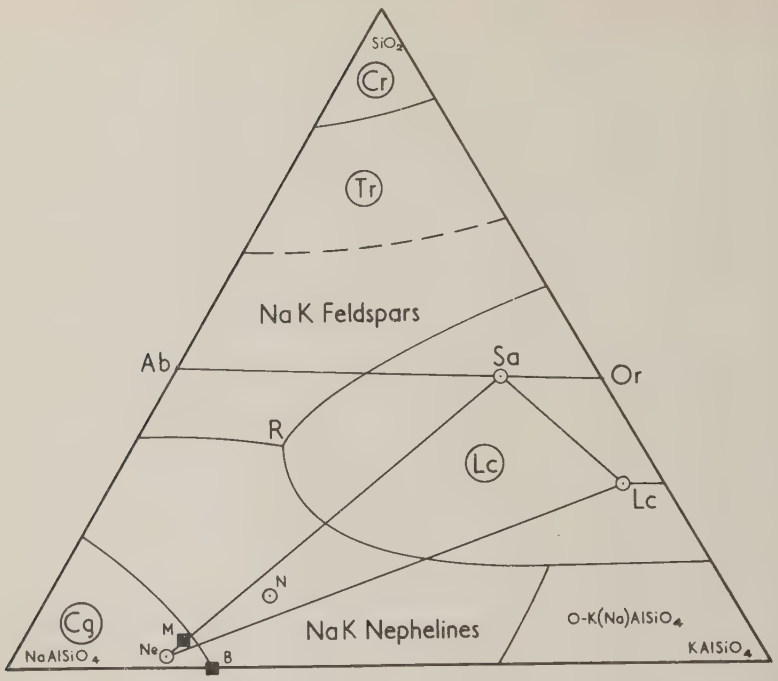

FIG. 1. Plot of the compositions of the Vogelsberg leucite nepheline dolerite and its salic minerals in the system $NaAlSiO_4$—$KAlSiO_4$—SiO_2.

N = rock, Ne = nepheline, Lc = leucite, Sa = sanidine, M and B nepheline formulae of Morozewicz and Buerger respectively (Tilley, 1954, pp. 65–66).

calculation we cannot derive therefrom the relative proportions of the constituent phases.

It is clear however from the position of N that nepheline should be the primary phase among the salic minerals, and that in the course of crystallization it would be joined by leucite, the two crystallizing together to the reaction point R*, when crystallization would be completed by a reaction involving partial resorption of leucite and precipitation of sanidine along with nepheline.

$$R_{liq} + \text{leucite} \rightarrow \text{nepheline} + \text{sanidine}$$

The observed textural relations of the minerals are as already noted in conformity with this sequence of crystallization and indeed with the

* In Dr. Schairer's revision of the $NaAlSiO_4$—$KAlSiO_4$—SiO_2 system (1950, fig. 1, p. 514) the temperature of this ternary point is redetermined at 1020° ± 5° C. On my enquiry, Dr. Schairer informed me that he believed the minimum on the boundary curve feldspar-nepheline lies so close to the ternary point in temperature and composition as to be within experimental error in these viscous melts where equilibrium is attained so slowly.

crystallization history now inferred from the bulk chemical composition of the rock and the known phase relations within the ternary system.

References

Knop, A. 1865. Ueber den Nephelin dolerit von Meiches im Vogelsberge: *Neues Jbuch Min.*, 674–710.

Rosenbusch, H. 1923. *Elemente der Gesteinslehre* (4th edition revised by A. Osann), Stuttgart, 480.

Schairer, J. F. 1950. The alkali-feldspar join in the system $NaAlSiO_4$—$KAlSiO_4$—SiO_2: *Jour. Geol.* **58,** 512–517.

Schairer, J. F. and Bowen, N. L. 1935. Preliminary report on equilibrium-relations between feldspathoids, alkali feldspars and silica: *Am. Geophys. Union Trans.*, 16th Ann. Meeting, 325–328.

Sobolev, V. S. 1956. Additions to the melting diagrams in the systems nepheline-kaliophilite-silica and orthoclase-albite-anorthite: (in Russian) *Mineral. Symposium Geol. Soc. Lvov*, No. 10, 68–76.

Sommerlad, H. 1883. Ueber Nephelingesteine aus dem Vogelsberg: *Ber. d. Oberh. Ges. f. Natur u Heilkunde*, **22,** 263–284.

Tilley, C. E. 1954. Nepheline-alkali feldspar parageneses: *Amer. Jour. Sci.*, **252,** 65–75.

———. 1956. Nepheline Associations: *Verh. Geol. Mijnb. Gen. Ned.* Geol. Ser., 16, 403–413 (Brouwer volume).

THE AMERICAN MINERALOGIST, VOL. 43, JULY-AUGUST, 1958

NOTE ON LITHIOPHOSPHATE

D. Jerome Fisher, *University of Chicago, Chicago, Illinois.*

This name has been given by V. V. Matias and A. M. Bondareva to Li_3PO_4 occurring as a hydrothermal replacement of montebrasite in a Kola pegmatite according to an abstract by M. Fleischer. Over eight years ago the writer took an *x*-ray diffraction pattern of the synthetic powder of this material (see the table), suspecting that it would be present in his pegmatite collections, but it never turned up. This pattern agrees well with that by A. P. Denisov quoted in the Fleischer abstract.

Zambonini and Laves found synthetic Li_3PO_4 to be orthorhombic with the olivine-triphylite structure with unit cell $a=10.26$, $b=4.86$, $c=6.07$kX. (orientation of chondrodite with $c<a$), space group *Pnam*. The indices shown in the table are accordingly taken from those given for the corresponding olivine reflections by Swanson and Tatge.

C. Guillemin's suggestion that this should be called lithiophosphatite is one that should meet with general agreement. Dana's System has in class 38 no place for the $A_3(XO_4)$ type that would seem to include lithiophosphatite. However it is proper to place it near the triphylite group of $AB(XO_4)$ type, just as the heterosites are put here rather than with

Powder Diffraction Data on Synthetic Li_3PO_4

Int.	d(kX.)	Indices	Int.	d	Int.	d
5	5.217	200	2	1.676	2	1.191
1	4.372	110	1	1.640	2	1.185
1	4.180	—	2	1.606	2	1.166†
10	3.976	201	1	1.584	2	1.159†
10−	3.792	011	2	1.559	1	1.150
6	3.547	111, 210	1	1.542	1	1.139
4	3.053	211	3	1.526	omit two weak lines	
½	2.902	—	5	1.513	2	1.101
8+	2.667 *	310	1	1.494	1	1.086
5	2.608 *	311	1	1.468	2	1.081
7	2.420	112	1	1.402	1	1.069
5	2.309†	212, 410	5	1.377	omit about three weak lines	
½	2.194	121	omit two weak lines		3	1.023 *
1	2.152	312	2	1.293	1	1.020 *
1	2.067	402	3	1.285 *	omit two weak lines	
½	1.897	510	2	1.278 *	2	1.003 *
1	1.875	113	1	1.264	2	1.002 *
2	1.838	511	1	1.254	omit five weak lines	
4	1.783 *	222				
3	1.767 *	421				
½	1.741	601				
¾	1.706	313				

Fe/Mn radiation in a Straumanis-type 114.6 mm. camera. Intensities by visual estimation; measured by Leon Atlas. * doublet; † diffuse line.

the $A(XO_4)$ type where they belong according to a strict purely-chemical interpretation.

References

Fleischer, M. (1957) *Am. Mineral.*, **42,** 585.

Guillemin, C. (1957) *Bull. Soc. fran. Min. et Crist.*, **80,** 217.

Palache, C., Berman, H., and Frondel, C. (1951) The System of Mineralogy of the Danas (7th ed.) **2,** 654.

Swanson, H. E. and Tatge, E. (1951) *J. Res., Nat. Bur. St.*, **46,** 325.

Zambonini, F. and Laves, F. (1932) *Zeit. Krist.*, **83,** 26.

THE AMERICAN MINERALOGIST, VOL. 43, JULY–AUGUST, 1958

AN OCCURRENCE OF GORCEIXITE IN ARKANSAS*

Edward J. Young, *U. S. Geological Survey, Denver, Colorado.*

An unusual occurrence of radially fibrous botryoidal gorceixite, $BaAl_3(PO_4)_2(OH)_5 \cdot H_2O$, has been found in sec. 16, T. 2 S., R. 18 W., 6

* Publication authorized by the Director, U. S. Geological Survey.

miles from Hot Springs, Garland County, Arkansas. Material collected in July 1956, by the Arkansas Geological and Conservation Division, was submitted to the Denver Area office of the U. S. Atomic Energy Commission. The gorceixite occurs on the south limb of one of the southwest plunging anticlines in the Zig Zag Mountains in the Arkansas novaculite, which is Devonian and Mississippian in age. The locality is within 10 miles of the Magnet Cove intrusive area and the Chamberlain Creek barite deposit.

The gorceixite in the form of spheroids, up to one centimeter in diameter, coated with black goethite (Fig. 1), occurs as incrustations in narrow fractures about $\frac{1}{4}$ inch wide in the Arkansas novaculite. The interiors consist of whitish radially fibrous gorceixite containing soft brown limonite between the fibers (Fig. 2). Under the microscope the gorceixite is very clouded and seems almost opaque. It has low birefringence and an index of refraction of approximately 1.61. Lathlike grains are length positive and show parallel extinction in polarized light.

A semiquantitative spectrographic analysis by Pauline J. Dunton of the U. S. Geological Survey follows:

Weight per cent	*Element*
M	Al, P
7	Ba, Fe
3	Sr
1.5	Ca
0.3	Si, As, U
0.15	Y, V
0.07	Mo, Sb
<0.05	Na
0.03	Ce, Cr, Cu, Nd
0.015	Dy, Er, Gd, La, Sc
0.007	Mg, Ti, Yb
0.003	Zr
0.0015	Mn, Ga
0.0007	Pb
0.0003	Be, Co, Ni

NOTE: Figures are reported to the nearest number in the series 7, 3, 1.5, 0.7, 0.3, 0.15, etc. M=major constituent—greater than 10 per cent. Sixty per cent of the reported results may be expected to agree with the results of quantitative methods.

Practically all the iron represents limonite impurity, which was demonstrated by first dissolving the limonite with repeated washings of concentrated HCl. From obviously impure gorceixite, the resultant product became almost white gorceixite, which was then sintered with Na_2O_2 at 440° C. After bringing the sinter product into solution and acidifying it, the sensitive potassium ferrocyanide test for Fe^{+++} was applied and only a trace of Fe was indicated. Gorceixite is extremely insoluble—so

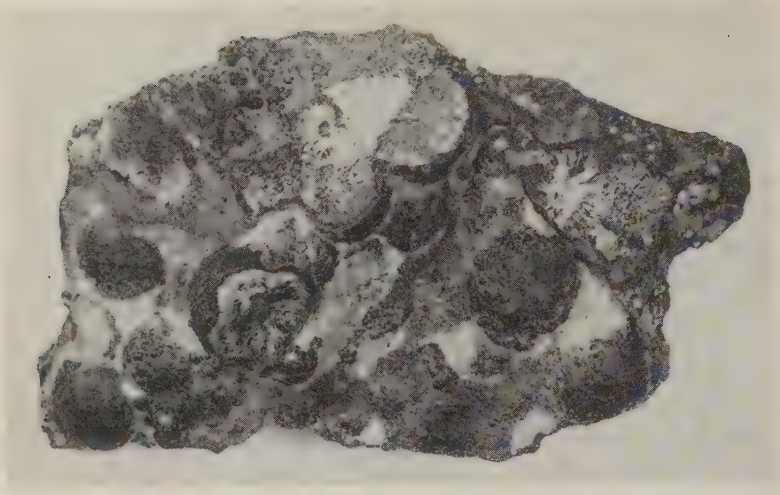

FIG. 1. Spheroids of gorceixite. ×2.5.

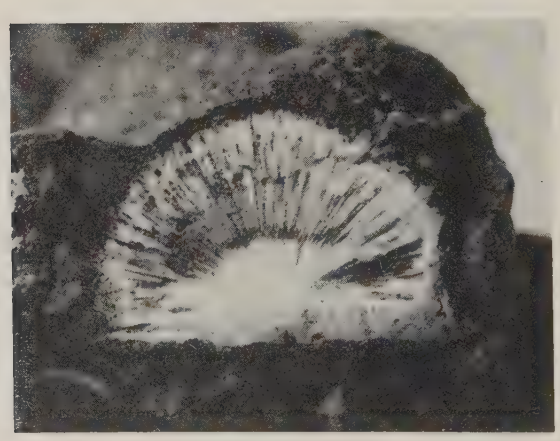

Photographs by Wendell Walker, U. S. Geological Survey

FIG. 2. Interior of spheroid showing radially fibrous gorceixite. ×8.

much so that Na_2CO_3 and $NaHSO_4$ fusions failed to bring it into solution. Presence of water in the mineral is shown by closed-tube test on material leached free of limonite by acid. Sulfate was tested for and not found.

Uranium and the rare earths are important trace elements in this occurrence of gorceixite. The rather large amount of Sr present suggests an isomorphous series between gorceixite and goyazite, $SrAl_3(PO_4)_2(OH)_5 \cdot H_2O$.

An x-ray powder photograph of this mineral taken by Richard P. Marquiss of the U. S. Geological Survey matched a mineral described as gorceixite from Dale County, Alabama (Charles Milton et al., this issue).

This work is part of a program being conducted by the U. S. Geological Survey on behalf of the Division of Raw Materials of the U. S. Atomic Energy Commission.

THE AMERICAN MINERALOGIST, VOL. 43, JULY-AUGUST, 1958

OPTICS OF THE EOSPHORITE-CHILDRENITE SERIES

HORACE WINCHELL, *Yale University, New Haven, Connecticut.*

Hurlbut (1950) discussed the evidence that the childrenite-eosphorite series $Mn_{1-x}Fe_xAl(PO_4)(OH)_2(H_2O)$ is indeed a continuous isomorphous series, citing examples with $x=0.04$, 0.14, 0.16, 0.23, 0.32, 0.33, 0.39, 0.47, 0.85, and 0.91, and giving in summary a variation diagram relating the optical properties and specific gravity to the weight per cent of FeO as determined by chemical analysis. Hurlbut's Table 2, summarizing the data on which his diagram is based, shows two apparently discontinuous changes. The optic orientation is practically constant with $X=b$ and $Z\wedge c=3°$ to 8° throughout the eosphorite half of the series ($x<0.5$), then changes to $X=b$ and $Y\wedge c=6°$ to 8° for childrenite ($x>0.8$); moreover, in the interval $0.5<x<0.8$, for which there are no data, the dispersion of 2V also reverses.

These changes can be explained easily if the curves for $n_\perp$ and $n_\parallel$, representing the refractive indices for the principal vibration-directions that are respectively almost perpendicular and almost parallel to c, cross one another in the neighborhood of $x=0.6$ to 0.7; analogous changes of axial plane are well known in other mineral series such as lithiophilite-triphylite, and always result in a change of the dispersion of 2V in passing through the composition for which $2V=0°$, in addition to the exchange of positions by two of the principal vibration directions—either X and Y, or Y and Z. In such a case there should also be a small range of compositions with crossed-axial-plane dispersion, *i.e.*, with the optic plane for one end of the spectrum at right angles to that for the opposite end; such a condition is easily recognized by abnormal interference colors in certain grains and thin sections of the mineral. Dispersion of 2V, if observable in such minerals, is $r>v$ on one side of the uniaxial composition and $r<v$ on the other. The obvious test of this hypothesis for eosphorite-childrenite is to find or make a crystal of manganoan childrenite with composition near $x=.65$, and observe whether such a crystal has

small 2V; with good luck, one might even hope to find a crystal with crossed-axial-plane dispersion and abnormal interference colors.

Lacking a crystal of the necessary composition, we may turn to the other available optical data to seek internal evidence concerning this hypothesis. For example, if precise enough refractive index figures are available, one may compare the goodness of fit, (a) between the data

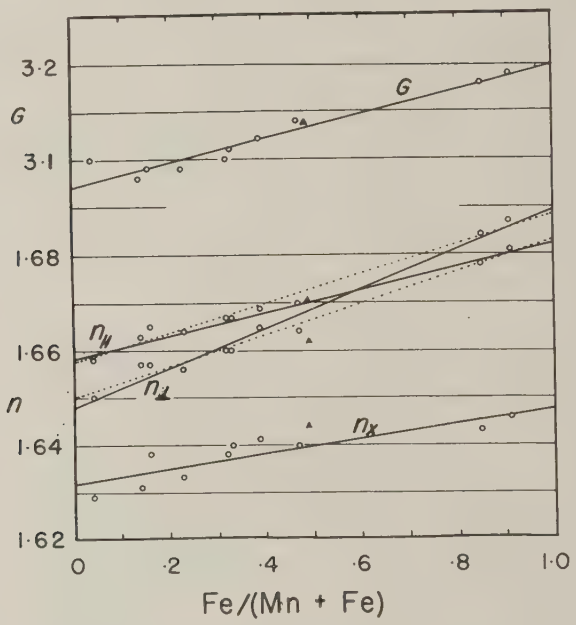

FIG. 1. Variations in physical properties in the Eosphorite—Childrenite series (modified from Hurlbut, 1950). The lines represent the regression equations (2) given in the text.

Dotted lines are n_y and n_z according to Hurlbut's interpretation; the solid lines $n_{\parallel}$ and $n_{\perp}$ show the preferred hypothesis.

and a pair of variation curves that cross somewhere in the range $0.5 < x < 0.8$, with (b) the fit obtained using curves that do not cross. This is attempted without decisive results in Fig. 1 and in the following:

Hurlbut's data (1950, Table 2, p. 803) appear to be by far the best available describing the variations of physical with chemical properties. His independent variable was the weight percentage of FeO in the analyses; for convenience these weight percentages were divided by 31.26, the percentage by weight of FeO in the childrenite end-member, $FeAl(PO_4)(OH)_2(H_2O)$, giving a number $x'(0 \leqq x' \leqq 1)$ that differs from the atomic proportion x by less than 0.005, well within the probable limits of chemical-analytical uncertainty. Considering x[or x'] as the independent

variable, linear regression formulas were computed by the method of least squares for each of the physical properties G, n_x, n_y, n_z as given by Hurlbut, and also for $n_\perp$ and $n_\parallel$. The equation for linear variation is

$$y_i = a_i + b_i x + s_i \tag{1}$$

where y_i is the measure of one of the physical properties, considered as the dependent variable; a_i and b_i are parameters to be determined; x is the independent variable defined above; i refers in turn to each of the physical properties G, n_x, n_y, n_z, $n_\parallel$, $n_\perp$; and s_i is the root-mean-square deviation of the observations from the calculated values. Least-squares evaluations of the several a's, b's, and s's give

$$\left.\begin{aligned} G &= 3.071 + 0.127x \pm 0.010 \\ n_x &= 1.6317 + 0.0160x \pm 0.0025 \\ n_y &= 1.6500 + 0.0332x \pm 0.0015 \\ n_z &= 1.6574 + 0.0312x \pm 0.0013 \quad (2a) \\ n_\parallel &= 1.6592 + 0.0233x \pm 0.0011 \\ n_\perp &= 1.6482 + 0.0411x \pm 0.0019 \quad (2b) \end{aligned}\right\} \quad (2)$$

There is no significant difference in the s-values in equations (2a) as compared with equations (2b). A careful plot of the data (Fig. 1) tends to confirm the same conclusion, and also shows that the hypothesis of linear regression is satisfactory for G, n_y, n_z, $n_\parallel$, and $n_\perp$, but perhaps not for n_x.

Strunz and Fischer (1957) provide further data that are shown in Fig. 1 by small triangles, but are not included in the above calculation. Their values for a specimen from Hagendorf with FeO = 14.86% (wt.) and unusually high CaO (3.587% wt.), are $n_x = 1.644$, $n_y = 1.662$, $n_z = 1.671$, $2V = (-)25°$, $Y \| c$ and $G = 3.11$ to 3.15, agreeing essentially with Hurlbut's data for material from Red Hill, Rumford, Maine (14.62% FeO, $n_x = 1.640$, $n_y = 1.664$, $n_z = 1.670$, $2V = (-)45°$, $Z \wedge \mathbf{c} = 4°$, $r < v$, $G = 3.14$). Strunz and Fischer's value of n_x also helps suggest that n_x does not vary linearly. They discuss the x-ray data so far published and conclude that the mineral is orthorhombic, and that the small extinction angles generally observed are anomalous. The change of optic orientation discussed here is probably due to intersection of the curves for $n_\parallel$ and $n_\perp$ regardless of the question of orthorhombic or lower symmetry.

Equations (2b) show that the uniaxial composition (if one exists) is near $x = .62$. The change in optic orientation and the reversal of the dispersion of $2V$ strongly favor the existence of such a composition. A sample of eosphorite-childrenite with x near .62 would probably afford the data needed to settle the question. The alternative hypothesis that childrenite-eosphorite is not in fact a continuous isomorphous series seems improbable on the basis of known data.

References

Hurlbut, C. S., Jr., (1950) Childrenite-Eosphorite Series: *Am. Mineral.*, **35**, 793–805.
Strunz, H. and Fischer, M. (1957) *Neues Jahrbuch fur Mineralogie*, Monatshefte, p. 78.

THE AMERICAN MINERALOGIST, VOL. 43, JULY–AUGUST, 1958

ADDITIONAL DATA ON BIKITAITE

Cornelius S. Hurlbut, Jr., *Harvard University, Cambridge, Mass.*

A new mineral, *bikitaite*, $LiAl_2O_6 \cdot H_2O$, was described in the November-December, 1957 *American Mineralogist.** The description was made on fine grained material interstitial to granular eucryptite and quartz. The largest fragments of single crystals were measured in tenths of millimeters.

Shortly after the manuscript on bikitaite was submitted for publication, Mr. George H. Nolan sent the writer another specimen from his mine in Southern Rhodesia. This specimen, measuring $25 \times 15 \times 15$ centimeters is largely granular eucryptite and quartz as in the original material. However, one surface is covered by bikitaite with individual crystals measuring up to six centimeters in length, and one centimeter across (Fig. 1). In addition, massive bikitaite forms a layer beneath the crystals two to five centimeters thick.

The bikitaite crystals are coated with a thin crust of stilbite so that, although the crystal habit is well displayed, there are no faces visible. Two other minerals, formed later than the stilbite, are present on the specimen. These are calcite, in scalenohedral crystals; and allophane, filling voids between some of the bikitaite crystals.

When the stilbite crust is removed, the bikitaite crystals are seen to be colorless and transparent. They are elongated on [010] (Fig. 2); and the faces in this zone are of high quality. The faces of the [001] zone, that terminate the elongated crystals, are deeply etched and thus give poor measurements on the reflecting goniometer. At the end of some crystals etching has produced slots several millimeters deep parallel to (100).

All the crystals are of the same habit with $c\{001\}$ and $t\{\bar{1}01\}$ the dominant forms in the [010] zone. Because these two forms have nearly equal development and similar rho angles, the crystals have a pseudo-orthorhombic appearance. Three etched forms, $b\{010\}$, $m\{110\}$ and $n\{210\}$, terminate the crystals. Of these, the faces of $\{210\}$ are the largest and also the most deeply etched. $o\{\bar{1}12\}$ was noted on only one

* C. S. Hurlbut, Jr., Bikitaite, $LiAlSi_2O_6 \cdot H_2O$, a new mineral from southern Rhodesia. *Am. Mineral.*, **42**, p. 792–797, 1957.

crystal as small faces of poor quality. From the faces that can be measured on the two-circle goniometer are obtained angular measurements that show a remarkably close agreement with the angles calculated for these forms using x-ray measurements. For example, $(100)\wedge(001) = 65°28'$, measured; whereas the calculated angle is $65°26'$. Because of

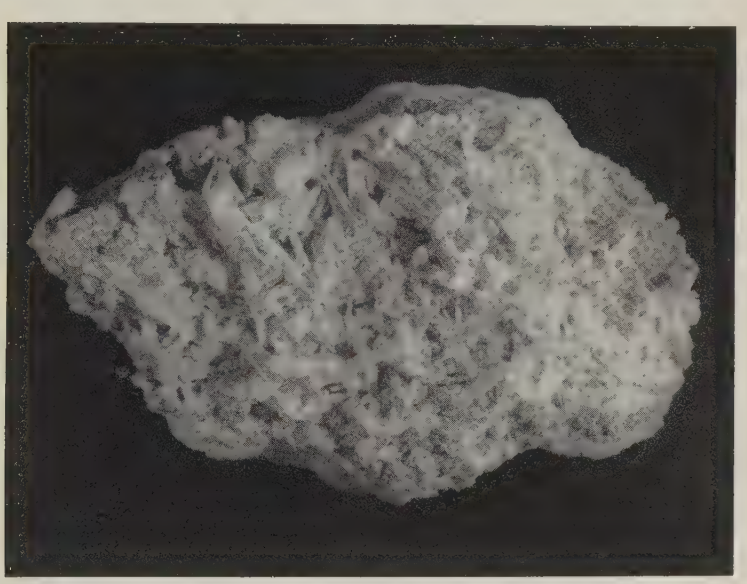

FIG. 1. Specimen coated with bikitaite crystals. Surface 25×15 centimeters.

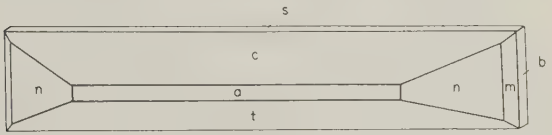

FIG. 2. Bikitaite crystal.

this good agreement and because of the poor angular readings of the etched terminal faces, the angles given in Table 1 are calculated from x-ray measurements.

In the original description it was noted that, when examined microscopically, some grains show parallel extinction with positive elongation. Since two different optical orientations were observed in these grains, it was argued that there might be poor $\{001\}$ and $\{100\}$ cleavage. This conclusion is supported by examination of the larger crystals which show

TABLE 1. BIKITAITE: ANGLE TABLE
Monoclinic: prismatic—2/m

$a:b:c = 1.7434:1:1.5434$ $\beta = 114°34'$ $p_0:q_0:r_0 = 0.8853:1.4033:1$
$r_2:p_2:q_2 = 0.7126:0.6309:1$; $\mu = 65°26'$ p_0' 0.9734, q_0' 1.5434, x_0' 0.4571

Forms	ϕ	ρ	ϕ_2	$\rho_2 = B$	C	A
c 001	90°00′	24°34′	65°26′	90°00′	—	65°26′
b 010	0°00′	90°00′	—	0°00′	90°00′	90°00′
a 100	90°00′	90°00′	0°00′	90°00′	65°26′	—
m 110	32°16′	90°00′	0°00′	32°16′	77°11′	57°44′
n 210	51°36′	90°00′	0°00′	51°36′	70°59′	38°24′
s $\bar{1}02$	−90°00′	1°42′	91°42′	90°00′	26°16′	91°42′
t $\bar{1}01$	−90°00′	27°18′	117°18′	90°00′	51°52′	117°18′
o $\bar{1}12$	− 2°12′	37°38′	91°42′	52°18′	44°48′	91°21′

a perfect {100} cleavage and a good, though less easily developed, {001} cleavage. Across these cleavages there is a conchoidal fracture.

The specific gravity, determined by suspension in bromoform, was reported earlier as 2.34 ± 0.04. The calculated specific gravity is 2.29. The specific gravity redetermined with the Berman balance using larger fragments is 2.29.

THE AMERICAN MINERALOGIST, VOL. 43, JULY–AUGUST, 1958

THE APPLICATION OF A MULTIPLE GUINIER CAMERA (AFTER P.M. DE WOLFF) IN CLAY MINERAL STUDIES

D. H. PORRENGA, *Physical-geographical Laboratory, Municipal Univ. of Amsterdam.*

The type of Guinier camera used by us for an *x*-ray investigation of clay minerals is characterized by a combination of four cameras in a compact unit, using a single focusing monochromator and a single film, and by an asymmetric disposition of the camera relative to the monochromator. According to GUINIER (1945, p. 147.) and DE WOLFF (Delft 1948, p. 207.) we can enumerate the following advantages:

1. An exceptionally high resolving power in the 2θ-range for which the camera is suited, i.e. $2\theta < 70°$. The resolving power ($1° 2\theta = 4$ mm.) is essentially much better than with a Debye-Scherrer camera of the same dispersion, because the focusing property eliminates to a large extent the influence of the thickness of the specimen. In addition, pairs of diffraction lines corresponding to both wavelengths of the α-doublet can be made to coincide for any desired value of 2θ, while their separation is much reduced in a region extending considerably on both sides of this value.

The fact that only a restricted 2θ-range is covered by the Guinier camera is not a handicap: all characteristic lines of clay minerals fall within the obtained range.

2. A low background intensity arising from the absence of white radiation.
3. The possibility of taking simultaneous exposures of four samples for serial work or comparison purposes. This ability is very important in the field of clay mineralogy, since many samples possess small differences in their qualitative or quantitative composition or in their degree of crystal perfection.
4. Very low-order reflections can be made visible, i.e. up to ca. 30 kX. (LIPPMANN, 1954, p. 131).

However, BRINDLEY (1951, p. 8) points out that the arrangement of the specimen is likely to give rather weak basal reflections, since the basal planes will tend to be aligned in the plane of the specimen.

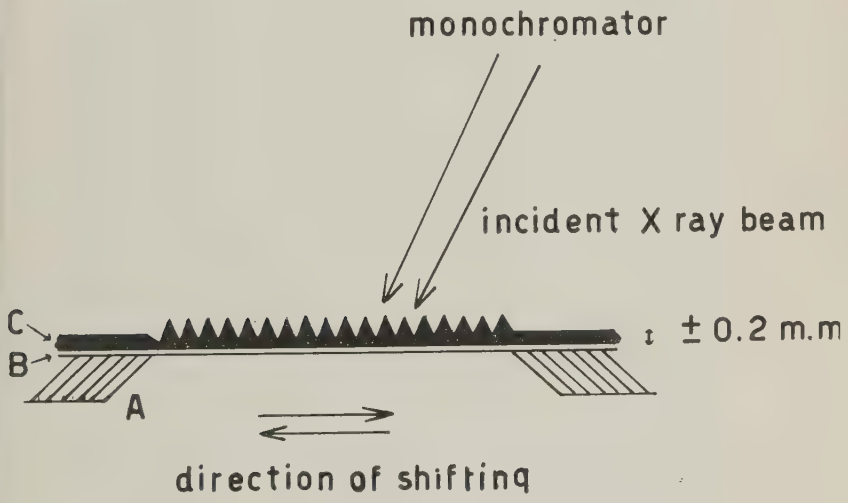

FIG. 1. Design of the sample holder (A), with cellophane (B) and the rippled clay surface (C).

In a study on the possibilities of a Guinier camera after VON WOLFF (Göttingen, Germany) in clay mineral research, LIPPMANN (1954, p. 251–254) describes the difficulty of obtaining basal reflections. He therefore was advised to employ another technique, giving exclusively non-basal reflections, which are in some cases characteristic too.

The present author, however, in cooperation with MR. A. KREUGER of the Netherlands Organisation for Pure Scientific Research, has tried to obtain distinct basal and non-basal reflections by making very fine parallel ribs on the surface of the specimen in order to give the clay crystals favorable orientations to the x-ray beam (Fig. 1). First the clay is embedded in paraffin wax, glycerol, ethylene diamine or any desired medium. Then the clay-paste is mounted on the cellophane of the

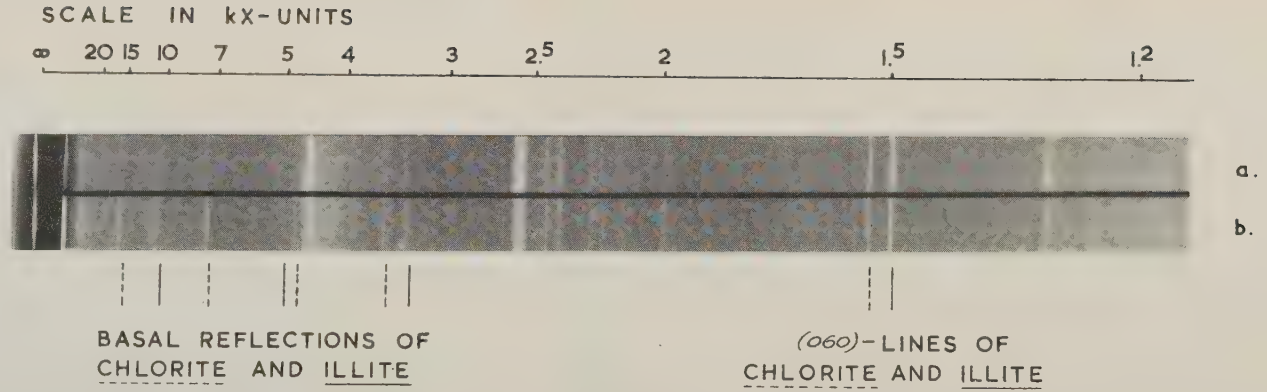

FIG. 2. a) Film taken of sample mounted by the previous methods. b) Film taken of sample mounted with the saw-tooth surface. In both cases the same clay sample was used containing chlorite, illite and quartz (fraction $<1\mu$). CuKx radiation, 35 KV, 20 ma., exposure time 4 hours.

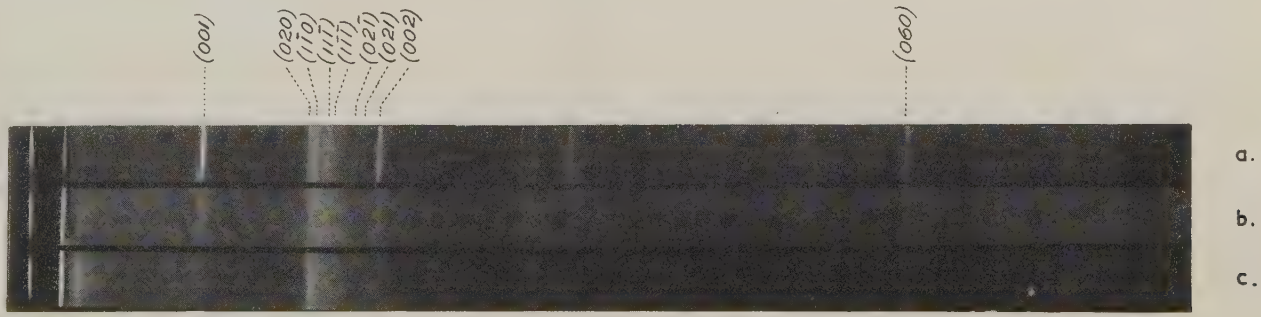

FIG. 3. Film of kaolinite samples. a) reasonably well-crystallized kaolinite from Surinam. b) Poorly crystallized kaolinite from Surinam, and c) Very poorly crystallized kaolinite from Chile, collected by Dr. W. Weischet (Münich). CuKx radiation, 35 KV, 20 ma., exposure time 4 hours.

sample holder. Saw-like ribs are made on the clay surface (thickness ca 0.2 mm.) using a knife blade.

The differences obtained by the old (BRINDLEY, 1951; LIPPMANN, 1954) and the new methods are illustrated by Fig. 2.

Figure 3 shows the advantage of photographing several samples on a

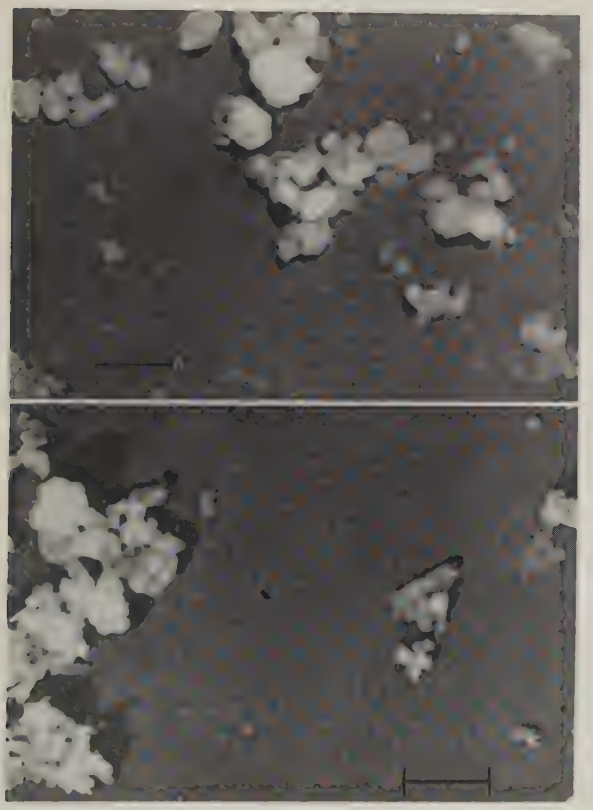

FIG. 4. Electron micrographs of kaolinite samples 0-34-15 (above) and V-56-200, (below) showing the difference in crystallization. Pd-shadow.

single film for comparison purposes. For all three diagrams kaolinite samples (fraction $< 1\mu$) from Surinam and Chile are used. In the upper diagram the high resolving power of the Guinier camera enables us to see how in sample 0-34-15 (Northern Surinam) the (020)-, (110)-, (11$\bar{1}$)-, (111)-, (021)-, (02$\bar{1}$)- and (002)-lines are clearly separated: a well crystallized kaolinite. The middle diagram is obtained from a rather poorly crystallized kaolinite of a sample derived from the Voltzberg area (V-56-200) in Surinam and shows a broadening of some of the lines together

with a decreased intensity. Some lines have even disappeared. The last diagram shows the fewer, broader and weaker lines, characteristic of a very poorly crystallized kaolinite (Chile, W9.).

From the same three samples electron micrographs have been made to investigate the particle size and the degree of crystal perfection. The results appear in good agreement with the *x*-ray examinations. Since in all samples the clay particles are about the same size, it seems likely that the broadening and the decreasing intensities of the lines, as shown in Fig. 3, are not only caused by decreasing particle size but in addition by crystal imperfections (cf. Fig. 4).

Acknowledgments

The helpful guidance and encouragement of Prof. Dr. Carolina H. MacGillavry and Mr. A. Kreuger of the Laboratory for Chemical Crystallography is gratefully acknowledged. The Netherlands Organization for Pure Scientific Research kindly permitted the use of their *x*-ray equipment. We are very indebted to Miss W. van Iterson of the Laboratory for Electron Microscopy and to Mr. H. Van Heuven who made the electron micrographs. Finally we would like to thank Prof. Dr. J. P. Bakker and Dr. H. J. Müller of the Physical-geographical Laboratory for furnishing the clay samples.

References

Brindley, G. W. and Others. *X*-ray identification and crystal structures of clay minerals. Monograph, Mineralogical Society, London, 1951.

Guinier, A. J. Radiocristallographie. Dunod, Paris, 1945.

Lippmann, Fr. Anwendungsmöglichkeiten der Guinier-Kamera nach v. Wolff bei der röntgenographischen Tonuntersuchung. *Heidelberger Beiträge zur Mineralogie und Petrographie*, Bd **4**, 1/2 Heft, 251–254, 1954.

Lippmann, Fr. Über einen Keuperton von Zaisersweiher bei Maulbronn. *Heidelberger Beiträge zur Mineralogie und Petrographie*, Bd **4**, 130–134, 1954.

Wolff, P. M. De. Multiple focusing camera. *Acta Cryst.*, **1**, 207–211, 1948.

THE AMERICAN MINERALOGIST, VOL. 43, JULY–AUGUST, 1958

MINERALOGICAL CHANGES IN WEATHERED SEDIMENTARY IRONSTONES

R. F. Youell, *University of Leeds, Leeds, England.*

The sedimentary ironstones of Liassic and Oolitic ages vary in the state of oxidation of their iron content from ferrous in the green ores to ferric in the red-brown ores which have undergone weathering at deposition or on exposure. Taylor (1) has surveyed the principal physical, chemical and mineralogical changes which accompany weathering. Loss of

lime, magnesia, alumina and carbonate takes place during the oxidation of iron. Previous workers have attributed the formation of kaolinite, sericite or hydrous mica, goethite and "clay" to the alteration of the chamosite which occurs in the parent ore. Recent research (2) on the properties of chamosite has enabled a fresh approach to be made to the study of weathered ironstones.

A stable oxidized chamosite has been identified as a common constituent of weathered ironstones. Its composition is $(Fe^{3+},Al,Mg)_{2.9}$ $(Si,Al)_2$ $O_{6.9}$ $(OH)_{2.1}$ for half the orthohexagonal unit cell, corresponding to $(Fe^{2+},Al,Mg)_{2.9}$ $(Si,Al)_2$ $O_{5.0}$ $(OH)_{4.0}$ for the parent mineral. Laboratory oxidation of the latter under hydrating conditions gave a closely similar product to the natural oxidized form, whereas dehydrating conditions (2) had given a composition with only $O_{7.3}$ $(OH)_{1.0}$ per half unit cell. Its appearance resembles goethite, and much material formerly classed as goethite or limonite must now be regarded as oxidized chamosite. The colour of weathered ores is of little value as a guide to the mineral content, as both goethite and oxidized chamosite may appear in rocks coloured yellow, brown or red. The inference by Taylor (1) that "a silicate of ferric iron" might be present in weathered ironstones has proved an accurate prediction.

The first stage of alteration of siderite-chamosite ores is the breakdown of the siderite to a fine state of subdivision, followed by conversion to goethite. The second stage, which may to some extent overlap the first, is the conversion of chamosite to the ferric form; in some specimens chamosite and oxidized chamosite occur in equal amounts. The final stage is the breakdown of the oxidized chamosite to goethite and a residue which is usually amorphous and consists of the silicate sheets, $Si(Al)\text{-}O_x$, leached of all octahedral ions. The Al replacing Si in these sheets is more resistant than octahedral Al, and the residue has an Al/Si ratio less than for kaolin and chamosite, for which it is about unity.

There is no evidence that kaolinite, sericite or "clay" is produced from chamosite during alteration. The kaolinite which has been inferred from chemical analytical data is often the chamosite residue. Bannister's conclusion, in Taylor (1), that kaolinite is invariably present in weathered ironstones is not confirmed. The oxidized chamosite has similar (00*l*) spacings to kaolinite, and these reflections might be attributed to kaolinite in *x*-ray analysis of a mixture. Where a kaolin mineral occurs, the amount detected by *x*-ray diffraction is in general very much less than that deduced from chemical data. True kaolinite is rare, and in the Northampton Sand Ironstone is confined to the chamosite-kaolinite beds; the kaolin mineral which usually occurs gives a "fireclay" diffraction pattern.

Sericite, or hydrous mica, appears to be formed, not from chamosite,

but from small amounts of primary mica present in the parent ore, and detectable by *x*-ray analysis of the residue from acid extraction, even when it cannot be detected optically. The mica becomes hydrated during weathering and is concentrated by removal of soluble parts of the ore.

The occurrence of oxidized chamosite in weathered ironstones throws some light on the formation of "Box-stones," which consist of alternating layers of red and brown material concentrically arranged and sometimes enclosing unweathered ore. Although the mechanism of their production is not fully understood, it involves the transport of ferric iron as a solution or a colloid. The formation of box-stones is not solely a function of the iron content of the ore. The stability of oxidized chamosite except in extreme conditions of weathering means that the iron content, even if ferric, is not capable of solution and redeposition until a late stage. Siderite, however, produces finely divided goethite very early in the weathering process, and this apparently facilitates mobility of the ferric iron. Ores with only a low iron content, but entirely as siderite (siderite mudstones) produce box-stones, while ores containing much larger amounts of iron as chamosite (chamosite-kaolinite beds) tend to produce uniform brown weathering instead of box-stones. The state of the iron, carbonate or silicate, appears to be the controlling factor in box-stone formation. In general, the red layers of box-stones are richer in goethite, and the brown layers are richer in quartz, mica and kaolin. Unoxidized siderite is often present even in well-developed box-stones.

In some cases, doubt has arisen as to whether goethite is present in ooliths in the ore as a primary constituent or as an alteration product. If accompanied by a white residue, formerly identified as "clay," the goethite is probably an alteration product of chamosite. If not so accompanied, it may be either primary, or secondary after siderite.

Considerable attention has been directed to the problem of beneficiation of sedimentary ironstones. The occurrence of chamosite in unweathered ores is an obstacle to beneficiation processes based on physical methods, since the iron is chemically combined with slag-forming silica and alumina. The identification of oxidized chamosite in weathered ores means that a similar difficulty arises in this case, although previous work had indicated that the iron and the slag-forming constituents were not chemically combined.

Thanks are due to Professor Taylor and Drs. Davies, Dixie and Hemingway for specimens and much valuable discussion.

References

1. Taylor, J. H., Petrology of the Northamptonshire Sand Ironstone. *Mem. Geol. Survey. Gt. Brit. H.M.S.O.*, 1949.
2. Brindley, G. W. and Youell, R. F., *Min. Mag.*, **30**, 57 (1953).

THE AMERICAN MINERALOGIST, VOL. 43, JULY–AUGUST, 1958

REFRACTOMETER PERILS

D. Jerome Fisher, *University of Chicago, Chicago, Illinois.*

The determination of indices of refraction by the immersion technique is very common in mineralogical work. As long as one is satisfied with results to .002 or .003, slapstick methods are in order. But if the limit is to be .001 or better, considerable care is required, in spite of what one might gather from the mineralogical literature. This note is concerned with the ordinary Abbe prism refractometer which is so commonly used for standardizing the immersion media in the range below 1.84. This instrument may be read directly to .001 and by estimation to .0001, but Emmons as well as Fairbairn and Sheppard state that it is correct to .0002 in its lower range, but is less accurate in its upper range.

This refractometer is not given suitable description in any mineralogical text book in English with which the writer is familiar. A fairly good brief résumé appears in Gibb; a more complete and generally satisfactory treatment is by Bauer. Using this instrument (without Amici prisms) with a mercury-vapor lamp having suitable filters to effectively isolate the light of the 4358, 5461, and "5780" lines should yield quite satisfactory results. But the writer failed to get consistent figures, and so a more careful examination was carried out.

First the setting of the instrument was checked. This is normally done by comparing the reading given by a test glass plate against its n_D value (supplied with the instrument). The writer was unable to get satisfactory checks of his readings on subsequent days, in spite of the fact that he was very careful with the illumination. That is, the light was so directed against the non-polished (i.e., diffusing) end of the test plate that true grazing incidence was bound to occur between it and the contact oil (of higher n than that of the test plate). Checks of this nature were attempted on two different instruments (a standard one with range 1.30–1.70, and a high-index one of range 1.45-1.84) with five different test plates (see Table 1), using four different contact oils.

After consulting Tilton's excellent papers, it was concluded that the major trouble lay in the shape of the contact oil film. Thereafter the writer was very careful to use a minimum amount of oil, wiping off any excess at the base with lens tissue, and pressing the test plate tightly against the refractometer glass. Obviously this last must be done with considerable care, but it seems to be essential to avoid a wedge-shaped oil film instead of a parallel-surfaced film. The best way to make sure that one does not have a wedge-shaped oil film is to take readings from a

Table 1. Indices of Refraction Measured for the Five Glass Test Plates at Four Different Wavelengths

Test plate→	1.5174				1.6107				1.6495				1.7205		1.7898	
Instrument→	1.45–1.84		1.30–1.70		1.45–1.84		1.30–1.70		1.45–1.84		1.30–1.70		1.45–1.84		1.45–1.84	
n of oil→ / Light	1.66	1.74	1.66	1.74	1.66	1.74	1.66	1.74	1.66	1.74	1.74	1.82	1.74	1.82	1.775	1.82
5893	1.5177	1.5177	1.5176	1.5176−	1.6109	1.6109	1.6107	1.6107	1.6497	1.6495	1.6495	1.6495	1.7203	1.7203	—	1.7896
5780±0010	1.5182	1.5182	1.5182	1.5182	1.6114	1.6114	1.6114	1.6113	1.6507	1.6506	1.6504	1.6504	1.7220	1.7219	—	1.7913
5461	1.5194	1.5193+	1.5195	1.5195	1.6132	1.6130−	1.6134	1.6133	1.6541	1.6540	1.6541	1.6542−	1.7262	1.7262	—	1.7969
4358	1.5269	1.5269	1.5273	1.5272	1.6235	1.6236	1.6238	1.6238	1.6737	1.6736	1.6741	1.6741	1.7521	1.7521	1.8289	—

The corrections added to the actual readings to yield the above results were as follows:

5780±0010	.0022	.0015	.0022	.0015	.0022	.0015	.0022	—	.0022
5461	.0093	.0065	.0092	.0065	.0092	.0065	.0092	—	.0094
4358	.0524	.0348	.0518	.0347	.0515	.0348	.0515	.0519	—

Table 2. Assumed Correct *n*-Values of the Glass Test Plates

λ	1.5174	1.6107	1.6495	1.7205	1.7898
578	1.5178	1.6113	1.6505	1.7219	1.7917
546	1.5191	1.6132	1.6541	1.7266	1.7975
436	1.5268	1.6236	1.6738	1.7523	1.8291

Table 3. Difference between Measured Values and Assumed True Values

Plate→	1.5174		1.6107		1.6495		1.7205	1.7898
R→ / λ	High-*n*	Standard	High-*n*	Standard	High-*n*	Standard	High-*n*	High-*n*
589	+.0003	+.0002	+.0002	—	+.0001	—	−.0002	−.0002
578	+.0004	+.0004	+.0001	+.0001−	+.0001+	−.0001	—	−.0004
546	+.0003	+.0004	−.0001	+.0001+	—	—	−.0004	−.0006

single test plate using oils of two different n-values. If these readings do not check each other, and the error is due to the presence of a wedge-shaped film, it is obvious that other things being equal the result obtained using the film of lower n will be the smaller, and nearer to the true value. Unless the image of the total reflection boundary line was perfectly straight and sharp, no readings were taken. Thus any oil or dirt on the non-polished end of the test plate or on the refractometer glass surface just below it might cast a shadow that would break the regularity of this line. It should be unnecessary to emphasize that when one is looking at the true total reflection boundary line between light and dark, small movements of the mirror or lamp will not cause it to change position, as will occur if one is dealing with a false line. If the observed boundary line is not straight and sharp, this may be due to an unsatisfactory oil contact film or light source, or the latter or/and the mirror may not be properly adjusted. It is very important to focus the ocular so that the cross-lines are sharp; the shorter the wavelength, the lower the eye-lens. A pin-hole cap for the eye-lens should improve the results.

Having observed all the precautions cited above, the writer obtained data as shown in Table 1. Each value given represents a checked result of two or more readings. The contact oils used were as follows: 1.66-alpha bromonaphthalene; 1.74-methylene iodide; 1.775-sulphur in methylene iodide; 1.82-methylene iodide in phenyldiiodoarsine. The true indices of refraction of the test plates were assumed to be those values given in Table 2. These were obtained by taking the figures measured for $\lambda = 436$ (corrected for a true zero-setting) to be correct, and drawing straight lines on Hartmann dispersion paper through these and the (assumed true) given n_D values, as is shown in Fig. 1. Even if the $\lambda = 436$ figures are in error by a small amount, this will have no appreciable affect on the other numbers shown in Table 2.

In effect Table 3 gives the differences between corresponding values in Tables 1 and 2. From Table 3 the following conclusions may be drawn. The standard refractometer reads slightly high in the low-n range, and substantially correct elsewhere. The high-n instrument is substantially correct in its middle range, but reads too high in its low range and too low in its high range.

The above tests were made at room temperature (*ca.* 20° C.). Bauer (p. 1208) notes that the value obtained for a liquid is usually too low (by up to .0003 for low n liquids) if the instrument is adjusted by using a test glass plate. In any case for accurate work with liquids, the refractometer should be calibrated with these; certified samples can be obtained from the Bureau of Standards.

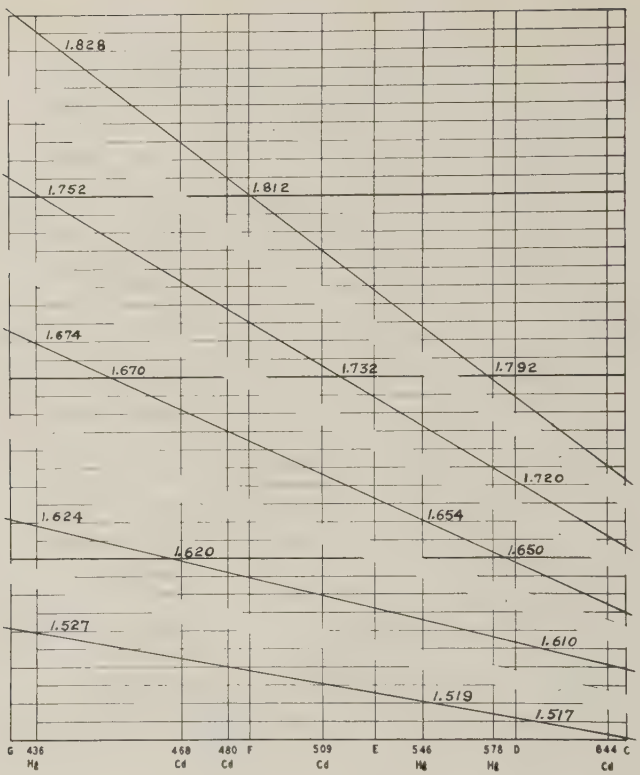

FIG. 1. Dispersion curves for the five glass test plates (see Table 2). The n values assigned to certain horizontal lines are given by the numbers shown above three (four in the central part) lines in each of the five parts of the graph. The spacing between adjacent horizontal lines represents an n-difference of .002 in each case.

REFERENCES

BAUER, N.; see Weissberger.

EMMONS, R. C., The universal stage. *Geol. Soc. Amer., Mem.* **8, 94, 98** (1943).

FAIRBAIRN, H. W. AND SHEPPARD, C. W., Maximum error in some mineralogic computations. *Am. Mineral.*, **30,** 683 (1945)

GIBB, T. R. P., Optical methods of chemical analysis, 326–330 (1942).

RATH, R., Dispersionsbestimmung mit Zeisschen Abbe Refraktometern. *Neues Jb. Min. Abh.*, **87,** 163–184 (1954) and **90,** 1–6, (1957).

TILTON, L. W., Testing and accurate use of Abbe-type refractometers. *Journ. Opt. Soc. Amer.*, **32,** 371–381 (1942).

TILTON, L. W., Sources of error in precise commercial refractometry. *J. Research Natl. Bur. Standards*, **30,** 311–328 (1943).

VON WOLFF, T. F., Methodisches zur quantitativen Gesteins-und Mineral-Untersuchung mit Hilfe der Phasenanalyse. *Mineral. und Petrogr. Mitt.*, **54,** 1–122 (1942). See especially pp. 45–60.

WEISSBERGER, A. (ed.), Physical methods of organic chemistry. Vol. 1, Pt. 2, Chap. XX on refractometry by N. Bauer. 1203–1214 (1949).

THE AMERICAN MINERALOGIST, VOL. 43, JULY–AUGUST, 1958

OCCURRENCE OF WAIRAKITE AT THE GEYSERS, CALIFORNIA

A. Steiner, *New Zealand Geological Survey, Wellington, New Zealand.*

Wairakite, the lime analogue of analcime, first discovered in hydrothermally altered rocks at Wairakei, New Zealand (1, 2) has been identified recently in a greywacke fragment from The Geysers, California. This fragment, made available by courtesy of Dr. Donald E. White, United States Geological Survey, was erupted in 1955 from a new well drilled to a depth of 600 feet and cased to 200 feet.

At The Geysers, wairakite, undoubtedly of hydrothermal origin, replaces feldspar almost completely, and lines cavities and fractures in the greywacke. Thus its occurrence resembles that at Wairakei. The Californian wairakite displays the characteristic two sets of polysynthetic twinning and possesses the same refractive indices as its counterpart from New Zealand.

References

1. Steiner, A. (1955): Wairakite, the Calcium Analogue of Analcime, a New Zeolite Mineral. *Min. Mag.*, **30,** 691.
2. Coombs, D. S. (1955): *X*-ray Observations on Wairakite and Non-cubic Analcime. *Min. Mag.*, **20,** 699.

THE AMERICAN MINERALOGIST, VOL. 43, JULY–AUGUST, 1958

MICROHARDNESS OF ALUMINUM BORIDE MONOCRYSTALS

Perry G. Cotter, *Bureau of Mines, Norris, Tennessee.*

Synthesis and General Description

Single crystals of aluminum boride (AlB_{12}) were obtained by two methods of synthesis at the Bureau of Mines Electrochemical Experiment Station, Norris, Tenn. In the first method aluminum chips and anhydrous boron oxide (B_2O_3) were heated in a graphite crucible, under vacuum, to the point of incipient melting. Argon at 2–5 psi was then admitted, and the temperature was raised rapidly to the reaction point. The first reaction occurred at 1140–1200° C., and the final reaction took place at 1350° C. The regulus from this final reaction was digested first in hydrochloric acid and then in hydrofluoric acid. From this synthesis three types of crystals were obtained, as shown in Figures 1–3.

The maximum diameter of crystals obtained by this method of synthesis was 2 mm. The maximum length of the long yellow crystals was 5 mm. Some showed distinct red-yellow pleochroism.

For the second synthesis the ordinary aluminothermic method was used. (1) The crystals obtained by this method, shown in Fig. 4,

FIG. 1. Long yellow orthorhombic crystals of aluminum boride. ×42.

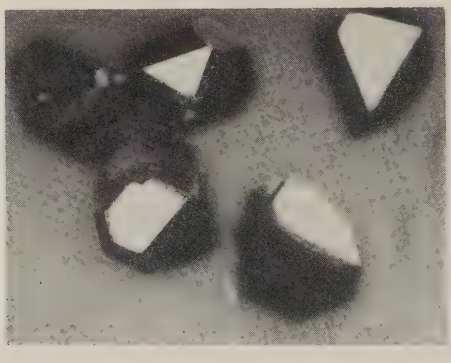

FIG. 2. Yellow orthorhombic, short bipyramidal crystals. ×42.

were red by transmitted light, flat tabular, pseudo-hexagonal and probably monoclinic. The maximum diameter was 5 mm. The quantity of crystals recovered from both methods of synthesis was small.

PROPERTIES

Density.—The density of selected crystals was determined by the sink-float method, using bromoform diluted with carbon tetrachloride as the immersion liquid. The figures obtained are shown in Table 1.

TABLE 1. DENSITY OF ALUMINUM BORIDE CRYSTALS

Type of crystal	Density (gm./cc.)
1. Solid yellow orthorhombic, short bipyramidal	2.591±0.005
2. Red hexagonal, flat tabular	2.534±0.008
3. Long yellow, pseudo-hexagonal	2.574±0.003

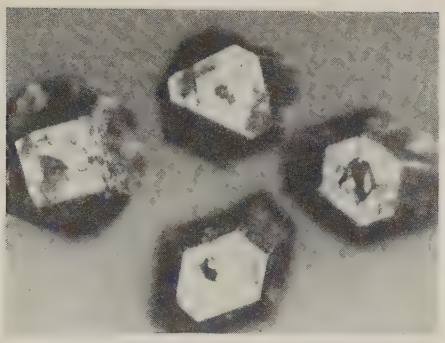

FIG. 3. Yellow "dished" orthorhombic crystals. ×42.

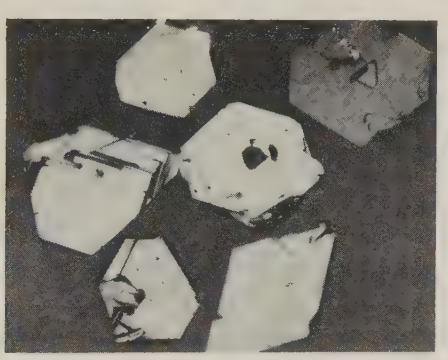

FIG. 4. Red tabular pseudohexagonal crystals. ×42.

Hardness.—The crystals selected for hardness testing were mounted in bakelite, surfaced first on a 600-grit diamond wheel, then on a 1000-grit diamond wheel, and were finally polished with 0 to 2 micron diamond paste on a teakwood wheel. This method gave optically flat surfaces of sufficient area for indenting.

Indentations were made with a Tukon microhardness tester, using a Knoop indenter and a 100-gram load. An oil-immersion objective (97×, 1.25 N.A.) was used to measure the length of indentations. Accuracy and reproducibility of the tests were determined by making indentations in molded boron carbide (Norbide) and in crystals of black silicon carbide.

Of the three types of yellow aluminum boride crystals tested, none showed a distinct variation in hardness. The average hardness value obtained from thirty indentations was 2754 K_{100}. The range in hardness was 2715–2788 K_{100}. Coincident indentations made in the molded boron carbide specimen gave an average hardness value of 2755 K_{100}, with a range of 2695–2841 K_{100}, while those made in the silicon carbide speci-

men gave an average hardness value of 2520 K_{100}, with a range of 2410–2600 K_{100}. These figures are comparable with those obtained by Thibault and Nyquist (2), 2760 K_{100} for molded boron carbide and 2550 K_{100} for gray silicon carbide, in their study of Knoop hardness.

Thirty indentations, made in four of the red pseudohexagonal crystals, gave an average hardness value of 2433 K_{100}, with a range of 2354–2527 K_{100}. Abrasion tests on the polished surfaces of silicon carbide and molded boron carbide, using crushed crystals of yellow aluminum boride, showed that the silicon carbide was scratched and pitted by the crystals, while the boron carbide was unaffected. A similar test using crushed red crystals showed no abrasion on either the silicon carbide or the boron carbide.

From the foregoing tests it appears that the hardness of yellow aluminum boride crystals is ≈ 2700 K_{100} and that they are harder than silicon carbide and very nearly as hard as boron carbide. The hardness value for the red pseudo-hexagonal crystals is ≈ 2400 K_{100}.

References

1. Biltz, Heinreich, (1908), Über krystalliziertes Bor I. *Berichte der Deutschen Chemischen Gesellschaft* **41,** 2634–2645.
2. Thibault, N. W., and Nyquist, H. L. (1947), Measured Knoop hardness of hard substances and factors affecting its determination. *Trans. Am. Soc. Metals,* **38,** 271–330.

THE AMERICAN MINERALOGIST, VOL. 43, JULY–AUGUST, 1958

DEVICE FOR PRECISELY CONTROLLING AN IRIS DIAPHRAGM*

P. A. Sabine, R. H. Rowe and G. Day
Geological Survey and Museum, London, England.

The photoelectric measurement of the reflectivity of ore-minerals, ably discussed by Bowie (1957), is facilitated if precise control of the light is achieved by means of an iris diaphragm. The device described below was designed for use on an ore-microscope, but could be used in any optical system where fine adjustment of the iris is desired.

The instrument is shown assembled on a microscope tube (Fig. 1*a*) and in "exploded" view (Fig. 1*b*).

The conventional control of an iris diaphragm is usually by means of a lever (K) acting more or less concentrically with the iris. The present device is mounted beside the lever and is coupled to it. An additional lever (A) moves coaxially on the microscope tube, resting on a flange. Mounted on the lever (A) is a flat knurled disk (D) in which is cut a spiral groove.

* Publication authorized by the Director, Geological Survey and Museum.

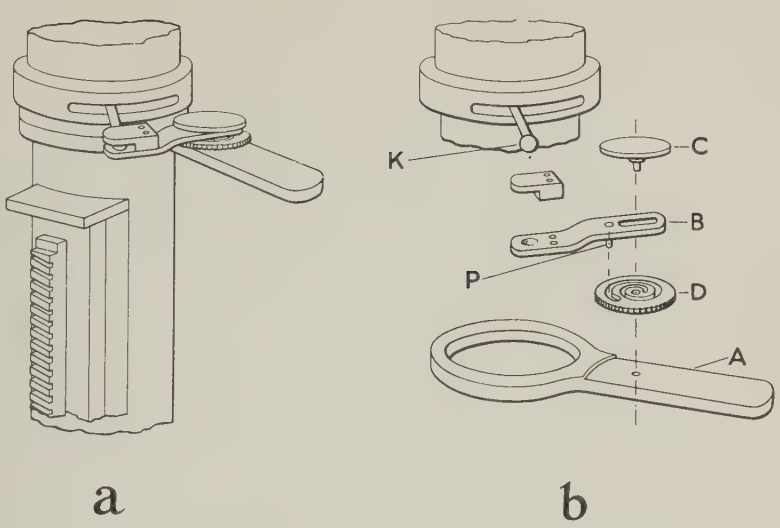

Fig. 1. Iris diaphragm device. (a) assembled. (b) "exploded" view.

A bracket (B) is attached to the lever (A) and disk (D) by means of a flat cover and screw (C). Pin (P) engages the spiral groove in the disk. The other end of the bracket is attached loosely by means of a clamp to the original lever of the iris.

Operation.—The lever (A) is used for coarse adjustment of the iris. For fine adjustment lever (A) is slightly depressed with the thumb in order to hold it by friction against the bearing surfaces above and below. The disk (D) is then turned with the forefinger so that bracket (B), engaging in the groove, moves slightly sideways in a direction along its length, thus finely adjusting the iris knob (K).

For use with an ore-microscope the device is not calibrated numerically but if calibration were wanted it could be done by arranging the lever (A) to have "click" stops at a number of equally-spaced definite positions, and engraving the edge of the knurled disk for movement between these positions.

Reference

Bowie, S. H. U. (1957), The photoelectric measurement of reflectivity: *Mineral Mag.*, **31**, 476–86.

THE AMERICAN MINERALOGIST, VOL. 43, JULY–AUGUST, 1958

THE SO-CALLED "OXYGEN EXCESS"

DUNCAN MCCONNELL, *Ohio State University, Columbus, Ohio.*

In view of discussions which arose at the annual meeting of the Mineralogical Society of America (Atlantic City, New Jersey, November 1957), coupled with the recent usage of the term in the *Mineralogical Magazine*, it seems appropriate to comment on the misleading expression "oxygen excess."

This so-called "oxygen excess" has been erroneously interpreted to mean, rather than a deficiency of smaller interstitial cations, exactly what the term implies, an excessive number of oxygen atoms occurring in a particular structure. Except in unusual situations which require special elucidation, "excess" oxygens do not exist in structures composed of fairly closely packed oxygen atoms.

It would seem axiomatic, for example, from the symmetrical requirements that a garnet structure cannot contain 99 oxygen atoms instead of 96. Nevertheless, it has been claimed that $12CaO \cdot 7Al_2O_3$ exists in "solid solution" with grossularite. Here, a portion of the failure in semantics probably stems from the term, "solid solution." Were one discussing a *glass*, for which "solid solution" would be most appropriate terminology, no such enigma as the assignment of 99 large anions (oxygens) to 96 equivalent points of a symmetrical lattice would arise, because of the known irregularities of glassy substances.

However, the problem at hand is quite simple. If, indeed, some substance composed of CaO and Al_2O_3 is isostructural with $Ca_3Al_2(SiO_4)_3$—and such a substance may exist—its correct composition cannot be represented by $12CaO \cdot 7Al_2O_3$ (actually $3[Ca_{12}Al_{14}O_{33}]$) because three additional oxygens cannot be placed in this structure without destroying the essential symmetrical arrangement required by *Ia3d*.

Such vague, illusive terminology as "oxygen excess" and "solid solution" should be abandoned in favor of *cation deficiency* and *isomorphic variant* in connection with description of silicates and related structures.

Alexander Newton Winchell died June 7, 1958. Professor Winchell was president of the Mineralogical Society of America in 1932, and received the Roebling Medal in 1955. A memorial will appear in the March-April, 1959 issue of the *American Mineralogist.*

S. J. Thugutt, emeritus professor of Warsaw University, died at Krakow, December 27, 1956, aged 95. Volume 20 (1957) of Archiwum Mineralogiczne is dedicated to him.

BOOK REVIEWS

FERROELECTRICITY IN CRYSTALS, by HELEN D. MEGAW. 220 pp. Methuen and Co. Ltd. (1957). 27s 6d.

The significant advances up to 1955 in this new field are assembled and reviewed in this book in a form which is readily assimilated and easily read. The emphasis here, in contrast to other treatments which stress the physical phenomena, is entirely on the matter of crystal structure and its influence on the electrical properties of this peculiar class of compounds. Such an approach, given to us by a veteran crystal chemist, is welcome for two reasons. First, it provides an easy and excellent introduction to the subject for those who are not primarily concerned with solid state physics. Second, it will provide the physicist a guide to the controlling factors of crystal chemistry and crystallography which are often not fully appreciated by workers in solid state physics.

Ferroelectricity was first discovered in Rochelle salt in 1921, but extensive study of the phenomenon was not begun until 1945 when the ferroelectric behavior of barium titanate was discovered. Since then, a diligent search for other crystals of this type has been carried on by many laboratories, yielding many new discoveries which are described in detail in Dr. Megaw's book. The one common feature of these structures is stressed, namely, that they are polar in symmetry, but have the special property of being only slight distortions of arrangements of higher symmetry. The measurement of these distortions is the most difficult task of the x-ray and neutron diffraction worker and the results which have been published are ably collected and evaluated. In spite of the advances that have been made, the collection of ferroelectric structures is a confusing picture of transition points, parallel and antiparallel displacements, hydrogen bonds, superlattices, and many other factors all of which, at one point or another, seem to play a key role in the development of ferroelectricity. The known examples of ferroelectric compounds grow in number at an increasing rate, but appear to defy any attempts to classify or systematize them. In fact, the study of ferroelectrics has served to reveal the inner complexity of many seemingly simple structures, which on closer examination have been found to exhibit a bewildering variety of first and second order transitions, by no means always associated with ferroelectricity.

The author has done her best to bring to bear the technique of crystal chemistry in combination with the current model theories for the physical properties of these crystals, but the failure of present-day theoretical methods is apparent. One reason why the discovery of ferroelectric barium titanate touched off such a storm of scientific investigation was that it was felt by workers in the solid state field that here was a structure basically so simple that it should be possible to evolve a unified theory relating the spontaneous polarization and other physical phenomena to the parameters of the structure directly. The investigations, especially in connection with the structure determinations, have proved to be far more difficult than had been anticipated, and the failure of a unified theory to emerge has been disappointing.

As Dr. Megaw points out, all of the model theories are based mainly on an analysis of the long-range electrostatic forces, and take no account of the short-range exchange forces involved in covalent bonding between the atoms. She stresses the need to take account of these latter forces in order to find the true source of ferroelectric behavior in crystals. Unfortunately, we are least well equipped to handle this part of the theoretical problem at the present time. Thus, we are brought directly to the fundamental problem of chemical bonding, and on this common ground solid state physicists, chemists, geochemists and mineralogists find each other standing side by side.

Dr. Megaw has enriched her book with cogent quotations from English literature at the

head of each chapter. The most appropriate is found before the introduction, from the "Testament of Beauty" by Bridges:

> "Wisdom will repudiate thee, if thou think to enquire WHY things are as they are, or whence they came: thy task is first to learn WHAT is."

This book makes it clear that in the field of ferroelectrics, we are still learning WHAT is.

Howard T. Evans, Jr.
U. S. Geological Survey
Washington 25 D. C.

CHEMICAL ENGINEERING IN THE COAL INDUSTRY. Edited by Forbes W. Sharpley. 141 pp. Pergamon Press, London, 1957. Price, $8.50.

During a period when there is much discussion about atomic power and exotic solid fuels, it is interesting to read that the economy of Europe, including Russia, will be dependent for 20 to 30 years upon technical progress in the seemingly commonplace coal industry.

This short book contains seven technical papers presented at an international conference held in Cheltenham, England, in June, 1956. Subjects discussed cover briquetting, controlled oxidation, carbonization, and analysis and industrial use of low-temperature coal tar. Particular emphasis is placed upon the fact that, although coal is classified as a mineral substance, the extent of its heterogeneity is unknown in the ore-processing industries.

Information presented in the various papers summarizes recent developments in several European countries. Each paper is followed by an extensive discussion; in one instance a 6-page text is followed by 8 pages of comments. Data on engineering, scientific, and economic factors in the preparation and utilization of coal are presented in interesting fashion.

The book is attractive in its assembly, and the figures and microphotographs are excellent. Very few typographical errors were noted, but in future efforts of this type an attempt should be made to eliminate inconsistencies in units that arise during translation. Although expensive, the book is highly recommended as a source of information on recent European developments in the preparation of coal.

Irving A. Breger
U. S. Geological Survey
Washington 25, D. C.

EINFÜHRUNG IN DIE KRISTALLOGRAPHIE, by W. Kleber. VEB Verlag Technic, Berlin, 1956, 312 pp., 316 figs., 44 tables. Price about $5.

The English philosopher Bertrand Russel stated in "The Analysis of Matter," p. 4, that "What were, in Peano's methods, primitive terms are . . . replaced by logical structures. . . ." The same process has taken place in many branches of geological science during the last five decades: The primitive terms, in our case unrelated observations on individual minerals, were replaced by logical structures; and we can understand the word structures even in a non-figurative way. Modern crystallography has provided a most remarkable, most valuable arsenal of logical concepts. In many ways it has thus counterbalanced the tremendous amount of new knowledge: by providing principles which reduce the number of unrelated data considerably.

Yet, in many schools mineralogy is still taught in the "old way" and the attitude is still alive that "what was good for many years will be good for many more," thus defying progress in science. Still a course in crystal structures is, in too many cases, pushed off into the graduate school, instead of forming an integral part of elementary crystallography.

Many attempts to condense the principles of crystallography exist in German, a few in English. However, a few only have been able to crystallize the most essential information into a course which is short and condensed enough to serve as a one semester textbook. Among these attempts KLEBER's new book appears to me to be the most successful one. On only 312 pages was he able to treat the subject of crystallography all the way from the symmetry principles and classes and the other aspects of morphological crystallography (p. 22–115), to crystal chemistry (p. 116–190), and to crystal physics, including excellent chapters on deformation, electrical and magnetic properties, optics and x-ray analyses (p. 191–299), followed by a ten-page index and a chart of the interference colors.

Again, one of the most outstanding features of the book is its clear and condensed style. The chapter on projections, e.g., takes up three and a half pages only, and yet the stereographic, the Schmidt, and the gnomonic projection are discussed in a well conceived way.

Building up on the tradition set by von Laue, W. H. and W. L. Bragg, Paul Niggli and V. M. Goldschmidt, this book is a masterpiece of teaching in the field of mineralogy.

The editors and printers have done a fine piece of clean organization and printing, and anyone interested in an excellent modern mineralogy textbook will want to add a copy of KLEBER's book to his library.

G. C. AMSTUTZ
Missouri School of Mines and Metallurgy

NEW MINERAL NAMES

Kirschsteinite

Th. G. Sahama and Kai Hytönen. Kirschsteinite, a natural analogue to synthetic iron monticellite, from the Belgian Congo. *Mineralog. Mag.*, **31,** 698–699 (1957).

The new mineral, the iron analogue of monticellite, occurs in melilite-nephelinite lava from Mt. Shaheru, Belgian Congo, associated with melilite, nepheline, clinopyroxene, kalsilite, götzenite, combeite, sodalite, magnetite, perovskite, apatite, hornblende, biotite, and an unidentified mineral.

Analysis gave SiO_2 32.71, TiO_2 0.23, Al_2O_3 0.26, Fe_2O_3 0.66, FeO 29.34, MnO 1.65, MgO 4.95, CaO 29.30, Na_2O 0.34, K_2O 0.36, P_2O_5 0.07, H_2O^+ 0.25, H_2O^- 0.06, sum 100.18%. This corresponds (in mol %) to Ca(Fe, Mg, Mn)SiO_4 96.3 with Fe:Mg:Mn = 69.4:22.6:4.3, Fe_2SiO_4 3.7. The analyzed mineral is therefore a magnesian kirschsteinite.

The mineral is slightly greenish; it is colorless in thin section. G. (pycnometer) 3.434. Optically biaxial, negative, α1.689, β 1.720, γ 1.728, 2Vα 51±; $\alpha = b$, $\beta = c$, $\gamma = a$.

X-ray powder data, indexed from the data on fayalite, are given. The strongest lines are 2.949 (100), 2.680 (85), 2.604 (80), 3.658 (70), 1.839 (60). From the powder data, the unit cell has $a = 5.859$, $b = 11.132$, $c = 6.420$ Å, all ±0.005. These were confirmed by Weissenberg and rotation photographs. Presumably the mineral is orthorhombic.

The name is for the late Egon Kirschstein, German geologist, pioneer in geological exploration of North Kivu.

Michael Fleischer

Götzenite

Th. G. Sahama and Kai Hytönen. Götzenite and combeite, two new silicates from the Belgian Congo. *Mineralog. Mag.*, **31,** 503–510 (1957).

Analysis gave SiO_2 32.50, TiO_2 9.72, Al_2O_3 4.26, Fe_2O_3 0.35, FeO 0.45, MnO 0.07, MgO 0.29, CaO 41.80, BaO 0.09, SrO none, Na_2O 4.85, K_2O 0.14, P_2O_5 0.01, CO_2 none, F 8.33, Cl 0.15, SO_3 0.19, H_2O^- 0.14, H_2O^+ 0.26, sum 103.60—(O = F_2) 3.54 = 100.06%. This is said to correspond to $5Ca(Si, Ti)O_3 \cdot (Na, Ca, Al)_2F_{3.5}$. The unit cell content is $(Ca, Na)_{6.66}(Ti, Al, etc.)_{1.66}Si_4O_{15}(F, OH)_{3.49}$ (compare the rinkite group new data). The mineral is close in chemical composition to calcium-rinkite but contains much more calcium, somewhat less sodium, and no rare-earths, compared to 2.3%. Spectrographic analysis showed no Ce, Y, Nb.

The mineral is easily soluble in hot dilute HCl. When heated, it shows decreasing birefringence and at 955±10° C. becomes isotropic; *x*-ray study shows that it has decomposed.

Götzenite occurs in colorless prismatic crystals up to 0.5 mm. long. Goniometric data (all ±1/2°) gave (100):(403) = 138°, (403):(001) = 143°, (001):($\bar{1}$01) = 145°, ($\bar{1}$01):(100) = 113°, ($\bar{1}$00):($\bar{2}$0$\bar{1}$) = 147°, ($\bar{2}$0$\bar{1}$):(00$\bar{1}$) = 135°, (00$\bar{1}$):(10$\bar{1}$) = 146°, (10$\bar{1}$):(100) = 113°. Weissenberg photographs show the mineral to be triclinic with $a = 10.93 \pm 0.05$, $b = 7.32 \pm 0.03$, $c = 5.74 \pm 0.03$ Å, alpha 90°, beta 100±1°, gamma 120±1°, $a:b:c = 1.493:1:0.784$. Cleavage perfect (100), good (001). Most crystals show lamellar twinning with twin axis *b* and composition plane perpendicular to (001). *X*-ray powder data (not indexed) are given and agree fairly well with those of Slepnev for the rinkite group, although the unit cell and symmetry do not agree. The strongest lines given for götzenite are 3.100 (100), 2.986 (100), 1.911 (50), 2.648 (40), 2.511 (25), 1.690 (25).

The mineral is biaxial, positive, with *n*s, alpha 1.660, beta 1.662, gamma 1.670, 2V 52° (measured), 53½° (calcd.) Dispersion strong, 2V greater for red than blue. A diagram of the optical orientation is given. D_4^{20} 3.138 (pycnometer). Hardness not given.

Götzenite occurs in a nephelinite found on the wall of Mt. Shaheru, the extinct southern tributary of the active volcano Mt. Nyiragongo, North Kiva, Belgian Congo.

The name is for the German traveller, Count G. A. von Götzen, the first white man to climb Mt. Shaheru (1894).

Discussion—I do not agree that "the entire absence of the rare earths (and Cb, Sr) and the somewhat higher fluorine content of götzenite as well as its slightly differing optical properties seem to justify the mineral being distinguished from calcium rinkite." However, the name calcium rinkite was somewhat unsuitable for a mineral with the same calcium content as rinkite and it may be abandoned in favor of götzenite, which is much closer to being an end-member.

M. F.

Combeite

Th. G. Sahama and Kai Hytönen. Götzenite and combeite, two new silicates from the Belgian Congo. *Mineralog. Mag.*, **31**, 503–510 (1957).

Analysis of combeite containing some alteration product gave SiO_2 49.78, TiO_2 0.32, ZrO_2 0.44, Al_2O_3 2.45, Fe_2O_3 1.86, FeO 0.54, MnO 0.58, MgO 0.41, CaO 22.68, BaO 0.09, SrO none, Na_2O 16.14, K_2O 1.18, P_2O_5 0.02, CO_2 none, F 1.87, Cl 0.30, SO_3 0.19, H_2O^- 0.42 H_2O^+ 1.39, sum $100.66-(O=F_2, Cl_2)$ $0.86=99.80\%$. Spectrographic tests showed rare earths to be absent. This is interpreted as corresponding to the simplified formula $Na_4(Ca, Al, Fe)_3Si_6O_{16}(OH, F)_2$; the unit cell contains 3 formula weights. Combeite is easily soluble in hot dilute HCl.

The mineral occurs in poorly developed colorless stout hexagonal prisms a few tenths of a mm. in length. No terminal faces were observed. Cleavage none. D_4^{20} 2.844 (pycnometer). It is optically uniaxial, negative, birefringence very low, $\epsilon \approx \omega = 1.598 \pm 0.002$. Weissenberg photographs show the mineral to be hexagonal rhombohedral, $\bar{3}mR$, possible space groups $R3m$, $R32$, $R\bar{3}m$. The unit cell has $a = 10.43$, $c = 13.14$, both ± 0.03 Å, $c/a = 1.260$. Indexed x-ray powder data are given; the strongest lines are 2.657 (100), 2.607 (80), 3.304 (70), 2.722 (50), 3.354 (40), 1.861 (40).

The mineral has altered to a product of higher birefringence with wavy extinction, uniaxial, negative, with optic axis parallel to that of unaltered combeite, and with ns 1.56–1.57. Its x-ray pattern is very similar to that of combeite.

Combeite occurs in the same rock as götzenite, see above. The name is for the late A. D. Combe of the Geological Survey of Uganda; pronounced koombite. Perhaps an analogue of eudialyte.

M. F.

Vibertite

N. R. Goodman. Gypsum in Nova Scotia and its associated minerals. The geology of Canadian industrial mineral deposits, pp. 110–114, Canadian Inst. Mining and Metallurgy, 1957.

$CaSO_4 \cdot 0.5H_2O$ was identified optically and by x-ray powder study in many samples of well borings from the upper 1,000 feet drilled at Nappan, Cumberland County, Nova Scotia. It replaces gypsum or anhydrite and is believed to have been present in the rocks, and not formed during drilling or in making sections.

The name is for G. Vibert Douglas, Professor of Geology, Dalhousie University.

Discussion.—The name bassanite has priority, see Dana's System, 7th Ed., Vol. II, p. 476, and remarks on the name miltonite (*Am. Mineral.*, **36**, 640 (1951)).

M. F.

Nioboloparite

I. P. Tikhonenkov and M. E. Kazakova. Niobloparite—a new mineral of the perovskite group. *Zapiski Vses. Mineralog. Obshch.*, **86**, 641–644 (1957) (in Russian).

The mineral occurs as crystals up to 1.5 mm. in diameter, with the octahedron dominant, and the cube minor but usually present. It is black, reddish-brown in fine splinters. Streak grayish-brown. Luster strong, metallic. No cleavage, fracture conchoidal. Hardness $5\frac{1}{2}$–6, G. 4.657 Isotropic, with n about 2.35.

Analysis (by M. E. K.) gave TiO_2 32.01, (Nb, Ta)$_2O_5$ 26.26, ΣCe_2O_3 25.55, ThO_2 1.16, FeO (total iron) 0.94, CaO 1.32, MgO 0.18, Na_2O 10.53, K_2O 0.80, H_2O 0.85, sum 99.60%. This corresponds to $(Na_{0.59}\ Ce_{0.27}\ Ca_{0.07})\ (Ti_{0.67}\ Nb_{0.33})\ O_{2.87}\ (OH)_{0.13}$, with a slight deficiency in the A position of the formula $A_2B_2(O, OH)_6$. A dehydration curve shows that most of the water was lost at 150°, the remainder at 700–800°. The mineral is insoluble in acids.

X-ray powder data are given. The strongest lines (kX) are 2.756 (10), 1.951 (6), 1.592 (6), 1.378 (4). This corresponds to a cubic cell with a_0 3.905 ± 0.005 A., but the mineral may be pseudo-cubic.

The mineral occurs in a pegmatite vein cutting pyroxene-bearing rischorrites of Kukisvumchorr Mt., Khibina Tundra, Kola Peninsula. It occurs only in parts of the vein in which the principal minerals (K feldspar, nepheline, arfvedsonite, and aegirine) have been largely replaced by natrolite and hackmanite, and appears to have been formed at the expense of rinkolite.

Discussion.—This member of the perovskite group contains 26% Nb_2O_5, whereas loparite contains about 10%. Nevertheless, since Ti is still >Nb, the name seems to be an unnecessary one for niobian loparite.

M. F.

Orthochamosite

Frantisek Novak, Jiri Vtelensky, Jiri Losert, Frantisek Kupa, and Zdenek Valcha. The orthochamosite from the ore veins of Kank near Kutna Hora—a new specific mineral. Frantisek Slavik Memorial Vol., *Czech Acad. Sci.*, **1957**, 315–344. (Czeck with English summary).

The name orthochamosite is given to the orthohexagonal modification first described by Brindley (*Mineralog. Mag.*, **29**, 502–522 (1951), and since by Brindley and Youell (*Ibid.*, **30**, 57–70 (1953), and Deudon (*Bull soc franc. mineral. crist.* **78**, 475–480 (1955)).

Analysis gives the formula:

$$(Fe^{2+}_{3.60}Mg_{1.06}Ca_{0.06})\ (Fe^{3+}_{0.46}Al_{0.71})\ (Si_{3.02}Al_{0.98})O_{10}(OH)_8.$$

G. 3.078, H. about 2, mean n 1.649. *X*-ray powder data give a_0 5.355, b_0 9.293, c_0 7.043 kX Dehydration and D.T.A. data are given.

M. F.

Parapitchblende

Jacques Geffroy and Jacqueline A. Sarcia. Contribution a l'etude des pechblendes francaises. *Sciences de la Terre* (*Ann. école natl. superieure géol. appliquée et prospection minière Univ. Nancy*) **2**, No. 1–2, 1–157 (1954).

The name parapitchblende is provisionally given to a black, isotropic alteration product of the pitchblende variety of uraninite from veins at Bauzot and Ruaux, Saone-et-Loire, France. It is apparently an oxide of uranium containing chiefly U^{+6} and minor U^{+4}. It differs from ordinary pitchblende in polished section in lower hardness and inferior reflectivity.

Discussion.—*X*-ray and chemical study would probably establish the identity of the substance as one of the known gummite-type alteration products of uraninite or perhaps a relatively highly oxidized type of uraninite itself. In the absence of diagnostic *x*-ray and other criteria, it would have been preferable to have simply called the substance an unidentified mineral and not to have advanced a new name, even provisionally.

Clifford Frondel

Unnamed Manganese Silicate

Smirnov, S. S., Mineralogy of some polymetallic ores of the Transbaikal region, p. 18–128 in *Selected works*, *Moscow, Acad. Sci. USSR*, 248 p. (1955).

An unnamed manganese silicate is described (p. 115–116) in this posthumous paper, never before published. The silicate occurs in highly oxidized material not visibly connected with lead-zinc ores of the Donin area, Nerchinsk district. The mineral, rosy-red where fresh, is veined by bustamite. Other paragenetic details could not be determined, owing to the strong oxidation. Optical properties: colorless in thin section, nX$\sim$1.780, nZ$\sim$1.810, nZ$-n$X$=0.031$, $2V_X=60°$; cleavage $\perp$Y distinct, cleavage $\perp$X less distinct. One grain showed a very good cleavage whose coördinates relative to X, Y, and Z are 45°, 0, and 45°. Analysis by M. M. Stukalova in 1930, on material highly contaminated with bustamite and some calcite, gave: SiO_2 37.72, TiO_2 nil, Al_2O_3 nil, Fe_2O_3 2.01, FeO 6.33, MnO 45.65, MgO 1.35, CaO 5.94, CO_2 1.13; sum 100.15% [100.13%]. Deducting CO_2 as calcite and the remaining CaO as bustamite ($6MnSiO_3 \cdot 5CaSiO_3$—the formula of analyzed bustamite from the Donin area), the author gets the molecular proportions 668 (Mn, Fe, Mg)O:452SiO_2, or very nearly 3(Mn, Fe, Mg)O.2SiO_2 [equivalent to $(Mn_{2.43}Fe_{0.42}Mg_{0.15})O.2SiO_2$; total iron as FeO]. Though no mineral of like physical and chemical character was known to him, the author thought his data inadequate for establishing a new mineral species.

Discussion.—Chemically, Smirnov's manganese silicate is analogous to artificial $Mn_3Si_2O_7$, named *Manganiustit* [manganjustite] by O. Glaser (1926, *Centralbl. Mineralogie*, Abt. A, p. 81–96). Optical data for the artificial compound have never been reported, and *x*-ray data are lacking for both substances. Because physical correspondence between these substances has not been demonstrated, one can state only that a mineral chemically resembling the manganjustite of Glaser has been reported by Smirnov.

B. F. Leonard

Strunzite

Clifford Frondel. Strunzite, a new mineral. *Die Naturwissenschaften* **45**, 37–38 (1958).

The new mineral forms divergent tufts and felted coatings of tiny hair-like or lath-like crystals. Color straw-yellow to brownish-yellow. G. variable, 2.47–2.56, mostly near 2.52.

Weissenberg and precession photographs show it to be monoclinic, $a_0=9.80$, $b_0=18.06$, $c_0=7.34$ (A. or kX?), β 100°10′, $a_0:b_0:c_0=0.543:1:0.406$. Space group probably $C2/c$. The laths are flattened on (010) and twins on (100) have been observed. *X*-ray powder patterns (not given) are nearly identical, but show slight variations in spacings.

"An approximate chemical analysis on 150 mg" gave P_2O_5 33.0, MnO 9.1, Fe_2O_3 36.0, $H_2O(\pm)$ 22.5, sum 100.6%. Spectrographic analysis showed also 0.X% Mg and Zn. This is close to $MnFe_2(PO_4)_2(OH)_2 \cdot 8H_2O$. The unit cell contains 4 molecules.

The optical properties vary, both from the same locality and from different localities. For Hagendorf material, α 1.619, β 1.670, γ 1.720, $Z:c=10°$, pleochroism faint in yellow, absorption $Z>X$, Y. There is no obvious correlation between optical properties, *x*-ray spacings, and Fe/Mn ratio.

The mineral occurs as a near-surface weathering product in 10 pegmatites that contain

triphylite (Palermo and Fletcher, N. H.; Norway, Rumford, Newry, and Unity, Maine; Hagendorf and three others in Bavaria), also as films in weathered outcrops of phosphate rock of the Phosphoria Formation at Rasmussen Valley, Idaho.

The name is for Professor Hugo Strunz of Berlin and Regensburg.

M. F.

Revoredite

G. C. Amstutz, P. Ramdohr, and F. de las Casas. A new low temperature mineral of hydrothermal origin from Cerro de Pasco. *Bol. soc. geol. Peru*, **32**, 25–33 (1957).

The mineral, first thought to be botryoidal supergene limonite, was found on the 1400 level of the Cerro de Pasco mine in cavities in the lead-zinc sections. It occurs as stalactitic tubes, as massive reniform crusts, and as powdery incrustations; the vugs range from very small ones to one probably containing several tons of the mineral. The mineral is associated with quartz, galena, sphalerite, pyrite, and gratonite.

The color ranges from silvery-gray to orange to carmine-red; streak brownish-red. Fracture conchoidal. Optically isotropic, semi-opaque, pleochroism not detected. Fairly soft. *X*-ray studies at Harvard, Heidelberg, and the U. S. Geological Survey show the material to be amorphous.

Chemical analyses (by Research Dept., Cerro de Pasco Corp.) gave As 52.1, 51.9; Pb 8.7, 2.7; S 34.9, 34.7, Tl 0.5–1%. Semiquant. spectrographic analyses of 6 samples of different color show As major in all, Pb major in 3, minor (1–10%) in 3, Fe 1–10% in 3, 0.1–1% in 3, Tl 1–10% in 2, 0.1–1% in 3, 0.01–0.1% in 1. Also detected Cd, Al, In, Sn, Zn, Sb and others. When heated, the material turns black and melts.

The name revoredite, for Juan Francisco Aguilar Revoredo, a Peruvian mineralogist, is proposed "in case that a crystalline sample should be found or that, by some method, it might be possible to attribute a crystalline structure to this so far amorphous mineral."

M. F.

Koutekite

Zdeněk Johan. Koutekite: a new mineral. *Nature*, **181**, no. 4622, 1553–1554 (1958).

The mineral occurs with arsenic, silver, smaltite, loellingite and chalcocite "in the bicarbonate gangue" of specimens from Černy Dul in the Krkonoše (Giant Mts.), Bohemia. It occurs as fine grains intergrown with an unknown copper arsenide. Synthetic alloys corresponding closely to Cu_2As were identical with the new mineral by optical and *x*-ray study.

Under the microscope the mineral is bluish-gray (markedly blue compared to chalcocite). Strongly anisotropic, no internal reflections. Etched by HNO_3 (1+1), HCl (1+1), 20% $FeCl_3$ solution, giving first a crimson color, then a light gray; partly positive, partly negative results were obtained with 5% $HgCl_2$ solution, negative with 40% KOH. Apparently hexagonal; the strongest lines of the *x*-ray pattern have spacings (intensities not given) 3.32, 2.446, 2.078, 2.024, 1.994, 1.374, 1.324, 1.197, 1.178, 1.147A. G. (synthetic) 8.48.

The name is for J. Koutek, professor of economic geology, Charles University, Prague.

Discussion.—Nearly all these lines are fairly close to strong lines of "β-domeykite" (see Padera, *Rozpravy Ceske Akad.* **61**, No. 4 (1951)), but many lines of the latter are missing here. More data are needed.

M. F.

Kobokobite

J. Thoreau. Sur un mineral de la famille des "Dufrenites" dans la pegmatite de Kobokobo (Congo Belge). *Acad. royale Belg., Bull. classe sci.*, **43**, 705–710 (1957).

The mineral occurs as crusts of radiating fibers and as masses in the Kobokobo pegmatite, South Kivu. Fresh material is dull green, altered material is brown. Analyses by P. Ronchesne of the green and brown material gave FeO 9.36, —; MnO 8.40, 4.14; CaO, MgO, Al_2O_3 n.d., n.d.; Fe_2O_3 41.33, 49.21; Mn_2O_3 —, 4.96; P_2O_5 32.20, 31.67; H_2O 8.38, 10.90; sum 99.67, 100.88%. The first analysis gives approximately $RO:Fe_2O_3:P_2O_5 = 10:10:9$, or if slight oxidation is assumed, $(Fe'', Mn'')_2Fe_3'''(PO_4)_3(OH)_4 \cdot nH_2O$, whereas Frondel had proposed $Fe''Fe_6'''(PO_4)_4(OH)_8$ and Lindberg $(Fe'', Mn'')Fe_4'''(PO_4)_3(OH)_5 \cdot 2H_2O$ for the rockbridgeite-frondelite series.

X-ray powder data are given; they agree closely with those of rockbridgeite and frondelite. The green mineral is optically biaxial, positive, with α 1.798 ± 0.003, β 1.820 ± 0.002, 2V very large, Z perpendicular to the cleavage, γ parallel to elongation, pleochroism marked, X green to bluish, γ pale brown. The brown variety has *n*s approximately α 1.86, β above 1.88, X parallel elongation, X pale brown, γ dark brown.

The new name is justified on the basis of the composition (higher content of FeO + MnO) and the lower indices of refraction than those reported for the rockbridgeite-frondelite series (see Frondel, *Am. Mineral.*, **34**, 513–540 (1949, Lindberg, Ibid., 541–549).

Discussion.—Should not have been named. The formulas of these minerals are uncertain because of doubt as to the degree of oxidation of FeO.

M. F.

Unnamed (β-MnS)

Guy Baron and Jacques Debyser. Sur la presence dans les vases organiques de la mer Baltique du sulfure manganeux β hexagonal. *Compt. rendu acad. sci. France*, **245**, 1148–1150 (1957).

Rose-colored beds 0.5–2 mm. thick were found in cores taken at 2.15–4.45 m. below the water-sediment interface at Landortsdjupet on the Baltic Sea. These very fine grained layers contained 2.35–3.40% organic carbon and consisted chiefly of quartz, alkali feldspar, plagioclase, illite, and kaolinite. Minute bipyramidal black prisms in the clay were found spectrographically to contain much Mn, less Si and Al, no Fe. A microchemical analysis gave S 27.3 ± 0.3%. The *x*-ray powder diagram is identical with that of synthetic hexagonal red β-MnS (Schnaase, *Zeitschr phys. Chem.* **B20**, 89 117 (1933)). Indexed *x*-ray powder data (no intensities given) show lines at 3.43, 3.21, 3.03, 2.352, 1.992, 1.82, 1.725, 1.693, 1.666, 1.52, 1.45, 1.344, 1.204, 1.149, 1.113. The mineral is believed to be authigenic.

Discussion.—Apparently a member of the wurtzite group.

M. F.

NEW DATA

Rinkite, Johnstrupite, Rinkolite, Lovchorrite, and Calcium Rinkite (all = Mosandrite)

Yu. S. Slepnev. The minerals of the rinkite group. *Izvest. Akad. Nauk S.S.S.R., Ser. geol.*, 1957, No. **3**, 63–75 (in Russian).

Th. G. Sahama and Kai Hytönen. Unit cell of mosandrite, johnstrupite, and rinkite. *Geol. Foren. Forh.*, **79**, 791–796 (1957) (in English).

Slepnev gives the results of new *x*-ray and D.T.A. studies of these minerals. Only calcium-rinkite gave an *x*-ray pattern; the others were metamict, but gave essentially the

same pattern after being heated to 800°. All are essentially identical in composition; special tests showed that mosandrite, rinkite, and johnstrupite, previously reported to contain up to about 7% ZrO_2, actually contain about 1%. Calcium-rinkite contains only 2.3% rare earths, compared to 13–21% for the others; however, the content of CaO and Na_2O is not correspondingly increased. Mosandrite is somewhat lower in Na_2O and F and higher in H_2O than the others and may represent an early stage of alteration. The general formula of the group is $Na_2Ca_4CeTiSi_4O_{15}(F, OH)_3$.

Vud'yavrite is highly altered, all the Na_2O and F having been leached out, and is highly hydrated. It is considered to be a distinct mineral.

Slepnev believes the minerals to be monoclinic; he gives for rinkolite $a = 18.52$, $b = 5.71$, $c = 7.52$, β 91°30′–92°; for rinkite $a = 18.47$, $b = 5.67$, $c = 7.46$, β 91°13′; for mosandrite $a = 18.37$, $b = 5.63$, $c = 7.42$, β 93°4′ (?). S. and H. find the minerals to be triclinic. Mosandrite and johnstrupite have $a_0 = 18.45 \pm 0.06$, $b_0 = 7.44 \pm 0.03$, $c_0 = 5.63 \pm 0.02$, alpha 90.2°, beta 91.0°, gamma 100.9°; rinkite has $a_0 = 18.51 \pm 0.1$, $b_0 = 7.45 \pm 0.03$, $c_0 = 5.64 \pm 0.03$, alpha 90°, beta 91°, gamma 101°. (These are clearly identical within experimental error, S. and H. having reversed the b and c of Slepnev. M. F.) The x-ray powder data of S. and H. agree fairly well with those of Slepnev. The unit cell of götzenite (see above) is, however, distinctly different.

The only recommendation made by Slepnev as to nomenclature is that all these minerals be placed in a single group, to be called the rinkite group because mosandrite is partially altered. S. and H. consider that despite the near identity of unit cells, rinkite clearly differs from mosandrite and johnstrupite and is to be regarded as a separate species (The differences seem to me to consist only in that the pattern of rinkite showed many additional lines. M.F.).

Discussion.—The minerals appear to be identical and some names can be dropped, including rinkite (1884), johnstrupite (1890), rinkolite (1926, *Am. Mineral.*, **14,** 440 (1929)), and lovchorrite (1926, *Am. Mineral*, **15,** 203 (1930)), all in favor of mosandrite (1841). The slight degree of alteration of the latter seems insufficient reason for dropping the name. Calcium-rinkite (1935) differs somewhat in composition, but not enough to justify retaining the name (see Götzenite, above).

M. F.

Schuilingite

C. Guillemin and R. Pierrot. Nouvelles donnees sur la schuilingite. *Bull. soc franc. mineral. crist.*, **80,** p. 549–551 (1957).

The original fragmentary description (see *Am. Mineral.*, **33,** 385–386 (1948) is greatly amplified. The mineral occurs in crusts of crystals rarely up to 0.3 mm in length. Apparently monoclinic, with one good cleavage parallel to the elongation. Color turquoise –to azure-blue, powder pale blue. H. 3–4. G. (hydrostatic) 5.2 ± 0.1.

Optically biaxial, negative, ns, α (calcd.) 1.710, β 1.755 ± 0.005, γ 1.775 ± 0.005, 2V 66°. Most crystals show parallel extinction, but some show extinction at 8–10° from parallel.

Microchemical analysis (on 20 mg. for CO_2 and H_2O, 20 mg. for others) gave PbO 37.4, CuO 9.4, CaO 19.8, CO_2 20.9, H_2O 9.9, insol. 3.1, sum 100.5% This corresponds to $Pb_3Cu_2Ca_6(CO_3)_8(OH)_6 \cdot 6H_2O$. The mineral is readily decomposed by dilute acids, with strong effervescence. When heated, it blackens and melts with difficulty to a black bead.

Unindexed x-ray powder data are given. The strongest lines in Å. are 4.78 (S), 3.85 (mS), 9.56 (m), 6.08 (m), 4.51 (m), 3.18 (m), 2.95 (m).

Discussion.—Schuilingite is apparently a valid species, to be classed in Dana's System Seventh Ed., Class 16, Type 2.

M. F.

Obruchevite

A. P. KALITA. On the composition of obruchevite—a hydrated uranium-yttrium variety of pyrochlore. *Doklady Akad. Nauk S.S.S.R.*, **117,** 120 (1957) (in Russian).

Previous data are given in *Am. Mineral.* **43,** 380–381 (1958). Two new analyses by M. E. Kazakova and M. V. Kukharchik gave Na_2O 2.43, 2.03; K_2O 0.31, 0.70; CaO 2.82, 2.66; MgO 0.26, 0.18; MnO 0.35,——; Y_2O_3 11.34, 11.73; Ce_2O_3 0.66, 1.13; ThO_2 0.26, 0.11; UO_3 9.72, 10.50; Fe_2O_3 4.30, 3.52; Al_2O_3——, 1.40; SiO_2 3.78, 3.20; TiO_2 6.29, 2.74; Nb_2O_5 37.54, 37.30; Ta_2O_5 5.47, 7.23; H_2O^+ 7.77, 14.50 (total H_2O), H_2O^- 6.48,——; ignition loss ——, 1., sum 99.78, 99.93% (given as 100.33 M.F.). The first analysis corresponds to $(Y, Na, Ca, U)_{1.27}(Nb, Ta, Ti, Fe)_2O_{5.40}(OH)_{0.60}$. 1.13 H_2O. A D.T.A. curve shows a large endothermal effect at 200° and a small exothermic effect at 710°. A curve for loss of weight shows 7.2% to 200°, 10.8% to 500°, 13.4% to 1100°.

The mineral is metamict; when heated to 1100° it gives a powder pattern similar to that of the pyrochlore group with $a = 10.0$–10.34 Å. The strongest lines are 2.975 (10), 1.695 (9), 1.488 (7), 3.152 (5), 1.550 (5).

The color is brown of various shades, mainly chocolate-brown, luster vitreous to adamantine. G. 3.60–3.80, hardness $4\frac{1}{2}$–5. Isotropic, n 1.830–1.835. Fracture conchoidal.

Obruchevite occurs in a pegmatite in the Alakurtt region, north-west Karelia, in albite-muscovite replacement zones, associated with garnet, fergusonite, and columbite.

DISCUSSION.—Y predominates in the A group of the formula, so that obruchevite may be ranked as a species corresponding to the Ce-predominant member, loparite.

M. F.

Classification of the Alkali Amphiboles

A. MIYASHIRO. The chemistry, optics, and genesis of the alkali-amphiboles *Journ. Fac. Sci. Univ. Tokyo*, Sec. 2, **11,** 57–83 (1957).

AKIHO MIYASHIRO and MASAO IWASAKI. Magnesio-riebeckite in crystalline schists of Bizan in Sikoku, Japan. *Journ. Geol. Soc. Japan*, **63,** 698–703 (1957).

YU. K. ANDREEV. A new variety of alkali amphibole-magnesio-arfvedsonite *Trudy Inst. Geol. Rudnykh Mestorozhdenii, Petrog., Mineralog., Geokhim*, **10,** 12–20 (1957) (In Russian).

The first of these papers is an important study of these minerals, with consideration of 63 analyzed and optically studied samples. Eckermannite and holmquistite, in which there is appreciable Li, are omitted.

Taking the general formula of the alkali amphiboles as $(Na, K, Ca)_{2-3}(R'', R''')_5(Si, Al)_8O_{22}(OH)_2$, Miyashiro divides them into four main groups, with ideal formulas as follows:

A. Riebeckite-glaucophane	$Na_2R_3''R_2'''Si_8O_{22}(OH)_2$
B. Arfvedsonite	$Na_2Ca_{0.5}R_{3.5}''R_{1.5}'''(Si_{7.5}Al_{0.5})O_{22}(OH)_2$
C. Katophorite	$NaCaR_4''R'''(Si_7Al)O_{22}(OH)_2$
D. Soda-tremolite	$Na_2CaR_5''Si_8O_{22}(OH)_2$

The first three are in serial relation, with increasing amounts of the substitution CaR''Al for R'''Si. Soda-tremolite is derived from tremolite by substitution of Na_2 for Ca.

Within group A, the names used and ideal formulas are:

	R''	R'''	
Riebeckite	Fe_3	Fe_2	
Magnesioriebeckite	Mg_3	Fe_2	
Subglaucophane	$Mg_{1.5}Fe_{1.5}$	AlFe	$Fe'''/R''' = 0.3$–0.7
Glaucophane	Mg_3	Al_2	$Fe'''/R'' = <0.5$, $Fe'''/R''' = <0.3$
Ferroglaucophane	Fe_3	Al_2	

Osannite (Hlawatsch, 1906) is a variety of riebeckite.

Ternovskite (Polovinkina, 1924) is magnesioriebeckite.

Crocidolite has riebeckite or magnesioriebeckite composition.

Gastaldite (Struever, 1875) is near glaucophane; the original analysis appears to have been erroneous.

Crossite (Palache, 1894) has been defined both on chemical and optical bases. Miyashiro accepts the optical definition, i.e., optic axial plane normal to (010), $b=Z$, and $c:\gamma$ small. Such material is usually subglaucophane, rarely riebeckite or magnesioriebeckite.

Within group B, the names used and ideal formulas are:

	R''	R'''	
Arfvedsonite	Fe	Fe	Fe″>Mg
Magnesioarfvedsonite	Mg	Fe	Mg>Fe″

Heikolite (Kinosaki, 1935) is a variety of arfvedsonite with composition near the boundary with riebeckite.

Fluotaramite (Morozewicz, 1925) is mostly magnesioarfvedsonite, partly magnesioriebeckite.

Torendrikite (1920) belongs to magnesioarfvedsonite; some samples later placed here on the basis of optics are magnesioriebeckite.

Andreev describes occurrences of magnesio-arfvedsonite, for which he uses the slightly different formula $Na_3Mg_4Fe'''Si_8O_{22}(OH)_2$.

Within group C, the names used and ideal formulas are:

	R''	R'''	
Katophorite	Fe″	Fe‴	Fe″>Mg
Magnesiokatophorite	Mg	Fe‴	Mg>Fe″

Anophorite (Freudenberg, 1910) is a magnesio katophorite.

In group D, R″ is largely Mg. R‴ is low and predominantly Fe‴.

Imerinite (Lacroix, 1921) and Szechenyiite (Krenner, 1900) belong here. Richterite is manganoan soda-tremolite.

M. F.

Bellite

H. Strunz. Bellit, ein Chromat-Apatit, *Naturwissenschaften*, **45**, 127–128 (1958).

Bellite was originally described by Petterd (1904) as a lead chromate-arsenate, with CrO_3 22.61, As_2O_3 6.55 (= As_2O_5 7.61), SiO_2 7.59, PbO 61.68%. Tests by Palache (Dana, 7th Ed., Vol. II, p. 895) indicated it to be a mixture, mainly of mimetite. Strunz reports that red needles from the type locality are optically uniaxial, negative, with ϵ 2.16, ω 2.22 (much higher than those of Palache), a_0 10.13_5, c_0 7.39. The powder photograph is of the mimetite type. Spectrographic analysis showed the presence of Pb, Ag, Cr, and As. On this basis, the formula is written as $(Pb, Ag)_5Cl[(As, Cr, Si)O_4]_3$.

Discussion.—Quantitative analyses are required to establish this as being other than a chromatian variety of mimetite.

M. F.

AMERICAN MINERALOGIST

Price Information

Back issues of the AMERICAN MINERALOGIST can be purchased at the prices given below, but certain issues as listed are available only in microtext edition. The microtext edition is on 3 x 5 inch cards, each card containing 48 pages of text material, with a heading in regular type to indicate the volume, number, pages and date. Microtext will be furnished on all orders where necessary, unless specific instructions are received to the contrary. Prices apply to both the regular and microtext editions, and postage is charged except on indexes. Agents and dealers are allowed the usual 10% discount on orders. Subscriptions for the current volume (calendar year) are available to libraries, colleges, and other organizations at $6.00, postpaid. Individuals can receive the current volume by becoming members of the Mineralogical Society of America.

Volume	Year	Price per volume	Price per issue (except special issues)
1-9	1916-1924	$3.00	$ .50
10-19	1925-1934	4.00	.50
20-28	1935-1943	6.00	.80 (monthly issue)
29-42	1944-1957	6.00	1.60 (bimonthly issue)

Microtext Edition

Vol.	No.	Year	Vol.	No.	Year
1-5	Complete	1916-1920	27	1-12	1942
7	2	1922	28	1-8	1943
9	3	1924	29	1-8	1944
10	3	1925	30	1-4, 7-8	1945
11	3	1926	31	1-4	1946
25	5	1940	32	1-4	1947
26	1-3, 6-9, 12	1941			

Special Issues

Year	Issue	Vol.	No.	Price	Year	Issue	Vol.	No.	Price
1925	Michigan	10	9	$1.00	1945	Quartz Symposium	30	5-6	$3.00
1925	Harvard	10	11	1.00	1950	Larsen	35	9-10	2.50
1927	Harvard	12	4	1.00	1953	Hunt	38	1-2	2.00
1928	Harvard	13	7	1.00	1953	Ross-Schaller	38	11-12	3.00
1930	Harvard	15	8	1.00	1955	Kraus	40	11-12	2.00
1932	Harvard	17	7	1.00	1957	Harvard	42	11-12	2.00
1937	Palache	22	7	3.00					
1938	Harvard	23	11	1.50					

Indexes

Vols. 1-20 (1916-1935) $2.00; $1.00 to members; postpaid
21-30 (1936-1945) 3.00; 2.00 to members; postpaid
31-40 (1946-1955) 5.00; 3.00 to members; postpaid

Send all orders to

MINERALOGICAL SOCIETY OF AMERICA

Earl Ingerson, Treasurer

c/o U. S. Geological Survey, Washington 25, D.C.

NEW AT WARD'S—
2" X 2" ASTRONOMY SLIDES

LX 30 Astronomy slides. A splendid set of 25 black-and-white 2″ × 2″ slides of important astronomical subjects. The photographs were taken with the largest and most powerful astronomical instruments in the world, at the Mount Wilson and Palomar Observatories, and are of the best quality under the extremely difficult conditions of this type of photography. The moon, sun, galaxies, and nebulae are all represented. The set is excellent for general science, earth science, and astronomy courses, or for personal possession and pleasure.

LX 30 Set of 25 slides $18.75

BROKEN HILL COLLECTION

The Broken Hill lode in the New South Wales desert is a classic mining district. A representative series of its ores, gangue minerals and rocks should be made available to all students of economic geology. The 23 specimens in this suite average 2″ × 2″ to 3″ × 4″ and are accompanied by a descriptive list. $74.85

All prices are list at Rochester, N.Y.

NEW WARD CATALOGS

583 Ward's Geology Catalog—The most comprehensive geology catalog ever published by Ward's. It contains a listing of mineral, rock and fossil collections; minerals, rocks and reference clay minerals in bulk or student specimens; color slides for geology (physical geology, mineralogy, paleontology, astronomy). The section on equipment for field and laboratory includes expanded listings of storage equipment, and an especially fine section on thin section equipment. There is an illustrated section on crystallographic aids including crystal models. If you are not on our mailing list to receive this catalog, write for it today.